Title 40 CFR Part 191
Subparts B and C
Compliance Recertification Application 2026
for the
Waste Isolation Pilot Plant

Appendix SCR-2026
Feature, Event, and Process Screening for PA

United States Department of Energy
Waste Isolation Pilot Plant

Carlsbad Field Office
Carlsbad, New Mexico

Compliance Recertification Application 2026 Appendix SCR-2026 Feature, Event, and Process Screening for PA

Table of Contents

SCR-1.0 INTRODUCTION 1

SCR-2.0 BASIS FOR FEPS SCREENING PROCESS 2
SCR-2.1 Requirement for FEPs 2
SCR-2.2 FEPs List Development for the CCA 3
SCR-2.3 Criteria for Screening of FEPs and Categorization of Retained FEPs 3
SCR-2.3.1 Regulation (SO-R) 3
SCR-2.3.2 Probability of Occurrence of a FEP Leading to Significant Release of Radionuclides (SO-P) 3
SCR-2.3.3 Potential Consequences Associated with the Occurrence of the FEPs (SO-C) 4
SCR-2.3.4 UP FEPs 4
SCR-2.3.5 DP FEPs 5
SCR-2.4 FEPs Categories and Timeframes 5
SCR-2.4.1 Description of Natural FEPs 5
SCR-2.4.2 Description of Human-Induced EPs 5
SCR-2.4.3 Description of Waste- and Repository-Induced FEPs 8

SCR-3.0 FEPs 9

SCR-4.0 SCREENING OF NATURAL FEPS 25
SCR-4.1 Geological FEPs 25
SCR-4.1.1 Stratigraphy 25
SCR-4.1.2 Tectonics 26
SCR-4.2 Structural FEPs 30
SCR-4.2.1 Deformation 30
SCR-4.2.2 Fracture Development 32
SCR-4.2.3 Crustal Process 40
SCR-4.2.4 Geochemical Processes 43
SCR-4.3 Subsurface Hydrological FEPs 49
SCR-4.3.1 Groundwater Characteristics 49
SCR-4.3.2 Changes in Groundwater Flow 51
SCR-4.4 Subsurface Geochemical FEPs 55
SCR-4.4.1 Groundwater Geochemistry 55
SCR-4.5 Geomorphological FEPs 61
SCR-4.5.1 Physiography 61
SCR-4.6 Surface Hydrological FEPs 67
SCR-4.6.1 Depositional Processes 67
SCR-4.6.2 Streams and Lakes 68
SCR-4.6.3 Groundwater Recharge and Discharge 69
SCR-4.7 Climate EPs 73
SCR-4.7.1 Climate and Climate Changes 73

SCR-4.8 Marine FEPs 75
SCR-4.8.1 Seas, Sedimentation, and Level Changes 75
SCR-4.9 Ecological FEPs 77
SCR-4.9.1 Flora and Fauna 77

SCR-5.0 SCREENING OF HUMAN-INDUCED FEPS 84
SCR-5.1 Human-Induced Geological EPs 84
SCR-5.1.1 Drilling 84
SCR-5.1.2 Excavation Activities 90
SCR-5.1.3 Subsurface Explosions 94
SCR-5.2 Subsurface Hydrological and Geochemical EPs 96
SCR-5.2.1 Borehole Fluid Flow 96
SCR-5.2.2 Excavation-Induced Flow 130
SCR-5.2.3 Explosion-Induced Flow 141
SCR-5.3 Geomorphological EPs 142
SCR-5.3.1 Land Use Changes 142
SCR-5.4 Surface Hydrological EPs 145
SCR-5.4.1 Water Control and Use 145
SCR-5.5 Climatic EPs 148
SCR-5.5.1 Anthropogenic Climate Change 148
SCR-5.6 Marine EPs 149
SCR-5.6.1 Marine Activities 149
SCR-5.7 Ecological EPs 150
SCR-5.7.1 Agricultural Activities 150
SCR-5.7.2 Social and Technological Development 151

SCR-6.0 WASTE AND REPOSITORY-INDUCED FEPS 153
SCR-6.1 Waste and Repository Characteristics 153
SCR-6.1.1 Repository Characteristics 153
SCR-6.1.2 Waste Characteristics 154
SCR-6.1.3 Container Characteristics 156
SCR-6.1.4 Seal Characteristics 158
SCR-6.1.5 Backfill Characteristics 160
SCR-6.1.6 Post-Closure Monitoring Characteristics 164
SCR-6.2 Radiological FEPs 164
SCR-6.2.1 Radioactive Decay and Heat 164
SCR-6.2.2 Radiological Effects on Material Properties 181
SCR-6.3 Geological and Mechanical FEPs 182
SCR-6.3.1 Excavation-Induced Changes 182
SCR-6.3.2 Effects of Fluid Pressure Changes 190
SCR-6.3.3 Effects of Explosions 191
SCR-6.3.4 Thermal Effects 195
SCR-6.3.5 Mechanical Effects on Material Properties 206
SCR-6.4 Subsurface Hydrological and Fluid Dynamic FEPs 219

SCR-6.4.1 Repository-Induced Flow 219
SCR-6.4.2 Effects of Gas Generation 221
SCR-6.4.3 Thermal Effects 222
SCR-6.5 Geochemical and Chemical FEPs 224
SCR-6.5.1 Gas Generation 224
SCR-6.5.2 Speciation 242
SCR-6.5.3 Precipitation and Dissolution 245
SCR-6.5.4 Sorption 247
SCR-6.5.5 Reduction-Oxidation Chemistry 250
SCR-6.5.6 Organic Complexation 254
SCR-6.5.7 Chemical Effects on Material Properties 256
SCR-6.6 Contaminant Transport Mode FEPs 259
SCR-6.6.1 Solute and Colloid Transport 259
SCR-6.6.2 Particle Transport 261
SCR-6.6.3 Microbial Transport 262
SCR-6.6.4 Gas Transport 264
SCR-6.7 Contaminant Transport Processes 264
SCR-6.7.1 Advection 264
SCR-6.7.2 Diffusion 267
SCR-6.7.3 Thermochemical Transport Phenomena 270
SCR-6.7.4 Electrochemical Transport Phenomena 272
SCR-6.7.5 Physiochemical Transport Phenomena 274
SCR-6.8 Ecological FEPs 278
SCR-6.8.1 Plant, Animal, and Soil Uptake 278
SCR-6.8.2 Human Uptake 279

SCR-7.0 REFERENCES 280

List of Figures

Figure SCR-1. Thermal power for CRA-2026 and past performance assessment derives primarily from Pu isotopes and is less than the assumed 500 kW initial thermal power that resulted in a maximum ~2 °C temperature rise in the entire repository region (Kicker 2025/Van Soest 2025; Van Soest 2018; Van Soest 2012; Crawford et al. 2009; Thorne and Rudeen 1981) 168
Figure SCR-2. Categories of criticality for organizing arguments based on fast or slow assembly speed for a fissile configuration moderated by brine and hydrogenous material (Rechard et al. 1997, Fig. 7) 172
Figure SCR-3. Roof falls onto 3 tiers of POCs and CCOs emplaced in a WIPP disposal room does not significantly disrupt the array nor cause clustering or sorting of containers. Red and brown discs represent the top and bottom plywood stabilizer for the blue 12-inch inner pipe or 6-inch criticality control container inside the 55-gallon shell (which is hidden for visualization) (Rechard et al. 2025a, Fig. 12b; Rechard et al. 2025b, Fig. 3b) 174

Figure SCR-4. Compacted arrays of POCs and CCOs in disposal room buckle and tip over but groups of containers are not critical (Rechard et al. 2025a, Fig. 14b; Rechard et al. 2025b. Fig. 7b) 177
Figure SCR-5. Limiting hydrogenous material to less than 1.3 kg prevents criticality in CCOs (i.e., assembly is safely subcritical if k_{eff}<0.95—green line—if moderator mass inside CCO < 1.3 kg); reactivity decreases further if at least 2 kg miscellaneous filler present (based on Rechard et al. 2025b, Fig. 19b)..... 178
Figure SCR-6. Ten grams boron carbide sufficient to prevent criticality even with large mass of hydrogenous material (i.e., assembly is safely subcritical if k_{eff}<0.95—green line—if moderator mass inside CCO < 2.8 kg) (Rechard et al. 2025b, Fig. 39b) 178
Figure SCR-7. Categories of criticality for organizing arguments based on explosive, fast, or slow fissile assembly speed for fissile assembly with unmoderated, fast neutrons (Rechard et al. 1997, Fig. 7)..... 194
Figure SCR-8. Mass of magnesium oxide remaining in waste panel (MGOKG_W) for E1 intrusion, Replicate 1, CRA-2026 (Scenario S2-BF-t350-r1)..... 201
Figure SCR-9. Fraction of initial cellulose, plastic, and rubber remaining in waste panel (CPRREM_W) for E1 intrusion with intrusion at 350 years, Replicate 1, CRA-2026 (Scenario S2-BF-t350-r1) 202
Figure SCR-10. Mass of gas generated from equivalent cellulose biodegradation in waste panel (CELMOL_W) for E1 intrusion at 350 years, Replicate 1, CRA-2026 (Scenario S2-BF-t350-r1)..... 203
Figure SCR- 11. Four infinitely long cylindrical containers within a single-layer infinite array. 209
Figure SCR- 12 Waste cylinder movement velocities as a function of cylinder spacing for the 213
Figure SCR-13. Lagrangian porosity (based on initial room volume) is very small because of practically zero salt porosity that creeps into room when no gas is generated and is very large because of empty volume of expanded room when maximum gas is generated (Vignes et al. 2023, Fig. 3-6) 217
Figure SCR-14. Total repository gas generation from iron corrosion, cellulose biodegradation, and radiolysis (ALL_HTTC) for E1 intrusion with intrusion at 350 years, Replicate 1, CRA-2026 (Scenario S2-BF-t350-r1) 240
Figure SCR-15. Diffusion Penetration Distance as a Function of Diffusion Time 253

List of Tables

Table SCR-1. FEPs Summary for CRA 2026 10
Table SCR-2. Summary of cell sizes of microorganisms in WIPP groundwaters..... 79
Table SCR-3. Summary of conditions in microbe-Culebra experiments..... 81
Table SCR-4. Delaware Basin Brine Well Status..... 137
Table SCR-5. MgO Mass Already Placed in WIPP Panels 162
Table SCR-6. Initial Inventory Activity as Represented by EPA Waste Unit Factor 182
Table SCR-7. Potential Reactants in Disposal Area Associated with Waste for CCA-1996, and CRA-2026..... 198
Table SCR-8. Waste Material Mass Already Placed in WIPP Panels[a] 199
Table SCR-9. Temperature Increase from Exothermic Reactions in CCA-1996 and CRA-2026 205
Table SCR-10. Volumes of MgO in Full and Room Segment..... 218
Table SCR-11. WIPP-Relevant G-Values..... 235

Acronyms and Abbreviations

AIC	active institutional controls
API	American Petroleum Institute
Bq	becquerels
°C	degrees centigrade
CAG	Compliance Application Guidance
CCA	Compliance Certification Application
CCDF	complementary cumulative distribution function
CDF	cumulative distribution function
CFR	Code of Federal Regulations
CH-TRAMPAC	Contact-Handled Transuranic Waste Authorized Methods for Payload Control
CH-TRU	contact-handled transuranic
Ci	curie
cm	centimeter
CPR	cellulose, plastic, and rubber
CRA	Compliance Recertification Application
DBDSP	Delaware Basin Drilling Surveillance Program
DFR	driving force ratio
DNA	deoxyribonucleic acid
DOE	U.S. Department of Energy
DP	disturbed performance
DRZ	disturbed rock zone
E	a deep drilling scenario
Eh	reduction-oxidation (redox) potential
EP	event and process
EPA	U.S. Environmental Protection Agency
EPS	extracellular polymeric substances
ERMS	Electronic Record Management System
ERDA	Energy Research and Development Administration Well 6
°F	degrees Fahrenheit

FEP	feature, event, and process
FLAC	Fast Lagrangian Analysis Continua
FSU	Florida State University
ft	foot/feet
ft^2	square foot
ft^3	cubic foot
g	gram
gal	gallon
gpm	gallons per minute
GWB	Generic Weep Brine
H	human-initiated
HCN	historic, current, and near-future
hr	hour
IB	inside boundary
ID	identifier
in.	inch/inches
ka	kilo annum (one thousand years)
K_d	retardation distribution coefficient
kg	kilogram
kg/m^3	kilograms per cubic meter
km	kilometer
km^2	square kilometer
kW	kilowatt
kW/acre	kilowatts per acre
L	liter
lb/gal	pounds per gallon
LET	linear energy transfer
LWA	Land Withdrawal Act
LWB	Land Withdrawal Boundary
m	meter
m^2	square meter

m^3	cubic meter
Ma	million years
Ma BP	million years before present
MB	marker bed
MeV	megaelectron volt
MIS	marine isotope stages
mi	mile
mL	milliliter
M_L	local magnitude
Mm	millimeter
MPa	megapascal
MPI	Mississippi Potash Inc.
mrem/hr	millirem per hour
m/s	meters per second
µm	micrometer
mV	millivolt
N	natural
nCi/g	nanocuries per gram
nm	nanometer
NMOCD	New Mexico Oil Conservation Division
NMT	New Mexico Institute of Mining and Technology
NRC	U.S. Nuclear Regulatory Commission
OB	outside boundary
oz	ounce
PA	performance assessment
PABC	Performance Assessment Baseline Calculation
PAVT	Performance Assessment Verification Test
PCS	panel closure system
pH	negative logarithm of H^+ activity
PIC	passive institutional control
POC	pipe overpack container

ppm	parts per million
psi	pounds per square inch
RH-TRAMPAC	Remote-Handled Transuranic Waste Authorized Methods for Payload Control
RH-TRU	remote-handled transuranic
ROM	run-of-mine
ROS	reactive oxygen species
RPPCR	Replacement Panels Planned Change Request
s	second
SKI	Statens Kärnkraftinspektion
SNL	Sandia National Laboratories
SO-C	screened-out consequence
SO-P	screened-out probability
SO-R	screened-out regulatory
SWD	salt water disposal
t	metric tons
T-field	transmissivity field
TRU	transuranic
TSD	technical support document
US	United States
USGS	U.S. Geological Survey
UP	undisturbed performance
V	volt
W	waste and repository-induced
W	watt
W/drum	watts per drum
W/g	watts per gram
WIPP	Waste Isolation Pilot Plant
WUF	Waste Unit Factor
yr	year
yrs	years

Elements and Chemical Compounds

Al	aluminum
Am	americium
An	actinide
CH_4	methane
CO_2	carbon dioxide
Cs	cesium
EDTA	ethylenediaminetetraacetate
Fe	iron
MgO	magnesium oxide
Np	neptunium
Pm	promethium
Pu	plutonium
Rn	radon
Sr	strontium
Th	thorium
U	uranium

SCR-1.0 INTRODUCTION

The U.S. Department of Energy (DOE) has developed the Waste Isolation Pilot Plant (WIPP) in southeastern New Mexico for the disposal of transuranic (TRU) wastes generated by defense programs. In May of 1998, the U.S. Environmental Protection Agency (EPA) certified that the WIPP would meet the disposal standards (U.S. EPA 1998a, p. 27405) established in 40 Code of Federal Regulations (CFR) Part 191 Subparts B and C (U.S. EPA 1993), thereby allowing the WIPP to begin waste disposal operations. To a significant degree, this certification was based on performance assessment (PA) calculations that were included in the DOE's Compliance Certification Application (CCA) (U.S. DOE 1996a). These calculations demonstrate that cumulative radionuclide releases to the accessible environment will not exceed the levels allowed by the EPA standard.

The WIPP Land Withdrawal Act (LWA) (U.S. Congress 1992) requires the WIPP to demonstrate continued compliance with the disposal standards every five years (yrs.). This demonstration of continued compliance is documented in a Compliance Recertification Application (CRA) prepared and submitted by DOE to EPA for their approval. The EPA's approval of this application is formally called "Recertification," and allows WIPP to continue waste disposal activities until the next CRA has been prepared, submitted, and presumably approved. This regulatory cycle has been successfully executed by the DOE and EPA since the start of waste disposal operations at WIPP (March 26, 1999). These regulatory submittals are documented in the 2004 Compliance Recertification Application (CRA-2004) (U.S. DOE 2004), the CRA-2009 (U.S. DOE 2009), the CRA-2014 (U.S. DOE 2014), and the CRA-2019 (U.S. DOE 2019a), and EPA's respective regulatory actions are documented in U.S. EPA (2006), U.S. EPA (2010), U.S. EPA (2017a), and U.S. EPA (2022e). Currently, and in compliance with the requirements for periodic recertification, the DOE has prepared this CRA-2026, which documents changes since the CRA-2019 and demonstrates continued compliance with the long-term disposal requirements of 40 CFR 191 and the compliance criteria of 40 CFR 194.

The purpose of this Appendix is to present the WIPP features, events, and processes (FEPs) and their descriptions, screening arguments, and decisions in their most up-to-date and current form. Section 194.32, Scope of Performance Assessments, directs that PAs consider both natural and human-initiated FEPs that exist and/or may occur and affect the disposal system during the regulatory time frame. Therefore, compliance applications must include information that identifies all potential FEPs that may affect the disposal system, and document the screening process used to determine whether these FEPs are included or excluded from PA calculations.

For the WIPP CCA, a systematic process was used to identify, compile, analyze, screen, and document FEPs for use in PA. This FEP selection process for the WIPP is described in detail in the CCA, Chapter 6.0, Section 6.2, and Appendix SCR (U.S. DOE 1996a). Because Section 8(f)(2) of the WIPP LWA does not allow recertification applications to undergo rulemaking, significant changes to the WIPP compliance basis may not be introduced within the recertification process. Because of this regulatory constraint, as well as those imposed by 40 CFR 194.4(b)(3), changes

to the PA (and FEPs) baseline must be carefully evaluated and managed any time changes are desired, introduced, or imposed. Accordingly, the FEPs baseline is systematically managed in accordance with Project Specific Procedure 9-4, *Performing FEPs Baseline Impact Assessment for Planned or Unplanned Changes* (Kirkes 2024).

In response to EPA comments on the CRA-2019 (U.S. EPA 2022d), a broad reassessment of FEPs was conducted (Kirkes and McCormick 2023). Since the update of Kirkes and McCormick (2023), more recent activities such as the Replacement Panels Planned Change Request (RPPCR) (U.S. DOE 2024a) and annual inventory updates have prompted additional minor updates to the FEPs baseline. Therefore, this Appendix SCR-2026 presents the FEPs baseline in its most current form.

SCR-2.0 BASIS FOR FEPS SCREENING PROCESS

SCR-2.1 Requirement for FEPs

The origin of FEPs is related to the EPA's requirement, under radioactive waste disposal standards (40 CFR part 191), to use PA methodology. The DOE was required to demonstrate that the WIPP complied with the containment requirements of 40 CFR 191.13 (U.S. EPA 1993). These requirements state that the DOE must use PA to demonstrate that radionuclide releases from the disposal system during the 10,000 yrs following closure will fall below specified limits. The PA analyses supporting this determination must be quantitative. They must consider uncertainties caused by all significant processes and events that may affect the disposal system, including inadvertent human intrusion after closure. The scope of PA is further defined by the EPA at 40 CFR 194.32 (U.S. EPA 1996a), which states,

> Any compliance application(s) shall include information which:
>
> (1) Identifies all potential processes, events, or sequences and combinations of processes and events that may occur during the regulatory time frame and may affect the disposal system;
>
> (2) Identifies the processes, events, or sequences and combinations of processes and events included in performance assessments; and
>
> (3) Documents why any processes, events or sequences and combinations of processes and events identified pursuant to paragraph (e)(1) of this section were not included in performance assessment results provided in any compliance application.

Therefore, the PA methodology includes a process that compiles a comprehensive list of FEPs potentially relevant to disposal system performance. Those FEPs identified by screening analysis as potentially affecting performance are represented in scenarios and quantitative calculations using a system of linked computer models to describe the interaction between the repository and the natural system, both with and without human intrusion. For the CCA, the DOE first compiled a comprehensive list of potentially relevant FEPs, which was then screened,

leading to the set of FEPs used in PA to demonstrate the WIPP's compliance with the long-term disposal standards.

SCR-2.2 FEPs List Development for the CCA

The steps taken in the CCA to identify the FEPs list for the WIPP was included in the CRA-2019 (U.S. DOE 2019a). These steps resulted in a list of WIPP-relevant FEPs retained for further consideration in the first certification PA. These FEPs were screened to determine which would be included in the PA models and scenarios for the CCA PA. As mentioned in Section SCR-1.0, the FEPs baseline is managed by procedure to be systematically reviewed and updated prior to each recertification application. As a result of this process, the CRA-2004 included 235 WIPP FEPs, and the CRA-2009, CRA-2014, CRA-2019, and the CRA-2026 include 245 WIPP FEPs. These evaluations are documented in Wagner et al. (2003), Kirkes (2008), Kirkes (2013), Kirkes (2019a), and McCormick and Kirkes (2025) respectively.

SCR-2.3 Criteria for Screening of FEPs and Categorization of Retained FEPs

The purpose of FEP screening is to identify those FEPs that should be accounted for in PA, and those FEPs that need not be considered further. The DOE's process of removing FEPs from consideration in PA calculations involved the structured application of explicit screening criteria. The criteria used to screen out FEPs are explicit regulatory exclusion (SO-R), probability (SO-P), and consequence (SO-C). All three criteria are derived from regulatory requirements. FEPs not screened out as SO-R, SO-P, or SO-C were retained for inclusion in PA calculations in the undisturbed performance (UP) and disturbed performance (DP) scenarios.

SCR-2.3.1 Regulation (SO-R)

Specific FEP screening criteria are stated in 40 CFR 191 and 40 CFR 194. Such screening criteria relating to the applicability of particular FEPs represent screening decisions made by the EPA. That is, in the process of developing and demonstrating the feasibility of the 40 CFR 191 standard and the 40 CFR 194 criteria, the EPA considered and made conclusions on the relevance, consequence, and probability of particular FEPs occurring. In so doing, it allowed some FEPs to be eliminated from consideration.

SCR-2.3.2 Probability of Occurrence of a FEP Leading to Significant Release of Radionuclides (SO-P)

Low-probability events can be excluded on the basis of the criterion provided in 40 CFR 194.32(d), which states, "performance assessments need not consider processes and events that have less than one chance in 10,000 of occurring over 10,000 years." In practice, for most FEPs screened out on the basis of low probability of occurrence, it has not been possible to estimate a meaningful quantitative probability. In the absence of quantitative probability estimates, a qualitative argument was used.

SCR-2.3.3 Potential Consequences Associated with the Occurrence of the FEPs (SO-C)

The DOE recognizes two uses for this criterion:

1. FEPs can be eliminated from PA calculations on the basis of insignificant consequence. Consequence can refer to effects on the repository or site or to radiological consequence. In particular, 40 CFR 194.34(a) (U.S. EPA 1996a) states, "The results of performance assessments shall be assembled into 'complementary, cumulative distribution functions' (CCDFs) that represent the probability of exceeding various levels of cumulative release caused by all significant processes and events." The DOE has omitted events and processes (EPs) from PA calculations where there is a reasonable expectation that the remaining probability distribution of cumulative releases would not be significantly changed by such omissions.

2. FEPs that are potentially beneficial to subsystem performance may be eliminated from PA calculations if necessary to simplify the analysis. This argument may be used when there is uncertainty as to exactly how the FEP should be incorporated into assessment calculations or when incorporation would incur unreasonable difficulties.

In some cases, the effects of the particular event or process occurring, although not necessarily insignificant, can be shown to lie within the range of uncertainty of another FEP already accounted for in the PA calculations. In such cases, the event or process may be included in PA calculations implicitly, within the range of uncertainty associated with the included FEP.

Although some FEPs could be eliminated from PA calculations on the basis of more than one criterion, the most practical screening criterion was used for classification. In particular, a regulatory screening classification was used in preference to a probability or consequence screening classification. FEPs that have not been screened out based on any of the three criteria were included in the PA.

SCR-2.3.4 UP FEPs

FEPs classified as UP are accounted for in calculations of UP of the disposal system. UP is defined in 40 CFR 191.12 (U.S. EPA 1993) as "the predicted behavior of a disposal system, including consideration of the uncertainties in predicted behavior, if the disposal system is not disrupted by human intrusion or the occurrence of unlikely natural events." The UP FEPs are accounted for in the PA calculations to evaluate compliance with the containment requirements in 40 CFR 191.13. PA Calculations for the UP scenario are also used to demonstrate compliance with the individual and groundwater protection requirements of 40 CFR 191.15 (U.S. EPA 1993) and 40 CFR 191 Subpart C, respectively.

SCR-2.3.5 DP FEPs

The FEPs classified as DP are accounted for only in assessment calculations for the DP scenario. The DP FEPs that remain following the screening process relate to the potential disruptive effects of future drilling and mining events in the controlled area. Consideration of both DP and UP FEPs is required to evaluate compliance with 40 CFR 191.13.

SCR-2.4 FEPs Categories and Timeframes

In the following sections, FEPs are discussed under the categories Natural FEPs, Human-Induced EPs, and Waste- and Repository-Induced FEPs. Identifiers (IDs) of Natural FEPs begin with "N," IDs of Human-Induced EPs begin with "H," and IDs of Waste- and Repository-Induced FEPs begin with "W." The FEPs are also considered within time frames during which they may occur. Because of the regulatory requirements concerning human activities, two time periods were used when evaluating human-induced EPs. These time frames were defined as Historical, Current, and Near-Future Human Activities (HCN) and Future Human Activities (Future). These time frames are also discussed in Section SCR-2.4.2.

SCR-2.4.1 Description of Natural FEPs

Natural FEPs are those that relate to hydrologic, geologic, and climate conditions that have the potential to affect long-term performance of the WIPP disposal system over the regulatory time frame. These FEPs do not include the impacts of other human-related activities such as the effect of boreholes on FEPs related to natural changes in groundwater chemistry. Only natural FEPs are included in the screening process.

Consistent with 40 CFR 194.32(d), the DOE has screened out several natural FEPs from PA calculations on the basis of a low probability of occurrence at or near the WIPP site. In particular, natural events for which there is no evidence indicating that they have occurred within the Delaware Basin have been screened out on this basis. For FEPs analysis, the probabilities of occurrence of these events are assumed to be zero. Quantitative, nonzero probabilities for such events, based on numbers of occurrences, cannot be ascribed without considering regions much larger than the Delaware Basin, thus neglecting established geological understanding of the FEPs that occur within particular geographical provinces.

In considering the overall geological setting of the Delaware Basin, the DOE has eliminated many FEPs from PA calculations on the basis of low consequence. FEPs that have had little effect on the characteristics of the region in the past are expected to be of low consequence for the regulatory time period.

SCR-2.4.2 Description of Human-Induced EPs

Human-induced EPs (Human EPs) are those associated with human activities in the past, present, and future. The EPA provided guidance in their regulations concerning which human

activities are to be considered, their severity, and the manner in which to include them in the future predictions.

The scope of PAs is clarified with respect to human-induced EPs in 40 CFR 194.32. In 40 CFR 194.32(a), the EPA states,

> Performance assessments shall consider natural processes and events, mining, deep drilling, and shallow drilling that may affect the disposal system during the regulatory time frame.

Thus, PAs must include consideration of human-induced EPs relating to mining and drilling activities that might take place during the regulatory time frame. In particular, PAs must consider the potential effects of such activities that might take place within the controlled area[a] at a time when institutional controls cannot be assumed to completely eliminate the possibility of human intrusion.

Further criteria concerning the scope of PAs are provided at 40 CFR 194.32(c):

> Performance assessments shall include an analysis of the effects on the disposal system of any activities that occur in the vicinity of the disposal system prior to disposal and are expected to occur in the vicinity of the disposal system soon after disposal. Such activities shall include, but shall not be limited to, existing boreholes and the development of any existing leases that can be reasonably expected to be developed in the near future, including boreholes and leases that may be used for fluid injection activities.

In order to implement the criteria in 40 CFR 194.32 relating to the scope of PAs, the DOE has divided human activities into three categories: (1) human activities currently taking place and those that took place prior to the time of the compliance application, (2) human activities that might be initiated in the near future after submission of the compliance application, and (3) human activities that might be initiated after repository closure. The first two categories of EPs, corresponding to the HCN time frame, are considered under UP, and EPs in the third category, which belong to the Future time frame, may lead to DP conditions. A description of these three categories follows.

1. Historical and current human activities include resource-extraction activities that have historically taken place and are currently taking place outside the controlled area. These activities are of potential significance insofar as they could affect the geological, hydrological, or geochemical characteristics of the disposal system or groundwater flow pathways outside the disposal system. Current human activities taking place within the controlled area are essentially those associated with development of the WIPP repository. Historic human activities include existing boreholes.

2. Near-future human activities include resource-extraction activities that may be expected to occur outside the controlled area based on existing plans and leases. Thus, the near future includes the expected lives of existing mines and oil and gas fields, and the expected lives of new mines and oil and gas fields that the DOE expects will be developed based on existing

[a] For the purposes of this document, the *controlled area* is assumed to be the area within the WIPP LWA boundary.

plans and leases. These activities are of potential significance insofar as they could affect the geological, hydrological, or geochemical characteristics of the disposal system or groundwater flow pathways outside the disposal system. The only human activities expected to occur within the controlled area in the near future are those associated with development of the WIPP repository. The DOE expects that any activity initiated in the near future, based on existing plans and leases, will be initiated prior to repository closure. Activities initiated prior to repository closure are assumed to continue until their completion.

3. Future human activities include activities that might be initiated within or outside the controlled area after repository closure. This includes drilling and mining for resources within the disposal system at a time when institutional controls cannot be assumed to completely eliminate the possibility of such activities. Future human activities could influence the transport of contaminants within and outside the disposal system by directly removing waste from the disposal system or altering the geological, hydrological, or geochemical characteristics of the disposal system.

SCR-2.4.2.1 Scope of Future Human Activities in PA

PAs must consider the effects of future human activities on the performance of the disposal system. The EPA has provided criteria relating to future human activities in 40 CFR 194.32(a), which limits the scope of consideration of future human activities in PAs to mining and drilling.

SCR-2.4.2.1.1 Criteria Concerning Future Mining

The EPA provides the following additional criteria concerning the type of future mining that should be considered by the DOE in 40 CFR 194.32(b):

> Assessments of mining effects may be limited to changes in the hydraulic conductivity of the hydrogeologic units of the disposal system from excavation mining for natural resources. Mining shall be assumed to occur with a one in 100 probability in each century of the regulatory time frame. Performance assessments shall assume that mineral deposits of those resources, similar in quality and type to those resources currently extracted from the Delaware Basin, will be completely removed from the controlled area during the century in which such mining is randomly calculated to occur. Complete removal of such mineral resources shall be assumed to occur only once during the regulatory time frame.

Thus, consideration of future mining may be limited to mining within the controlled area at the locations of resources that are similar in quality and type to those currently extracted from the Delaware Basin. Potash is the only resource that has been identified within the controlled area in quality similar to that currently mined from underground deposits elsewhere in the Delaware Basin. The hydrogeological impacts of future potash mining within the controlled area are accounted for in calculations of the DP of the disposal system. Consistent with 40 CFR 194.32(b), all economically recoverable resources in the vicinity of the disposal system (outside the controlled area) are assumed to be extracted in the near future.

SCR-2.4.2.1.2 Criteria Concerning Future Drilling

With respect to consideration of future drilling, in the preamble to 40 CFR 194, the EPA:

> …reasoned that while the resources drilled for today may not be the same as those drilled for in the future, the present rates at which these boreholes are drilled can nonetheless provide an estimate of the future rate at which boreholes will be drilled.

Criteria concerning the consideration of future deep and shallow drilling in PAs are provided in 40 CFR 194.33 (U.S. EPA 1996a). The EPA also provides a criterion in 40 CFR 194.33(d) concerning the use of future boreholes subsequent to drilling:

> With respect to future drilling events, performance assessments need not analyze the effects of techniques used for resource recovery subsequent to the drilling of the borehole.

Thus, PAs need not consider the effects of techniques used for resource extraction and recovery that would occur subsequent to the drilling of a borehole in the future. These activities are screened SO-R.

The EPA provides an additional criterion that limits the severity of human intrusion scenarios that must be considered in PAs. In 40 CFR 194.33(b)(1) the EPA states,

> Inadvertent and intermittent intrusion by drilling for resources (other than those resources provided by the waste in the disposal system or engineered barriers designed to isolate such waste) is the most severe human intrusion scenario.

SCR-2.4.2.1.3 Screening of Future Human EPs

Future Human EPs accounted for in PA for the WIPP are those associated with mining and deep drilling within the controlled area at a time when institutional controls cannot be assumed to completely eliminate the possibility of such activities. All other future Human EPs, if not eliminated from PA calculations based on regulation, have been eliminated based on low consequence or low probability. For example, the effects of future shallow drilling within the controlled area were eliminated from CCA PA calculations on the basis of low consequence to the performance of the disposal system.

SCR-2.4.3 Description of Waste- and Repository-Induced FEPs

The waste- and repository-induced FEPs are those that relate specifically to the waste material, waste containers, shaft seals, magnesium oxide (MgO) backfill, panel closure system (PCS), repository structures, and investigation boreholes. All FEPs related to radionuclide chemistry and radionuclide migration are included in this category. The FEPs related to radionuclide transport resulting from future borehole intersections of the WIPP excavation are defined as waste- and repository-induced FEPs.

SCR-3.0 FEPs

The presentation, evaluation and screening of the FEPs in this Appendix result in a new FEPs baseline for CRA-2026. The reassessment of FEPs and evaluation of new data and information since the CRA-2019 has resulted in the update of 151 of the 245 WIPP FEPs, and 94 WIPP FEPs remain unchanged. Five FEPs have had their screening decisions changed, although none of these changes result in additional FEPs being screened into PA calculations. A summary of these five changes follows:

FEP N71 “Microbes” was changed to remove the reference to “UP-for colloidal effects and gas generation”. The screening decision for N71 has been changed to focus only on naturally-occurring microbes, which is SO-C. Colloidal effects and gas generation due to microbial degradation are no longer mentioned in FEP N71 and are solely discussed in FEP W44, “Degradation of Organic Material.”

FEP W8 “Shaft Seal Chemical Composition” was changed from “SO-C Beneficial” to simply “SO-C” (losing the “beneficial” indication) due to the lack of a clear and defensible beneficial consequence. The limited movement of brine in contact with the lower shaft seal components and the resulting minimal impact on pH are not assumed to provide any benefit.

FEP W59 “Precipitation of Secondary Minerals” was also changed from “SO-C Beneficial” to “SO-C.” FEP W59 is not impactful to the concentrations of radionuclides and does not provide a clear beneficial consequence to the performance of the disposal system.

FEP W82 “Suspension of Particles” was changed from DP to screened-out due to SO-C. The change in this classification eliminates inconsistencies within the FEPs baseline. This designation is consistent with the CCA (DOE 1996a), and properly emphasizes dissolved and colloidal actinides as currently implemented in PA.

FEP W111 “Panel Closure Chemical Composition” was changed from “SO-C Beneficial” to “SO-C.” FEP W111 does not provide a clear beneficial consequence to the performance of the disposal system.

Table SCR-1 outlines updates to the FEPs baseline since the CRA-2019, and subsequent sections of this document present the actual screening decisions and supporting arguments. Those FEPs not separated by gridlines in the first column of Table SCR-1 have been addressed by group because of close similarity with other FEPs within that group.

Finally, a new feature of this Appendix SCR-2026 is the addition of a brief implementation summary for those FEPs that are retained for inclusion in PA (either screened as UP or DP). This feature is meant to clarify how screened-in FEPs are accounted for in PA scenarios, whether through parameterization, assumptions, regulatory mandates, or other methods.

Table SCR-1. FEPs Summary for CRA 2026

EPA FEP I.D.[a,b,c, d]	FEP Name	Screening Argument Update?	Screening Decision Changed?	Screening Classification
N1	Stratigraphy	New references to stratigraphic data obtained during drilling of Shaft 5	No	UP
N2	Brine Reservoirs	Updated with new references	No	DP
N3	Changes in Regional Stress	Updated with new references and information	No	SO-C
N4	Regional Tectonics	Updated with new references and information	No	SO-C
N5	Regional Uplift and Subsidence	Updated with new references and information	No	SO-C
N6	Salt Deformation	Updated with new references	No	SO-P
N7	Diapirism	Updated with new references	No	SO-P
N8	Formation of Fractures	Updated with new references	No	SO-P (Far-field) UP (Repository)
N9	Changes in Fracture Properties	Updated with new references	No	SO-C UP (Near Repository)
N10	Formation of New Faults	Updated with new references	No	SO-P
N11	Fault Movement	Updated with new references	No	SO-P
N12	Seismic Activity	Updated with new references	No	UP
N13	Volcanic Activity	No change	No	SO-P
N14	Magmatic Activity	No change	No	SO-C
N15	Metamorphic Activity	No change	No	SO-P
N16	Shallow Dissolution	Updated with new references and information	No	UP
N18	Deep Dissolution	Updated with new references	No	SO-P
N20	Breccia Pipes	Updated with new references	No	SO-P

EPA FEP I.D.[a,b,c, d]	FEP Name	Screening Argument Update?	Screening Decision Changed?	Screening Classification
N21	Collapse Breccias	Updated with new references	No	SO-P
N22	Fracture Infills	Updated with new references	No	SO-C - Beneficial
N23	Saturated Groundwater Flow	No change	No	UP
N24	Unsaturated Groundwater Flow	No change	No	UP
N25	Fracture Flow	No change	No	UP
N27	Effects of Preferential Pathways	No change	No	UP
N26	Density Effects on Groundwater Flow	Updated to discuss new geometry	No	SO-C – Beneficial
N28	Thermal Effects on Groundwater Flow	Updated with new references	No	SO-C
N29	Saline Intrusion (Hydrogeological Effects)	No change	No	SO-P
N30	Freshwater Intrusion (Hydrogeological Effects)	Updated with new references	No	SO-P
N31	Hydrological Response to Earthquakes	Updated with new references and information	No	SO-C
N32	Natural Gas Intrusion	Updated with new references and information	No	SO-P
N33	Groundwater Geochemistry	Updated with new references	No	UP
N34	Saline Intrusion (Geochemical Effects)	Updated with new references	No	SO-C
N38	Effects of Dissolution	Updated with new references	No	SO-C
N35	Freshwater Intrusion (Geochemical Effects)	FEP text updated with new information	No	SO-C
N36	Changes in Groundwater Eh	FEP text updated with new information	No	SO-C
N37	Changes in Groundwater pH	FEP text updated with new information	No	SO-C
N39	Physiography	No change	No	UP
N40	Impact of a Large Meteorite	No change	No	SO-P

EPA FEP I.D.[a,b,c, d]	FEP Name	Screening Argument Update?	Screening Decision Changed?	Screening Classification
N41	Mechanical Weathering	No change	No	SO-C
N42	Chemical Weathering	No change	No	SO-C
N43	Aeolian Erosion	FEP text updated with new information	No	SO-C
N44	Fluvial Erosion	FEP text updated with new information	No	SO-C
N45	Mass Wasting (Erosion)	FEP text updated with new information	No	SO-C
N46	Aeolian Deposition	No change	No	SO-C
N47	Fluvial Deposition	No change	No	SO-C
N48	Lacustrine Deposition	No change	No	SO-C
N49	Mass Wasting (Deposition)	No change	No	SO-C
N50	Soil Development	Updated with new references	No	SO-C
N51	Stream and River Flow	No change	No	SO-C
N52	Surface Water Bodies	No change	No	SO-C
N53	Groundwater Discharge	Updated with new information	No	UP
N54	Groundwater Recharge	Updated with new information	No	UP
N55	Infiltration	Updated with new information	No	UP
N56	Changes in Groundwater Recharge and Discharge	Updated with new references and information	No	UP
N57	Lake Formation	No change	No	SO-C
N58	River Flooding	No change	No	SO-C
N59	Precipitation (e.g., Rainfall)	Updated with new references and climate data	No	UP
N60	Temperature	Updated with new references and climate data	No	UP
N61	Climate Change	No change	No	UP
N62	Glaciation	No change	No	SO-P
N63	Permafrost	No change	No	SO-P
N64	Seas and Oceans	No change	No	SO-C

EPA FEP I.D.[a,b,c, d]	FEP Name	Screening Argument Update?	Screening Decision Changed?	Screening Classification
N65	Estuaries	No change	No	SO-C
N66	Coastal Erosion	No change	No	SO-C
N67	Marine Sediment Transport and Deposition	No change	No	SO-C
N68	Sea Level Changes	No change	No	SO-C
N69	Plants	No change	No	SO-C
N70	Animals	No change	No	SO-C
N71	Microbes	FEP text updated with new information that states this FEP only applies to naturally-occurring microbes	Yes	SO-C
N72	Natural Ecological Development	No change	No	SO-C
H1	Oil and Gas Exploration	Updated with new drilling rate and references	No	SO-C (HCN) DP (Future)
H2	Potash Exploration	FEP text updated with new information	No	SO-C (HCN) DP (Future)
H4	Oil and Gas Exploitation	Updated with new drilling rate and references	No	SO-C (HCN) DP (Future)
H8	Other Resources	FEP text updated with new information	No	SO-C (HCN) DP (Future)
H9	Enhanced Oil and Gas Recovery	FEP text updated with new information	No	SO-C (HCN) DP (Future)
H3	Water Resources Exploration	Updated with the most recent monitoring information	No	SO-C (HCN) SO-C (Future)
H5	Groundwater Exploitation	Updated with the most recent monitoring information	No	SO-C (HCN) SO-C (Future)
H6	Archaeological Investigations	No change	No	SO-R (HCN) SO-R (Future)
H7	Geothermal Energy Production	No change	No	SO-R (HCN) SO-R (Future)

EPA FEP I.D.[a,b,c, d]	FEP Name	Screening Argument Update?	Screening Decision Changed?	Screening Classification
H10	Liquid Waste Disposal	No change	No	SO-R (HCN) SO-R (Future)
H11	Hydrocarbon Storage	No change	No	SO-R (HCN) SO-R (Future)
H12	Deliberate Drilling Intrusion	No change	No	SO-R (HCN) SO-R (Future)
H13	Conventional Underground Potash Mining	No change	No	UP (HCN) DP (Future)
H14	Other Resources (Mining For)	No change	No	SO-C (HCN) SO-R (Future)
H15	Tunneling	No change	No	SO-R (HCN) SO-R (Future)
H16	Construction of Underground Facilities (e.g., Storage, Disposal, Accommodation)	No change	No	SO-R (HCN) SO-R (Future)
H17	Archaeological Excavations	No change	No	SO-C (HCN) SO-R (Future)
H18	Deliberate Mining Intrusion	No change	No	SO-R (HCN) SO-R (Future)
H19	Explosions for Resource Recovery	No change	No	SO-C (HCN) SO-R (Future)
H20	Underground Nuclear Device Testing	Updated for clarity. No new information.	No	SO-C (HCN) SO-R (Future)
H21	Drilling Fluid Flow	Updated to screen H21, H22, and H23 together	No	SO-C (HCN) DP (Future)
H22	Drilling Fluid Loss	Updated to screen H21, H22, and H23 together	No	SO-C (HCN) DP (Future)
H23	Blowouts	Updated to screen H21, H22, and H23 together	No	SO-C (HCN) DP (Future)
H24	Drilling-Induced Geochemical Changes	Updated for clarity	No	UP (HCN) DP (Future)
H25	Oil and Gas Extraction	FEP text updated with new information	No	SO-C (HCN) SO-R (Future)
H26	Groundwater Extraction	Updated with new references	No	SO-C (HCN) SO-R (Future)
H27	Liquid Waste Disposal–Outside Boundary (OB)	Updated with new references	No	SO-C (HCN) SO-C (Future)

EPA FEP I.D.[a,b,c, d]	FEP Name	Screening Argument Update?	Screening Decision Changed?	Screening Classification
H28	Enhanced Oil and Gas Production–OB	Updated with new references	No	SO-C (HCN) SO-C (Future)
H29	Hydrocarbon Storage–OB	No change	No	SO-C (HCN) SO-C (Future)
H60	Liquid Waste Disposal–Inside Boundary (IB)	No change	No	SO-R (HCN) SO-R (Future)
H61	Enhanced Oil and Gas Production–IB	No change	No	SO-R (HCN) SO-R (Future)
H62	Hydrocarbon Storage–IB	No change	No	SO-R (HCN) SO-R (Future)
H30	Fluid-Injection Induced Geochemical Changes	No change	No	UP (HCN) SO-R (Future)
H31	Natural Borehole Fluid Flow	Updated to reflect new plugging probabilities	No	SO-C (HCN) SO-C (Future, holes not penetrating waste panels) DP (Future, holes penetrating panels)
H32	Waste-Induced Borehole Flow	Updated to reflect new plugging probabilities	No	SO-R (HCN) DP (Future)
H34	Borehole-Induced Solution and Subsidence	Updated with new references and information	No	SO-C (HCN) SO-C (Future)
H35	Borehole-Induced Mineralization	Updated with new references and information	No	SO-C (HCN) SO-C (Future)
H36	Borehole-Induced Geochemical Changes	Updated to reflect new plugging probabilities	No	UP (HCN) DP (Future) SO-C – Beneficial (for units other than the Culebra)
H37	Changes in Groundwater Flow Due to Mining	Updated with new references and mining leases	No	UP (HCN) DP (Future)
H38	Changes in Geochemistry Due to Mining	Argument edited for clarity	No	SO-C (HCN) SO-R (Future)
H39	Changes in Groundwater Flow Due to Explosions	No change	No	SO-C (HCN) SO-R (Future)
H40	Land Use Changes	FEP text updated with new information	No	SO-R (HCN) SO-R (Future)

EPA FEP I.D.[a,b,c, d]	FEP Name	Screening Argument Update?	Screening Decision Changed?	Screening Classification
H41	Surface Disruptions	FEP text updated with new information	No	UP (HCN) SO-C (Future)
H42	Damming of Streams and Rivers	No change	No	SO-C (HCN) SO-R (Future)
H43	Reservoirs	No change	No	SO-C (HCN) SO-R (Future)
H44	Irrigation	No change	No	SO-C (HCN) SO-R (Future)
H45	Lake Usage	No change	No	SO-R (HCN) SO-R (Future)
H46	Altered Soil or Surface Water Chemistry by Human Activities	No change	No	SO-C (HCN) SO-R (Future)
H47	Greenhouse Gas Effects	No change	No	SO-R (HCN) SO-R (Future)
H48	Acid Rain	No change	No	SO-R (HCN) SO-R (Future)
H49	Damage to the Ozone Layer	No change	No	SO-R (HCN) SO-R (Future)
H50	Coastal Water Use	No change	No	SO-R (HCN) SO-R (Future)
H51	Sea Water Use	No change	No	SO-R (HCN) SO-R (Future)
H52	Estuarine Water Use	No change	No	SO-R (HCN) SO-R (Future)
H53	Arable Farming	No change	No	SO-C (HCN) SO-R (Future)
H54	Ranching	No change	No	SO-C (HCN) SO-R (Future)
H55	Fish Farming	No change	No	SO-R (HCN) SO-R (Future)
H56	Demographic Change and Urban Development	No change	No	SO-R (HCN) SO-R (Future)
H57	Loss of Records	No change	No	NA (HCN) DP (Future)
H58	Solution Mining for Potash	No change	No	SO-R (HCN) SO-R (Future)
H59	Solution Mining for Other Resources	Updated with new information regarding brine wells in the region	No	SO-C (HCN) SO-C (Future)

EPA FEP I.D.[a,b,c, d]	FEP Name	Screening Argument Update?	Screening Decision Changed?	Screening Classification
W1	Disposal Geometry	Updated with additional and replacement panel information.	No	UP
W2	Waste Inventory	Updated with new inventory data	No	UP
W3	Heterogeneity of Waste Forms	Updated with new inventory data	No	DP
W4	Container Form	Updated with new container material masses	No	SO-C – Beneficial
W34	Container Integrity	Updated to screen W4 and W34 together	No	SO-C – Beneficial
W5	Container Material Inventory	Updated to reflect new inventory data and container variants.	No	UP
W6	Shaft Seal Geometry	FEP text updated with new information	No	UP
W7	Shaft Seal Physical Properties	FEP text updated with new information	No	UP
W109	Panel Closure Geometry	FEP text updated with new information	No	UP
W110	Panel Closure Physical Properties	FEP text updated with new information	No	UP
W8	Shaft Seal Chemical Composition	Screened separately from W111	Yes	SO-C
W9	Backfill Physical Properties	FEP text updated with new information	No	SO-C
W10	Backfill Chemical Composition	No change	No	UP
W11	Post-Closure Monitoring	No change	No	SO-C
W12	Radionuclide Decay and In-Growth	No change	No	UP
W13	Heat from Radioactive Decay	FEP text updated with new information	No	SO-C

EPA FEP I.D.[a,b,c, d]	FEP Name	Screening Argument Update?	Screening Decision Changed?	Screening Classification
W14	Nuclear Criticality: Heat	FEP text updated with new information.	No	SO-P
W15	Radiological Effects on Waste	Updated to reflect the new radionuclide inventory	No	SO-C
W16	Radiological Effects on Containers	Updated to reflect the new radionuclide inventory	No	SO-C
W17	Radiological Effects on Shaft Seals	Updated to reflect the new radionuclide inventory	No	SO-C
W112	Radiological Effects on Panel Closures	Updated to reflect the new radionuclide inventory	No	SO-C
W18	Disturbed Rock Zone (DRZ)	Updated with information on new panels	No	UP
W19	Excavation-Induced Changes in Stress	Updated with information on new panels	No	UP
W20	Salt Creep	Updated with new references	No	UP
W21	Changes in the Stress Field	Updated with new references	No	UP
W22	Roof Falls	Updated with information about new panels	No	UP
W23	Subsidence	Updated with new references and information	No	SO-C
W24	Large Scale Rock Fracturing	Updated with new references and information	No	SO-P
W25	Disruption Due to Gas Effects	Updated with information on the mechanical effects of gas generation	No	UP
W26	Pressurization	Updated with information on	No	UP

EPA FEP I.D.[a,b,c, d]	FEP Name	Screening Argument Update?	Screening Decision Changed?	Screening Classification
		mechanical effects of gas generation		
W27	Gas Explosions	FEP text updated with new information	No	UP
W28	Nuclear Explosions	Updated with new references and information	No	SO-P
W29	Thermal Effects on Material Properties	Updated to reflect new inventory information	No	SO-C
W30	Thermally-Induced Stress Changes	Updated to reflect new inventory information	No	SO-C
W31	Differing Thermal Expansion of Repository Components	Updated to reflect new inventory information	No	SO-C
W72	Exothermic Reactions	Updated to reflect new inventory information	No	SO-C
W73	Concrete Hydration	Updated to reflect new inventory information	No	SO-C
W32	Consolidation of Waste	Updated disposal room porosity surface	No	UP
W36	Consolidation of Shaft Seals	No change	No	UP
W37	Mechanical Degradation of Shaft Seals	No change	No	UP
W39	Underground Boreholes	No change	No	UP
W113	Consolidation of Panel Closures	No change	No	UP
W114	Mechanical Degradation of Panel Closures	No change	No	SO-P
W33	Movement of Containers	Updated with new references	No	SO-C
W35	Mechanical Effects of Backfill	Updated with new information and references	No	SO-C
W40	Brine Inflow	Updated with new formulas and references	No	UP

EPA FEP I.D.[a,b,c, d]	FEP Name	Screening Argument Update?	Screening Decision Changed?	Screening Classification
W41	Wicking	Updated with new formulas and references	No	UP
W42	Fluid Flow Due to Gas Production	Updated with new references	No	UP
W43	Convection	Updated with new estimates of heat produced from inventory data	No	SO-C
W44	Degradation of Organic Material	Updated with new information and screened separately from W45 and W48	No	UP
W45	Effects of Temperature on Microbial Gas Generation	Updated with new thermal increase calculations and screened separately from W44	No	UP
W48	Effects of Biofilms on Microbial Gas Generation	Updated with new thermal increase calculations and screened separately from W44	No	UP
W46	Effects of Pressure on Microbial Gas Generation	Updated with new references and information. Modified to more directly discuss the effects of pressure on gas generation	No	SO-C
W47	Effects of Radiation on Microbial Gas Generation	Updated with new information	No	SO-C
W49	Gases from Metal Corrosion	Updated to reflect new inventory information and address EPA comments	No	UP
W51	Chemical Effects of Corrosion	Updated to reflect new inventory information and address EPA comments	No	UP
W50	Galvanic Coupling (Within the Repository)	Updated with information on lead inventory	No	SO-C

EPA FEP I.D.[a,b,c, d]	FEP Name	Screening Argument Update?	Screening Decision Changed?	Screening Classification
W52	Radiolysis of Brine	Updated with new references	No	UP
W53	Radiolysis of Cellulose	Updated with new information and references	No	SO-C
W54	Helium Gas Production	Updated to reflect new inventory	No	SO-C
W55	Radioactive Gases	Updated to reflect new inventory	No	SO-C
W56	Speciation	Updated with new information and references	No	UP in disposal rooms and Culebra. SO-C elsewhere, and SO-C Beneficial in shaft seals
W57	Kinetics of Speciation	No change	No	SO-C
W58	Dissolution of Waste	No change	No	UP
W59	Precipitation of Secondary Minerals	No change	Yes	SO-C
W60	Kinetics of Precipitation and Dissolution	No change	No	SO-C
W61	Actinide Sorption	Updated with new references	No	UP in the Culebra and Dewey Lake; SO-C—Beneficial in the disposal room, shaft seals, panel closures, and other geologic units.
W62	Kinetics of Sorption	Updated with new references	No	UP in the Culebra and Dewey Lake; SO-C—Beneficial in the disposal room, shaft seals, panel closures, and other geologic units.
W63	Changes in Sorptive Surfaces	Updated with new references	No	UP
W64	Effects of Metal Corrosion	No change	No	UP
W66	Reduction-Oxidation Kinetics	No change	No	UP
W65	Reduction-Oxidation Fronts	No change	No	SO-P
W67	Localized Reducing Zones	No change	No	SO-C
W68	Organic Complexation	Updated with new references	No	UP

EPA FEP I.D.[a,b,c, d]	FEP Name	Screening Argument Update?	Screening Decision Changed?	Screening Classification
W69	Organic Ligands	Updated with new references	No	UP
W71	Kinetics of Organic Complexation	Updated with new references	No	SO-C
W70	Humic and Fulvic Acids	No change	No	UP
W74	Chemical Degradation of Shaft Seals	No change to the argument. FEP W115 removed from screening.	No	UP
W76	Microbial Growth on Concrete	No change to the argument. FEP W115 was removed from screening.	No	UP
W75	Chemical Degradation of Backfill	No change	No	SO-C
W77	Solute Transport	Updated for clarity	No	UP
W78	Colloid Transport	Updated with new references	No	UP
W79	Colloid Formation and Stability	Updated with new references	No	UP
W80	Colloid Filtration	Updated with new references	No	UP
W81	Colloid Sorption	Updated with new references	No	UP
W82	Suspension of Particles	Updated with arguments for screening out this FEP	Yes	SO-C
W83	Rinse	No change	No	SO-C
W84	Cuttings	No change	No	DP
W85	Cavings	No change	No	DP
W86	Spallings	No change	No	DP
W87	Microbial Transport	Updated with new references	No	UP
W88	Biofilms	Updated with new references and information	No	SO-C – Beneficial
W89	Transport of Radioactive Gases	Updated with new references and information	No	SO-C

EPA FEP I.D.[a,b,c, d]	FEP Name	Screening Argument Update?	Screening Decision Changed?	Screening Classification
W90	Advection	Updated with new references and information	No	UP
W91	Diffusion	Updated with new information	No	UP
W92	Matrix Diffusion	Updated with new information	No	UP
W93	Soret Effect	Updated with new references and information	No	SO-C
W94	Electrochemical Effects	No change	No	SO-C
W95	Galvanic Coupling (Outside the Repository)	No change	No	SO-P
W96	Electrophoresis	No change	No	SO-C
W97	Chemical Gradients	Updated with new references and information	No	SO-C
W98	Osmotic Processes	No change	No	SO-C
W99	Alpha Recoil	No change	No	SO-C
W100	Enhanced Diffusion	No change	No	SO-C
W101	Plant Uptake	Updated with new references and information	No	SO-R (for section 191.13) SO-C (for section 191.15)
W102	Animal Uptake	Updated with new references and information	No	SO-R (for section 191.13) SO-C (for section 191.15)
W103	Accumulation in Soils	Updated with new references and information	No	SO-C Beneficial (for section 191.13) SO-C (for section 191.15)
W104	Ingestion	Updated with new references and information	No	SO-R SO-C (for section 191.15)
W105	Inhalation	Updated with new references and information	No	SO-R SO-C (for section 191.15)
W106	Irradiation	Updated with new references and information	No	SO-R SO-C (for section 191.15)

EPA FEP I.D.[a,b,c,d]	FEP Name	Screening Argument Update?	Screening Decision Changed?	Screening Classification
W107	Dermal Sorption	Updated with new references and information	No	SO-R SO-C (for section 191.15)
W108	Injection	Updated with new references and information	No	SO-R SO-C (for section 191.15)
W111	Panel Closure Chemical Composition	Screened separately from W8	Yes	SO-C
W115	Chemical Degradation of Panel Closures	Screened separately from W74 and W76	No	SO-P

[a] N = Natural FEP
[b] H = Human-induced event and process (EP)
[c] W = Waste- and Repository-induced FEP
[d] FEPs in this column that are not separated by rows represent FEPs that are similar in nature and are discussed and screened as a common group.

SCR-4.0 SCREENING OF NATURAL FEPS

This section presents the screening arguments and decisions for natural FEPs. Screening of natural FEPs is conducted without human influence. Table SCR-1 provides summary information regarding changes to natural FEPs since the CRA-2019. Seventy (70) natural FEPs are included in the CRA-2026. Of the 70 natural FEPs, 31 remain completely unchanged, and 39 have been updated to include additional information. One screening decision (classification) has been changed to remove reference to a classification discussed in a separate FEP. No additional natural FEPs have been identified.

SCR-4.1 Geological FEPs

SCR-4.1.1 Stratigraphy

SCR-4.1.1.1 **FEP Numbers: N1 and N2**
FEP Titles: Stratigraphy (N1)
Brine Reservoirs (N2)

SCR-4.1.1.1.1 Screening Decision: UP (N1)
DP (N2)

The *Stratigraphy* of the geological formations in the region of the WIPP is accounted for in PA. The presence of *Brine Reservoirs* in the Castile Formation (hereafter referred to as the Castile) is accounted for in PA.

SCR-4.1.1.1.2 Summary of New Information

New stratigraphic data at the WIPP site were acquired by drilling and coring in 2016 and 2017 to support construction of a new utility shaft (Shaft 5) for WIPP (Powers et al., 2018; Powers et al. 2019a,b,c,d). Powers et al. (2018) describe the geology and stratigraphy of corehole C-3977 based on cores and geophysical logs at the location of the new shaft. C-3977 was drilled and cored to a depth of 2,308 feet, approximately 180 ft below the disposal horizon at WIPP. Stratigraphic units were correlated to the air intake shaft, and no anomalous features or stratigraphy were encountered. The other four coreholes examined shallow stratigraphy (maximum depth of 201.5 ft) and were observed for water inflow. The upper Dewey Lake was encountered in each, and the stratigraphy of each borehole was consistent with this location.

The PBRINE parameter distribution is adjusted due to the correction of the error found in the PRELHS code (SNL 2022).

The Delaware Basin Monitoring Annual Report (U.S. DOE 2025) reported no additional Castile pressurized brine reservoir encounters during the reporting period. The total number of reported encounters in the vicinity of WIPP is 40.

SCR-4.1.1.1.3 Screening Argument

The stratigraphy and geology of the region around the WIPP, including the distribution and characteristics of pressurized brine reservoirs in the Castile, are discussed in detail in the CCA, Chapter 2.0, Section 2.1.3. The stratigraphy of the geological formations in the WIPP region is accounted for in PA through the model geometries (Appendix MASS-3.1). The presence of brine reservoirs is accounted for in the treatment of inadvertent drilling (Appendix PA-4.2.10). The hypothesized brine reservoir properties are described in Appendix MASS-16.0.

SCR-4.1.1.1.4 FEP Implementation in PA

Stratigraphy is represented in the following WIPP conceptual models: Disposal System Geometry, Shaft and Shaft Seals, Culebra Hydrogeology, Salado, Impure Halite, Salado Interbeds, Units Above the Salado, Exploration Boreholes, and Castile and Brine Reservoir. Important aspects of *Stratigraphy* as they relate to these conceptual models are implemented primarily by the code BRAGFLO and in the construction of the BRAGLO grid. To a lesser extent, the codes MODFLOW6 and SECOTP2D incorporate various aspects of the stratigraphic column in PA. *Brine Reservoirs* are represented in the "Castile and Brine Reservoir" and "Exploration Boreholes" conceptual models, as implemented in the code BRAGFLO. Key parameters used for *Brine Reservoirs* are GLOBAL:PBRINE, CASTILER:COMP_RCK, CASTILER:PRESSURE, and CASTILER:PRMX_LOG.

SCR-4.1.2 Tectonics

SCR-4.1.2.1 **FEP Numbers: N3, N4, and N5**
FEP Titles: Changes in Regional Stress (N3)
Regional Tectonics (N4)
Regional Uplift and Subsidence (N5)

SCR-4.1.2.1.1 Screening Decision: SO-C

The effects of *Regional Tectonics*, *Regional Uplift and Subsidence*, and *Change in Regional Stress* have been eliminated from PA calculations on the basis of low consequence to the performance of the disposal system.

SCR-4.1.2.1.2 Summary of New Information

This FEP has been updated to reference recent geologic studies. This new information does not affect the screening decision or arguments presented previously.

SCR-4.1.2.1.3 Screening Argument

Regional tectonics encompasses two related issues: the overall level of regional stress and the possibility of significant changes in regional stress.

The tectonic setting and structural features of the area around the WIPP are described in the CCA, Chapter 2.0, Section 2.1.5. In summary, there is no geological evidence for Quaternary regional tectonics in the Delaware Basin. The eastward tilting of the region has been dated as mid-Miocene to Pliocene by King (1948, pp. 120–21) and is associated with the uplift of the Guadalupe Mountains to the west. Fault zones along the eastern margin of the basin, where it flanks the Central Basin Platform, were active during the Late Permian. Evidence for this includes the displacement of the Rustler Formation (hereafter referred to as the Rustler) observed by Holt and Powers (1988, pp. 4–14) and the thinning of the Dewey Lake Redbeds Formation (hereafter referred to as the Dewey Lake) reported by Schiel (1994). There is, however, no surface displacement along the trend of these fault zones, indicating that there has been no significant Quaternary movement. Other faults identified within the evaporite sequence of the Delaware Basin are inferred by Barrows' figures in Borns et al. (1983, pp. 58–60) to be the result of salt deformation rather than regional tectonic processes. According to Muehlberger, Belcher, and Goetz (1978, p. 338), the nearest faults on which Quaternary movement has been identified lie to the west of the Guadalupe Mountains and are of minor regional significance. Hayes and Bachman (1979) re-examined the eastern escarpment of the Guadalupe Mountains and concluded that proposed Barrera and Carlsbad faults (Kelley 1971 and 1972) were misinterpreted surficial features and jointing. The effects of regional tectonics and changes in regional stress have therefore been eliminated from PA calculations on the basis of low consequence to the performance of the disposal system.

There are no reported stress measurements from the Delaware Basin, but a low–level, regional stress regime with low deviatoric stress has been inferred from the geological setting of the area (see the CCA, Chapter 2.0, Section 2.1.5). The inferred low level of regional stress and the lack of Quaternary tectonic activity indicate that regional tectonics and any changes in regional stress will be minor and therefore of low consequence to the performance of the disposal system. Even if rates of regional tectonic movement experienced over the past 10 million yrs continue, the extent of regional uplift and subsidence over the next 10,000 yrs would only be approximately 1 meter (m) (about several ft). This amount of uplift or subsidence would not lead to a breach of the Salado because the salt would deform plastically to accommodate this slow rate of movement. Uniform regional uplift or a small increase in regional dip consistent with this past rate could give rise to downcutting by rivers and streams in the region. The extent of this downcutting would be little more than the extent of uplift and reducing the overburden by 1 or 2 m would have no significant effect on groundwater flow or contaminant transport in units above or below the Salado. Thus, the effects of regional uplift and subsidence have been eliminated from PA calculations on the basis of low consequence to the performance of the disposal system.

SCR-4.1.2.1.3.1 Tectonic Setting and Site Structural Features

The DOE has screened out, on the basis of either probability or consequence or both, all tectonic, magmatic, and structural processes. The screening discussions can be found in the CCA, Appendix SCR (U.S. DOE 1996a). The information needed for this screening is included here and covers (1) regional tectonic processes such as subsidence, uplift, and basin tilting; (2)

magmatic processes such as igneous intrusion and events such as volcanism; and (3) structural processes such as faulting and loading and unloading of the rocks because of long-term sedimentation or erosion. Discussions of structural events, such as earthquakes, are considered to the extent that they may create new faults or activate old faults. The seismicity of the area is considered in the CCA, Chapter 2.0, Section 2.6 for the purposes of determining seismic design parameters for the facility.

SCR-4.1.2.1.3.2 Tectonics

The processes and features included in this section are those more traditionally considered part of tectonics–processes that develop the broad-scale features of the Earth. Salt dissolution is a different process that can develop some features resembling those of tectonics.

Most broad-scale structural elements of the area around the WIPP developed during the Late Paleozoic (see the CCA, Appendix GCR, pp. 3-58 through 3-77). There is little historical or geological evidence of significant tectonic activity in the vicinity, and the level of stress in the region is low. The entire region tilted slightly during the Tertiary, and activity related to Basin and Range tectonics formed major structures southwest of the area. Seismic activity is specifically addressed in a separate section.

Broad subsidence began in the area as early as the Ordovician, developing a sag called the Tobosa Basin. By Late Pennsylvanian to Early Permian time, the Central Basin Platform developed (see the CCA, Chapter 2.0, Figure 2-19), separating the Tobosa Basin into two parts: the Delaware Basin to the west and the Midland Basin to the east. The Permian Basin refers to the collective set of depositional basins in the area during the Permian Period. Southwest of the Delaware Basin, the Diablo Platform began developing either in the Late Pennsylvanian or Early Permian. The Marathon Uplift and Ouachita tectonic belt limited the southern extent of the Delaware Basin.

According to Brokaw et al. (1972, p. 30), pre-Ochoan sedimentary rocks in the Delaware Basin show evidence of gentle downwarping during deposition. Ochoan rocks also show subsidence eastward in the form of thickening and facies changes. A relatively uniform eastward tilt, generally from about 14 to 19 meters per kilometer (m/km) (75 to 100 ft per mile [ft/mi]), has been superimposed on the sedimentary sequence. King (1948, pp. 108 and 121) generally attributes the uplift of the Guadalupe and Delaware mountains along the west side of the Delaware Basin to the later Cenozoic, though he also notes that some faults along the west margin of the Guadalupe Mountains have displaced Quaternary gravels.

King (1948, p. 144) also infers the uplift from the Pliocene-age deposits of the Llano Estacado. Subsequent studies of the Ogallala of the Llano Estacado show that it varies in age from Miocene (about 12 million yrs before present) to Pliocene (Hawley 1993). This is the most likely range for uplift of the Guadalupe Mountains and broad tilting to the east of the Delaware Basin sequence.

Analysis of the present regional stress field indicates that the Delaware Basin lies within the Southern Great Plains stress province. This province is a transition zone between the extensional stress regime to the west and the region of compressive stress to the east. An interpretation by Zoback and Zoback (1991, p. 350) of the available data indicates that the level of stress in the Southern Great Plains stress province is low. Changes to the tectonic setting, such as the development of subduction zones and a consequent change in the driving forces, would take much longer than 10,000 yrs to occur.

To the west of the Southern Great Plains province is the Basin and Range province, or Cordilleran Extension province, where according to Zoback and Zoback (1991, pp. 348–51) normal faulting is the characteristic style of deformation. The eastern boundary of the Basin and Range province is marked by the Rio Grande Rift. Sanford, Jakasha, and Cash (1991, p. 230) note that, as a geological structure, the Rift extends beyond the relatively narrow geomorphological feature seen at the surface, with a magnetic anomaly at least 500 km (300 mi) wide. On this basis, the Rio Grande Rift can be regarded as a system of axial grabens along a major north-south trending structural uplift (a continuation of the Southern Rocky Mountains). The magnetic anomaly extends beneath the Southern Great Plains stress province, and regional-scale uplift of about 1,000 m (3,300 ft) over the past 10 million yrs also extends into eastern New Mexico.

To the east of the Southern Great Plains province is the large Mid-Plate province that encompasses central and eastern regions of the conterminous United States and the Atlantic basin west of the Mid-Atlantic Ridge. The Mid-Plate province is characterized by low levels of paleo- and historic seismicity. Where Quaternary faulting has occurred, it is generally strike-slip and appears to be associated with the reactivation of older structural elements.

Zoback et al. (1991) report no stress measurements from the Delaware Basin. The stress field in the Southern Great Plains stress province has been defined from borehole measurements in west Texas and from volcanic lineaments in northern New Mexico. These measurements were interpreted by Zoback and Zoback (1991, p. 353) to indicate that the least principal horizontal stress is oriented north-northeast and south-southwest and that most of the province is characterized by an extensional stress regime.

There is an abrupt change between the orientation of the least principal horizontal stress in the Southern Great Plains and the west-northwest orientation of the least principal horizontal stress characteristic of the Rio Grande Rift. In addition to the geological indications of a transition zone as described above, Zoback and Zoback (1980, p. 6,134) point out that there is also evidence for a sharp boundary between these two provinces. This is reinforced by the change in crustal thickness from about 40 km (24 mi) beneath the Colorado Plateau to about 50 km (30 mi) or more beneath the Southern Great Plains east of the Rio Grande Rift. The base of the crust within the Rio Grande Rift is poorly defined but is shallower than that of the Colorado Plateau (Thompson and Zoback 1979, p. 152). There is also markedly lower heat flow in the Southern Great Plains (typically < 60 m W m^{-2}) reported by Blackwell, Steele, and Carter (1991, p. 428) compared with that in the Rio Grande Rift (typically > 80 m W m^{-2}) reported by Reiter,

Barroll, and Minier (1991, p. 463). Mansure and Reiter (1977) measured temperatures in AEC 8 and estimated the heat flow at ~ 1 heat flow unit (~48.1 m W m^{-2}), consistent with the Southern Great Plains.

Recent articles provide considerably more evidence on the orientation of maximum horizontal stress in the region. Lundstern and Zoback (2016) added 200 new orientations in Texas; a portion of these is in the southern Delaware Basin (in Texas) or on the Central Basin Platform adjacent to the southeastern corner of New Mexico. The bulk of the orientations in the Delaware Basin are near E-W; those nearer the southern end of the basin are oriented approximately NW-SE. Snee and Zoback (2018) added 100 more orientations in west Texas and southeastern New Mexico. These orientations (Snee and Zoback 2018, fig. 1) within the Delaware Basin in New Mexico display a general fan shape. Orientations are nearly W-E in Lea County near the border with Texas, more NE-SW near WIPP, and NNE-SSW northwest of WIPP. As in earlier publications, orientations in the southeastern Delaware Basin are NW-SE. In a further update focusing on stress in areas of active unconventional oil and gas development across the United States (US), Lund Snee and Zoback (2022, fig. 7) provided additional stress orientations in the area around WIPP. Previous patterns or stress orientation around WIPP were confirmed. Snee and Zoback (2018) also noted that additional information on principal stress orientations available through the TexNet Seismic Monitoring Program were not included because of unresolved contradictions.

A broader look at stress throughout the US (Levandowski et al. 2018) shows few data points in the WIPP area from formal inversions of focal mechanisms, but they are consistent with Lund Snee and Zoback (2022) and other sources.

SCR-4.2 Structural FEPs

SCR-4.2.1 Deformation

SCR-4.2.1.1 **FEP Numbers: N6 and N7**
FEP Titles: Salt Deformation (N6)
Diapirism (N7)

SCR-4.2.1.1.1 Screening Decision: SO-P

Natural *Salt Deformation* and *Diapirism* at the WIPP site over the next 10,000 years have been excluded from PA. This exclusion is based on their low probability of occurring at a severity that would significantly affect the disposal system.

SCR-4.2.1.1.2 Summary of New Information

This FEP has been updated with information from additional references. These references and information do not affect the screening argument or decision of this FEP.

SCR-4.2.1.1.3 Screening Argument

Some of the evaporites in the northern Delaware Basin have been deformed and it has been proposed that the likely mechanism for deformation is gravity-driven foundering of denser anhydrites into less dense halite (e.g., Anderson and Powers 1978; Jones 1981; Borns et al. 1983; Borns 1987). Diapirism occurs when the deformation is penetrative, i.e., halite beds disrupt overlying anhydrites. As Anderson and Powers (1978) suggested, this may have happened northeast of the WIPP at the location of drillhole ERDA-6. This is the only location where diapirism has been suggested for the evaporites of the northern Delaware Basin. The geologic situation suggests that deformation occurred before the Miocene-Pliocene Ogallala Formation was deposited (Jones 1981). Mechanical modeling is consistent with salt deformation occurring over about 700,000 yrs to form the deformed features known in the northern part of the WIPP site (Borns et al. 1983). The DOE concluded that evaporites at the WIPP site deform too slowly to affect the performance of the disposal system.

Because brine reservoirs appear to be associated with deformation, Powers et al. (1996) prepared detailed structure elevation maps of various units from the base of the Castile upward through the evaporites in the northern Delaware Basin. Drillholes are far more numerous in this study than in the study by Anderson and Powers (1978). Subdivisions of the Castile appear to be continuous in the vicinity of ERDA-6 and at ERDA-6. There is little justification for interpreting diapiric piercement at that site. The location and distribution of evaporite deformation around the WIPP site are similar to those reported in earlier studies (e.g., Anderson and Powers 1978; Borns et al. 1983; Borns and Shaffer 1985).

Surface domal features at the northwestern end of Nash Draw were of undetermined origin prior to WIPP investigations (e.g., Vine 1963), but extensive geophysical studies of these features were conducated as part of early WIPP investigations (see Powers 1996). Two of the domal features were drilled, demonstrating that they had a solution-collapse origin (breccia pipes) and were unrelated to salt diapirism (Snyder and Gard 1982).

A more recent study of the structure of the Culebra Dolomite Member of the Rustler Formation (hereafter referred to as the Culebra) (Powers 2003a; Powers et al. 2003) shows that the larger deformation associated with deeper units is reflected in the Culebra, although the structural relief is muted. Elevations of the base of Rustler, top of Rustler, and top of Dewey Lake in Ewing et al. (2012; figs. 4.2.2, 4.2.1, and 4.2.10, respectively) also show the structure related to this deformation. In addition, evaporite deformation in the northern part of the WIPP site, associated with the area earlier termed the “disturbed zone” (Powers et al. 1978), is hardly observable on a map of Culebra structure (Powers 2003a). There is no evidence of more recent deformation at the WIPP site from these maps. Additional drilling since 1996-2003 would be expected to yield additional details of the extent and timing of deformation.

Deformed salt in the lower Salado and upper strata of the Castile has been encountered in a number of boreholes around the WIPP site; the extent of existing salt deformation is summarized in the CCA, Chapter 2.0, Section 2.1.6.1, and further detail is provided in the CCA, Appendix DEF.

A broader review of salt tectonics (Hudec and Jackson 2007) does not include the Delaware Basin or greater Permian Basin as displaying salt deformation (e.g., op. cit., figure 5a). Currently, knowledge of salt deformation around the WIPP site is contained in WIPP-related reports or articles beginning with Jones (1972) and Jones et al. (1973).

Several mechanisms may result in salt deformation: in massive salt deposits, buoyancy effects or diapirism may cause salt to rise through denser, overlying units; and in bedded salt with anhydrite or other interbeds, gravity-driven foundering of the interbeds into the halite may occur. Results from rock mechanics modeling studies (see the CCA, Appendix DEF) indicate that the time scale for the deformation process is such that significant natural deformation is unlikely to occur at the WIPP site over any time frame significant to waste isolation. Thus, natural salt deformation and diapirism severe enough to alter existing patterns of groundwater flow or the behavior of the disposal system over the regulatory period have been eliminated from PA calculations on the basis of low probability of occurrence over the next 10,000 years.

SCR-4.2.2 Fracture Development

SCR-4.2.2.1 **FEP Number: N8**
FEP Title: Formation of Fractures

SCR-4.2.2.1.1 Screening Decision: SO-P (Far-field), UP (Repository)

Formation of Fractures in the far-field have been eliminated from PA calculations on the basis of a low probability of occurrence over 10,000 yrs. The *Formation of Fractures* near the repository is accounted for in PA through treatment of the DRZ.

SCR-4.2.2.1.2 Summary of New Information

This FEP has been updated with recent references as well as a summary of the implementation of *Formation of Fractures* near the repository in PA.

SCR-4.2.2.1.3 Screening Argument

The formation of fractures requires larger changes in stress than are required for changes to the properties of existing fractures to overcome the shear and tensile strength of the rock. It has been concluded from the regional tectonic setting of the Delaware Basin that no significant changes in regional stress are expected over the regulatory period. The EPA agrees that fracture formation in the Rustler is likely a result of halite dissolution and subsequent overlying unit fracturing loading/unloading, as well as the syn- and postdepositional processes. Intraformational postdepositional dissolution of the Rustler has been ruled out as a major contributor to Rustler salt distribution and thus to new fracture formation based on work by Holt and Powers in the CCA (Appendix DEF, Section DEF 3.2) and Powers and Holt (1999 and 2000), who believe that depositional facies and syndepositional dissolution account for most of the patterns of halite distribution in the Rustler. The Rustler has been evaluated further with respect to such processes, supporting the conclusions regarding fracture formation (Powers et

al., 2003; Holt et al., 2005; Powers et al. 2006a; Holt and Powers, 2010; Powers and Holt, 2021). The WIPP site lacks significant integrated drainage, and the Mescalero Paleosol (caliche) has been taken as an indicator of long-term stability of the surface. Erosion is not expected to cause unloading and new fracture formation in the regulatory period. The argument against developing new fractures in the Rustler during the regulatory period appears reasonable. The formation of new fracture sets in the Culebra has therefore been eliminated from PA calculations on the basis of a low probability of occurrence over 10,000 yrs.

Repository-induced fracturing of the DRZ and Salado interbeds is accounted for in PA.

A mechanism such as salt diapirism could develop fracturing in the Salado, but there is little evidence of diapirism in the Delaware Basin. Salt deformation has occurred in the vicinity of the WIPP, and fractures have developed in deeper Castile anhydrites as a consequence. Deformation rates are slow, and it is highly unlikely that this process will induce significant new fractures in the Salado during the regulatory time period. Surface domal features at the northwestern end of Nash Draw were of undetermined origin prior to WIPP investigations (e.g., Vine 1963), but extensive geophysical studies were conducted of these features as part of early WIPP studies (see Powers 1996). Two of the domal features were drilled, demonstrating that they had a solution-collapse origin (breccia pipes) and were not related in any way to salt diapirism (Snyder and Gard 1982).

SCR-4.2.2.1.4 FEP Implementation in PA

For the far-field, FEP N8 *Formation of Fractures* has been eliminated on the basis of low probability of occurrence and is not incorporated into PA. However, in the repository, the *Formation of Fractures* is associated with the *Disturbed Rock Zone* conceptual model. This conceptual model is implemented in the PA code BRAGFLO for the Salado Flow computation in the PA calculation (Appendix PA-4.2). This conceptual model is implemented by assigning different DRZ material properties to the host rock immediately surrounding the repository excavation. The DRZ material properties include increased porosity and permeability from the intact Salado Halite. The DRZ material also allows for a further increase in porosity and permeability above specified brine pressures to account for fracture openings.

SCR-4.2.2.2 FEP Number: N9
FEP Title: Changes in Fracture Properties

SCR-4.2.2.2.1 Screening Decision: SO-C, UP (near repository)

Naturally induced *Changes in Fracture Properties* that may affect groundwater flow or radionuclide transport in the region of the WIPP have been eliminated from PA calculations on the basis of low consequence to the performance of the disposal system. *Changes in Fracture Properties* near the repository are accounted for in PA through treatment of the DRZ.

SCR-4.2.2.2.2 Summary of New Information

This FEP has been updated with new references. The basis of the screening argument has not changed, nor has the screening decision.

SCR-4.2.2.2.3 Screening Argument

Groundwater flow in the region of the WIPP and transport of any released radionuclides may take place along fractures. The rate of flow and the extent of transport will be influenced by fracture characteristics. Changes in fracture properties could arise through natural changes in the local stress field; for example, through tectonic processes, erosion or sedimentation changing the amount of overburden, dissolution of soluble minerals along beds in the Rustler or upper Salado, or dissolution or precipitation of minerals in fractures.

Tectonic processes and features (*changes in regional stress* [N3]; *tectonics* [N4]; *regional uplift* and *subsidence* [N5]; *salt deformation* [N6]; *diapirism* [N7]) have been screened out of PA. These processes are not expected to significantly change the character of fractures during the regulatory period.

Surface erosion or deposition (e.g., N41–N49) are not expected to significantly change the overburden on the Culebra during the regulatory period. The relationship between Culebra transmissivity and depth is significant (Holt and Yarbrough 2002; Holt and Powers 2002; Powers et al. 2003), but the potential change to Culebra transmissivity based on deposition or erosion from these processes over the regulatory period is insignificant.

Shallow dissolution (N16), where soluble beds from the upper Salado or Rustler are removed by groundwater, has been extensively considered. There are no direct effects on the Salado at depths of the repository. Extensive study of the upper Salado and Rustler halite units (Holt and Powers 1988; the CCA, Appendix FAC; Powers and Holt 1999 and 2000; Powers 2003a; Powers et al. 2003, 2006b; Holt and Powers 2010) indicates little potential for dissolution at the WIPP site during the regulatory period.

Mineral precipitation within fractures (N22) is expected to be beneficial to performance, and it has been screened out on the basis of low consequence. Natural dissolution of fracture fillings within the Culebra is incorporated within FEP N16 (Shallow Dissolution). There is no new information on the distribution of fracture fillings within the Culebra. The effects of fracture fillings are also expected to be represented in the distribution of Culebra transmissivity values around the WIPP site and are thus incorporated into PA.

SCR-4.2.2.2.4 FEP Implementation in PA

Repository-induced fracturing of the DRZ and Salado interbeds is accounted for in PA (UP) and is discussed further in FEPs W18 and W19.

SCR-4.2.2.3 **FEP Numbers: N10 and N11**
FEP Titles: Formation of New Faults (N10)
Fault Movement (N11)

SCR-4.2.2.3.1 Screening Decision: SO-P

Naturally induced *Fault Movement* and *Formation of New Faults* of sufficient magnitude to significantly affect the performance of the disposal system have been eliminated from PA calculations on the basis of low probability of occurrence over 10,000 yrs.

SCR-4.2.2.3.2 Summary of New Information

This FEP has been updated with additional references since the CRA-2019. The basis of the screening argument has not changed, nor has the screening decision.

SCR-4.2.2.3.3 Screening Argument

Faults are present in the Delaware Basin in both the units underlying the Salado and in the Permian evaporite sequence (see the CCA, Section 2.1.5.3). According to Powers et al. (1978 included in the CCA, Appendix GCR), there is evidence that movement along faults within the pre-Permian units affected the thickness of Early Permian strata, but these faults did not exert a structural control on the deposition of the Castile, the Salado, or the Rustler. Fault zones along the margins of the Delaware Basin were active during the Late Permian Period. Along the eastern margin, where the Delaware Basin flanks the Central Basin Platform, Holt and Powers (1988; also included in the CCA, Appendix FAC) note that there is displacement of the Rustler, and Schiel (1994) notes that there is thinning of the Dewey Lake. There is, however, no surface displacement along the trend of these fault zones, indicating that there has been no significant Quaternary movement. Muehlberger et al. (1978, p. 338) note that the nearest faults on which Quaternary movement has been identified lie to the west of the Guadalupe Mountains. Hayes and Bachman (1979) re-examined the eastern escarpment of the Guadalupe Mountains and concluded that proposed Barrera and Carlsbad faults (Kelley 1971, 1972) were misinterpreted surficial features and jointing. The US Geological Survey website locating known faults of Quaternary age (<1.6 million years) shows no faults within 100 km of the WIPP site (U.S. Geological Survey [USGS] Quaternary Faults). The nearest known fault of that age is at the base of the Guadalupe-Delaware Mountains fault zone.

The WIPP is located in an area of tectonic quiescence. Seismic monitoring conducted for the WIPP since the CCA continues to record small events in southeastern New Mexico and west Texas, and these events are mainly in areas associated with resource production (see Section SCR-4.2.2.4 for more information on seismic events in the area). The absence of Quaternary fault scarps and the general tectonic setting and understanding of its evolution indicate that large-scale, tectonically induced fault movement within the Delaware Basin can be eliminated from PA calculations on the basis of low probability over 10,000 yrs. The stable tectonic setting also allows the formation of new faults within the basin over the next 10,000 yrs to be eliminated from PA calculations on the basis of low probability of occurrence.

Evaporite dissolution at or near the WIPP site has the potential for developing fractures in the overlying beds. Three zones with halite (top of Salado, M1/H1 of the Los Medaños Member, and M2/H2 of the Los Medaños Member) underlie the Culebra at the site (Powers 2003a). The upper Salado is present across the site, and there is no indication that dissolution of this area will occur in the regulatory period or cause faulting at the site. The Los Medaños units show both mudflat facies and halite-bearing facies within or adjacent to the WIPP site (Powers 2003a). Although the distribution of halite in the Rustler is mainly the result of depositional facies and syndepositional dissolution (Holt and Powers 1988; Powers and Holt 1999 and 2000), the possibility of past or future halite dissolution along the margins cannot be ruled out (Holt and Powers 1988; Beauheim and Holt 1990). If halite in the lower Rustler has been dissolved along the depositional margin, it has not occurred recently or has been of no consequence, as there is no indication on the surface or in Rustler structure of new (or old) faults in this area (e.g., Powers et al. 1978; Powers 2003a).

The absence of Quaternary fault scarps and the general tectonic setting and understanding of its evolution indicate that large-scale, tectonically induced fault movement within the Delaware Basin can be eliminated from PA calculations on the basis of low probability over 10,000 yrs. The stable tectonic setting also allows the formation of new faults within the basin over the next 10,000 yrs to be eliminated from PA calculations on the basis of low probability of occurrence.

SCR-4.2.2.4 **FEP Number: N12**
FEP Title: Seismic Activity

SCR-4.2.2.4.1 Screening Decision: UP

The post-closure effects of *Seismic Activity* on the repository and the DRZ are accounted for in PA.

SCR-4.2.2.4.2 Summary of New Information

Since the CCA, a much more rigorous seismic monitoring system has been developed by the New Mexico Institute of Mining and Technology (NMT). Seismic events have historically been obtained from NMT every quarter. This method of obtaining data has since changed and information is currently obtained monthly from the USGS and entered into the Delaware Basin Well Tracking Application. The Delaware Basin Monitoring Annual Report (U.S. DOE 2019b, 2020a, 2021d, 2022a, 2024b, and 2025a) reveals a total of 24,078 recorded events since the CRA-2019.

In general, the large increase in recorded events covers the same period as the increase in fracking, oil and gas production, and disposal of produced water (also referred to as saltwater disposal, or “SWD”) as well as the fielding of better and greater numbers of seismometer stations in New Mexico and west Texas in the area of interest (Delaware Basin) for WIPP. Event numbers, dates, epicenters and other information are tabulated variously for reporting or for

particular analyses (e.g., Froelich et al. 2016; Litherland and Record 2023a,b ; Litherland 2023; US DOE 2025a).

In general, explanations of seismic activity that go beyond data tabulation consider the recent increase in number of earthquakes to be a result of induced seismic activity. The main focus in most analyses is the association of event locations (epicenters) with the locations of industry activities (mainly SWD and fracking, with less emphasis on oil production/extraction). In contrast, Froelich et al. (2016) developed a five-question test as a means of distinguishing induced earthquakes from tectonic events.

Savvaidis et al. (2020) compared epicenters with relatively specific activity for fracking and, separately, SWD to develop associations between earthquakes and these activities (space-time clustering). They note uncertainties in epicenter locations as well as less well-constrained (in time) fracking or SWD operations. Savvaidis et al. (2020) provided an analysis to separate events related to fracking and those related to SWD. Their summary indicates earthquakes more promptly follow fracking, are clustered more closely, and diminish quickly following the fracking event. Earthquakes were more associated with a change in SWD activity after a long period of injection. Specific mechanisms to link deep earthquakes to fracking or SWD were not discussed.

Zhai et al. (2021) related deep seismicity to shallow injection in west Texas. Their analysis specifically recognized the geological separations between earthquakes in basement rocks and relatively shallow injection, mostly in the Delaware Mountain Group. Permian-age shale layers, such as Bone Spring and Wolfcamp, are common targets for oil production and associated well completion activities such as fracking. Overall, Zhai et al. (2021) conclude that it is unlikely that vertical fractures connect higher SWD zones to much deeper basement rock through these (and deeper) shales. They conclude that the lack of vertical conductivity eliminates pore pressure diffusion from shallow injection as a mechanism to cause deep earthquakes in west Texas. This contrasts with the conclusion of Woo and Ellsworth (2023) that deep injection in areas of the Midland basin does activate basement faults through pressure diffusion (and poroelastic effects). Zhai et al. (2021) concur with Woo and Ellsworth with respect to the Midland Basin induced seismicity. Zhai et al. propose that poroelastic stress is transmitted to cause deep earthquakes. Surface deformation data from synthetic aperture radar is analyzed to support their concept.

The analysis of high-volume data of seismicity, with the exception of Zhai et al. (2021), tends to minimize most geological aspects. Epicenter and hypocenter locations are noted as less precise than needed for certain analyses, and more dense and dedicated detection arrays would be needed to improve locations. In addition, the apparent limited historic “natural” seismicity of the Delaware Basin region is mainly lost from analysis in the face of the more abundant recent seismicity attributed to human activity. In an alternate view, Dvory and Zoback (2021) examine how oil and gas production affect pore-pressure and poroelastic stress, and therefore may limit subsequent injection-induced seismicity.

Magnitude of completeness for recent data for the Texas Seismological Network in selected areas has been reported as local magnitude (M_L)1.5 (Savvaidis et al. 2019, 2020). Magnitude of completeness has not been reported specifically for the WIPP seismic network to date, though Litherland (2023) indicated M_L 1.8. Litherland (2023) does not specifically indicate the methodology used to determine magnitude of completeness. For the first half of calendar year 2023, Litherland and Record (2023a, 2023b) reported 110 events within 50 km of WIPP. Seventy-five were below M_L 1.8. Thirty-five were M_L 1.8 or greater. The mean depths of the hypocenters for these two groupings were 8.09 km and 9.05 km, respectively. Deeper injection wells are commonly in the range of ~5.3 km or less, with one well ~6.1 km deep. Delaware Mountain Group injection wells are < ~3 km.

The WIPP continues to monitor seismic activity in the region to identify impacts and risk to the expected performance of the repository. As described in the following sections, this new information does not change the screening argument or conclusions.

SCR-4.2.2.4.3 Screening Argument

The following subsections present the screening argument for seismic activity (groundshaking).

SCR-4.2.2.4.3.1 Causes of Seismic Activity

Seismic activity describes transient ground motion that may be generated by several energy sources. There are two possible causes of seismic activity that could potentially affect the WIPP site: natural and human-induced. Natural seismic activity is caused by fault movement (earthquakes) when the buildup of strain in rock is released through sudden rupture or movement. Human-induced seismic activity may result from a variety of surface and subsurface activities, such as explosions (H19 and H20), mining (H13, H14, H58, and H59), fluid injection (H28), and fluid withdrawal (H25).

SCR-4.2.2.4.3.2 Groundshaking

Ground vibration and the consequent shaking of buildings and other structures are the most obvious effects of seismic activity. Once the repository and shafts have been sealed, however, existing surface structures will be dismantled. Post-closure PAs are concerned with the effects of seismic activity on the closed repository.

In regions of low and moderate seismic activity, such as the Delaware Basin, rocks behave elastically in response to the passage of seismic waves, and there are no long-term changes in rock properties. The effects of earthquakes beyond the DRZ have been eliminated from PA calculations on the basis of low consequence to the performance of the disposal system. An inelastic response, such as cracking, is only possible where there are free surfaces, as in the roof and walls of the repository prior to closure by creep. Seismic activity could, therefore, have an effect on the properties of the DRZ.

An assessment of the extent of damage in underground excavations caused by groundshaking depends largely on observations from mines and tunnels. Because such excavations tend to take place in rock types more brittle than halite, these observations cannot be related directly to the behavior of the WIPP. According to Wallner (1981, p. 244), the DRZ in brittle rock types is likely to be more highly fractured and hence more prone to spalling and rockfalls than an equivalent zone in salt. Relationships between groundshaking and subsequent damage observed in mines will therefore be conservative with respect to the extent of damage induced at the WIPP by seismic activity.

Dowding and Rozen (1978) classified damage in underground structures following seismic activity and found that no damage (cracks, spalling, or rockfalls) occurred at accelerations below 0.2 gravities (g) and that only minor damage occurred at accelerations up to 0.4 g. Lenhardt (1988, p. 392) showed that a magnitude 3 earthquake would have to be within 1 km (0.6 mi) of a deep hard-rock mine in South Africa to result in falls of loose rock. Literature relating induced seismicity to salt mines focuses on seismicity associated with the mine itself, including solution mining. The risk of seismic activity in the region of the WIPP reaching these thresholds is discussed below.

SCR-4.2.2.4.3.3 Seismic Risk in the Region of the WIPP

Prior to the introduction of a seismic monitoring network in 1960, most recorded earthquakes in New Mexico were associated with the Rio Grande Rift, although small earthquakes were detected in other parts of the region. In addition to continued activity in the Rio Grande Rift, the instrumental record has shown a significant amount of seismic activity originating from the Central Basin Platform and a number of small earthquakes in the Los Medaños area. Seismic activity in the Rio Grande Rift is associated with extensional tectonics in that area. Seismic activity in the Central Basin Platform may be associated with natural earthquakes, but there are also indications that this activity occurs in association with oil-field activities such as fluid injection. Small earthquakes in the Los Medaños region have not been precisely located but may be the result of mining activity in the region. The CCA, Chapter 2.0, Section 2.6.2 contains additional discussion of seismic activity and risk in the WIPP region.

The instrumental record was used as the basis of a seismic risk study primarily intended for design calculations of surface facilities rather than for postclosure PAs. The use of this study to define probable ground accelerations in the WIPP region over the next 10,000 yrs is based on the assumptions that hydrocarbon extraction and potash mining will continue in the region and that the regional tectonic setting precludes major changes over the next 10,000 yrs.

Three source regions were used in calculating seismic risk: the Rio Grande Rift, the Central Basin Platform, and part of the Delaware Basin province (including the Los Medaños). Using conservative assumptions about the maximum magnitude event in each zone, the study indicated a return period of about 10,000 yrs (annual probability of occurrence of 10^{-4}) for events producing ground accelerations of 0.1 g. Ground accelerations of 0.2 g would have an annual probability of occurrence of about 5×10^{-6}.

The results of the seismic risk study and the observations of damage in mines caused by groundshaking give an estimated annual probability of occurrence of between 10^{-8} and 10^{-6} for events that could increase the permeability of the DRZ. The DRZ is accounted for in PA as a zone of permanently high permeability (see Appendix PA-4.2.4); this treatment is considered to account for the effects of any potential seismic activity.

SCR-4.2.2.4.4 FEP Implementation in PA

FEP N12 *Seismic Activity*, which is accounted for in the UP scenario, is associated with the *Disturbed Rock Zone* conceptual model. This conceptual model is implemented in the PA code BRAGFLO for the Salado Flow computation in the PA calculation (Appendix PA-4.2). The DRZ conceptual model is implemented by assigning different DRZ material properties to the host rock immediately surrounding the repository excavation. The DRZ material properties include increased porosity and permeability from the intact Salado Halite. The DRZ material also allows for a further increase in porosity and permeability above specified brine pressures to account for fracture openings.

SCR-4.2.3 Crustal Process

SCR-4.2.3.1 **FEP Number: N13**
FEP Title: Volcanic Activity

SCR-4.2.3.1.1 Screening Decision: SO-P

Volcanic Activity has been eliminated from PA calculations on the basis of low probability of occurrence over 10,000 yrs.

SCR-4.2.3.1.2 Summary of New Information

No new information that affects the screening of this FEP has been identified since the CRA-2019.

SCR-4.2.3.1.3 Screening Argument

The Paleozoic and younger stratigraphic sequences within the Delaware Basin are devoid of locally derived volcanic rocks. Volcanic ashes (dated at 13 million yrs and 0.6 million yrs) do occur in the Gatuña Formation (hereafter referred to as the Gatuña), but these are not locally derived. Within eastern New Mexico and northern, central, and western Texas, the closest Tertiary volcanic rocks with notable areal extent or tectonic significance to the WIPP are approximately 160 km (100 mi) to the south in the Davis Mountains volcanic area. The closest Quaternary volcanic rocks are 250 km (150 mi) to the northwest in the Sacramento Mountains. No volcanic rocks are exposed at the surface within the Delaware Basin.

Volcanic activity is associated with particular tectonic settings: constructive and destructive plate margins, regions of intraplate rifting, and isolated hot spots in intraplate regions. The tectonic setting of the WIPP site and the Delaware Basin is remote from plate margins, and the absence of past volcanic activity indicates the absence of a major hot spot in the region. Intraplate rifting has taken place along the Rio Grande some 200 km (120 mi) west of the WIPP site during the Tertiary and Quaternary Periods. Igneous activity along this rift valley is comprised of sheet lavas intruded on by a host of small-to-large plugs, sills, and other intrusive bodies. However, the geological setting of the WIPP site within the large and stable Delaware Basin allows volcanic activity in the region of the WIPP repository to be eliminated from performance calculations on the basis of low probability of occurrence over the next 10,000 yrs.

SCR-4.2.3.2 **FEP Number: N14**
FEP Title: Magmatic Activity

SCR-4.2.3.2.1 Screening Decision: SO-C

The effects of *Magmatic Activity* have been eliminated from the PA calculations on the basis of low consequence to the performance of the disposal system.

SCR-4.2.3.2.2 Summary of New Information

No new information that affects the screening of this FEP has been identified since the CRA-2019.

SCR-4.2.3.2.3 Screening Argument

Magmatic activity is defined as the subsurface intrusion of igneous rocks into country rock. Deep intrusive igneous rocks crystallize at depths of several kilometers (several miles) and have no surface or near-surface expression until considerable erosion has taken place. Alternatively, intrusive rocks may form from magma that has risen to near the surface or in the vents that give rise to volcanoes and lava flows. Magma near the surface may be intruded along subvertical and subhorizontal discontinuities (forming dikes and sills, respectively), and magma in volcanic vents may solidify as plugs. The formation of such features close to a repository or the existence of a recently intruded rock mass could impose thermal stresses, inducing new fractures or altering the hydraulic characteristics of existing fractures.

The principal area of magmatic activity in New Mexico is the Rio Grande Rift, where extensive intrusions occurred during the Tertiary and Quaternary Periods. The Rio Grande Rift, however, is in a different tectonic province than the Delaware Basin, and its magmatic activity is related to the extensional stress regime and high heat flow in that region.

Within the Delaware Basin, there is a single identified outcrop of a lamprophyre dike about 70 km (40 mi) southwest of the WIPP (see the CCA, Chapter 2.0, Section 2.1.5.4 and the CCA, Appendix GCR for more detail). Closer to the WIPP site, similar rocks have been exposed within potash mines some 15 km (10 mi) to the northwest, and igneous rocks have been reported

from petroleum exploration boreholes. Material from the subsurface exposures has been dated at around 35 million yrs. Some recrystallization of the host rocks took place alongside the intrusion, and there is evidence that minor fracture development and fluid migration also occurred along the margins of the intrusion. However, the fractures have been sealed, and there is no evidence that the dike acted as a conduit for continued fluid flow.

Aeromagnetic surveys of the Delaware Basin have shown anomalies that lie on a linear southwest-northeast trend that coincides with the surface and subsurface exposures of magmatic rocks. There is a strong indication, therefore, of a dike or a closely related set of dikes extending for at least 120 km (70 mi) across the region (see the CCA, Chapter 2.0, Section 2.1.5.4). The aeromagnetic survey conducted to delineate the dike showed a magnetic anomaly that is several kilometers (several miles) wide at depth and narrows to a thin trace near the surface. This pattern is interpreted as the result of an extensive dike swarm at depths of less than approximately 4.0 km (2.5 mi) near the Precambrian basement, from which a limited number of dikes have extended towards the surface.

Magmatic activity has taken place in the vicinity of the WIPP site in the past, but the igneous rocks have cooled over a long period. Any enhanced fracturing or conduits for fluid flow have been sealed by salt creep and mineralization. Continuing magmatic activity in the Rio Grande Rift is too remote from the WIPP location to be of consequence to the performance of the disposal system. Thus, the effects of magmatic activity have been eliminated from PA calculations on the basis of low consequence to the performance of the disposal system.

SCR-4.2.3.3 **FEP Number: N15**
FEP Title: Metamorphic Activity

SCR-4.2.3.3.1 Screening Decision: SO-P

Metamorphic Activity has been eliminated from PA calculations on the basis of low probability of occurrence over the next 10,000 yrs.

SCR-4.2.3.3.2 Summary of New Information

No new information that affects the screening of this FEP has been identified since the CRA-2019.

SCR-4.2.3.3.3 Screening Argument

Metamorphic activity, that is, solid-state recrystallization changes to rock properties and geologic structures through the effects of heat and/or pressure, requires depths of burial much greater than the depth of the repository. Regional tectonics that would result in the burial of the repository to the depths at which the repository would be affected by metamorphic activity have been eliminated from PA calculations on the basis of low probability of occurrence; therefore, metamorphic activity has also been eliminated from PA calculations on the basis of low probability of occurrence over the next 10,000 yrs.

SCR-4.2.4 Geochemical Processes

SCR-4.2.4.1 **FEP Number: N16**
FEP Title: Shallow Dissolution (including lateral dissolution)

SCR-4.2.4.1.1 Screening Decision: UP

Shallow Dissolution is accounted for in PA.

SCR-4.2.4.1.2 Summary of New Information

This FEP has been updated with more recent references and information. Because this FEP is included in performance assessment calculations, implementation details have been added as well.

SCR-4.2.4.1.3 Screening Argument

This section discusses a variety of styles of dissolution that have been active in the region of the WIPP or in the Delaware Basin. A distinction has been drawn between shallow dissolution involving circulation of groundwater, mineral dissolution in the Rustler and at the top of the Salado in the region of the WIPP, and deep dissolution taking place in the Castile and the base of the Salado. Dissolution will initially enhance porosities, but continued dissolution may lead to compaction of the affected units with a consequent reduction in porosity. Compaction may result in fracturing of overlying brittle units and increased permeability. Extensive dissolution may create cavities (karst) and result in the total collapse of overlying units. This topic is discussed further in the CCA, Chapter 2.0, Section 2.1.6.2.

SCR-4.2.4.1.3.1 Shallow Dissolution

In the region around the WIPP, shallow dissolution by groundwater flow has removed soluble minerals from the upper Salado as well as the Rustler to form Nash Draw; extensive solution within the closed draw has created karst features including caves and dolines in the sulfate beds of the Rustler (see Lee 1925; Vine 1963, Bachman 1980, 1985, and 1987a; Powers et al. 2006b; Goodbar and Goodbar 2014; Goodbar et al. 2020). An alluvial doline drilled at WIPP 33, about 850 m (2,800 ft) west of the WIPP site boundary, is the nearest karst feature known in the vicinity of the site. Upper Salado halite dissolution in Nash Draw resulted in fracture propagation upward through the overlying Rustler (Holt and Powers 1988). The margin of dissolution of halite from the upper Salado has commonly been placed west of the WIPP site, near, but east of, Livingston Ridge, the eastern boundary of Nash Draw. Halite occurs in the Rustler east of Livingston Ridge, with the margin generally progressively eastward in higher stratigraphic units (e.g., Snyder 1985; Powers and Holt 1995). The distribution of halite in the Rustler has commonly been attributed to shallow dissolution (e.g., Powers et al. 1978; Lambert 1983; Bachman 1985; Snyder 1985; Lowenstein 1987). During early studies for the WIPP, the variability of Culebra transmissivity in the vicinity of the WIPP was commonly attributed to the effects of Rustler halite dissolution and changes in fracturing as a consequence.

After a detailed sedimentologic and stratigraphic investigation of WIPP cores, shafts, and geophysical logs from the region around the WIPP, the distribution of halite in the Rustler was attributed to depositional and syndepositional processes rather than postdepositional dissolution (Holt and Powers 1988; Powers and Holt 2000). Rustler exposures in shafts for the WIPP revealed extensive sedimentary structures in clastic units (Holt and Powers 1984, 1986, and 1990), and the suite of features in these beds led these investigators (Holt and Powers 1988; Powers and Holt 1990 and 2000) to reinterpret the clastic units. They conclude that the clastic facies represent mainly mudflat facies tracts adjacent to a salt pan. Although some halite was likely deposited in mudflat areas proximal to the salt pan, it was largely removed by syndepositional dissolution, as indicated by soil structures, soft sediment deformation, bedding, and small-scale vertical relationships (Holt and Powers 1988; Powers and Holt 1990, 1999 and 2000). The depositional margins of halite in the Rustler are the likely points for past or future dissolution (e.g., Holt and Powers 1988; Beauheim and Holt 1990). Cores from drillholes at the H-19 drillpad near the Tamarisk Member halite margin show evidence of some dissolution of halite in the Tamarisk (Mercer et al. 1998), consistent with these predictions. The distribution of Culebra transmissivity values is not considered related to dissolution of Rustler halite except in a narrow corridor along the margin of halite in the Tamarisk Member (Powers et al. 2003), and other geological factors (e.g., depth, upper Salado dissolution) correlate well with Culebra transmissivity (e.g., Powers and Holt 1995; Holt and Powers 2002; Holt and Yarbrough 2002; Powers et al. 2003; Holt et al. 2005).

Since the CCA was completed, the WIPP has conducted additional work on shallow dissolution, principally of the upper Salado, and its possible relationship to the distribution of transmissivity values for the Culebra as determined through testing of WIPP hydrology wells.

Analysis Plan 088 (AP-088) (Beauheim 2002) noted that potentiometric surface values for the Culebra in many monitoring wells were outside the uncertainty ranges used to calibrate models of steady-state heads for the unit. AP-088 directed the analysis of the relationship between geological factors and values of transmissivity at Culebra wells. The relationship between geological factors, including dissolution of the upper Salado as well as limited dissolution in the Rustler, and Culebra transmissivity has been used to evaluate differences between assuming steady-state Culebra heads and changing heads.

Task 1 for AP-088 (Powers 2003a) evaluated geological factors, including shallow dissolution in the vicinity of the WIPP site related to Culebra transmissivity. A much more extensive drillhole geological database was developed than was previously available, utilizing sources of data from WIPP, potash exploration, and oil and gas exploration and development. The principal findings related to shallow dissolution are (1) a relatively narrow zone (~ 200 – 400 m [656 – 1,312 ft] wide) could be defined as the margin of dissolution of the upper Salado in much of the area around the WIPP, (2) the upper Salado dissolution margin commonly underlies surface escarpments such as Livingston Ridge, and (3) there are possible extensions or reentrants of incipient upper Salado dissolution extending eastward from the general dissolution margin. The WIPP site proper is not affected by this process.

Culebra transmissivity correlates well with depth or overburden, which affects fracture apertures (Powers and Holt 1995; Holt 1997; Holt and Powers 2002; Holt and Yarbrough 2002; Powers et al. 2003; Holt et al. 2005). Dissolution of the upper Salado appears to increase transmissivity by one or more orders of magnitude (Holt and Yarbrough 2002). Because there is no indication of upper Salado dissolution at the WIPP site, Holt and Yarbrough (2002) did not include this factor for the WIPP site in estimates of base transmissivity values for the WIPP site and surroundings.

Shallow dissolution in Nash Draw continues to be investigated separately from WIPP (Goodbar and Goodbar 2014; Goodbar et al. 2020). Powers and Holt (2021) more recently provided an extensive review of dissolution as it relates to WIPP and included new data that addressed some long-standing claims.

The effects of shallow dissolution (including the impacts of lateral dissolution) have been included in PA calculations in the derivation of transmissivity fields for Culebra flow and transport.

SCR-4.2.4.1.4 FEP Implementation in PA

The effects of Salado dissolution are included within the Culebra Hydrogeology conceptual model, as implemented in construction of the base geostatistical transmissivity fields using various commercial-off-the-shelf software programs (Hart et al. 2008), and subsequent calibration of the transmissivity fields against observed heads using the parameter estimation software PEST and groundwater flow software MODFLOW (Bowman et al., 2023).

SCR-4.2.4.2 FEP Numbers: N18, N20, and N21

FEP Titles: **Deep Dissolution (N18)**
Breccia Pipes (N20)
Collapse Breccias (N21)

SCR-4.2.4.2.1 Screening Decision: SO-P

Deep Dissolution and the formation of associated features (for example, solution chimneys or *Breccia Pipes*, *Collapse Breccias*) at the WIPP site have been eliminated from PA calculations on the basis of low probability of occurrence over the next 10,000 yrs.

SCR-4.2.4.2.2 Summary of New Information

The screening argument for these FEPs has been updated with new relevant references and studies.

SCR-4.2.4.2.3 Screening Argument

This section discusses a variety of styles of dissolution that have been active in the region of the WIPP or in the Delaware Basin. A distinction has been drawn between shallow dissolution, involving circulation of groundwater and mineral dissolution in the Rustler and at the top of the

Salado in the region of the WIPP, and deep dissolution taking place in the Castile and the base of the Salado. Dissolution will initially enhance porosities, but continued dissolution may lead to compaction of the affected units with a consequent reduction in porosity. Compaction may result in fracturing of overlying brittle units and increased permeability. Extensive dissolution may create cavities (karst) and result in the total collapse of overlying units. This topic is discussed further in the CCA, Chapter 2.0, Section 2.1.6.2.

SCR-4.2.4.2.4 Deep Dissolution

Deep dissolution is limited to processes involving dissolution of the Castile or basal Salado and features such as breccia pipes (also known as solution chimneys) associated with this process (see the CCA, Chapter 2.0, Section 2.1.6.2). Deep dissolution is distinguished from shallow and lateral dissolution not only by depth, but also by the origin of the water. Dissolution by groundwater from deep water-bearing zones can lead to the formation of cavities. Collapse of overlying beds leads to the formation of collapse breccias if the overlying rocks are brittle, or to deformation if the overlying rocks are ductile. If dissolution is extensive, breccia pipes or solution chimneys may form above the cavity. These pipes may reach the surface or pass upwards into fractures and then into microcracks that do not extend to the surface. Breccia pipes may also form through the downward percolation of meteoric waters, as discussed earlier. Deep dissolution is of concern because it could accelerate contaminant transport through the creation of vertical flow paths that bypass low-permeability units in the Rustler. If dissolution occurred within or beneath the waste panels themselves, there could be increased circulation of groundwater through the waste, as well as a breach of the Salado host rock.

Features identified as being the result of deep dissolution are present along the northern and eastern margins of the Delaware Basin. In addition to features that have a surface expression or that appear within potash mine workings, deep dissolution has been cited by Anderson et al. (1972, p. 81) as the cause of lateral variability within evaporite sequences in the lower Salado.

Exposures of the McNutt Potash Member of the Salado within a mine near Nash Draw have shown a breccia pipe containing cemented brecciated fragments of formations higher in the stratigraphic sequence. At the surface, this feature is marked by a dome, and similar domes have been interpreted as dissolution features. The depth of dissolution has not been confirmed, but the collapse structures led Anderson (1978, p. 52), Bachman (1980), and Snyder and Gard (1982, p. 65) to postulate dissolution of the Capitan Limestone at depth; collapse of the Salado, Rustler, and younger formations; and subsequent dissolution and hydration by downward percolating waters. San Simon Sink (see the CCA, Chapter 2.0, Section 2.1.6.2), some 35 km (20 mi) east-southeast of the WIPP site, has also been interpreted as a solution chimney. Subsidence has occurred there in historical times according to Nicholson and Clebsch (1961, p. 14), suggesting that dissolution at depth is still taking place. Whether this is the result of downward-percolating surface water or deep groundwater has not been confirmed. The association of these dissolution features with the inner margin of the Capitan Reef suggest that they owe their origins, if not their continued development, to groundwaters derived from the Capitan Limestone.

SCR-4.2.4.2.5 Dissolution within the Castile and Lower Salado

The Castile contains sequences of varved anhydrite and carbonate (that is, laminae deposited on a cyclical basis) that can be correlated between several boreholes. On the basis of these deposits, a basin-wide uniformity in the depositional environment of the Castile evaporites was assumed. The absence of varves from all or part of a sequence and the presence of brecciated anhydrite beds have been interpreted by Anderson et al. (1972) as evidence of dissolution. Holt and Powers (the CCA, Appendix FAC) have questioned the assumption of a uniform depositional environment and contend that the anhydrite beds are lateral equivalents of halite sequences without significant postdepositional dissolution. Wedges of brecciated anhydrite along the margin of the Castile have been interpreted by Robinson and Powers (1987, p. 78) as gravity-driven clastic deposits, rather than the result of deep dissolution.

Localized depressions at the top of the Castile and inclined geophysical marker units at the base of the Salado have been interpreted by Davies (1983, p. 45) as the result of deep dissolution and subsequent collapse or deformation of overlying rocks. The postulated cause of this dissolution was circulation of undersaturated groundwaters from the Bell Canyon Formation (hereafter referred to as Bell Canyon). Additional boreholes (notably WIPP-13, WIPP-32, and DOE-2) and geophysical logging led Borns and Shaffer (1985) to conclude that the features interpreted by Davies as being dissolution features are the result of irregularities at the top of Bell Canyon. These irregularities led to localized depositional thickening of the Castile and lower Salado sediments.

Interpreted or inferred dissolution within these deeper formations, especially in eastern and central parts of the Delaware Basin, has largely relied on early assumptions and often many fewer data points than now exist. An important factor not taken into account into most earlier discussions and assertions regarding dissolution is the pore pressure within the very limited porosity existing in these bedded evaporites (e.g., Beauheim and Roberts 2002; Roberts et al. 1999). Near-lithostatic pressures due to the plasticity of halite will exceed the hydrostatic pressures from most situations where dissolution is postulated within an otherwise apparently normal sequence of bedded halite. Powers et al. (2001), Holt and Powers (2010, 2011), and Powers and Holt (2021) have explained in varying detail how this information contradicts assumptions and assertions about specific instances of “deep” dissolution in these bedded evaporites.

In addition, associations such as those by Davies (1983) to explain variations in the evaporite sequence by dissolution are now more readily tested due to the additional drilling in the Delaware Basin. Powers and Holt (2021) provide an example; drilling in the Bell Lake “sink” reveals there is no breccia pipe as has been suggested (e.g., Anderson 1978).

SCR-4.2.4.2.6 Collapse Breccias at Basin Margins

Collapse breccias are present at several places around the margins of the Delaware Basin. Their formation is attributed to relatively fresh groundwater from the Capitan Limestone that forms the margin of the basin. Collapse breccias corresponding to features on geophysical records

that have been ascribed to deep dissolution have not been found in boreholes away from the margins. These features have been reinterpreted as the result of early dissolution prior to the deposition of the Salado.

Research continues on the western margin of the Central Basin Platform, in part because the collapse areas and alluvial fill can contain significant volumes of fresh to low-salinity waters. Recent work includes Johnson (2005) and Powers and Holt (2021). Collapse structure interpreted on geophysical log data of the Rustler Formation top and base are included in Ewing et al. (2012, figs. 4.2.1 and 4.2.2).

SCR-4.2.4.2.7 Summary of Deep Dissolution

Deep dissolution features have been identified within the Delaware Basin, but only in marginal areas underlain by Capitan Reef. There is a low probability that deep dissolution will occur sufficiently close to the waste panels over the regulatory period to affect groundwater flow in the immediate region of the WIPP. Deep dissolution at the WIPP site has therefore been eliminated from PA calculations on the basis of low probability of occurrence over the next 10,000 yrs.

SCR-4.2.4.3 **FEP Number: N22**
FEP Title: Fracture Infill

SCR-4.2.4.3.1 Screening Decision: SO-C – Beneficial

The effects of *Fracture Infill* have been eliminated from PA calculations on the basis of beneficial consequence to the performance of the disposal system.

SCR-4.2.4.3.2 Summary of New Information

The screening argument for this FEP has been updated to include references to recent geologic studies. This new information does not alter the screening argument or decision.

SCR-4.2.4.3.3 Screening Argument

SCR-4.2.4.3.3.1 Mineralization

Precipitation of minerals as fracture infills can reduce hydraulic conductivities. The distribution of infilled fractures in the Culebra closely parallels the spatial variability of lateral transmissivity in the Culebra. The secondary gypsum veins in the Rustler have not been dated. Strontium isotope studies (Siegel et al. 1991, pp. 5-53 to 5-57) indicate that the infilling minerals are locally derived from the host rock rather than extrinsically derived, and it is inferred that they reflect an early phase of mineralization and are not associated with recent meteoric waters.

Stable isotope geochemistry in the Rustler has also provided information on mineral stabilities in these strata. Both Chapman (1986, p. 31) and Lambert and Harvey (1987, p. 207) imply that the mineralogical characteristics of units above the Salado have been stable or subject to only

minor changes under the various recharge conditions that have existed during the past 0.6 million yrs—the period since the formation of the Mescalero caliche and the establishment of a pattern of climate change and associated changes in recharge that led to present-day hydrogeological conditions. No changes in climate are expected other than those experienced during this period, and for this reason, no changes are expected in the mineralogical characteristics other than those expressed by the existing variability of fracture infills and diagenetic textures. Formation of fracture infills will reduce transmissivities and will therefore be of beneficial consequence to the performance of the disposal system.

The range in age of the Mescalero paleosol (caliche) is being revised to ~ 100-150 kilo annum (ka) based on optically stimulated luminescence (OSL) ages of ~90 ka for sand above the paleosol and ~153 ka for upper Gatuña below the paleosol Hall and Goble (2023a,b). See N50 Soil Development for additional details.

This more recent work reflects new techniques and information but does not change the assessment of this FEP.

SCR-4.3 Subsurface Hydrological FEPs

SCR-4.3.1 Groundwater Characteristics

SCR-4.3.1.1

FEP Numbers: N23, N24, N25, and N27
FEP Titles: Saturated Groundwater Flow (N23)
Unsaturated Groundwater Flow (N24)
Fracture Flow (N25)
Effects of Preferential Pathways (N27)

SCR-4.3.1.1.1 Screening Decision: UP

Saturated Groundwater Flow, *Unsaturated Groundwater Flow*, *Fracture Flow*, and *Effects of Preferential Pathways* are accounted for in PA.

SCR-4.3.1.1.2 Summary of New Information

No new information that affects the screening of these FEPs has been identified since the CRA-2019. A summary of the implementation of these FEPs in PA has been added.

SCR-4.3.1.1.3 Screening Argument

Saturated groundwater flow, unsaturated groundwater flow, fracture flow, and effects of preferential pathways are accounted for in PA calculations of subsurface radionuclide transport to the Land Withdrawal Boundary (LWB). Groundwater flow is discussed in the CCA, Chapter 2.0, Section 2.2.1; and Chapter 6.0, Section 6.4.5 and Section 6.4.6.

SCR-4.3.1.1.4 FEP Implementation in PA

The FEPs *Saturated Groundwater Flow*, *Unsaturated Groundwater Flow*, *Fracture Flow*, and *Effects of Preferential Pathways*, are incorporated in the Culebra Hydrogeology conceptual model and implemented via the MODFLOW Culebra groundwater flow model. The Culebra groundwater model simulates saturated, steady-state flow in the vicinity of the WIPP. Flow is driven by recharge and peripheral fixed-head boundary conditions derived from interpolation of measured groundwater head (Appendix TFIELD-2014). The effect of unsaturated flow, preferential pathways, and fracture flow are accounted for in PA through the estimates of heterogeneous Culebra transmissivity, storativity, anisotropy, and recharge (Appendix TFIELD-2014).

SCR-4.3.1.2 FEP Number: N26
FEP Title: Density Effect on Groundwater Flow

SCR-4.3.1.2.1 Screening Decision: SO-C – Beneficial

Density Effects on Groundwater Flow has been eliminated from PA calculations on the basis of beneficial consequence to the performance of the disposal system.

SCR-4.3.1.2.2 Summary of New Information

The screening argument was updated with a consideration of the repository geometry with replacement and additional waste panels. No other new information that affects the screening of this FEP has been identified since the CRA-2019**.**

SCR-4.3.1.2.3 Screening Argument

The most transmissive unit in the Rustler, and hence the most significant potential pathway for transport of radionuclides to the accessible environment, is the Culebra. The properties of Culebra groundwaters are not homogeneous, and spatial variations in groundwater density (the CCA, Chapter 2.0, Section 2.2.1.4.1.2) could influence the rate and direction of groundwater flow. A comparison of the gravity-driven flow component and the pressure-driven component in the Culebra, however, shows that only in the region to the south of the WIPP are head gradients low enough for density gradients to be significant (Davies 1989, p. 53). Accounting for this variability would rotate groundwater flow vectors towards the east (down-dip) and hence, the fluid in the high-transmissivity zone would move away from the zone. Furthermore, the repository footprint with replacement and additional waste panels is closer to the western edge of the controlled area than the eastern edge, therefore fluid flowing to the east must travel farther before it exits the controlled area. Excluding brine density variations within the Culebra from PA calculations is therefore a conservative assumption, and density effects on groundwater flow have been eliminated from PA calculations on the basis of beneficial consequence to the performance of the disposal system.

SCR-4.3.2 Changes in Groundwater Flow

SCR-4.3.2.1 **FEP Number: N28**
FEP Title: Thermal Effects on Groundwater Flow

SCR-4.3.2.1.1 Screening Decision: SO-C

Natural Thermal Effects on Groundwater Flow have been eliminated from PA calculations on the basis of low consequence to the performance of the disposal system.

SCR-4.3.2.1.2 Summary of New Information

New and previously uncited information has been presented here for completeness, but none affect the screening of this FEP since the CRA-2019.

SCR-4.3.2.1.3 Screening Argument

Sensitive temperature measurements made in AEC-8 (near WIPP) in 1977, after the drillhole had been stable for several years, revealed heat flow of ~ 1 heat flow unit (HFU), consistent with the Southern Great Plains area (Mansure and Reiter, 1977; see N4 Regional Tectonics). The temperature gradient from 4,242 ft to 1,056 ft (lower Castile Formation to upper Salado Formation) was 0.43 degrees Fahrenheit (°F)/100 ft (~0.78 degrees Celsius [°C]/100 m). The temperature gradient from 1,035 ft to 50 ft (upper Salado Formation to near ground level) was 0.85 °F/100 ft (1.55 °C/100 m). The temperatures at upper and lower Culebra Dolomite Member (Rustler Formation), respectively were 74.245 °F (23.469 °C) and 74.428 °F (23.571 °C), respectively. The last known thermal event directly affecting the later Permian evaporite deposits in the northern Delaware Basin is the Yeso Hills dikes and sills dated at 34.45±0.28 million years (Ma) (Attia et al. 2023). This dike system trends northeast from Yeso Hills, passing about 6 miles northwest of the northwest corner of the WIPP site. In this area, samples from mine encounters produce slightly younger ages (e.g., Brookins 1980). Thermal effects of the dike in the potash mines were limited to a distance of 10 m (Brookins 1981) to 12 m (Bodine and Lohr 1978). These most recent known thermal events in the Delaware Basin have no observable effect at the location of WIPP.

Given the generally low permeability in the region and the limited thickness of units in which groundwater flow occurs (for example, the Culebra), natural convection will be too weak to have a significant effect on groundwater flow. No natural FEPs have been identified that could significantly alter the temperature distribution of the disposal system or give rise to thermal effects on groundwater flow. Such effects have therefore been eliminated from PA calculations on the basis of low consequence to the performance of the disposal system.

SCR-4.3.2.2 **FEP Number: N29**
FEP Title: Saline Intrusion (hydrogeological effects)

SCR-4.3.2.2.1 Screening Decision: SO-P

Changes in groundwater flow arising from *Saline Intrusion* have been eliminated from PA calculations on the basis of low probability of occurrence over 10,000 yrs.

SCR-4.3.2.2.2 Summary of New Information

No new information that affects the screening of this FEP has been identified since the CRA-2019.

SCR-4.3.2.2.3 Screening Argument

No natural events or processes have been identified that could result in saline intrusion into units above the Salado or cause a significant increase in fluid density. Natural saline intrusion has therefore been eliminated from PA calculations on the basis of low probability of occurrence over the next 10,000 yrs. Saline intrusion arising from human events such as drilling into a pressurized brine pocket is discussed in FEPs H21 through H24 (Section SCR-5.2.1.1and SCR-5.2.1.2).

SCR-4.3.2.3 **FEP Number: N30**
FEP Title: Freshwater Intrusion (hydrogeological effects)

SCR-4.3.2.3.1 Screening Decision: SO-P

Changes in groundwater flow arising from *Freshwater Intrusion* have been eliminated from PA calculations on the basis of low probability of occurrence over 10,000 yrs.

SCR-4.3.2.3.2 Summary of New Information

This screening argument has been modified by referencing more recent studies on Culebra recharge.

SCR-4.3.2.3.3 Screening Argument

A number of FEPs, including climate change, can result in changes in infiltration and recharge (see discussions for FEPs N53 through N55, Section SCR-4.6.3.1). These changes will affect the height of the water table and, hence, could affect groundwater flow in the Rustler through changes in head gradients. The generally low transmissivity of the Dewey Lake and the Rustler, however, will prevent any significant changes in groundwater density from occurring within the Culebra over the timescales for which increased precipitation and recharge are anticipated. No other natural events or processes have been identified that could result in freshwater intrusion

into units above the Salado or cause a significant decrease in fluid density. Freshwater intrusion has therefore been eliminated from PA calculations on the basis of low probability of occurrence over the next 10,000 yrs.

Recent additional evidence (Sturchio et al. 2014) of Culebra ground-water ages of ~130,000 and ~330,000 years for higher and lower Culebra transmissivities, respectively, support and strengthen earlier conclusions about recharge reaching the Culebra at WIPP is longer, or even order of magnitude longer, than the regulatory period.

SCR-4.3.2.4 **FEP Number: N31**
FEP Title: Hydrological Response to Earthquakes

SCR-4.3.2.4.1 Screening Decision: SO-C

Hydrological Response to Earthquakes has been eliminated from PA calculations on the basis of low consequence to the performance of the disposal system.

SCR-4.3.2.4.2 Summary of New Information

This FEP has been updated to reference new information that relate to seismic activity in the Delaware Basin. This additional information does not affect the screening of this FEP.

SCR-4.3.2.4.3 Screening Argument

SCR-4.3.2.4.3.1 Hydrological Effects of Seismic Activity

There are a variety of hydrological responses to earthquakes. Some of these responses, such as changes in surface-water flow directions, result directly from fault movement. Others, such as changes in subsurface water chemistry and temperature, probably result from changes in flow pathways along the fault or fault zone. According to Bredehoeft et al. (1987, p. 139), further away from the region of fault movement, two types of changes to groundwater levels may take place as a result of changes in fluid pressure.

- The passage of seismic waves through a rock mass causes a volume change, inducing a transient response in the fluid pressure, which may be observed as a short-lived fluctuation of the water level in wells.

- Changes in volume strain can cause long-term changes in water level. A buildup of strain occurs prior to rupture and is released during an earthquake. The consequent change in fluid pressure may be manifested by the drying up or reactivation of springs some distance from the region of the epicenter.

Fluid-pressure changes induced by the transmission of seismic waves can produce changes of up to several meters (several yards) in groundwater levels in wells, even at distances of thousands of kilometers from the epicenter. These changes are temporary, however, and levels typically return to pre-earthquake levels in a few hours or days. Changes in fluid pressure

arising from changes in volume strain persist for much longer periods, but they are only potentially consequential in tectonic regimes where there is a significant buildup of strain. The regional tectonics of the Delaware Basin indicates that such a buildup has a low probability of occurring over the next 10,000 yrs (see FEPs N3 and N4, Section SCR-4.1.2.1).

The expected level of seismic activity in the region of the WIPP will be of low consequence to the performance of the disposal system in terms of groundwater flow or contaminant transport. Changes in groundwater levels resulting from more distant earthquakes will be too short in duration to be significant. Thus, hydrological response to earthquakes has been eliminated from PA calculations on the basis of low consequence to the performance of the disposal system.

Recent increases in seismic events (see N12 Seismic Activity, Section SCR-4.2.2.4) in the Delaware Basin are commonly designated as "induced seismicity" and attributed to, or associated with, petroleum activities (salt water disposal, hydrofracking, production). Within 50 km of WIPP, 110 events were recorded during the first half of calendar year 2023 (Litherland and Record 2023a,b). The maximum M_L was 3.3. Seventy-five were below M_L 1.8, the apparent magnitude of completeness (Litherland 2023). The average distance from WIPP was 33.8 km, with the closest at 7.2 km. The events are not assigned natural or induced origins.

Hydrological responses, as noted above, are not expected to differ for induced seismic events. Ingebritsen and Manga (2019) review the developing science around the hydrogeology of earthquakes. They particularly note that "permeability is not a static property." They also note that such temporal changes of permeability (as might be associated with recent seismicity) have not yet received much attention because spatial variations are comparatively large. Most attempts to use earthquake data to estimate hydraulic properties appear to use large magnitude events which may be at significant distances. These efforts commonly combine other stimuli, such as Earth tides, atmospheric tides, barometric variations, as well as seismic events to estimate hydraulic properties. These approaches have not been utilized for WIPP; the spatial variation (6-7 orders of magnitude) and distribution of transmissivity are the principal controls over fluid flow in the Culebra.

SCR-4.3.2.5 **FEP Number: N32**
FEP Title: Natural Gas Intrusion

SCR-4.3.2.5.1 Screening decision: SO-P

Changes in groundwater flow arising from *Natural Gas Intrusion* have been eliminated from PA calculations on the basis of low probability of occurrence over 10,000 yrs.

SCR-4.3.2.5.2 Summary of New Information

This FEP has been updated with new references and information regarding gas producing intervals and comments from the EPA on the CRA-2019.

SCR-4.3.2.5.3 Screening Argument

Hydrocarbon resources are present in formations beneath the WIPP (the CCA, Chapter 2.0, Section 2.3.1.2), and natural gas is extracted from these formations. These reserves are, however, some 1,830-2,440 m (6,000-8,000 ft) below the surface (Melzer and Hall 2023), and no natural events or processes have been identified that could result in natural gas intrusion into the Salado or the units above. Natural gas intrusion has therefore been eliminated from PA calculations on the basis of low probability of occurrence over the next 10,000 yrs.

SCR-4.4 Subsurface Geochemical FEPs

SCR-4.4.1 Groundwater Geochemistry

SCR-4.4.1.1 **FEP Number: N33**
FEP Title: Groundwater Geochemistry

SCR-4.4.1.1.1 Screening Decision: UP

Groundwater Geochemistry in the hydrological units of the disposal system is accounted for in PA.

SCR-4.4.1.1.2 Summary of New Information

Culebra geochemistry continues to be investigated. Recent new data and analysis of trends through time show modest changes and refinement of hydrogeochemical facies long associated with the Culebra (e.g., Kirkes et al. 2022; Appendix HYDRO-2026). The screening decision for this FEP is not changed.

SCR-4.4.1.1.3 Screening Argument

The most important aspect of groundwater geochemistry in the region of the WIPP in terms of chemical retardation and colloid stability is salinity. Groundwater geochemistry is discussed in detail in the CCA, Chapter 2.0, Section 2.2 and Section 2.4 and summarized here. The Delaware Mountain Group, Castile, and Salado contain basinal brines. Waters in the Castile and Salado are at or near halite saturation. Above the Salado, groundwaters are also relatively saline, and groundwater quality is poor in all of the permeable units. Waters from the Culebra vary spatially in salinity and chemistry. They range from saline sodium chloride-rich waters to brackish calcium sulfate-rich waters. In addition, a range of magnesium-to-calcium ratios has been observed, and some waters reflect the influence of potash mining activities, having elevated potassium-to-sodium ratios. Waters from the Santa Rosa are generally of better quality than those from the Rustler.

Kirkes et al. (2022) and Appendix HYDRO-2026 report recent geochemical data from the Culebra. Hydrogeochemical facies were developed much earlier for Culebra geochemistry at and around the WIPP site. The newer data, when compared to earlier results, are mainly

consistent with previous hydrogeochemical facies distribution. Kirkes et al. (2022) refined some boundaries; the work also resulted in finer definitions of ionic strength ranges and associated Mg/Ca ratios for each facies.

A correlation analysis of chemistry at all Culebra wells provides details of relationships between different parameters. Na^+/Cl^- and Ca^{2+}/Mg^{2+} are each highly correlated, indicating heavy influence of halite (NaCl) and dolomite ($CaMg(CO_3)_2$). SO_4^{2-} is correlated with K^+ and Cl^-, indicating possible presence of minerals polyhalite and/or carnallite as has previously been postulated. The detail of geological implications of some of these correlations have not been investigated.

Kirkes et al. (2022) further examined indicators of dolomite supersaturation in Culebra waters, finding supersaturation mainly east of the center of WIPP and west of WIPP in Nash Draw and somewhat following the distribution of halite in the lower Los Medaños Member. The molar ratio of Ca^{2+} to SO_4^{2-} was related to gypsum dissolution to compare with previous geological observations, finding general agreement.

SCR-4.4.1.1.4 FEP Implementation in PA

Salado and Castile brine geochemistry is accounted for in PA calculations of the actinide (An) source term (the CCA, Chapter 6.0, Section 6.4.3.4). In the Salado, the brine geochemistry is part of the Dissolved Actinide Source Term conceptual model and the closely related Colloidal Actinide Source Term conceptual model, as implemented in the PA codes EQ3/6 and PANEL. Culebra groundwater geochemistry is accounted for in the retardation factors used in PA calculations of actinide transport (see the CCA, Chapter 6.0, Section 6.4.6.2). In the Culebra, groundwater geochemistry is part of the Transport of Dissolved Actinides in the Culebra conceptual model and the closely related Transport of Colloidal Actinides in the Culebra conceptual model, as implemented in the PA code SECOTP2D.

SCR-4.4.1.2 FEP Numbers: N34 and N38

FEP Titles: **Saline Intrusion (N34)**
Effects of Dissolution (N38)

SCR-4.4.1.2.1 Screening Decision: SO-C

The effects of *Saline Intrusion* and *Dissolution* on groundwater chemistry have been eliminated from PA calculations on the basis of low consequence to the performance of the disposal system.

SCR-4.4.1.2.2 Summary of New Information

The screening argument for these FEPs has been updated with new references and information. The screening decision has not changed.

SCR-4.4.1.2.3 Screening Argument

Saline intrusion and effects of dissolution are considered together in this discussion because dissolution of minerals such as halite (NaCl), anhydrite ($CaSO_4$), or gypsum ($CaSO_4 \cdot 2H_2O$) (N38) could – in the most extreme case – increase the salinity of groundwaters in the Culebra to levels characteristic of those expected after saline intrusion (N34).

No natural events or processes have been identified that could result in saline intrusion into units above the Salado.

The possibility that dissolution of halite, anhydrite, or gypsum might result in a significant increase in the salinity of low- to moderate-ionic-strength groundwaters in the Culebra also appears unlikely. Halite occurs below the Culebra in the Los Medaños under most of the WIPP site (e.g., Siegel et al. 1991, Figure 1-13). This halite interval, designated H-1, in the lower Los Medaños, extends across the expected Culebra off-site transport pathway (the direction of flow from the point[s] at which brines from the repository would enter the Culebra, flow towards the south or south-southeast, and eventually to the boundary of the WIPP site) (Powers et al. 2003). H-2, the halite interval more immediately below the Culebra, is almost non-existent across WIPP, while H-3, the halite in the middle of the Tamarisk Member, exists across a narrow area along the eastern boundary of WIPP (Powers et al. 2003). Salinity of Culebra waters increases eastward across the WIPP site towards the limits of these two (H-2, H-3) halitic intervals (.e.g., Kirkes et al. 2022). This situation is generally addressed as conceptual model 2 (Holt and Powers 2010, figure 9) where diffusion is expected to be the dominant process at the dissolution margin, limiting both solute production and local movement of the solute into the general groundwater pathway. Sturchio et al. (2014, p. 17) include similar arguments for this area while also showing that a much greater ^{81}Kr -based model age (based on SNL-8 data) is consistent with very slow movement in a zone dominated by diffusion transport. Flow-model travel time from the artificial recharge boundary north of WIPP to a point immediately south of WIPP is greater than 10,000 years, and the ^{81}Kr -based model is significantly longer (~x4). The flow-model, if unchanged through the regulatory period, indicates any saline intrusion through this pathway would likely already be detected. The ^{81}Kr model times indicate that a saline intrusion would already have to be well within the model domain (and sample area) to reach the disposal area within the regulatory period.

A dissolution-induced increase in the salinity of Culebra groundwaters is unlikely. Halite beds within the Rustler have been areally limited by depositional processes with relatively smaller areas along original halite margins subject to post-depositional dissolution (e.g., Holt and Powers 1988). The Rustler halite margins are being affected mainly by the slow process of diffusion with advection becoming more important to the west, away from the halite margin. The general pattern of salinity increases to the east are consistent with this process. This contrasts with the assumed vertical hydraulic conductivities and infiltration into the Rustler across this same area (of bedded halite above and below the Culebra) used to develop the "basin model" (e.g., Corbet and Knupp 1996).

Injection of Castile or Salado brines into the Culebra as a result of human intrusion, an anthropogenically induced event, was included in past PA calculations. Laboratory studies carried out to evaluate radionuclide transport in the Culebra following human intrusion produced data that can also be used to evaluate the consequences of natural saline intrusion.

Nevertheless, saline intrusion would not affect the predicted transport of thorium (Th), uranium (U), plutonium (Pu), and americium (Am) in the Culebra. This is because (1) the laboratory studies that quantified the retardation of Th, U, Pu, and Am for the CCA PA were carried out with both moderate-ionic-strength solutions representative of Culebra groundwaters along the expected off-site transport pathway and high-ionic-strength solutions representative of brines from the Castile and the Salado (Brush 1996; Brush and Storz 1996); and (2) the results obtained with the Castile and Salado brines were – for the most part – used to predict the transport of Pu(III) and Am(III); Th(IV), U(IV), Np(IV), and Pu(IV); and U(VI). The results obtained with the saline solutions were used for these actinide oxidation states because the extent to which saline and Culebra brines will mix along the offsite transport pathway in the Culebra was unclear at the time of the CCA PA; therefore, Brush (1996) and Brush and Storz (1996) recommended that PA use the results that predict less retardation. In the case of Pu(III) and Am(III); Th(IV), U(IV), Np(IV), and Pu(IV); and U(VI), the retardation distribution coefficient (K_ds) obtained with the saline solutions were somewhat lower than those obtained with the Culebra fluids

Finally, it is important to reiterate that the use of results from laboratory studies with saline solutions to predict radionuclide transport in the Culebra for previous PAs and the CRA-2026 PA implement the effects of saline intrusion caused by human intrusion, not natural saline intrusion. The conclusions that natural saline intrusion is unlikely, that significant dissolution is unlikely, and that these events or processes would have no significant consequence – in the unlikely event that they occur – continue to be valid.

SCR-4.4.1.3 **FEP Numbers: N35, N36, and N37**
FEP Titles: Freshwater Intrusion (Geochemical Effects) (N35)
Changes in Groundwater Eh (N36)
Changes in Groundwater pH (N37)

SCR-4.4.1.3.1 Screening Decision: SO-C

The effects of *Freshwater Intrusion* on groundwater chemistry have been eliminated from PA calculations on the basis of low consequence to the performance of the disposal system. *Changes in Groundwater Eh* and *Changes in Groundwater pH* have been eliminated from PA calculations on the basis of low consequence to the performance of the disposal system.

SCR-4.4.1.3.2 Summary of New Information

Results of Culebra groundwater age estimates derived from analyses of radiokrypton isotopic ratios were added to the screening argument (Sturchio et al. 2014; Sturchio 2016). No other new information that affects the screening of this FEP has been identified since the CRA-2019.

SCR-4.4.1.3.3 Screening Argument

Natural changes in the groundwater chemistry of the Culebra and other units that resulted from saline intrusion or freshwater intrusion could potentially affect chemical retardation and the stability of colloids. Changes in groundwater Eh and groundwater pH could also affect the migration of radionuclides (see FEPs W65 to W70, Section SCR-6.5.5.2, Section SCR-6.5.5.3, Section SCR-6.5.6.1, and Section SCR-6.5.6.2). No natural EPs have been identified that could result in saline intrusion into units above the Salado, and the magnitude of any natural temporal variation from the effects of dissolution on groundwater chemistry, or because of changes in recharge, is likely to be no greater than the present spatial variation. These FEPs related to the effects of future natural changes in groundwater chemistry have been eliminated from PA calculations on the basis of low consequence to the performance of the disposal system. See Appendix SOTERM-3.2 and Appendix GEOCHEM-4.1.3 for a discussion of WIPP brine chemistry where a stronger case that the local geochemistry of emplaced waste will predominate continues to be made.

The most likely mechanism for (natural) freshwater intrusion into the Culebra (N35), changes in groundwater Eh (N36), and changes in groundwater pH (N37) is (natural) recharge of the Culebra (other FEPs consider possible anthropogenically induced recharge). These three FEPs are closely related because an increase in the rate of recharge could reduce the ionic strength(s) of Culebra groundwaters, possibly enough to significantly dilute the Culebra with fresh water, at least temporarily. Recharge driven dilution reduces the ionic strength, altering the chemical environment by decreasing the concentration of dissolved salts. The reduction in ionic strength can influence the solubility, speciation, and sorption behavior of radionuclides. Concurrently, if atmospheric oxygen remains dissolved during recharge, Eh may increase, shifting the redox conditions toward more oxidizing states. An increase in the Eh of Culebra groundwaters could potentially oxidize Pu from the relatively immobile III and IV oxidation states (Pu(III) and Pu(IV)) – the oxidation states expected under current conditions (Appendix SOTERM-5.5 and SOTERM-6.4) – to the relatively mobile V and VI oxidation states (Pu(V) and Pu(VI)). Similarly, recharge of the Culebra with freshwater could also change the pH of Culebra groundwaters from the currently observed range of about six to seven to mildly acidic values, thus (possibly) altering the retardation of dissolved radionuclides.

There is still considerable uncertainty regarding the extent and timing of recharge to the Culebra. Lambert (1986), Lambert and Carter (1987), and Lambert and Harvey (1987) used a variety of stable and radiogenic isotopic-dating techniques to conclude that the Rustler (and the Dewey Lake) has been a closed hydrologic systems for several thousand to a few tens of thousands of yrs. In this interpretation, the last significant recharge of the Rustler occurred during the late Pleistocene in response to higher levels of precipitation and infiltration associated with the most recent continental glaciation of North America, and the current flow field in the Culebra is the result of the slow discharge of groundwater from this event. Other investigators have agreed that it is possible that Pleistocene recharge has contributed to present-day flow patterns in the Culebra, but that current patterns are also consistent with significant current recharge (Haug et al. 1987; Davies 1989). Still others (Chapman 1986 and

1988) have rejected Lambert's interpretations in favor of exclusively modern recharge, at least in some areas. For example, the lower ionic strength of Hydrochemical Zone B south of the WIPP site could represent dilution of Culebra groundwater with recently introduced meteoric water (see Siegel et al. 1991, pp. 2-57–2-62 and Figure 2-17 for definitions and locations of the four hydrochemical facies in the Culebra in and around the WIPP site). Radiokrypton studies have been completed to help resolve questions around extent and timing of recharge. However, Culebra monitoring well water samples age dated with radiokrypton are similarly inconclusive, with ages ranging from 17,000 yrs in SNL-16 to 79,000 yrs in SNL-8 (Sturchio 2016).

Precipitation and overall climate affects *Freshwater Intrusion*. Precipitation and recharge responses to climate changes are relatively slow and it is unlikely that they reach maximum rates during the 10,000 year regulatory period. The review by Swift et al. (1991), later incorporated in the CCA, Appendix CLI, provides evidence that precipitation in New Mexico did not attain peak precipitation rates (about 60-100% greater than current precipitation) until a few thousand yrs before the last glacial maximum. High-resolution, deep-sea $\delta^{18}O$ data (and other data) reviewed by Servant (2001, Figure 1 and Figure 2) support the conclusion that, although the volume of ice incorporated in continental ice sheets can expand rapidly at the start of a glaciation, attainment of maximum volume does not occur until a few thousand or a few tens of thousands of yrs prior to the termination of the approximately 100,000-yr glaciations that have occurred during the last 0.5 to 1 million years before present (Ma BP). Therefore, it is likely that levels characteristic of the most recent glacial maximum until about 70,000 to 75,000 yrs after glaciations had begun.

Past hydrogeological investigations into the cause and effect from observed water-level rises in the Culebra led to a revised groundwater conceptual model (Appendix TFIELD-2014, Section 3.0). Continuing hydrogeological studies have seen responses to precipitation events in Culebra wells. This is not to say, however, that present-day rainfall actually enters the Culebra wherever a pressure response to rainfall is observed. Rather, the rainfall reaches a water table in a higher stratigraphic unit that is in sufficient hydraulic communication with the Culebra to transmit a *pressure* response rapidly.

However, geochemical impacts of recharge to the Culebra may be screened out regardless of whether recharge is primarily derived from pluvials concomitant with continental glaciation or modern precipitation. If recharge occurs mainly during periods of pluvials associated with periods of continental glaciation, the consequences of such recharge are likely reflected in the ranges of geochemical conditions currently observed in the Culebra as a whole, as well as along the likely offsite transport pathway through the Culebra to the LWB. The effects of pluvial recharge are already included among existing variations in geochemical conditions because (1) as many as 50 continental glaciations and associated pluvials have occurred since the late Pliocene Epoch 2.5 Ma BP; (2) the glaciations and pluvials that have occurred since about 0.5 to 1 Ma BP have been significantly more severe than those that occurred prior to 1 Ma BP (see, for example, Servant 2001); and (3) it is unlikely that precipitation and recharge would reach their maximum levels during the 10,000-yr regulatory period. Considering that conditions in the

Culebra are favorable for retardation of actinides despite the effects of as many as 50 periods of recharge, further impacts from future pluvials are likely to be inconsequential. Therefore, the effects of future natural changes in groundwater chemistry have been eliminated from PA calculations on the basis of low consequence to the performance of the disposal system.

If, on the other hand, significant recharge occurs throughout both phases of the glacial-interglacial cycles, the effects of ongoing pluvial and modern recharge are already reflected by existing variations in geochemical conditions and PA input parameters.

SCR-4.5 Geomorphological FEPs

SCR-4.5.1 Physiography

SCR-4.5.1.1 **FEP Number: N39**
FEP Title: Physiography

SCR-4.5.1.1.1 Screening Decision: UP

Relevant aspects of the *Physiography*, geomorphology, and topography of the region around the WIPP are accounted for in PA.

SCR-4.5.1.1.2 Summary of New Information

No new information that affects the screening of this FEP has been identified since the CRA-2019. A summary of the implementation of this FEP has been provided below.

SCR-4.5.1.1.3 Screening Argument

Physiography and geomorphology are discussed in detail in the CCA, Chapter 2.0, Section 2.1.4.

SCR-4.5.1.1.4 FEP Implementation in PA

Physiography is incorporated in the Culebra Hydrogeology conceptual model. Through this conceptual model, Physiography is implemented in the PA as boundary conditions in the basin scale groundwater model and the Culebra fluid flow model. Both the basin scale groundwater model and the Culebra fluid flow model use major topographic features to locate no-flow boundary conditions. The Culebra fluid flow model is implemented with the PA code MODFLOW6.

SCR-4.5.1.2 **FEP Number: N40**
FEP Title: Impact of a Large Meteorite

SCR-4.5.1.2.1 Screening Decision: SO-P

Disruption arising from the *Impact of a Large Meteorite* has been eliminated from PA calculations on the basis of low probability of occurrence over 10,000 yrs.

SCR-4.5.1.2.2 Summary of New Information

No new information that affects the screening of this FEP has been identified since the CRA-2019.

SCR-4.5.1.2.3 Screening Argument

Meteors frequently enter the Earth's atmosphere, but most of these are small and burn up before reaching the ground. Of those that reach the ground, most produce only small impact craters that would have no effect on the postclosure integrity of a repository 650 m (2,150 ft) below the ground surface. While the depth of a crater may be only one-eighth of its diameter, the depth of the disrupted and brecciated material is typically one-third of the overall crater diameter (Grieve 1987, p. 248). Direct disruption of waste at the WIPP would only occur with a crater larger than 1.8 km (1.1 mi) in diameter. Even if waste were not directly disrupted, the impact of a large meteorite could create a zone of fractured rocks beneath and around the crater. The extent of such a zone would depend on the rock type. For sedimentary rocks, the zone may extend to a depth of half the crater diameter or more (Dence et al. 1977, p. 263). The impact of a meteorite causing a crater larger than 1 km (0.6 mi) in diameter could thus fracture the Salado above the repository.

Geological evidence for meteorite impacts on Earth is rare because many meteorites fall into the oceans and erosion and sedimentation serve to obscure craters that form on land. Dietz (1961) estimated that meteorites that cause craters larger than 1 km (0.6 mi) in diameter strike the Earth at the rate of about one every 10,000 yrs (equivalent to about 2×10^{-13} impacts per square kilometer [km^2] per yr). Using observations from the Canadian Shield, Hartmann (1965, p. 161) estimated a frequency of between 0.8×10^{-13} and 17×10^{-13} impacts/km^2/yr for impacts causing craters larger than 1 km (0.6 mi). Frequencies estimated for larger impacts in studies reported by Grieve (1987, p. 263) can be extrapolated to give a rate of about 1.3×10^{-12} impacts/km^2/yr for craters larger than 1 km (0.6 mi). It is commonly assumed that meteorite impacts are randomly distributed across the Earth's surface, although Halliday (1964, pp. 267-277) calculated that the rate of impact in polar regions would be some 50 to 60 percent of that in equatorial regions. The frequencies reported by Grieve (1987) would correspond to an overall rate of about 1 per 1,000 yrs on the basis of a random distribution.

Assuming the higher estimated impact rate of 17×10^{-13} impacts per square kilometer per yr for impacts leading to fracturing of sufficient extent to affect a deep repository, and assuming a repository footprint of 1.4 km × 1.6 km (0.9 mi × 1.0 mi) for the WIPP, yields a frequency of about 4×10^{-12} impacts per yr for a direct hit above the repository. This impact frequency is several orders of magnitude below the screening threshold of 10^{-4} per 10,000 yrs provided in 40 CFR 194.32(d).

Meteorite hits directly above the repository footprint are not the only impacts of concern, however, because large craters may disrupt the waste panels even if the center of the crater is outside the repository area. It is possible to calculate the frequency of meteorite impacts that could disrupt a deep repository such as the WIPP by using the conservative model of a cylinder

of rock fractured to a depth equal to one-half the crater diameter, as shown in the CCA, Appendix SCR, Figure SCR-1. The area within which a meteorite could impact the repository is calculated by

$$S_D = \left(L + 2 \times \frac{D}{2}\right) \times \left(W + 2 \times \frac{D}{2}\right), \quad \text{(SCR.1)}$$

where

L = length of the repository footprint (km)
W = width of the repository footprint (km)
D = diameter of the impact crater (km)
S_D = area of the region where the crater would disrupt the repository (km^2)

There are insufficient data on meteorites that have struck the Earth to derive a distribution function for the size of craters directly. Using meteorite impacts on the moon as an analogy, however, Grieve (1987, p. 257) derived the following distribution function:

$$F_D \propto D^{-1.8} \quad \text{(SCR.2)}$$

where

F_D = frequency of impacts resulting in craters larger than D (impacts/km^2/yr).

If $f(D)$ denotes the frequency of impacts giving craters of diameter D, then the frequency of impacts giving craters larger than D is

$$F_D = \int_D^{\infty} f(D)dD \quad \text{(SCR.3)}$$

and

$$f(D) = F_1 \times 1.8 \times D^{-2.8}, \quad \text{(SCR.4)}$$

where

F_1 = frequency of impacts resulting in craters larger than 1 km (impacts/km^2/yr)
$f(D)$ = frequency of impacts resulting in craters of diameter D (impacts/km^2/yr)

The overall frequency of meteorite impacts, in the size range of interest, that could disrupt or fracture the repository is thus given by

$$N = \int_{2h}^{M} f(D) \times S_D dD, \quad \text{(SCR.5)}$$

where

h = depth to repository (kilometers),
M = maximum size of meteorite considered (kilometers)

N = frequency of impacts leading to disruption of the repository (impacts per yr), and

$$N = 1.8F_1\left[\frac{(M)^{0.2}-(2h)^{0.2}}{0.2} - LW\frac{(M)^{-1.8}-(2h)^{-1.8}}{1.8} - (L+W)\frac{(M)^{-0.8}-(2h)^{-0.8}}{0.8}\right]. \quad \text{(SCR.6)}$$

Conservatively using the size (933 km [550 mi]) of the largest known asteroid, Ceres (Tedesco 1992), for the maximum size considered and if it is assumed that the repository is located at a depth of 650 m (2,150 ft) and has a footprint area of 1.4 km × 1.6 km (0.9 mi × 1.0 mi) and that meteorites creating craters larger than 1 km in diameter hit the Earth at a frequency (F_1) of 17 × 10^{-13} impacts/km^2/yr, then Equation (SCR.6) gives a frequency of approximately 5.6 × 10^{-11} impacts per yr for impacts disrupting the repository. If impacts are randomly distributed over time, this corresponds to a probability of 5.6 × 10^{-7} over 10,000 yrs.

Similar calculations have been performed that indicate rates of impact of between 10^{-12} and 10^{-13} per yr for meteorites large enough to disrupt a deep repository (see, for example, Hartmann 1979, Kärnbränslesakerhet 1978, Claiborne and Gera 1974, Cranwell et al. 1990, and Thorne 1992). Meteorite impact can thus be eliminated from PA calculations on the basis of low probability of occurrence over 10,000 yrs.

Assuming a random or nearly random distribution of meteorite impacts, cratering at any location is inevitable given sufficient time. Although repository depth and host-rock lithology may reduce the consequences of a meteorite impact, there are no repository locations or engineered systems that can reduce the probability of impact over 10,000 yrs.

SCR-4.5.1.3 **FEP Number: N41 and N42**
FEP Titles: Mechanical Weathering (N41)
Chemical Weathering (N42)

SCR-4.5.1.3.1 Screening Decision: SO-C

The effects of *Chemical Weathering* and *Mechanical Weathering* have been eliminated from PA calculations on the basis of low consequence to the performance of the disposal system.

SCR-4.5.1.3.2 Summary of New Information

No new information that affects the screening of these FEPs has been identified since the CRA-2019.

SCR-4.5.1.3.3 Screening Argument

Mechanical weathering and chemical weathering are assumed to be occurring at or near the surface around the WIPP site through processes such as exfoliation and leaching. The extent of these processes is limited and they will contribute little to the overall rate of erosion in the area or to the availability of material for other erosional processes. The effects of chemical

weathering and mechanical weathering have been eliminated from PA calculations on the basis of low consequence to the performance of the disposal system.

SCR-4.5.1.4 **FEP Numbers: N43, N44, and N45**
FEP Titles: Aeolian Erosion (N43)
Fluvial Erosion (N44)
Mass Wasting (N45)

SCR-4.5.1.4.1 Screening Decision: SO-C

The effects of *Fluvial Erosion*, *Aeolian Erosion*, and *Mass Wasting* in the region of the WIPP have been eliminated from PA calculations on the basis of low consequence to the performance of the disposal system.

SCR-4.5.1.4.2 Summary of New Information

The DOE monitors and documents changes to mean annual rainfall and temperature in the Waste Isolation Pilot Plant Annual Site Environment Report (U.S. DOE 2025b). This screening argument has been updated with the most recent data.

SCR-4.5.1.4.3 Screening Argument

The geomorphological regime on the Mescalero Plain (Los Medaños) in the region of the WIPP is dominated by aeolian processes. Dunes are present in the area, and although some are stabilized by vegetation, aeolian erosion will occur as they migrate across the area. Old dunes will be replaced by new dunes, and no significant changes in the overall thickness of aeolian material are likely to occur.

The average yearly rainfall recorded at the meteorological tower since 1996 is 269.38 millimeter (mm) (10.61 inches [in]) (U.S. DOE 2025b). This is too low to cause perennial streams, and the relief in the area is too low for extensive sheet flood erosion during storms. An increase in precipitation to around 61 centimeters (cm) (24 in.) per yr in cooler climatic conditions could result in perennial streams, but the nature of the relief and the presence of dissolution hollows and sinks will ensure that these streams remain small. Significant fluvial erosion is not expected during the next 10,000 yrs.

Mass wasting (the downslope movement of material caused by the direct effect of gravity) is important only in terms of sediment erosion in regions of steep slopes. In the vicinity of the WIPP, mass wasting will be insignificant under the climatic conditions expected over the next 10,000 yrs.

Erosion from wind, water, and mass wasting will continue in the WIPP region throughout the next 10,000 yrs at rates similar to those occurring at present. These rates are too low to affect the performance of the disposal system significantly. Thus, the effects of fluvial erosion, aeolian erosion, and mass wasting have been eliminated from PA calculations on the basis of low consequence to the performance of the disposal system.

SCR-4.5.1.5 **FEP Number: N50**
FEP Title: Soil Development

SCR-4.5.1.5.1 Screening Decision: SO-C

Soil Development has been eliminated from PA calculations on the basis of low consequence to the performance of the disposal system.

SCR-4.5.1.5.2 Summary of New Information

The screening argument for this FEP has been updated with references to recent studies that relate to the surface geology in the region around the WIPP. These studies do not alter the screening decision for this FEP.

SCR-4.5.1.5.3 Screening Argument

The Mescalero caliche is a well-developed calcareous remnant of an extensive soil profile across the WIPP site and adjacent areas. Although this unit may be up to 3 m (10 ft) thick, it is not continuous and does not prevent infiltration to the underlying formations. At Nash Draw, this caliche, dated in Lappin et al. (1989, pp. 2-4) at 410,000 to 510,000 yrs old, is present in collapse blocks, indicating some growth of Nash Draw in the late Pleistocene. Localized gypsite spring deposits about 25,000 yrs old occur along the eastern flank of Nash Draw, but the springs are not currently active. The Berino soil, interpreted as 333,000 yrs old (Rosholt and McKinney 1980, Table 5), is a thin soil horizon above the Mescalero caliche. The persistence of these soils on the Livingston Ridge and the lack of deformation indicates the relative stability of the WIPP region over the past half-million yrs.

More recent and extensive studies of the Mescalero paleosol (caliche) and overlying geologically young deposits have been summarized by Hall and Goble (2023a), with more limited discussion for the 2023 New Mexico Geological Society fall field conference (Hall and Goble 2023b; Attia et al. 2023).

Attia et al. sampled the Gatuña Formation along Livingston Ridge below the Lava Creek B ash (~0.63 Ma). The sediment sample yielded detrital sanidine ages with a youngest age ≤ 1.3 Ma. As this sample is close to a contact with underlying Dewey Lake Formation, Attia et al. conclude that the Gatuña at this location is Quaternary in age.

Hall and Goble (2023a, b) report OSL ages of upper Gatuña from 3 locations, each underlying the Mescalero paleosol and ranging from ~169 ka to 153 ka.

The Mescalero sand sheet, including paleosols above the Mescalero paleosol, have been investigated extensively by Hall and Goble (2023a). including sampling from areas relatively close to WIPP. The oldest part of the sand sheet ("Lower sand") yields OSL ages of ~90 ka. A sample of the Berino soil from near the intersection of NM 128 and South Access Road (to WIPP) was sampled and yielded an OSL age of ~52 ka (Hall and Goble 2012).

These ages contrast with the ~0.5 Ma age previously assigned to the Mescalero paleosol and ~330 ka age for the Berino. These ages reflect at least more recent techniques and more reliable inferences about the period of stability reflected by the soil formation of the Mescalero. Nevertheless, these ages represent a long period of stability for formation and preservation at the site relative to the period of performance and do not change the assessment.

Continued growth of caliche may occur in the future but will be of low consequence in terms of its effect on infiltration. Other soils in the area are not extensive enough to affect the amount of infiltration that reaches underlying aquifers. Soil development has been eliminated from PA calculations on the basis of low consequence to the performance of the disposal system.

SCR-4.6 Surface Hydrological FEPs

SCR-4.6.1 Depositional Processes

SCR-4.6.1.1 **FEP Numbers: N46, N47, N48, and N49**
FEP Titles: Aeolian Deposition (N46)
Fluvial Deposition (47)
Lacustrine Deposition (N48)
Mass Waste (Deposition) (N49)

SCR-4.6.1.1.1 Screening Decision: SO-C

The effects of *Aeolian Deposition*, *Fluvial Deposition*, and *Lacustrine Deposition* and sedimentation in the region of the WIPP have been eliminated from PA calculations on the basis of low consequence to the performance of the disposal system.

SCR-4.6.1.1.2 Summary of New Information

No new information that affects the screening of these FEPs has been identified since the CRA-2019.

SCR-4.6.1.1.3 Screening Argument

The geomorphological regime on the Mescalero Plain (Los Medaños) in the region of the WIPP is dominated by aeolian processes, but although some dunes are stabilized by vegetation, no significant changes in the overall thickness of aeolian material are expected to occur. Vegetational changes during periods of wetter climate may further stabilize the dune fields, but aeolian deposition is not expected to significantly increase the overall thickness of the superficial deposits.

The limited extent of water courses in the region of the WIPP, under both present-day conditions and under the expected climatic conditions, will restrict the amount of fluvial deposition and lacustrine deposition in the region.

Mass wasting (deposition) may be significant if it results in dams or modifies streams. In the region around the WIPP, the Pecos River forms a significant water course some 19 km (12 mi) away, but the broadness of its valley precludes either significant mass wasting or the formation of large impoundments.

Sedimentation from wind, water, and mass wasting is expected to continue in the WIPP region throughout the next 10,000 yrs at the low rates similar to those occurring at present. These rates are too low to significantly affect the performance of the disposal system. Thus, the effects of aeolian deposition, fluvial deposition, and lacustrine deposition and sedimentation resulting from mass wasting have been eliminated from PA calculations on the basis of low consequence.

SCR-4.6.2 Streams and Lakes

SCR-4.6.2.1 **FEPs Number: N51**
FEPs Title: Stream and River Flow

SCR-4.6.2.1.1 Screening Decision: SO-C

Stream and River Flow has been eliminated from PA calculations on the basis of low consequence to the performance of the disposal system.

SCR-4.6.2.1.2 Summary of New Information

No new information that affects the screening of this FEP has been identified since the CRA-2019.

SCR-4.6.2.1.3 Screening Argument

No perennial streams are present at the WIPP site, and there is no evidence in the literature indicating that such features existed at this location since the Pleistocene (see, for example, Powers et al. 1978; Bachman 1974, 1981, and 1987b). The Pecos River is approximately 19 km (12 mi) from the WIPP site and more than 90 m (300 ft) lower in elevation. Stream and river flow has been eliminated from PA calculations on the basis of low consequence to the performance of the disposal system.

SCR-4.6.2.2 **FEP Number: N52**
FEP Title: Surface Water Bodies

SCR-4.6.2.2.1 Screening Decision: SO-C

The effects of *Surface Water Bodies* have been eliminated from PA calculations on the basis of low consequence to the performance of the disposal system.

SCR-4.6.2.2.2 Summary of New Information

No new information that affects the screening of this FEP has been identified since the CRA-2019.

SCR-4.6.2.2.3 Screening Argument

No standing surface water bodies are present at the WIPP site, and there is no evidence in the literature indicating that such features existed at this location during or after the Pleistocene (see, for example, Powers et al. 1978, and Bachman 1974, 1981, and 1987b). In Nash Draw, lakes and spoil ponds associated with potash mines are located at elevations 30 m (100 ft) below the elevation of the land surface at the location of the waste panels. There is no evidence in the literature to suggest that Nash Draw was formed by stream erosion or was at any time the location of a deep body of standing water, although shallow playa lakes have existed there at various times. Based on these factors, the formation of large lakes is unlikely and the formation of smaller lakes and ponds is of little consequence to the performance of the disposal system. The effects of surface water bodies have therefore been eliminated from PA calculations on the basis of low consequence to the performance of the disposal system.

SCR-4.6.3 Groundwater Recharge and Discharge

SCR-4.6.3.1 **FEP Numbers: N53, N54, and N55**
FEP Titles: Groundwater Discharge (N53)
Groundwater Recharge (N54)
Infiltration (N55)

SCR-4.6.3.1.1 Screening Decision: UP

Groundwater Recharge, *Groundwater Discharge*, and *Infiltration* are accounted for in PA.

SCR-4.6.3.1.2 Summary of New Information

These FEPs have been updated with additional information. This new information does not change the screening decision. A brief summary of the implementation of these FEPs has been added as well.

SCR-4.6.3.1.3 Screening Argument

The groundwater basin described in the CCA, Chapter 2.0, Section 2.2.1.4 is governed by flow from areas where the water table is high to areas where the water table is low. The height of the water table is governed by the amount of groundwater recharge reaching the water table, which in turn is a function of the vertical hydraulic conductivity and the partitioning of precipitation between evapotranspiration, runoff, and infiltration. Flow within the Rustler is also governed by the amount of groundwater discharge that takes place from the basin. In the region around the WIPP, the principal discharge areas are along Nash Draw and the Pecos River. Groundwater flow modeling accounts for infiltration, recharge, and discharge (the CCA, Chapter 2.0, Section 2.2.1.4 and Chapter 6.0, Section 6.4.10.2).

Groundwater basin modeling, as formulated for the CCA, provided a means of bounding groundwater movement at WIPP under conditions assumed to represent a recent glacial maximum. The basin domain considered extends considerably beyond WIPP boundaries or model domains used to assess performance of the repository. Significant assumptions for the basin model include vertical hydraulic conductivities from ground level to top of (impermeable) Salado across the basin model domain, all recharge is vertical (percolation of precipitation), selected boundaries are groundwater divides, and recharge rates were selected to mimic conditions today as well as assumed conditions of greater recharge resulting in a water table near the land surface (Corbet and Knupp 1996).

The results of the groundwater basin model have been incorporated into PA since the CCA as an uncertain parameter accounting for the uncertainty of future groundwater conditions is implemented as a scaling factor on fluid flow in the Culebra.

Fundamental information about the hydrogeology of the WIPP site and, especially for the Culebra, has significantly increased since the CCA (1996). Vertical hydraulic conductivities assumed for various geological units could be replaced or modified by newer information. However, bedded salt above and below the Culebra in areas of the model basin indicate no vertical conductivity through geologic time and thus no recharge to the Culebra from infiltration. Additionally, halite within the Culebra indicates no horizontal conductivity through geologic time (Beauheim and Holt 1990). These occurrences would also limit boundaries assumed in the original model. Extensive drilling for resources since 1996 also provide a source for new data to refine the geology across the groundwater basin model area although new data are unlikely to change the general structure of the groundwater basin model.

SCR-4.6.3.1.4 FEP Implementation in PA

Groundwater Discharge, *Groundwater Recharge*, and *Infiltration* are accounted for in PA through the Culebra hydrogeology conceptual model. Groundwater Discharge and Groundwater Recharge are simulated in the Culebra groundwater flow model with the software MODFLOW6. Since the 2009 Performance Assessment Baseline Calculation (PABC-2009), recharge in the Culebra flow model has been calibrated by the parameter estimation software PEST++, along with estimates of transmissivity, storativity, and anisotropy (Appendix TFIELD-

2014; Appendix TFIELD-2026). The impact of uncertain future climate conditions on recharge, infiltration, and groundwater discharge was evaluated with the software MWT3D, the results of which were used to derive an uncertain parameter distribution (GLOBAL:CLIMTIDX) implemented as multipliers on fluid flow in the PA Culebra flow model.

SCR-4.6.3.2 **FEP Number: N56**
FEP Title: Changes in Groundwater Recharge and Discharge

SCR-4.6.3.2.1 Screening Decision: UP

Changes in Groundwater Recharge and Discharge arising as a result of climate change are accounted for in PA.

SCR-4.6.3.2.2 Summary of New Information

Recent regional studies (e.g., southwestern United States) related to natural climate change during more recent glacial and interglacial periods provide more specific data regarding metrics such as oxygen isotopes and techniques for determining geologic age. These studies mainly document events and relate them to global standards such as ice cores or marine isotope stages (MIS). Some attempt to explain or discuss the purported meteorological phenomena or processes related to this region (e.g., Wagner et al. 2010; Morrill et al. 2018) in light of new data.

A few of these studies are more closely related geographically to WIPP.

A study of organic compounds from sediments in the Valles Caldera (near Santa Fe, NM) estimated the strength of monsoons during the period ~550,000 - ~360,000 years ago, which includes MIS 11, thought to be similar to the interglacial period of today (Cisneros-Dozal et al. 2014). In general, they found monsoonal strength and variability were greater during such interglacial periods. Nevertheless, they also found an exception during MIS 11 when data indicate higher temperatures and decreased monsoonal strength.

Estancia Basin (east of Albuquerque, NM) has been re-examined as a source of climatic history from 69-10 ka (thousand years). New age data have been combined with indicators of hydrologic conditions to provide a more detailed and consistent relationship between hydrologic conditions and global climatic indicators (Menking et al. 2018).

A core from a stalagmite in Carlsbad Caverns yielded ages and climatic indicators related to conditions from 560 to 145 ka (Railsback et al 2015). Again, the work mainly indicated consistency with global patterns. As others have noted, Railsback et al. (2015) noted that continued warming during the current interglacial period likely will lead to increasing aridity in the region. These newer studies do not change the screening or implementation of this FEP.

SCR-4.6.3.2.3 Screening Argument

Changes in recharge may affect groundwater flow and radionuclide transport in units such as the Culebra and Magenta dolomites. Changes in the surface environment driven by natural climate change are expected to occur over the next 10,000 yrs (see FEPs N59 to N63). Groundwater basin modeling (the CCA, Chapter 2.0, Section 2.2.1.4) indicates that a change in recharge will affect the height of the water table in the area of the WIPP, and that this will in turn affect the direction and rate of groundwater flow.

The present-day water table in the vicinity of the WIPP is within the Dewey Lake at about 980 m (3,215 ft) above mean sea level (the CCA, Chapter 2.0, Section 2.2.1.4.2.1). An increase in recharge relative to present-day conditions would raise the water table, potentially as far as the local ground surface. Similarly, a decrease in recharge could result in a lowering of the water table. The low transmissivity of the Dewey Lake and the Rustler ensures that any such lowering of the water table will be at a slow rate, and lateral discharge from the groundwater basin is expected to persist for several thousand yrs after any decrease in recharge. Under the anticipated changes in climate over the next 10,000 yrs, the water table will not fall below the base of the Dewey Lake, and dewatering of the Culebra is not expected to occur during this period (the CCA, Chapter 2.0, Section 2.2.1.4).

Changes in groundwater recharge and discharge are accounted for in PA through definition of the boundary conditions for flow and transport in the Culebra (the CCA, Chapter 6.0, Section 6.4.9, and Appendix PA-4.9.3). Information from newer sources do not change the assessment that climatic conditions in the future are expected to be in the range of conditions found in the more recent geological past.

SCR-4.6.3.2.4 FEP Implementation in PA

Changes in Groundwater Recharge and Discharge is included in the UP scenario and is associated with the Culebra Hydrogeology conceptual model by use of a sampled parameter to scale flow velocity in the Culebra (Appendix PA-4.9). This is done using the climate scaling factor, which is implemented by the PRESECOTP2D Culebra transport preprocessing code.

SCR-4.6.3.3 FEP Numbers: N57 and N58
FEP Titles: Lake Formation (N57)
River Flooding (N58)

SCR-4.6.3.3.1 Screening Decision: SO-C

The effects of *River Flooding* and *Lake Formation* have been eliminated from PA calculations on the basis of low consequence to the performance of the disposal system.

SCR-4.6.3.3.2 Summary of New Information

No new information that affects the screening of this FEP has been identified since the CRA-2019.

SCR-4.6.3.3.3 Screening Argument

Intermittent flooding of stream channels and the formation of shallow lakes will occur in the WIPP region over the next 10,000 yrs. These may have a short-lived and local effect on the height of the water table but are unlikely to affect groundwater flow in the Culebra.

Future occurrences of playa lakes or other longer-term floods will be remote from the WIPP and will have little consequence on system performance in terms of groundwater flow at the site. There is no reason to believe that any impoundments or lakes could form over the WIPP site itself. Thus, river flooding and lake formation have been eliminated from PA calculations on the basis of low consequence to the performance of the disposal system.

SCR-4.7 Climate EPs

SCR-4.7.1 Climate and Climate Changes

SCR-4.7.1.1 **FEP Numbers: N59 and N60**
FEP Titles: Precipitation (N59)
Temperature (N60)

SCR-4.7.1.1.1 Screening Decision: UP

Precipitation and *Temperature* are accounted for in PA.

SCR-4.7.1.1.2 Summary of New Information

Since the CCA, there have been changes to mean annual rainfall and temperature. DOE publishes the Waste Isolation Pilot Plant Annual Site Environment Report (U.S. DOE 2025b) that includes this data.

SCR-4.7.1.1.3 Screening Argument

The climate and meteorology of the region around the WIPP are described in the CCA, Section 2.5.2. The average yearly rainfall recorded at the meteorological tower since 1996 is 269.38 mm (10.61 in) and mean annual temperature for 2024 was 67.23 °F (19.57 °C) (U.S. DOE 2025b). Precipitation and temperature are important controls on the amount of recharge that reaches the groundwater system and are accounted for in PA by use of a sampled parameter for scaling flow velocity in the Culebra (see Appendix PA-4.9).

SCR-4.7.1.1.4 FEP Implementation in PA

Precipitation (N59) and *Temperature* (N60) are included in the UP scenario and are associated with the Culebra Hydrogeology conceptual model by use of a sampled parameter to scale flow velocity in the Culebra. The climate scaling factor is implemented by the PRESECOTP2D Culebra transport preprocessing code.

SCR-4.7.1.2 **FEP Number: N61**
FEP Title: Climate Change

SCR-4.7.1.2.1 Screening Decision: UP

Climate Change is accounted for in PA.

SCR-4.7.1.2.2 Summary of New Information

No new information that affects the screening of this FEP has been identified since the CRA-2019. A brief summary of the implementation of this FEP has been added.

SCR-4.7.1.2.3 Screening Argument

Climate changes are instigated by changes in the Earth's orbit and by feedback mechanisms within the atmosphere and hydrosphere. Models of these mechanisms, combined with interpretations of the geological record, suggest that the climate will become cooler and wetter in the WIPP region during the next 10,000 yrs as a result of natural causes (Swift 1992). Other changes, such as fluctuations in radiation intensity from the sun and variability within the many feedback mechanisms, will modify this climatic response to orbital changes. The available evidence suggests that these changes will be less extreme than those arising from orbital fluctuations.

The effect of a change to cooler and wetter conditions is considered to be an increase in the amount of recharge, which in turn will affect the height of the water table (see FEPs N53 through N56, Section SCR-4.6.3.1 and SCR-4.6.3.2). The height of the water table across the groundwater basin is an important control on the rate and direction of groundwater flow within the Culebra (see the CCA, Chapter 2.0, Section 2.2.1.4), and hence potentially on transport of radionuclides released to the Culebra through the shafts or intrusion boreholes.

SCR-4.7.1.2.4 FEP Implementation in PA

Climate Change (N61) is included in the UP scenario and is associated with the Culebra Hydrogeology conceptual model by use of a sampled parameter to scale flow velocity in the Culebra (Appendix PA-4.9). The climate scaling factor is implemented by the PRESECOTP2D Culebra transport preprocessing code.

SCR-4.7.1.3 **FEP Numbers: N62 and N63**
FEP Titles: Glaciation (N62)
Permafrost (N63)

SCR-4.7.1.3.1 Screening Decision: SO-P

Glaciation and the effects of *Permafrost* have been eliminated from PA calculations on the basis of low probability of occurrence over 10,000 yrs.

SCR-4.7.1.3.2 Summary of New Information

No new information that affects the screening of these FEPs has been identified since the CRA-2019.

SCR-4.7.1.3.3 Screening Argument

No evidence exists to suggest that the northern part of the Delaware Basin has been covered by continental glaciers at any time since the beginning of the Paleozoic Era. During the maximum extent of continental glaciation in the Pleistocene Epoch, glaciers extended into northeastern Kansas at their closest approach to southeastern New Mexico. There is no evidence that alpine glaciers formed in the region of the WIPP during the Pleistocene glacial periods.

According to the theory that relates the periodicity of climate change to perturbations in the Earth's orbit, a return to a full glacial cycle within the next 10,000 yrs is highly unlikely (Imbrie and Imbrie 1980, p. 951).

Thus, glaciation has been eliminated from PA calculations on the basis of low probability of occurrence over the next 10,000 yrs. Similarly, a number of processes associated with the proximity of an ice sheet or valley glacier, such as permafrost and accelerated slope erosion (solifluction) have been eliminated from PA calculations on the basis of low probability of occurrence over the next 10,000 yrs.

SCR-4.8 Marine FEPs

SCR-4.8.1 Seas, Sedimentation, and Level Changes

SCR-4.8.1.1 **FEP Numbers: N64 and N65**
FEP Titles: Seas and Oceans (N64)
Estuaries (N65)

SCR-4.8.1.1.1 Screening Decision: SO-C

The effects of *Estuaries* and *Seas and Oceans* have been eliminated from PA calculations on the basis of low consequence to the performance of the disposal system.

SCR-4.8.1.1.2 Summary of New Information

No new information that affects the screening of these FEPs has been identified since the CRA-2019.

SCR-4.8.1.1.3 Screening Argument

The WIPP site is more than 800 km (480 mi) from the Pacific Ocean and from the Gulf of America. Estuaries and seas and oceans have therefore been eliminated from PA calculations on the basis of low consequence to the disposal system.

SCR-4.8.1.2 **FEP Numbers: N66 and N67**
FEP Titles: Coastal Erosion (N66)
Marine Sediment Transport and Deposition (N67)

SCR-4.8.1.2.1 Screening Decision: SO-C

Coastal Erosion and *Marine Sediment Transport and Deposition* have been eliminated from PA calculations on the basis of low consequence to the performance of the disposal system.

SCR-4.8.1.2.2 Summary of New Information

No new information that affects the screening of these FEPs has been identified since the CRA-2019.

SCR-4.8.1.2.3 Screening Argument

The WIPP site is more than 800 km (480 mi) from the Pacific Ocean and Gulf of America. The effects of coastal erosion and marine sediment transport and deposition have therefore been eliminated from PA calculations on the basis of low consequence to the performance of the disposal system.

SCR-4.8.1.3 **FEP Number: N68**
FEP Title: Sea Level Changes

SCR-4.8.1.3.1 Screening Decision: SO-C

The effects of both short-term and long-term *Sea Level Changes* have been eliminated from PA calculations on the basis of low consequence to the performance of the disposal system.

SCR-4.8.1.3.2 Summary of New Information

No new information that affects the screening of this FEP has been identified since the CRA-2019.

SCR-4.8.1.3.3 Screening Argument

The WIPP site is some 1,036 m (3,400 ft) above sea level. Global sea level changes may result in sea levels as much as 140 m (460 ft) below that of the present day during glacial periods, according to Chappell and Shackleton (1986, p. 138). This can have marked effects on coastal aquifers. During the next 10,000 yrs, the global sea level can be expected to drop towards this glacial minimum, but this will not affect the groundwater system in the vicinity of the WIPP. Short-term changes in sea level, brought about by events such as meteorite impact, tsunamis, seiches, and hurricanes may raise water levels by several tens of meters. Such events have a maximum duration of a few days and will have no effect on the surface or groundwater systems at the WIPP site. Anthropogenic-induced global warming has been conjectured by Warrick and

Oerlemans (1990, p. 278) to result in longer-term sea level rise. The magnitude of this rise, however, is not expected to be more than a few meters, and such a variation will have no effect on the groundwater system in the WIPP region. Thus, the effects of both short-term and long-term sea level changes have been eliminated from PA calculations on the basis of low consequence to the performance of the disposal system.

SCR-4.9 Ecological FEPs

SCR-4.9.1 Flora and Fauna

SCR-4.9.1.1 **FEP Numbers: N69 and N70**
FEP Titles: Plants (N69)
Animals (N70)

SCR-4.9.1.1.1 Screening Decision: SO-C

The effects of the natural *Plants* and *Animals* (flora and fauna) in the region of the WIPP have been eliminated from PA calculations on the basis of low consequence to the performance of the disposal system.

SCR-4.9.1.1.2 Summary of New Information

No new information that affects the screening of this FEP has been identified since the CRA-2019.

SCR-4.9.1.1.3 Screening Argument

The terrestrial and aquatic ecology of the region around the WIPP is described in the CCA, Chapter 2.0, Section 2.4.1. The plants in the region are predominantly shrubs and grasses. The most conspicuous animals in the area are jackrabbits and cottontail rabbits. The effects of this flora and fauna in the region have been eliminated from PA calculations on the basis of low consequence to the performance of the disposal system.

SCR-4.9.1.2 **FEP Number: N71**
FEP Title: Microbes

SCR-4.9.1.2.1 Screening Decision: SO-C

The effects of indigenous *Microbes* on the region of the WIPP have been eliminated from PA calculations on the basis of low consequence to the performance of the disposal system.

SCR-4.9.1.2.2 Summary of New Information

The screening decision for FEP N71 “Microbes” was changed to remove the reference to “UP-for colloidal effects and gas generation”. This FEP has been edited to clearly identify that N71 relates only to naturally-occurring microbes in soils and groundwater near WIPP, and to

reference newer experiments. Colloidal effects and gas generation due to microbial degradation are no longer mentioned in FEP N71 and are solely discussed in FEP W44, "Degradation of Organic Material."

SCR-4.9.1.2.3 Screening Argument

This FEP addresses the possible role of indigenous microorganisms from the WIPP far-field as biocolloids involved in the transport of radionuclides through the Culebra. The assumption is that affected microbes will not be transported through the Culebra dolomite member due to size exclusion. In reality, cell mobilization depends not only on the traits of the microbes but also on features in the Culebra, and the argument is better made taking into consideration all of these factors, rather than size alone.

The Culebra displays characteristics of a double porosity medium in which solutes are carried by groundwater flow through fractures and by slow advection or diffusion in fracture-bound matrix blocks. Transport simulations predict that very little radionuclide mass breaks through at the Land Withdrawal Boundary by 10,000 years (Kuhlman 2010).

Microorganisms are not like particles or dissolved radionuclides. Their potential passage through the Culebra will depend on several other factors, including: their size distribution and morphology as a function of growth stage, organism type, the presence of nutrients; the size distribution of dolomite grains; cell dispersion as a function of fluid viscosity, flow rates and cell size/density; sorption/desorption from grains as a function of pH, ionic strength, flow rate, organism type, growth stage, surface roughness, and collision/contact frequency; their ability to establish biofilms, as a function of numbers, flow rate, and nutrient flux.

Microbial size and shape influence filtration in porous media. If the "limiting dimension" of a cell is more than 5% of the mean diameter of grain particles in the porous matrix, then filtration-based retardation can be significant (Herzig et al. 1970; Pepper et al. 2014). Cell diameters typically range from 0.2-2.0 micrometers (µm) (Madigan et al. 2018), with the lowest recorded diameter of 0.12 µm in a marine bacterium (Rappé et al. 2002). The smallest documented archaea are nanohaloarchaea measured at 0.3-0.5 µm (Huber et al. 2002). Cell lengths are more variable and can reach up to hundreds of microns in length. Cell shape also influences retardation, and smaller, rounder morphologies tend to move more quickly through porous media. Table SCR-2 provides sizes of microorganisms present in WIPP groundwaters.

Table SCR-2. Summary of cell sizes of microorganisms in WIPP groundwaters

Source (as described in reference)	Length (µm)	Width (µm)	Reference
Culebra groundwater	0.82 ± 0.14	0.66 ± 0.14	Francis et al. 1998
WIPP-1A culture (*Halomonas* sp.)	1.53 ± 0.09	0.79 ± 0.03	Francis et al. 1998
Mixed culture* (BAB):	1.46 ± 0.45 (mean)	0.66 ± 0.07	Francis et al. 1998
Group A	0.54 ± 0.03	0.48 ± 0.03	
Group B	0.66 ± 0.01	0.62 ± 0.02	
Group C	1.47 ± 0.14	0.76 ± 0.04	
Group D	2.66 ± 0.29	0.92 ± 0.06	
Group E	7.73 ± 0.96	0.67 ± 0.04	
Culebra groundwater	0.75 ± 0.04	0.58 ± 0.02	Gillow et al. 2000
WIPP monitoring well (*Chromohalobacter* sp.)	3.5	0.5	Ams et al. 2013
WIPP monitoring well (*Halococcus* sp.)	~1	~1	Swanson and Simmons, 2013
WIPP-1A culture (*Halomonas* sp.) formalin-fixed	No measurements of length and width; measurements of cell volumes range from 0.2-0.4 µm^3	No measurements of length and width; measurements of cell volumes range from 0.2-0.4 µm^3	Lucero et al. 1996

*based on descriptions of pink pigmentation, this culture is presumed to be and/or contain haloarchaea; many of these organisms are pleomorphic, so it is likely that some of these groups are different morphologies of the same organism.

There are limited, yet conflicting, data on microbial transport through dolomite matrices. Studies have investigated microbial transport through crushed and intact Culebra rock (Table SCR-3; Yelton et al. 1996; Lucero et al. 1996; Zengotita et al. 2019). Yelton et al. (Yelton et al. 1996) found that the flow of latex microspheres (ranging in diameter from 0.48-1.05 µm to approximate microbial sizes) through crushed dolomite was significantly retarded under their test conditions, even when larger grains were used (maximum elution of 11% of the smallest spheres at the larger grain sizes). Microbial cells in the presence of nutrients caused complete blockage of the crushed dolomite. In the absence of nutrients, less than 1% of the injected cells broke through. More retardation occurred when the dolomite particle size fraction was smaller or when the cell size was larger.

In similar experiments using an intact dolomite core with much lower porosity, Lucero et al. (Lucero et al. 1996) showed a reduction in the number of injected cells versus cells in the effluent, and it was suggested that the effluent cells may have already been resident within the core at the start of the experiment. The presence of bacteria did not affect the transport of uranium, americium, or plutonium through the column.

Zengotita et al. (Zengotita et al. 2019) found that actively growing cells of *Chromohalobacter* sp. were retarded in crushed dolomite more than stationary phase cells (~65% recovery versus 80% recovery). These are similar to the results of Yelton et al. (above) and could have been due to

either the straining of larger growing cells or differing surface characteristics that allowed for interaction with the dolomite. This study used a flow rate approximating the maximum hydraulic conductivity previously measured in the Culebra (10^{-5} meters per second [m/s]).

Table SCR-3. Summary of conditions in microbe-Culebra experiments

Cells	Eluent	Flow Rate	Grain size fraction	Average porosity	Reference
Mixed culture (from Francis & Gillow, 1994); binned into different size fractions, ranging 0.2-1 µm length; stationary phase live	3 m brine simulant, primarily NaCl	0.5 mL/min	250-500 nm	0.46	Yelton et al. 1996
Mixed culture (from Francis & Gillow, 1994); binned into different size fractions, ranging 0.2-1 µm length; preserved at stationary phase using formalin	3 m brine simulant, primarily NaCl	0.5 mL/min	250-500 nm	0.44	Yelton et al. 1996
WIPP-1A culture (*Halomonas* sp.) + possible indigenous organisms from crushed dolomite (cells formalin-fixed prior to size determination but not fixed for experiment)	Brine simulant, low sodium (~0.6 M)	0.1 mL/min	Intact core	0.15	Lucero et al. 1996
Chromohalobacter sp.; stationary phase live	2.6 M NaCl + 15 mM bicarb	0.013 mL/min	355-500 µm	0.43	Zengotita et al. 2019
Chromohalobacter sp.; dimensions; stationary phase "heat-stressed"	2.6 M NaCl + 15 mM bicarb	0.013 mL/min	355-500 µm	0.43	Zengotita et al. 2019
Chromohalobacter sp.; dimensions; log phase	2.6 M NaCl + 15 mM bicarb	0.013 mL/min	355-500 µm	0.43	Zengotita et al. 2019

Other dolomite transport studies have been conducted in the context of pathogens entering drinking water aquifers. Mondal and Sleep (Mondal and Sleep 2012) investigated latex microsphere transport through dolomite with manmade fractures and found little retention of 500 nm spheres, independent of flow rate and ionic strength. In contrast, smaller spheres (20 and 200 nm) were retained as ionic strength increased or flow rate decreased. Increasing ionic strength also led to less transport of *E. coli* through a fractured dolomite block, although in most cases it moved through easily (Xu and Feriancikova 2014). However, those tests were conducted at a flow rate (5.03 ml/min) close to 400-times that expected in the Culebra, and the flow was directed along the fracture plane.

Ionic strength effects are thought to be due to an increase in collision efficiency and adhesion, as a function of the interaction between cell characteristics (e.g., surface zeta potential and morphology) and matrix composition (e.g., dominant cations leading to effects on surface functional groups and/or extracellular polymeric substances [EPS]) (Jewett et al. 1995; Kim and Walker 2009). Higher ionic strengths compress the electrostatic double layer, such that a negatively charged cell surface proximal to negatively charged dolomite grains is not repelled (Jewett et al. 1995). This permits more interactions between cells and dolomite, as well as between cells, resulting in agglomeration and clogging (Samari-Kermani et al. 2021).

Should microbial transport through the Culebra occur, it will do so at a slow rate. During that time, other factors can come into play—such as redox processes, biofilm formation, or mineralization—that could lead to radionuclide immobilization. Microbial populations in the Culebra are diverse, containing aerobes, denitrifiers, metal reducers, and sulfate reducers (Swanson and Simmons 2013), some of which would be capable of reducing radionuclides or incorporating them into minerals (Sánchez-Roman et al. 2011, Swanson 2025a). Finally, microorganisms can catalyze dolomite formation (Kenward et al. 2013; Qiu et al. 2019). Deposition of dolomite could result in further straining of cells or their co-deposition within the Culebra. Therefore, indigenous *Microbes* have been eliminated from PA calculations on the basis of low-consequence to the performance of the disposal system.

SCR-4.9.1.3 **FEP Number: N72**
FEP Title: Natural Ecological Development

SCR-4.9.1.3.1 Screening Decision: SO-C

The effects of *Natural Ecological Development* likely to occur in the region of the WIPP have been eliminated from PA calculations on the basis of low consequence to the performance of the disposal system.

SCR-4.9.1.3.2 Summary of New Information

No new information that affects the screening of this FEP has been identified since the CRA-2019.

SCR-4.9.1.3.3 Screening Argument

The region around the WIPP is sparsely vegetated as a result of the climate and poor soil quality. Wetter periods are expected during the regulatory period, but botanical records indicate that, even under these conditions, dense vegetation will not be present in the region (Swift 1992; see the CCA, Appendix CLI, p. 17). The effects of the indigenous fauna are of low consequence to the performance of the disposal system and no natural events or processes have been identified that would lead to a change in this fauna that would be of consequence to system performance. Natural ecological development in the region of the WIPP has therefore been eliminated from PA calculations on the basis of low consequence to the performance of the disposal system.

SCR-5.0 SCREENING OF HUMAN-INDUCED FEPS

The following section presents screening arguments and decisions for human-induced FEPs. Table SCR-1 provides summary information regarding changes to human-induced EPs since the CRA-2019. There are 61 human-induced FEPs included in the CRA-2026. Of the 61 human-induced EPs included in the CRA-2026, 35 remain unchanged, and 26 were updated with new information.

SCR-5.1 Human-Induced Geological EPs

SCR-5.1.1 Drilling

SCR-5.1.1.1 **FEP Numbers: H1, H2, H4, H8, and H9**
FEP Titles: Oil and Gas Exploration (H1)
Potash Exploration (H2)
Oil and Gas Exploitation (H4)
Other Resources (drilling for) (H8)
Enhanced Oil and Gas Recovery (drilling for) (H9)

SCR-5.1.1.1.1 Screening Decision: SO-C (HCN)
DP (Future)

The effects of historical, current, and near-future drilling associated with *Oil and Gas Exploration*, *Potash Exploration*, *Oil and Gas Exploitation*, *Drilling for Other Resources*, and *Drilling for Enhanced Oil and Gas Recovery* have been eliminated from PA calculations on the basis of low consequence to the performance of the disposal system (see screening discussion for H21, H22, and H23). Oil and gas exploration, potash exploration, oil and gas exploitation, drilling for other resources, and enhanced oil and gas recovery in the future is accounted for in DP scenarios through incorporation of the rate of future drilling as specified in 40 CFR 194.33.

SCR-5.1.1.1.2 Summary of New Information

The CRA-2026 will use an updated drilling rate as required by 40 CFR 194.33. This new rate does not change the screening argument or decision for FEPs H1, *Oil and Gas Exploration*, H4, *Oil and Gas Exploitation*, H8, *Other Resources*, and H9, *Enhanced Oil and Gas Recovery*. This updated deep drilling rate is implemented through the PA parameter GLOBAL:LAMBDAD. For the CRA-2026, the value for this parameter is 1.534×10^{-2} boreholes per km^2 per yr. This is an increase from the values of 1.389×10^{-2} boreholes per km^2 per yr in the RPPCR and 9.90×10^{-3} boreholes per km^2 per yr used in the CRA-2019. Permeability capillary pressure of an open borehole (PA parameter BH_OPEN:RELP_MOD) within the BRAGFLO code remains the same as the CRA-2019 with a value of 11.

SCR-5.1.1.1.3 Historical, Current, and Near-Future Human EPs

Resource exploration and exploitation are the most common reasons for drilling in the Delaware Basin and are the most likely reasons for drilling in the near future. The WIPP location has been evaluated for the occurrence of natural resources in economic quantities. Powers et al. (1978) (the CCA, Appendix GCR, Chapter 8) investigated the potential for exploitation of potash, hydrocarbons, caliche, gypsum, salt, uranium, sulfur, and lithium. Also, in 1995, the New Mexico Bureau of Mines and Mineral Resources performed a reevaluation of the mineral resources at and within 1.6 km (1 mi) around the WIPP site (New Mexico Bureau of Mines and Mineral Resources 1995). While some resources do exist at the WIPP site, for the HCN time frames, such drilling is assumed to only occur outside the WIPP site boundary, with the exception of horizontal wells beneath Section 31 (the southwest corner of the WIPP site). Oil leases that pre-existed the withdrawal of land by the Federal government for the WIPP in Section 31 were not condemned, as it was determined that production of these resources could be conducted without adverse effects to the WIPP. As such, the DOE only controls from the surface to 6,000 ft (1,829 m) below ground surface. Operators have continued to produce these leases utilizing horizontal drilling techniques (Melzer and Hall 2023). This continued development and production is consistent with the expectations of the DOE and the EPA (U.S. EPA 1998c). These wells originate outside the WIPP boundary and transition to horizontal orientation at depths below 6,000 ft (1,829 m). The vertical portion of these drill holes lie outside the WIPP boundary. Therefore, it is not expected that vertical wells will be initiated within the WIPP site during the HCN time frame. This assumption is based on current federal ownership and management of the WIPP during operations and assumed effectiveness of institutional controls for the 100-yr period immediately following site closure.

Drilling associated with oil and gas exploration and oil and gas exploitation currently takes place in the vicinity of the WIPP. Oil and gas are produced from several different formations, including Delaware Mountain Group, Bone Spring, Wolfcamp, Atoka, and Morrow. Horizontal drilling technology represents 95 percent of all rigs running in the Permian Basin and has led to increased recoveries when compared to older vertical completions (Melzer and Hall 2023).

Potash resources in the vicinity of the WIPP are discussed in the CCA, Chapter 2.0, Section 2.3.1.1. Throughout the Carlsbad Potash District, commercial quantities of potash are restricted to the McNutt, which forms part of the Salado above the repository horizon. Potash exploration and evaluation boreholes have been drilled within and outside the controlled area. Such drilling will continue outside the WIPP land withdrawal boundary, but no longer occurs within the boundary because rights and controls have been transferred to the DOE. Moreover, drilling for the evaluation of potash resources within the boundary will not occur throughout the time period of active institutional controls (AICs).

Drilling for other resources has taken place within the Delaware Basin. For example, sulfur extraction using the Frasch process began in 1969 and continued for three decades at the Culberson County Rustler Springs mine near Orla, Texas. In addition, brine wells have been in operation in and about the Delaware Basin for at least as long. Solution mining processes for

sulfur, salt (brine), potash, or any other mineral are not addressed in this FEP; only the drilling of the borehole is addressed here. Resource extraction through solution mining and any potential effects are evaluated in Section SCR-5.2.2.3 (*Solution Mining for Potash* [H58]). Nonetheless, the drilling activity associated with the production of other resources is not notably different than drilling for petroleum exploration and exploitation.

Drilling for the purposes of reservoir stimulation and subsequent enhanced oil and gas recovery does take place within the Delaware Basin, although systematic, planned waterflooding has not taken place near the WIPP. Instead, injection near the WIPP consists of single-point injectors, rather than broad, grid-type waterflood projects (Melzer and Hall 2023). In the vicinity of the WIPP, fluid injection usually takes place using boreholes initially drilled as producing wells. Therefore, regardless of the initial intent of a deep borehole, whether in search of petroleum reserves or as an injection point, the drilling event and associated processes are virtually the same. These drilling-related processes are addressed more fully in Section SCR-5.2.1.1 (*Drilling Fluid Flow* [H21], *Drilling Fluid Loss* [H22], and *Blowouts* [H23]). Discussion on the effects subsequent to drilling a borehole for the purpose of enhancing oil and gas recovery is discussed in Section SCR-5.2.1.4 *(Enhanced Oil and Gas Production* [H28]).

In summary, drilling associated with *Oil and Gas Exploration, Potash Exploration, Oil and Gas Exploitation, Drilling for Other Resources*, and *Drilling for Enhanced Oil and Gas Recovery* has taken place and is expected to continue in the Delaware Basin. The potential effects of existing and possible near-future boreholes on fluid flow and radionuclide transport within the disposal system are discussed in FEPs H25 through H36 (Section SCR-5.2.1.3, Section SCR-5.2.1.4, Section SCR-5.2.1.6, Section SCR-5.2.1.7, Section SCR-5.2.1.8, Section SCR-5.2.1.9, Section SCR-5.2.1.10, and Section SCR-5.2.1.11), where low-consequence screening arguments are provided.

SCR-5.1.1.1.4 Future Human EPs

Criteria in 40 CFR 194.33 require the DOE to examine the historical rate of drilling for resources in the Delaware Basin. Thus, consistent with 40 CFR 194.33(b)(3)(i), the DOE has used the historical record of deep drilling associated with oil and gas exploration, potash exploration, oil and gas exploitation, enhanced oil and gas recovery, and drilling associated with other resources (sulfur exploration) in the Delaware Basin in calculations to determine the rate of future deep drilling in the Delaware Basin (see Section 33 of this application). Implementation of the drilling intrusion event is described in Appendix PA-3.2.

SCR-5.1.1.1.5 FEP Implementation in PA

Oil and Gas Exploration (H1), Potash Exploration (H2), Oil and Gas Exploitation (H4), Other Resources (drilling for) (H8), and Enhanced Oil and Gas Recovery (drilling for) (H9) are associated with the Exploratory Boreholes conceptual model. This conceptual model is implemented in the deterministic scenarios defined in PA and implemented in the random futures defined by the CCDFGF code.

SCR-5.1.1.2 **FEP Numbers: H3 and H5**
FEP Titles: Water Resources Exploration (H3)
Groundwater Exploitation (H5)

SCR-5.1.1.2.1 Screening Decision: SO-C (HCN)
SO-C (Future)

The effects of HCN and future drilling associated with *Water Resources Exploration* and *Groundwater Exploitation* have been eliminated from PA calculations on the basis of low consequence to the performance of the disposal system.

SCR-5.1.1.2.2 Summary of New Information

As with all previous compliance applications, shallow drilling continues to be screened out of PA calculations because of low consequence. The DOE collects data on shallow wells drilled within the Delaware Basin (U.S. DOE 2025b). However, since such wells are not included in performance analyses, the derivation of the shallow drilling rate has not been done for the CRA-2026.

SCR-5.1.1.2.3 Screening Argument

Drilling associated with water resources exploration and groundwater exploitation has taken place and is expected to continue in the Delaware Basin. For the most part, water resources in the vicinity of the WIPP are scarce. Elsewhere in the Delaware Basin, potable surface water occurs in places while some communities rely solely on groundwater sources for drinking water. Even though water resources exploration and groundwater exploitation occur in the Basin, all such exploration/exploitation is confined to shallow drilling that extends no deeper than the Rustler. Thus, it will not impact repository performance because of the limited drilling anticipated in the future and the sizeable thickness of low-permeability Salado salt between the waste panels and the shallow groundwaters. Given the limited groundwater resources and minimal consequence of shallow drilling on performance, the effects of HCN and future drilling associated with water resources exploration and groundwater exploitation have been eliminated from PA calculations on the basis of low consequence to the performance of the disposal system. The screening argument therefore remains the same as given previously in the CCA.

Although shallow drilling for water resources exploration and groundwater exploitation have been eliminated from PA calculations, the Delaware Basin Drilling Surveillance Program (DBDSP) continues to collect drilling data related to water resources, as well as other shallow drilling activities. As shown in the DBDSP 2024 Annual Report (U.S. DOE 2025a), the total number of shallow water wells in the Delaware Basin is currently 4,602. This number has decreased significantly from the CRA-2019, where the shallow well count was 10,496 (U.S. DOE 2018a). This decrease is primarily due to fewer wells designated as “Drilling or waiting on paperwork.”

SCR-5.1.1.2.4 Historical, Current, and Near-Future Human EPs

Water is currently extracted from formations above the Salado, as discussed in the CCA, Chapter 2.0, Section 2.3.1.3. The distribution of groundwater wells in the Delaware Basin is included in the CCA, Appendix USDW, Section USDW.3. Water resources exploration and groundwater exploitation are expected to continue in the Delaware Basin.

In summary, drilling associated with water resources exploration, groundwater exploitation, potash exploration, oil and gas exploration, oil and gas exploitation, enhanced oil and gas recovery, and drilling to explore other resources has taken place and is expected to continue in the Delaware Basin. The potential effects of existing and possible near-future boreholes on fluid flow and radionuclide transport within the disposal system are discussed in Section SCR-5.2, where low-consequence screening arguments are provided.

SCR-5.1.1.2.5 Future Human EPs

Criteria in 40 CFR 194.33 require that, to calculate the rates of future shallow and deep drilling in the Delaware Basin, the DOE should examine the historical rate of drilling for resources in the Delaware Basin.

Shallow drilling associated with water, potash, sulfur, oil, and gas extraction has taken place in the Delaware Basin over the past 100 yrs. However, of these resources, only water and potash are present at shallow depths (less than 641 m (2,104 ft) below the surface) within the controlled area. Thus, consistent with 40 CFR 194.33(b)(4), drilling associated with water resources exploration, potash exploration, and groundwater exploitation is included in calculations to determine the rate of future shallow drilling in the Delaware Basin. However, the effects of such events are not included in PA calculations because of low consequence to the performance of the disposal system.

SCR-5.1.1.3 **FEP Numbers: H6, H7, H10, H11, and H12**
FEP Titles: Archaeological Investigations (H6)
Geothermal Energy Production (H7)
Liquid Waste Disposal (H10)
Hydrocarbon Storage (H11)
Deliberate Drilling Intrusion (H12)

SCR-5.1.1.3.1 Screening Decision: SO-R (HCN)
SO-R (Future)

Drilling associated with *Archaeological Investigations*, *Geothermal Energy Production*, *Liquid Waste Disposal*, *Hydrocarbon Storage*, and *Deliberate Drilling Intrusion* have been eliminated from PA calculations on regulatory grounds.

SCR-5.1.1.3.2 Summary of New Information

No new information that affects the screening of these FEPs has been identified since the CRA-2019.

SCR-5.1.1.3.3 Screening Argument

SCR-5.1.1.3.3.1 Historic, Current, and Near-Future EPs

No drilling associated with archaeology or geothermal energy production has taken place in the Delaware Basin. Consistent with the future states assumptions in 40 CFR 194.25(a) (U.S. EPA 1996a), such drilling activities have been eliminated from PA calculations on regulatory grounds.

While numerous archaeological sites exist at and near the WIPP site, drilling for archaeological purposes has not occurred. Archaeological investigations have only involved shallow surface disruptions, and do not require deeper investigation by any method, drilling or otherwise. Geothermal energy is not considered to be a potentially exploitable resource because economically attractive geothermal conditions do not exist in the northern Delaware Basin.

Oil and gas production byproducts are disposed of underground in the WIPP region, but such liquid waste disposal does not involve drilling of additional boreholes (see H27, Section SCR-5.2.1.4); therefore drilling of boreholes for the explicit purpose of disposal has not occurred.

Hydrocarbon storage takes place in the Delaware Basin, but it involves gas injection through existing boreholes into depleted reservoirs (see, for example, Burton et al. 1993, pp. 66-67). Therefore, drilling of boreholes for the explicit purpose of hydrocarbon storage has not occurred.

Consistent with 40 CFR 194.33(b)(1), all near-future Human EPs relating to deliberate drilling intrusion into the WIPP excavation have been eliminated from PA calculations on regulatory grounds.

SCR-5.1.1.3.3.2 Future Human EPs

Consistent with 40 CFR 194.33 and the future states assumptions in 40 CFR 194.25(a), drilling for purposes other than resource recovery (such as WIPP site investigation) and drilling activities that have not taken place in the Delaware Basin over the past 100 yrs need not be considered in determining future drilling rates. Thus, drilling associated with archaeological investigations, geothermal energy production, liquid waste disposal, hydrocarbon storage, and deliberate drilling intrusion have been eliminated from PA calculations on regulatory grounds.

SCR-5.1.2 Excavation Activities

SCR-5.1.2.1 **FEP Number: H13**
FEP Title: Conventional Underground Potash Mining

SCR-5.1.2.1.1 Screening Decision: UP (HCN)
DP (Future)

As prescribed by 40 CFR 194.32(b), the effects of HCN and future *Conventional Underground Potash Mining* are accounted for in PA (see also FEP H37).

SCR-5.1.2.1.2 Summary of New Information

No new information that affects the screening of this FEP has been identified since the CRA-2019. However, an explanation of the implementation of this FEP within PA has been provided.

SCR-5.1.2.1.3 Screening Argument

Potash is the only known economically viable resource in the vicinity of the WIPP that is recovered by underground mining (see the CCA, Chapter 2.0, Section 2.3.1). Potash is mined extensively by conventional techniques in the region east of Carlsbad from leases extending to the boundaries of the controlled area of the WIPP. According to existing plans and leases (see the CCA, Chapter 2.0, Section 2.3.1.1), potash mining is expected to continue in the vicinity of the WIPP in the near future. The DOE assumes that all economically recoverable potash in the vicinity of the disposal system will be extracted in the near future, although there are no economical reserves above the WIPP waste panels (Griswold and Griswold 1999) (see also Section SCR-5.2.2.1, FEP H37 *"Changes in Groundwater Flow Due to Mining"*).

In summary, conventional underground potash mining is currently taking place and is expected to continue in the vicinity of the WIPP in the near future. The potential effects of HCN and future conventional underground potash mining are accounted for in PA as prescribed by 40 CFR 194.32(b), and as further described in the supplementary information to 40 CFR 194 Subpart C, Compliance Certification and Recertification and in the Compliance Application Guidance (CAG), Subpart C, 194.32, Scope of Performance Assessments.

SCR-5.1.2.1.4 FEP Implementation in PA

The Culebra hydrogeology conceptual model accounts for localized increases in Culebra horizontal transmissivity due to mining underlying potash reserves. The impacts of potash mining are implemented in PA by applying the sampled parameter CULEBRA:MINP_FAC as a multiplier on the transmissivity values of MODFLOW Culebra flow model cells that are determined to be disturbed by potash mining. The areas disturbed by mining activities in the Culebra are larger than mined areas due to angle-of-draw effects; the subsidence effects propagate up and out at 45° angles between horizontal and vertical. To accommodate the angle of draw, the mining zone boundaries, as overlaid on the current model grid, are extended

outward three model cells (300 meters) in the x- and y-directions, and two model cells (283 meters) in the diagonal directions.

Mining impacts are included in two scenarios, the partial mining scenario in which only potash reserves outside of the LWB are assumed to be mined, and the full mining scenario in which potash reserves are assumed to be mined wherever they are present throughout the model domain. The DOE assumes that all potash reserves outside of the land withdrawal boundary will be mined by the time of repository closure. Thereafter, the DOE assumes that the probability that full mining conditions will occur is 1% every 100 years.

SCR-5.1.2.2 **FEP Number: H14**
FEP Title: Other Resources (mining for)

SCR-5.1.2.2.1 Screening Decision: **SO-C (HCN)**
SO-R (Future)

HCN *Mining for Other Resources* has been eliminated from PA calculations on the basis of low consequence to the performance of the disposal system. Future *Mining for Other Resources* has been eliminated from PA calculations on regulatory grounds.

SCR-5.1.2.2.2 Summary of New Information

No new information that affects the screening of this FEP has been identified since the CRA-2019.

SCR-5.1.2.2.3 Screening Argument

Potash is the only known economically viable resource in the vicinity of the WIPP that is recovered by underground mining. Potash is mined extensively in the region east of Carlsbad and up to 5 km (3.1 mi) from the boundaries of the controlled area. According to existing plans and leases, potash mining is expected to continue in the vicinity of the WIPP in the near future. The DOE assumes that all economically recoverable potash in the vicinity of the disposal system will be extracted in the near future. Excavation for resources other than potash and archaeological excavations have taken place or are currently taking place in the Delaware Basin. These activities have not altered the geology of the controlled area significantly and have been eliminated from PA calculations for the HCN timeframe on the basis of low consequence to the performance of the disposal system.

Potash is the only resource that has been identified within the controlled area in a quality similar to that currently mined elsewhere in the Delaware Basin. Future mining for other resources has been eliminated from PA calculations on the regulatory basis of 40 CFR 194.25(a).

SCR-5.1.2.3 **FEP Numbers: H15 and H16**
FEP Titles: Tunneling (H15)
Construction of Underground Facilities (H16)

SCR-5.1.2.3.1 Screening Decision: SO-R (HCN)
SO-R (Future)

Consistent with 40 CFR 194.33(b)(1), near-future, human-induced EPs relating to *Tunneling* into the WIPP excavation and *Construction of Underground Facilities* have been eliminated from PA calculations on regulatory grounds. Furthermore, consistent with 40 CFR 194.25(a), future human-induced EPs relating to *Tunneling* into the WIPP excavation and *Construction of Underground Facilities* have been eliminated from PA calculations on regulatory grounds.

SCR-5.1.2.3.2 Summary

No new information that affects the screening of this FEP has been identified since the CRA-2019.

SCR-5.1.2.3.3 Screening Argument

No tunneling or construction of underground facilities (for example, storage, disposal, accommodation [i.e., dwellings]) has taken place in the Delaware Basin. Mining for potash occurs (a form of tunneling) but is addressed specifically in (Section SCR-5.1.2.1 (*Conventional Underground Potash Mining* [H13])). Gas storage does take place in the Delaware Basin, but it involves injection through boreholes into depleted reservoirs, and not excavation (see, for example, Burton et al. 1993, pp. 66–67).

Because tunneling and construction of underground facilities (other than the WIPP) have not taken place in the Delaware Basin, and consistent with the future-states assumptions in 40 CFR 194.25(a), such excavation activities have been eliminated from PA calculations on regulatory grounds.

SCR-5.1.2.4 **FEP Number: H17**
FEP Title: Archaeological Excavations

SCR-5.1.2.4.1 Screening Decision: SO-C (HCN)
SO-R (Future)

HCN *Archaeological Excavations* have been eliminated from PA calculations on the basis of low consequence to the performance of the disposal system. Future *Archaeological Excavations* into the disposal system have been eliminated from PA calculations on regulatory grounds.

SCR-5.1.2.4.2 Summary of New Information

No new information that affects the screening of this FEP has been identified since the CRA-2019.

SCR-5.1.2.4.3 Screening Argument

Archaeological excavations have occurred at or near the WIPP but involved only minor surface disturbances. These archaeological excavations may continue into the foreseeable future as other archaeological sites are discovered. These activities have not altered the geology of the controlled area significantly and have been eliminated from PA calculations on the basis of low consequence to the performance of the disposal system for the HCN timeframe.

Also, consistent with 40 CFR 194.32(a), which limits the scope of consideration of future human actions to mining and drilling, future archaeological excavations have been eliminated from PA calculations on regulatory grounds.

SCR-5.1.2.5 **FEP Number: H18**
FEP Title: Deliberate Mining Intrusion

SCR-5.1.2.5.1 Screening Decision: SO-R (HCN)
SO-R (Future)

Consistent with 40 CFR 194.33(b)(1), near-future, human-induced EPs relating to *Deliberate Mining Intrusion* into the WIPP excavation have been eliminated from PA calculations on regulatory grounds. Furthermore, consistent with 40 CFR 194.33(b)(1), future human-induced EPs relating to *Deliberate Mining Intrusion* into the WIPP excavation have been eliminated from PA calculations on regulatory grounds.

SCR-5.1.2.5.2 Summary of New Information

No new information that affects the screening of this FEP has been identified since the CRA-2019.

SCR-5.1.2.5.3 Screening Argument

Consistent with 40 CFR 194.33(b)(1), all future human-related EPs relating to deliberate mining intrusion into the WIPP excavation have been eliminated from PA calculations on regulatory grounds.

SCR-5.1.3 Subsurface Explosions

SCR-5.1.3.1 **FEPs Number: H19**
FEP Title: Explosions for Resource Recovery

SCR-5.1.3.1.1 Screening Decision: SO-C (HCN)
SO-R (Future)

Historical underground *Explosions for Resource Recovery* have been eliminated from PA calculations on the basis of low consequence to the performance of the disposal system. Future underground *Explosions for Resource Recovery* have been eliminated from PA calculations on regulatory grounds.

SCR-5.1.3.1.2 Summary of New Information

No new information that affects the screening of this FEP has been identified since the CRA-2019.

SCR-5.1.3.1.3 Screening Argument

This section discusses subsurface explosions associated with resource recovery that may result in pathways for fluid flow between hydraulically conductive horizons. The potential effects of explosions on the hydrological characteristics of the disposal system are discussed in Section SCR-5.2.3.1 (*Changes in Groundwater Flow Due to Explosions* [H39]).

SCR-5.1.3.1.4 Historical, Current, and Near-Future Human EPs

Neither small-scale nor regional-scale explosive techniques to enhance the formation of hydraulic conductivity form a part of current mainstream oil- and gas-production technology. Instead, controlled perforating and hydrofracturing are used to improve the performance of oil and gas boreholes in the Delaware Basin. However, small-scale explosions have been used in the past to fracture oil- and natural-gas-bearing units to enhance resource recovery. The size of explosion used to fracture an oil- or gas-bearing unit is limited by the need to contain the damage within the unit being exploited. In the area surrounding the WIPP, the stratigraphic units with oil and gas resources are too deep for explosions to affect the performance of the disposal system. Thus, the effects of explosions for resource recovery have been eliminated from PA calculations on the basis of low consequence to the performance of the disposal system.

Potash mining is currently taking place and is expected to continue in the vicinity of the WIPP in the near future. Potash is mined extensively in the region east of Carlsbad and up to 2.4 km (1.3 mi) from the boundaries of the controlled area. In earlier years, conventional drill, blast, load, and rail-haulage methods were used. Today, continuous miners similar to those used in coal-mining have been adapted to fit the potash-salt formations. Hence, drilling and blasting technology is not used in the present-day potash mines. Thus, the effects of explosions for

resource recovery during the HCN timeframe have been eliminated from PA calculations on the basis of low consequence to the performance of the disposal system.

Consistent with 40 CFR 194.33(d), PAs need not analyze the effects of techniques used for resource recovery subsequent to the drilling of a future borehole. Therefore, future underground explosions for resource recovery have been eliminated from PA calculations on regulatory grounds.

SCR-5.1.3.2 **FEP Number: H20**
FEP Title: Underground Nuclear Device Testing

SCR-5.1.3.2.1 Screening Decision: SO-C (HCN)
SO-R (Future)

Historical *Underground Nuclear Device Testing* has been eliminated from PA calculations on the basis of low consequence to the performance of the disposal system. Future *Underground Nuclear Device Testing* has been eliminated from PA calculations on regulatory grounds.

SCR-5.1.3.2.2 Summary of New Information

No new information that affects the screening of this FEP has been identified since the CRA-2019. The screening argument has been edited for clarity.

SCR-5.1.3.2.3 Screening Argument

SCR-5.1.3.2.3.1 Historical, Current, and Near-Future Human EPs

The Delaware Basin was used for an isolated nuclear test. This test, Project Gnome (Rawson et al. 1965), took place in 1961 at a location about 13 km (8 mi) southwest of the WIPP waste disposal region. The primary objective of Project Gnome was to study the effects of an underground nuclear explosion in salt. It was the first test conducted under Project Plowshare.

The Gnome experiment involved the detonation of a 3.1 kiloton nuclear device at a depth of 360 m (1,190 ft) in the bedded salt of the Salado. The explosion created an approximately spherical cavity with a void volume of about 27,200 cubic meters (m^3) (950,000 ft^3). The bottom hemisphere, with average radius of 17.4 m, was filled with salt melt and then was covered with rubble from the cavity walls (porosity void of 3,030 m^3). The hemispherical cavity above the rock melt and rubble had an average radius of 22.6 m (void volume of 24,180 m^3). Observed fractures extended 40 m laterally, 38 m above, and 25 m below the explosion center, and evidence of gaseous injection in bedding planes was observed out to 65.5 m. Increased permeability was observed (from loss of fluid when drilling exploratory boreholes) in a cone that extended 46 m (150 ft) laterally and 105 m (344 ft) above the explosion center. The surface was displaced in a radius of 360 m (1,180 ft) with a maximum uplift of 0.6 m.

The test had no observable effects on the geological characteristics of the WIPP disposal system 13 km away. No Earth tremors perceptible to humans were reported at distances over 40 km (25 mi) from the explosion. Thus, historical underground nuclear device testing has

been excluded from PA calculations on the basis of low consequence to the performance of the disposal system. Because of the US moratorium on underground nuclear testing, no plans exist for underground nuclear device testing in the vicinity of the WIPP facility in the near future.

SCR-5.1.3.2.3.2 Future Human EPs

The criterion on the scope of performance assessments in 40 CFR 194.32(a) limits consideration of future human actions to mining and drilling. Therefore, future underground nuclear device testing has been excluded from PA calculations on regulatory grounds.

SCR-5.2 Subsurface Hydrological and Geochemical EPs

SCR-5.2.1 Borehole Fluid Flow

SCR-5.2.1.1 **FEP Number: H21, H22, H23**
FEP Title: Drilling Fluid Flow (H21)
Drilling Fluid Loss (H22)
Blowouts (H23)

SCR-5.2.1.1.1 Screening Decision: SO-C (HCN)
DP (Future)

Drilling Fluid Flow (H21), *Drilling Fluid Loss* (H22), *and Blowouts* (H23) associated with historical, current, near-future, and future boreholes that do not intersect the waste disposal region have been eliminated from PA calculations on the basis of low consequence to the performance of the disposal system. The possibility of a future deep borehole penetrating a waste panel, such that drilling-induced flow results in transport of radionuclides to the land surface or to overlying hydraulically conductive units, is accounted for in PA. The possibility of a deep borehole penetrating both the waste disposal region and a Castile brine reservoir is accounted for in PA.

SCR-5.2.1.1.2 Summary of New Information

Drilling Fluid Flow (H21)*, Drilling Fluid Loss* (H22), and *Blowouts* (H23) have been screened together for CRA-2026. A summary of the implementation of these FEPs within PA has been added.

SCR-5.2.1.1.3 Screening Argument

Inadvertent human intrusion into the repository by a borehole could result in transport of waste material to the ground surface through drilling-induced flow. This waste could include material eroded from the borehole wall by circulating drilling fluid (cavings). Transport of radionuclides by these materials and in brine is accounted for in PA and is discussed in Appendix PA-4.6 and PA-4.7. Effects of *Drilling Fluid Flow* is therefore included in PA calculations.

Drilling Fluid Loss is a short-term event that can result in the flow of pressurized fluid from one geologic stratum to another. Large fluid losses would lead a driller to inject materials to reduce permeability, or it would lead to the borehole being cased and cemented to limit the loss of drilling fluid. Assuming such operations are successful, drilling fluid loss in the near future outside the controlled area will not significantly affect the hydrology of the disposal system. Thus, *Drilling Fluid Loss* associated with historical, current, and near-future boreholes has been eliminated from PA calculations on the basis of low consequence to the performance of the disposal system.

Blowouts are short-term events that can result in the flow of pressurized fluid from one geologic stratum to another. For the near future, a blowout may occur in the vicinity of the WIPP but is not likely to affect the disposal system because of the distance from the well to the waste panels, assuming that AICs are in place which restrict borehole installation to outside the WIPP boundary. *Blowouts* associated with HCN and future boreholes that do not intersect the waste disposal region have been eliminated from PA calculations on the basis of low consequence to the performance of the disposal system. For the future, the drill holes may intersect the waste disposal region and these effects could be more profound. Thus, *Blowouts* that occur in the waste area of the repository are included in the assessment of future activities and their consequences are accounted for in PA.

Fluid could flow from pressurized zones through the borehole to the land surface (*Blowout*) or to a thief zone. Such drilling-related EPs could influence groundwater flow and, potentially, radionuclide transport in the affected units. Movement of brine from a pressurized zone through a borehole into potential thief zones such as the Salado interbeds or the Culebra could result in geochemical changes and altered radionuclide migration rates in these units.

SCR-5.2.1.1.3.1 Historical, Current, and Near-Future Human EPs

Drilling associated with water resources exploration, groundwater exploitation, potash exploration, oil and gas exploration, oil and gas exploitation, enhanced oil, and gas recovery, and drilling to explore other resources has taken place or is currently taking place outside the controlled area in the Delaware Basin. These drilling activities are expected to continue in the vicinity of the WIPP in the near future.

Drilling Fluid Flow will not affect hydraulic conditions in the disposal system significantly unless there is substantial *Drilling Fluid Loss* to a thief zone, such as the Culebra. Typically, zones into which significant borehole circulation fluid is lost are isolated through injection of materials to reduce permeability or through casing and cementing programs. Assuming such operations are successful, *Drilling Fluid Loss* in the near future outside the controlled area will not affect the hydrology of the disposal system significantly and be of no consequence.

Naturally occurring brine and gas pockets have been encountered during drilling in the Delaware Basin. Brine pockets have been intersected in the Castile (as discussed in the CCA, Chapter 2.0, Section 2.2.1.2). Gas *Blowouts* have occurred during drilling in the Salado. Usually, such events result in brief interruptions in drilling while the intersected fluid pocket is allowed

to depressurize through flow to the surface (for a period lasting from a few hours to a few days). Drilling then restarts with an increased drilling mud weight. Under these conditions, *Blowouts* in the near future will cause isolated hydraulic disturbances but will not affect the hydrology of the disposal system significantly. *Blowouts* associated with historical, current, and near-future boreholes have been eliminated from PA calculations on the basis of low consequence to the performance of the disposal system.

Potentially, the most significant disturbance to the disposal system could occur if an uncontrolled blowout during drilling resulted in substantial flow through the borehole from a pressurized zone to a thief zone. For example, if a borehole penetrates a brine reservoir in the Castile, brine could flow through the borehole to the Culebra over the long term, and, as a result, could affect hydraulic conditions in the Culebra. The potential effects of such an event can be compared to the effects of long-term fluid flow from deep overpressurized units to the Culebra through abandoned boreholes. Wallace (1996a) analyzed the potential effects of flow through abandoned boreholes in the future within the controlled area and concluded that interconnections between the Culebra and deep units could be eliminated from PA calculations on the basis of low consequence. Long-term flow through abandoned boreholes would have a greater hydrological impact in the Culebra than short-term, drilling-induced flow outside the controlled area. Thus, the effects of fluid flow during drilling in the near future have been eliminated from PA calculations on the basis of low consequence to the performance of the disposal system.

SCR-5.2.1.1.3.2 Future Human EPs

For the future, drill holes may intersect the waste disposal region and their effects could be more profound. The possibility of a future borehole penetrating a waste panel, so that *Drilling Fluid Flow,* or *Blowout* results in transport of radionuclides to the land surface or to overlying hydraulically conductive units, is accounted for in PA. Drilling events through the experimental and operational regions of the repository are not accounted for in PA as it was determined that they could be excluded due to low consequence (Wilson et al. 1996). This conclusion of low consequence was reconfirmed by Zeitler (2015).

The units intersected by the borehole may provide sources for fluid flow (brine, oil, or gas) to the waste panel during drilling. In the vicinity of the WIPP, the Castile that underlies the Salado contains isolated volumes of brine at fluid pressures greater than hydrostatic. A future borehole that penetrates a Castile brine reservoir could provide a connection for brine flow from the reservoir to the waste panel, thus increasing fluid pressure and brine volume in the waste panel. The possibility of a deep borehole penetrating both a waste panel and a brine reservoir is accounted for in PA.

Penetration of an underpressurized unit underlying the Salado could result in flow and radionuclide transport from the waste panel to the underlying unit during drilling, although drillers would minimize such fluid loss to a thief zone through the injection of materials to reduce permeability or through the use of casing and cementing. Also, the permeabilities of formations underlying the Salado are less than the permeability of the Culebra (Wallace 1996a).

Thus, the consequences associated with radionuclide transport to an underpressurized unit below the waste panels during drilling will be less significant, in terms of disposal system performance, than the consequences associated with radionuclide transport to the land surface or to the Culebra during drilling. Through this comparison, drilling events that result in penetration of underpressurized units below the waste-disposal region have been eliminated from PA calculations on the basis of low consequence to the performance of the disposal system.

For boreholes that do not intersect pressurized brine reservoirs (but do penetrate the waste-disposal region), the treatment of the disposal room implicitly accounts for the potential for greater gas generation resulting from drilling fluid loss. Thus, the hydrological effects of *Drilling Fluid Loss* for E2 drilling events (see PA-2.2.2.2) are accounted for in PA within the conceptual model of the disposal room for drilling intrusions.

SCR-5.2.1.1.4 FEP Implementation in PA

Drilling Fluid Flow and *Drilling Fluid Loss* from future boreholes that intersect the waste panels is implemented in the Exploratory Boreholes and Repository Fluid Flow conceptual models. This fluid flow is implemented in the PA code BRAGFLO.

Blowouts are implemented in the Direct Brine Release conceptual model. The duration of a blowout event is controlled by the BLOWOUT:MAXFLOW parameter. The volume of brine released during a blowout event is calculated by the PA code BRAGFLO.

SCR-5.2.1.2 **FEP Number: H24**
FEP Title: Drilling-Induced Geochemical Changes

SCR-5.2.1.2.1 Screening Decision: UP (HCN)
DP (Future)

Drilling-Induced Geochemical Changes that occur within the controlled area during the HCN and future time periods are accounted for in PA.

SCR-5.2.1.2.2 Summary of New Information

No new information that affects the screening of this FEP has been identified since the CRA-2019. However, it has been edited for clarity and a summary of the PA implementation has been provided.

SCR-5.2.1.2.3 Screening Argument

Borehole circulation fluid could be introduced into the waste disposal area during drilling. Movement of brine from a pressurized reservoir in the Castile through a borehole into potential thief zones, such as the Salado interbeds or the Culebra, could cause drilling-induced geochemical changes resulting in altered radionuclide migration rates in these units through

their effects on colloid transport and sorption (colloid transport may enhance radionuclide migration, while radionuclide migration may be retarded by sorption).

SCR-5.2.1.2.3.1 Historical, Current, and Near-Future Human EPs

Drilling associated with resource exploration, exploitation, and recovery has taken place or is currently taking place outside the controlled area in the Delaware Basin. These drilling activities are expected to continue in the vicinity of the WIPP in the near future. Chemical changes induced by such drilling are discussed below.

SCR-5.2.1.2.3.1.1 Geochemical Effects of Drilling-Induced Flow–HCN

Radionuclide migration rates are governed by the coupled effects of hydrological and geochemical processes (see discussions in FEPs W77 through W100, Section SCR-6.6.1.1, Section SCR-6.6.1.2, Section SCR-6.6.2.1, Section SCR-6.6.3.1, Section SCR-6.6.3.2, Section SCR-6.6.4.1, Section SCR-6.7.1.1, Section SCR-6.7.2.1, Section SCR-6.7.3.1, Section SCR-6.7.4.1, Section SCR-6.7.4.2, Section SCR-6.7.4.3, Section SCR-6.7.5.1, Section SCR-6.7.5.2, Section SCR-6.7.5.3, and Section SCR-6.7.5.4). Human EPs outside the controlled area could affect the geochemistry of units within the controlled area if they occur sufficiently close to the edge of the controlled area.

The treatment of colloids in PA calculations is described in Appendix GEOCHEM-5. The repository and its contents provide the main source of colloids in the disposal system. By comparison, Castile brines have relatively low total colloid concentrations. Therefore, changes in colloid transport in units within the controlled area as a result of HCN drilling-induced flow have been eliminated from PA calculations on the basis of low consequence to the performance of the disposal system.

Sorption within the Culebra is accounted for in PA as discussed in the CCA, Chapter 6.0, Section 6.4.6.2. The sorption model comprises an equilibrium, sorption isotherm approximation, employing K_ds applicable to dolomite in the Culebra (Appendix PA-2004, Attachment MASS, Section MASS-15.2). The cumulative distribution functions (CDFs) of K_ds used in PA were modified in the CRA-2009 PABC as a result of EPA comments (Clayton 2009). These values continue to be used in PA. Any changes in sorption geochemistry in the Culebra within the controlled area as a result of HCN drilling-induced flow are accounted for in PA.

Sorption within the Dewey Lake is accounted for in PA, as discussed in the CCA, Chapter 6.0, Section 6.4.6.6. It is assumed that the sorptive capacity of the Dewey Lake is sufficiently large to prevent any radionuclides that enter the Dewey Lake from being released over 10,000 yrs (Wallace et al. 1995). Sorption within other geological units of the disposal system has been eliminated from PA calculations on the basis of beneficial consequence to the performance of the disposal system. The effects of changes in sorption in the Dewey Lake and other units within the controlled area as a result of HCN drilling-induced flow have been eliminated from PA calculations on the basis of low consequence to the performance of the disposal system.

SCR-5.2.1.2.3.2 Future Human EPs — Boreholes that Intersect the Waste Disposal Region

The consequences of drilling within the controlled area in the future will primarily depend on the location of the borehole. Future deep drilling could potentially penetrate the waste disposal region. If the borehole intersects the waste in the disposal rooms, radionuclides could be transported as a result of drilling fluid flow and geochemical conditions in the waste panel could be affected as a result of drilling-induced geochemical changes.

SCR-5.2.1.2.3.3 Future Human EPs — Boreholes That Do Not Intersect the Waste Disposal Region

Future boreholes that do not intersect the waste disposal region could nevertheless encounter contaminated material by intersecting a region into which radionuclides have migrated from the disposal panels, or could affect hydrogeological conditions within the disposal system. Consistent with the containment requirements in 40 CFR 191.13(a), PAs need not evaluate the effects of the intersection of contaminated material outside the controlled area.

Movement of brine from a pressurized reservoir in the Castile, through a borehole and into thief zones such as the Salado interbeds or the Culebra could result in drilling-induced geochemical changes and altered radionuclide migration rates in these units.

SCR-5.2.1.2.3.3.1 Geochemical Effects of Drilling-Induced Flow

Movement of brine from a pressurized reservoir in the Castile through a borehole into thief zones, such as the Salado interbeds or the Culebra, could cause geochemical changes resulting in altered radionuclide migration rates in these units through their effects on colloid transport and sorption.

The contents of the waste disposal panels provide the main source of colloids in the disposal system. Thus, consistent with the discussion in FEPs H21, H22, and H23 (Section SCR-5.2.1.1), colloid transport as a result of drilling-induced flow associated with future boreholes that do not intersect the waste disposal region has been eliminated from PA calculations on the basis of low consequence to the performance of the disposal system.

As discussed in FEPs H21, H22, and H23 (Section SCR-5.2.1.1), sorption within the Culebra is accounted for in PA. The sorption model accounts for the effects of changes in sorption in the Culebra as a result of drilling-induced flow associated with boreholes that do not intersect the waste disposal region.

Consistent with the screening discussion in FEPs H21, H22, and H23 (Section SCR-5.2.1.1), the effects of changes in sorption in the Dewey Lake within the controlled area as a result of drilling-induced flow associated with boreholes that do not intersect the waste disposal region have been eliminated from PA calculations on the basis of low consequence to the performance of the disposal system. Sorption within other geological units of the disposal system has been

eliminated from PA calculations on the basis of beneficial consequence to the performance of the disposal system.

In summary, the effects of drilling-induced geochemical changes that occur within the controlled area as a result of HCN and future drilling-induced flow are accounted for in PA. Those that occur outside the controlled area have been eliminated from PA calculations.

SCR-5.2.1.2.4 FEP Implementation in PA

***Drilling-Induced Geochemical Changes* is associated with the Transport of Dissolved Actinides in the Culebra and Transport of Colloidal Actinides in the Culebra conceptual models and is implemented in the PA code SECOTP2D.**

SCR-5.2.1.3 **FEP Numbers: H25 and H26**
FEP Titles: Oil and Gas Extraction (H25)
Groundwater Extraction (H26)

SCR-5.2.1.3.1 Screening Decision: **SO-C (HCN)**
SO-R (Future)

HCN *Groundwater Extraction* and *Oil and Gas Extraction* outside the controlled area has been eliminated from PA calculations on the basis of low consequence to the performance of the disposal system. *Groundwater Extraction* and *Oil and Gas Extraction* through future boreholes has been eliminated from PA calculations on regulatory grounds.

SCR-5.2.1.3.2 Summary of New Information

These FEPs have been updated with information related to nearby water pumping for industrial use. Additionally, the screening argument has been edited to more clearly differentiate between the HCN and Future timeframes.

SCR-5.2.1.3.3 Screening Argument

The extraction of fluid could alter fluid-flow patterns in the target horizons, or in overlying units as a result of a failed borehole casing. Also, the removal of confined fluid from oil- or gas-bearing units can cause compaction in some geologic settings, potentially resulting in subvertical fracturing and surface subsidence.

SCR-5.2.1.3.3.1 Historical, Current, and Near-Future Human EPs

As discussed in FEPs H25 through H36, water, oil, and gas production are the only activities involving fluid extraction through boreholes that have taken place or are currently taking place in the vicinity of the WIPP. These activities are expected to continue in the vicinity of the WIPP in the near future.

Groundwater Extraction outside the controlled area from formations above the Salado could affect groundwater flow. The Dewey Lake contains a productive zone of saturation south of the WIPP site. Several wells operated by the J.C. Mills Ranch south of the WIPP produce water from the Dewey Lake to supply livestock (see the CCA, Chapter 2.0, Section 2.2.1.4.2.1). Water has also been extracted from the Culebra at the Engle Well approximately 9.66 km (6 mi) south of the controlled area to provide water for livestock. Additionally, a water well at the Sandia National Laboratories (SNL) wellpad SNL-14 also provides livestock water for the Mills ranch. This well is approximately 3,000 ft (0.9 km) from the WIPP site boundary.

Historic pumping from wells at the J.C. Mills Ranch may have resulted in reductions in hydraulic head in the Dewey Lake within southern regions of the controlled area, leading to increased hydraulic head gradients. However, these changes in the groundwater flow conditions in the Dewey Lake will have no significant effects on the performance of the disposal system, primarily because of the sorptive capacity of the Dewey Lake (see the CCA, Chapter 6.0, Section 6.4.6.6). Retardation of any radionuclides that enter the Dewey Lake will be such that no radionuclides will migrate through the Dewey Lake to the accessible environment within the 10,000-yr regulatory period.

The effects of *Groundwater Extraction* from the Culebra from a well 9.66 km (6 mi) south of the controlled area have been evaluated by Wallace (1996b), using an analytical solution for Darcian fluid flow in a continuous porous medium. Wallace (1996b) showed that such a well pumping at about 1.9 liters (L) (0.5 gallons per minute [gpm]) for 10,000 yrs will induce a hydraulic head gradient across the controlled area of about 4×10^{-5}. The hydraulic head gradient across the controlled area currently ranges from between 0.001 to 0.007. Therefore, pumping from the Engle Well will have only minor effects on the hydraulic head gradient within the controlled area even if pumping were to continue for 10,000 yrs. Thus, the effects of HCN groundwater extraction outside the controlled area have been eliminated from PA calculations on the basis of low consequence to the performance of the disposal system.

Groundwater extraction from an industrial use well installed in 2013 at the J.C. Mills Ranch south of the controlled area impacted water levels in monitoring wells screened into the Culebra over a broad region south of the WIPP facilities (Kuhlman and Corbet 2017). The timing and discharge volumes are unknown, but drawdown observations indicate intermittent pumping from 2013 through 2017 and recovery to near pre-pumping levels in 2018. The U.S. DOE evaluates the impact of Culebra water level changes on conservative particle travel times from the repository to the boundary line of the controlled area as a part of its annual site environmental report submittal. No impacts from Mills Ranch pumping were noted as of 2021 (U.S. DOE 2022b). Therefore, this event of relatively intense but short-term pumping does not impact the long-term groundwater flow conditions at the site.

Oil and Gas Extraction outside the controlled area could affect the hydrology of the disposal system. However, the horizons that act as oil and gas reservoirs are sufficiently below the repository for changes in fluid-flow patterns to be of low consequence, unless there is fluid leakage through a failed borehole casing. Also, oil and gas extraction horizons in the Delaware

Basin are well-lithified rigid strata, so Oil and Gas Extraction is not likely to result in compaction and subsidence (Brausch et al. 1982, pp. 52, 61). Furthermore, the plasticity of the salt formations in the Delaware Basin will limit the extent of any fracturing caused by compaction of underlying units. Thus, neither the extraction of gas from reservoirs in the Morrow Formation (some 4,200 m [14,000 ft] below the surface), nor extraction of oil from the shallower units within the Delaware Mountain Group (about 1,250 to 2,450 m [4,000 to 8,000 ft] below the surface) will lead to compaction and subsidence. In summary, historical, current, and near-future *Oil and Gas Extraction* outside the controlled area has been eliminated from PA calculations on the basis of low consequence to the performance of the disposal system.

SCR-5.2.1.3.3.2 Future Human EPs

Oil and Gas Extraction outside the controlled area could affect the hydrology of the disposal system in the future but, as discussed in the section above, the effects are of low consequence to disposal system performance. Similarly, future extraction of oil and gas will not lead to compaction and subsidence and have been eliminated from PA calculation on the basis of low consequence to the performance of the disposal system.

Consistent with 40 CFR 194.33(d), PAs need not analyze the effects of techniques used for resource recovery within the WIPP site boundary subsequent to the drilling of a future borehole. Therefore, *Groundwater Extraction* and *Oil and Gas Extraction* through future boreholes have been eliminated from PA calculations on regulatory grounds.

If contaminated water intersects a well while it is producing, then contaminants could be pumped to the surface. Consistent with the containment requirements in 40 CFR 191.13(b), PAs need not evaluate radiation doses that might result from such an event. However, compliance assessments must include any such events in dose calculations for evaluating compliance with the individual protection requirements in 40 CFR 191.15. For undisturbed conditions, there are no radionuclide releases to units above the Salado (Appendix PA-7.2), and therefore no releases to the accessible environment or producing water wells in the area.

SCR-5.2.1.4 **FEP Numbers: H27, H28, and H29**
FEP Titles: Liquid Waste Disposal – OB (H27)
Enhanced Oil and Gas Production – OB (H28)
Hydrocarbon Storage – OB (H29)

SCR-5.2.1.4.1 Screening Decision: SO-C (HCN)
SO-C (Future)

The hydrological effects of HCN fluid injection (*Liquid Waste Disposal*, *Enhanced Oil and Gas Production*, and *Hydrocarbon Storage*) through boreholes outside the controlled area have been eliminated from PA calculations on the basis of low consequence to the performance of the disposal system. *Liquid Waste Disposal*, *Enhanced Oil and Gas Production*, and *Hydrocarbon Storage* in the future have been eliminated from PA calculations based on low consequence.

SCR-5.2.1.4.2 Summary of New Information

This FEP has been updated with information from recent studies conducted by Melzer and Hall (2023), and Melzer (2023).

SCR-5.2.1.4.3 Screening Argument

The injection of fluids could alter fluid-flow patterns in the target horizons or, if there is accidental leakage through a borehole casing, in any other intersected hydraulically conductive zone. Injection of fluids through a leaking borehole could also result in geochemical changes and altered radionuclide migration rates in the thief units.

SCR-5.2.1.4.3.1 Historical, Current, and Near-Future Human EPs

The only historical and current activities involving fluid injection through boreholes in the Delaware Basin are *Enhanced Oil and Gas Production* (waterflooding or carbon dioxide [CO_2] injection), *Hydrocarbon Storage* (gas reinjection), and *Liquid Waste Disposal* (byproducts from oil and gas production). These fluid injection activities are expected to continue in the future. Only liquid waste disposal (produced water) occurs within the vicinity of the WIPP.

Hydraulic fracturing of oil- or gas-bearing units is currently used as a well completion technique to improve the performance of hydrocarbon reservoirs in the Delaware Basin. Fracturing is induced during a short period of high-pressure fluid injection, resulting in increased hydraulic conductivity near the borehole and has been used on the overwhelming majority of wells drilled within the Delaware Basin for several decades. This completion technique, however, does not classify as a method of enhanced production, as it occurs before primary production begins. Because the majority of wells drilled within the last 5-10 yrs are horizontal wells, the hydrofracking process is of greater importance than for conventional (vertical) wells. For horizontal wells, the wellbore lies within the hydrocarbon-bearing “payzone.” This contrasts with a conventional well where the wellbore only intercepts the payzone vertically. Starting in 2016, laterals within the payzone are being drilled up to 4.5 miles in length (Melzer and Hall 2023). Note that a typical payzone in the Delaware Basin may be only 30-ft thick. Hydrofracking a 4.5-mile-long horizontal well requires fracking in stages, and may require anywhere from 60-120 stages to complete, whereas a conventional well will be fractured in a single stage, due to the thinness of the payzone. As such, surface activities and equipment used to conduct a multi-stage hydrofracturing operation will be significantly greater due to the quantities of water, sand, and treatment products used. While these multi-stage hydrofracturing activities are labor intensive and use significant amounts of water, they result in much greater production from a single well. Horizontal wells are often drilled parallel to one another at spacings that maximize payzone contact while not being so close as to allow fractures to communicate with adjacent parallel wells, which would reduce production and well control. For this reason, hydraulic fracturing is a carefully controlled process. Normally, this controlled fracturing is confined to the pay zone and is unlikely to affect overlying strata.

Enhanced production techniques, such as waterflooding (secondary) and CO_2 miscible flooding (tertiary), are used to produce the residual oil in place that primary production did not yield. Waterflooding is used to maintain reservoir pressure and to drive or move residual oil towards the well bore. Tertiary recovery techniques, such as CO_2 miscible flooding, have been implemented with limited success in the Delaware Basin, but CO_2 miscible flooding is not an attractive recovery method for reservoirs near the WIPP (Melzer 2023). Even if CO_2 flooding were to occur, the effects, if any, would be very similar to those associated with waterflooding.

Reinjection of gas for storage currently takes place at one location in the Delaware Basin in a depleted gas field in the Morrow Formation at the Washington Ranch near Carlsbad Caverns (Burton et al. 1993, pp. 66-67; Appendix DATA-2004, Attachment A). This field is too far (approximately 50 mi [80 km]) from the WIPP site to have any effect on WIPP groundwaters under any circumstances. Disposal of liquid by-products from oil and gas production involves injection of fluid into depleted reservoirs. Such fluid injection techniques result in repressurization of the depleted target reservoir and mitigates any effects of fluid withdrawal.

The most significant effects of fluid injection would arise from substantial and uncontrolled fluid leakage through a failed borehole casing. The highly saline environment of some units can promote rapid corrosion of well casings and may result in fluid loss from boreholes.

SCR-5.2.1.4.3.2 Hydraulic Effects of Leakage through Injection Boreholes

The Vacuum Field (located in the Capitan Reef, some 30 km [20 mi] northeast of the WIPP site) and the Rhodes-Yates Field (located in the back reef of the Capitan, some 70 km [45 mi] southeast of the WIPP site) have been waterflooded for 40 yrs with confirmed leaking wells, which have resulted in brine entering the Salado and other formations above the Salado (see, for example, Silva 1994, pp. 67-68). Currently, saltwater disposal takes place in the vicinity of the WIPP into formations below the Castile. However, leakages from saltwater disposal wells or waterflood wells in the near future in the vicinity of the WIPP are unlikely to occur because of the following:

- There are significant differences between the geology and lithology in the vicinity of the disposal system and that of the Vacuum and Rhodes-Yates Fields. The WIPP is located in the Delaware Basin in a fore-reef environment, where a thick zone of anhydrite and halite (the Castile) exists. In the vicinity of the WIPP, oil is produced from the Brushy Canyon Formation at depths greater than 2,100 m (7,000 ft). By contrast, the Castile is not present at either the Vacuum or the Rhodes-Yates Field, which lie outside the Delaware Basin. Oil production at the Vacuum Field is from the San Andres and Grayburg Formations at depths of approximately 1,400 m (4,500 ft), and oil production at the Rhodes-Yates Field is from the Yates and Seven Rivers Formations at depths of approximately 900 m (3,000 ft). Waterflooding at the Rhodes-Yates Field involves injection into a zone only 60 m (200 ft) below the Salado. There are more potential thief zones below the Salado near the WIPP than at the Rhodes-Yates or Vacuum Fields; the Salado in the vicinity of the WIPP is therefore less likely to receive any fluid that leaks from an injection borehole. Additionally, the oil pools in the vicinity of the WIPP are

characterized by channel sands with thin net pay zones, low permeabilities, high irreducible water saturations, and high residual oil saturations. Therefore, waterflooding of oil fields in the vicinity of the WIPP on the scale of that undertaken in the Vacuum or the Rhodes-Yates Field is unlikely.

- New Mexico state regulations require the emplacement of a salt isolation casing string for all wells drilled in the potash enclave, which includes the WIPP area, to reduce the possibility of petroleum wells leaking into the Salado. Also, injection pressures are not allowed to exceed the pressure at which the rocks fracture. The injection pressure gradient must be kept below 4.5×10^3 pascals per meter above hydrostatic if fracture pressures are unknown. Such controls on fluid injection pressures limit the potential magnitude of any leakages from injection boreholes.

- Recent improvements in well completion practices and reservoir operations management have reduced the occurrences of leakages from injection wells. For example, injection pressures during waterflooding are typically kept below about 23×10^3 pascals per meter to avoid fracture initiation. Also, wells are currently completed using cemented and perforated casing, rather than the open-hole completions used in the early Rhodes-Yates wells.

Any injection well leakages that do occur in the vicinity of the WIPP in the near future are more likely to be associated with liquid waste disposal than waterflooding. Disposal typically involves fluid injection though old and potentially corroded well casings and does not include monitoring to the same extent as waterflooding. Such fluid injection could affect the performance of the disposal system if sufficient fluid leaked into the Salado interbeds to affect the rate of brine flow into the waste disposal panels.

Stoelzel and O'Brien (1996) evaluated the potential effects on the disposal system of leakage from a hypothetical salt water disposal borehole near the WIPP. Stoelzel and O'Brien (1996) used the two-dimensional BRAGFLO model (vertical north-south cross-section) to simulate saltwater disposal to the north and to the south of the disposal system. The disposal system model included the waste disposal region, the marker beds (MBs) and anhydrite intervals near the excavation horizon, and the rock strata associated with local oil and gas developments. A worst-case simulation was run using high values of borehole and anhydrite permeability and a low value of halite permeability to encourage flow to the disposal panels via the anhydrite. The boreholes were assumed to be plugged immediately above the Salado (consistent with the plugging configurations described in the CCA, Chapter 6.0, Section 6.4.7.2). Saltwater disposal into the Upper Bell Canyon was simulated, with annular leakage through the Salado. A total of approximately 7×10^5 m^3 (2.47×10^7 ft^3) of brine was injected through the boreholes during a 50-yr simulated disposal period. In this time, approximately 50 m^3 (1,765.5 ft^3) of brine entered the anhydrite interval at the horizon of the waste disposal region. For the next 200 yrs, the boreholes were assumed to be abandoned (with open-hole permeabilities of 1×10^{-9} square meters [m^2] [4×10^{-8} in.^{2}]). Cement plugs (of permeability 1×10^{-17} m^2 [4×10^{-16} in.^{2}]) were assumed to be placed at the injection interval and at the top of the Salado. Subsequently, the

boreholes were prescribed the permeability of silty sand (see the CCA, Chapter 6.0, Section 6.4.7.2), and the simulation was continued until the end of the 10,000-yr regulatory period. During this period, approximately 400 m^3 (14,124 ft^3) of brine entered the waste disposal region from the anhydrite interval. This value of cumulative brine inflow is within the bounds of the values generated by PA calculations for the UP scenario. During the disposal well simulation, leakage from the injection boreholes would have had no significant effect on the inflow rate at the waste panels.

Stoelzel and Swift (1997) expanded on Stoelzel and O'Brien's (1996) work by considering injection for a longer period of time (up to 150 yrs) and into deeper horizons at higher pressures. They developed two computational models (a modified cross-sectional model and an axisymmetric radial model) that are alternatives to the cross-sectional model used by Stoelzel and O'Brien (1996). Rather than repeat the conservative and bounding approach used by Stoelzel and O'Brien (1996), Stoelzel and Swift (1997) focused on reasonable and realistic conditions for most aspects of the modeling, including setting parameters that were sampled in the CCA at their median values. Model results indicate that, for the cases considered, the largest volume of brine entering MB 139 (the primary pathway to the WIPP) from the borehole is approximately 1,500 m^3 (52,974 ft^3), which is a small enough volume that it would not affect Stoelzel and O'Brien's (1996) conclusion even if it somehow all reached the WIPP. Other cases showed from 0 to 600 m^3 (21,190 ft^3) of brine entering MB 139 from the injection well. In all cases, high-permeability fractures created in the Castile and Salado anhydrite layers by the modeled injection pressures were restricted to less than 400 m (1,312 ft) from the wellbore and did not extend more than 250 m in MB 138 and MB 139.

No flow entered MB 139, nor was fracturing of the unit calculated to occur away from the borehole, in cases in which leaks in the cement sheath had permeabilities of $10^{-12.5}$ m^2 (corresponding to the median value used to characterize fully degraded boreholes in the CCA) or lower. The cases modeled in which flow entered MB 139 from the borehole and fracturing occurred away from the borehole required injection pressures conservatively higher than any currently in use near the WIPP and either 150 yrs of leakage through a fully degraded cement sheath or 10 yrs of simultaneous tubing and casing leaks from a waterflood operation. These conditions are not likely to occur in the future. If leaks like these do occur from brine injection near the WIPP, however, results of the Stoelzel and Swift (1997) modeling study indicate that they will not affect the performance of the repository.

Thus, the hydraulic effects of leakage through HCN boreholes outside the controlled area have been eliminated from PA calculations on the basis of low consequence to the performance of the disposal system.

SCR-5.2.1.4.3.3 Effects of Density Changes Resulting from Leakage Through Injection Boreholes

Leakage through a failed borehole casing during a fluid injection operation in the vicinity of the WIPP could alter fluid density in the affected unit, which could result in changes in fluid flow rates and directions within the disposal system. Disposal of oil and gas production byproducts

through boreholes could increase fluid densities in transmissive units affected by leakage in the casing. Operations such as waterflooding use fluids derived from the target reservoir, or fluids with a similar composition, to avoid scaling and other reactions. Therefore, the effects of leakage from waterflood boreholes would be similar to leakage from disposal wells.

Denser fluids have a tendency to sink relative to less dense fluids, and, if the hydrogeological unit concerned has a dip, there will be a tendency for the dense fluid to travel in the downdip direction. If this direction is the same as the direction of the groundwater pressure gradient, there would be an increase in flow velocity, and conversely, if the downdip direction is opposed to the direction of the groundwater pressure gradient, there would be a decrease in flow velocity. In general terms, taking account of density-related flow will cause a rotation of the flow vector towards the downdip direction that is dependent on the density contrast and the dip.

Wilmot and Galson (1996) showed that brine density changes in the Culebra resulting from leakage through an injection borehole outside the controlled area will not affect fluid flow in the Culebra significantly. Potash mining activities assumed on the basis of regulatory criteria to occur in the near future outside the controlled area will have a more significant effect on modeled Culebra hydrology. The distribution of existing leases suggests that near-future mining will take place to the north, west, and south of the controlled area (see the CCA, Chapter 2.0, Section 2.3.1.1). The effects of such potash mining are accounted for in calculations of UP of the disposal system (through an increase in the transmissivity of the Culebra above the mined region, as discussed in FEPs H37, H38, and H39 [Section SCR-5.2.2.1, Section SCR-5.2.2.2, and Section SCR-5.2.3.1]). Groundwater modeling that accounts for potash mining shows a change in the fluid pressure distribution and a consequent shift of flow directions towards the west in the Culebra within the controlled area (Wallace 1996c). A localized increase in fluid density in the Culebra resulting from leakage from an injection borehole would rotate the flow vector towards the downdip direction (towards the east).

Wilmot and Galson (1996) compared the relative magnitudes of the freshwater head gradient and the gravitational gradient and showed that the density effect is of low consequence to the performance of the disposal system. According to Darcy's Law, flow in an isotropic porous medium is governed by the gradient of fluid pressure and a gravitational term

$$\bar{v} = -\frac{k}{\mu}[\nabla p - \rho \bar{g}] \qquad \text{(SCR.7)}$$

where

v	=	Darcy velocity vector	(m s^{-1})
k	=	intrinsic permeability	(m^2)
μ	=	fluid viscosity	(Pa s)
∇p	=	gradient of fluid pressure	(Pa m^{-1})
ρ	=	fluid density	(kg m^{-3})
g	=	gravitational acceleration vector	(m s^{-2})

The relationship between the gravity-driven flow component and the pressure-driven component can be shown by expressing the velocity vector in terms of a freshwater head gradient and a density-related elevation gradient

$$\tilde{v} = -K \left[\nabla H_f + \frac{\Delta\rho}{\rho_f}\nabla E\right] \quad \text{(SCR.8)}$$

where

K	=	hydraulic conductivity	(m s^{-1})
∇H_f	=	gradient of freshwater head	
$\Delta\rho$	=	difference between actual fluid density and reference fluid density	(kg m^{-3})
ρ_f	=	density of freshwater	(kg m^{-3})
∇E	=	gradient of elevation	

Davies (1989, p. 28) defined a driving force ratio (DFR) to assess the potential significance of the density gradient

$$DFR = \frac{\Delta\rho|\nabla E|}{\rho_f|\nabla H_f|} \quad \text{(SCR.9)}$$

and concluded that a DFR of 0.5 can be considered an approximate threshold at which density-related gravity effects may become significant (Davies 1989, p. 28).

The dip of the Culebra in the vicinity of the WIPP is about 0.44 degrees or 8 m/km (26 ft/mi) to the east (Davies 1989, p. 42). According to Davies (1989, pp. 47–48), freshwater head gradients in the Culebra between the waste panels and the southwestern and western boundaries of the accessible environment range from 4 m/km (13 ft/mi) to 7 m/km (23 ft/mi). Only small changes in gradient arise from the calculated effects of near-future mining. Culebra brines have densities ranging from 998 to 1,158 kilograms per cubic meter (kg/m^3) (998 to 1,158 parts per million [ppm]) (Cauffman et al. 1990, Table E1.b). Assuming the density of fluid leaking from a waterflood borehole or a disposal well to be 1,215 kg/m^3 (1,215 ppm) (a conservative high value similar to the density of Castile brine [Popielak et al. 1983, Table C-2]) leads to a DFR of between 0.07 and 0.43. These values of the DFR show that density-related effects caused by leakage of brine into the Culebra during fluid injection operations are not significant. In summary, the effects of HCN fluid injection (liquid waste disposal, enhanced oil and gas production, and hydrocarbon storage) through boreholes outside the controlled area have been eliminated from PA calculations on the basis of low consequence to the performance of the disposal system.

SCR-5.2.1.4.3.4 Geochemical Effects of Leakage through Injection Boreholes

Injection of fluids through a leaking borehole could affect the geochemical conditions in thief zones, such as the Salado interbeds or the Culebra. Such fluid injection-induced geochemical changes could alter radionuclide migration rates within the disposal system in the affected

units if they occur sufficiently close to the edge of the controlled area through their effects on colloid transport and sorption.

The majority of fluids injected (for example, during brine disposal) have been extracted locally during production activities. Because they have been derived locally, their compositions are similar to fluids currently present in the disposal system, and they will have low total colloid concentrations compared to those in the waste disposal panels (see FEPs discussion for H21 through H24, Section SCR-5.2.1.1 and SCR-5.2.1.2). The repository will remain the main source of colloids in the disposal system. Therefore, colloid transport as a result of HCN fluid injection has been eliminated from PA calculations on the basis of low consequence to the performance of the disposal system.

As discussed in FEPs H21 through H24 (Section SCR-5.2.1.1 and SCR-5.2.1.2), sorption within the Culebra is accounted for in PA. The sorption model used accounts for the effects of any changes in sorption in the Culebra as a result of leakage through HCN injection boreholes.

Consistent with the screening discussion in FEPs H21 through H24, the effects of changes in sorption in the Dewey Lake within the controlled area as a result of leakage through HCN injection boreholes have been eliminated from PA calculations on the basis of low consequence to the performance of the disposal system. Sorption within other geological units of the disposal system has been eliminated from PA calculations on the basis of beneficial consequence to the performance of the disposal system.

Non-locally derived fluids could be used during hydraulic fracturing operations. However, such fluid-injection operations would be carefully controlled to minimize leakage to thief zones. Therefore, any potential geochemical effects of such leakages have been eliminated from PA calculations on the basis of low consequence to the performance of the disposal system.

SCR-5.2.1.4.3.5 Future Human EPs

Consistent with 40 CFR 194.33(d), PAs need not analyze the effects of techniques used for resource recovery subsequent to the drilling of a future borehole within the site boundary. Liquid waste disposal (byproducts from oil and gas production), enhanced oil and gas production, and hydrocarbon storage are techniques associated with resource recovery and are expected to continue into the future outside the site boundary. Analyses have shown that these activities have little consequence on repository performance (Stoelzel and Swift 1997). Therefore, activities such as liquid waste disposal, enhanced oil and gas production, and hydrocarbon storage outside the site boundary have been eliminated from PA calculations on the basis of low consequence.

SCR-5.2.1.5 **FEP Numbers: H60, H61, and H62**
FEP Titles: Liquid Waste Disposal – IB (H60)
Enhanced Oil and Gas Production – IB

(H61)
Hydrocarbon Storage – IB (H62)

SCR-5.2.1.5.1 Screening Decision: SO-R (HCN)
SO-R (Future)

The hydrological effects of HCN fluid injection (*Liquid Waste Disposal*, *Enhanced Oil and Gas Production*, and *Hydrocarbon Storage*) through boreholes inside the controlled area have been eliminated from PA calculations on regulatory grounds (40 CFR 194.25(a)). *Liquid Waste Disposal*, *Enhanced Oil and Gas Production*, and *Hydrocarbon Storage* (within the controlled area) in the future have been eliminated from PA calculations on regulatory grounds (40 CFR 194.33(d)).

SCR-5.2.1.5.2 Summary of New Information

No new information that affects the screening of this FEP has been identified since the CRA-2019.

SCR-5.2.1.5.3 Screening Argument

The injection of fluids in a borehole within the WIPP boundary could alter fluid-flow patterns in the target horizons or, if there is accidental leakage through a borehole casing, in any other intersected hydraulically conductive zone. Injection of fluids through a leaking borehole within the WIPP boundary could also result in geochemical changes and altered radionuclide migration rates in the thief units.

SCR-5.2.1.5.3.1 Historical, Current, and Near-Future Human EPs

Injection of fluids for the purposes of liquid disposal, enhanced oil and gas production, or hydrocarbon storage has not occurred within the WIPP boundary. Therefore, based on the future states assumption provided by 40 CFR 194.25(a), it is assumed that such activities will not occur within the near-future time frame, which includes the period of WIPP AICs. These activities are excluded from PA calculations on regulatory grounds.

SCR-5.2.1.5.3.2 Future Human EPs

The provisions of 40 CFR 194.33(d) state, “that performance assessments need not analyze the effects of techniques used for resource recovery subsequent to the drilling of the borehole.” Therefore, the future injection of fluids for the purposes of liquid disposal, enhanced oil and gas production, and hydrocarbon storage within the WIPP boundary have been excluded from PA calculations on regulatory grounds.

SCR-5.2.1.6 **FEP Number: H30**
FEP Title: Fluid Injection-Induced Geochemical Changes

SCR-5.2.1.6.1 Screening Decision: UP (HCN)
SO-R (Future)

Geochemical changes that occur inside the controlled area as a result of fluid flow associated with HCN fluid injection are accounted for in PA. Geochemical changes resulting from fluid injection in the future inside the controlled area have been eliminated from PA calculations on regulatory grounds.

SCR-5.2.1.6.2 Summary of New Information

No new information that affects the screening of this FEP has been identified since the CRA-2019.

SCR-5.2.1.6.3 Screening Argument

The injection of fluids could alter fluid-flow patterns in the target horizons or, if there is accidental leakage through a borehole casing, in any other intersected hydraulically conductive zone. Injection of fluids through a leaking borehole could also result in geochemical changes and altered radionuclide migration rates in the thief units.

SCR-5.2.1.6.3.1 Geochemical Effects of Leakage through Injection Boreholes

Injection of fluids through a leaking borehole could affect the geochemical conditions in thief zones, such as the Salado interbeds or the Culebra. Such fluid injection-induced geochemical changes could alter radionuclide migration rates within the disposal system in the affected units if they occur sufficiently close to the edge of the controlled area through their effects on colloid transport and sorption.

The majority of fluids injected (for example, during brine disposal) have been extracted locally during production activities. Because they have been derived locally, their compositions are similar to fluids currently present in the disposal system, and they will have low total colloid concentrations compared to those in the waste disposal panels (see FEPs H21 through H24, Section SCR-5.2.1.1 and SCR-5.2.1.2). The repository will remain the main source of colloids in the disposal system. Therefore, colloid transport as a result of HCN fluid injection has been eliminated from PA calculations on the basis of low consequence to the performance of the disposal system.

As discussed in FEPs H21 through H24 (Section SCR-5.2.1.1 and SCR-5.2.1.2), sorption within the Culebra is accounted for in PA. The sorption model used accounts for the effects of any changes in sorption in the Culebra as a result of leakage through HCN injection boreholes.

Consistent with the screening discussion in FEPs H21 through H24, the effects of changes in sorption in the Dewey Lake within the controlled area as a result of leakage through HCN injection boreholes have been eliminated from PA calculations on the basis of low consequence to the performance of the disposal system. Sorption within other geological units of the disposal system has been eliminated from PA calculations on the basis of beneficial consequence to the performance of the disposal system.

Non-locally derived fluids could be used during hydraulic fracturing operations. However, such fluid injection operations would be carefully controlled to minimize leakage to thief zones. Therefore, any potential geochemical effects of such leakages have been eliminated from PA calculations on the basis of low consequence to the performance of the disposal system.

SCR-5.2.1.6.3.2 Future Human EPs

Consistent with 40 CFR 194.33(d), PAs need not analyze the effects of techniques used for resource recovery subsequent to the drilling of a future borehole. Liquid waste disposal (byproducts from oil and gas production), enhanced oil and gas production, and hydrocarbon storage are techniques associated with resource recovery. Therefore, the use of future boreholes for such activities and fluid injection-induced geochemical changes have been eliminated from PA calculations on regulatory grounds.

SCR-5.2.1.6.4 FEP Implementation in PA

Impacts on sorption in the Culebra from FEP H30 *Fluid Injection-Induced Geochemical Changes* are accounted for in the Transport of Dissolved Actinides in the Culebra and Transport of Colloidal Actinides in the Culebra conceptual models. These conceptual models are implemented in the PA code SECOTP2D.

SCR-5.2.1.7 FEP Number: H31
FEP Title: Natural Borehole Fluid Flow (H31)

SCR-5.2.1.7.1 Screening Decision: SO-C (HCN)
SO-C (Future, holes not penetrating waste panels)
DP (Future, holes through waste panels)

The effects of *Natural Borehole Fluid Flow* through existing or near-future abandoned boreholes, known or unknown, have been eliminated from PA calculations on the basis of low consequence to the performance of the disposal system. The effects of *Natural Borehole Fluid Flow* through a future borehole that does not intersect the waste-disposal region have been eliminated from PA calculations on the basis of low consequence to the performance of the disposal system. *Natural Borehole Fluid Flow* through a future borehole that intersects a waste panel is accounted for in PA.

SCR-5.2.1.7.2 Summary of New Information

Since the CRA-2019, the target area for reporting borehole plugging has been changed to the nine-township area. This change was made based on information provided in EPA's TSD for 194.33 (U.S. EPA 2022a), Day (2023), and Santillan (2023). Probabilities for the various borehole plug types have been updated for use in PA (King 2025). This is an implementation change within PA and does not affect the screening argument or decision for this FEP.

SCR-5.2.1.7.3 Screening Argument

Abandoned boreholes could provide pathways for fluid flow and, potentially, contaminant transport between any intersected zones. For example, such boreholes could provide pathways for vertical flow between transmissive units in the Rustler, specifically the Culebra dolomite, or between the Rustler and units below the Salado, which could affect fluid densities, flow rates, and flow directions.

Movement of fluids through abandoned boreholes could result in borehole-induced geochemical changes in the receiving units, such as the Salado interbeds or Culebra, and thus alter radionuclide migration rates in these units.

Potentially, boreholes could provide pathways for surface-derived water or groundwater to percolate through low-permeability strata and into formations containing soluble minerals. Large-scale dissolution through this mechanism could lead to subsidence and changes in groundwater flow patterns. Also, fluid flow between hydraulically conductive horizons through a borehole may result in changes in permeability in the affected units through mineral precipitation.

SCR-5.2.1.7.3.1 Historical, Current, and Near-Future Human EPs

Abandoned water, potash, oil and gas exploration and production boreholes exist within and outside the controlled area. Most of these boreholes have been plugged in some way, but some have simply been abandoned. Over time, even the boreholes that have been plugged may provide hydraulic connections among the units they penetrate as the plugs degrade. The DOE assumes that records of past and present drilling activities in New Mexico are largely accurate, and that evidence of most boreholes would be included in these records. However, the potential effects of boreholes do not change depending on whether their existence is known, hence flow through unrecorded boreholes and flow through recorded boreholes can be evaluated together.

SCR-5.2.1.7.3.2 Hydraulic Effects of Flow through Abandoned Boreholes

Fluid flow and radionuclide transport within the Culebra could be affected if deep boreholes result in hydraulic connections between the Culebra and deep, overpressurized or underpressurized units, or if boreholes provide interconnections for flow between shallow units.

SCR-5.2.1.7.3.3 Connections Between the Culebra and Deeper Units

Fluid flow and radionuclide transport within the Culebra could be affected if deep boreholes result in hydraulic connections between the Culebra and deep, overpressurized or underpressurized units. Over the past 80 years, a large number of deep boreholes have been drilled within and around the controlled area (see the CCA, Chapter 6.0, Section 6.4.12.2). The effects on the performance of the disposal system of long-term hydraulic connections between the Culebra and deep units depends on the locations of the boreholes. In some cases, changes in the Culebra flow field caused by interconnections with deep units could decrease lateral radionuclide travel times to the accessible environment.

As part of an analysis to determine the impact of such interconnections, Wallace (1996a) gathered information on the pressures, permeabilities, and thicknesses of potential oil- or gas-bearing sedimentary units; such units exist to a depth of about 5,500 m (18,044 ft) in the vicinity of the WIPP. Of these units, the Atoka, some 4,000 m (13,123 ft) below the land surface, has the highest documented pressure of about 64 megapascals (MPa) (9,600 pounds per square inch [psi]), with permeability of about 2×10^{-14} m^2 (2.1×10^{-13} square ft [ft^2]) and thickness of about 210 m (689 ft). The Strawn, 3,900 m (12,795 ft) below the land surface, has the lowest pressures (35 MPa [5,000 psi], which is lower than hydrostatic) and highest permeability (10^{-13} m^2 [1.1×10^{-12} ft^2]) of the deep units, with a thickness of about 90 m (295 ft).

PA calculations indicate that the shortest radionuclide travel times to the accessible environment through the Culebra occur when flow in the Culebra over the disposal system is from north to south. Wallace (1996a) selected the steady-state Culebra flow model with the PA input that generated the shortest radionuclide travel times (with and without mining in the controlled area) and perturbed the flow field by placing a borehole connecting the contributive Atoka to the Culebra just north of the waste disposal panels and a borehole connecting the Culebra to the consumptive Strawn just south of the controlled area. The borehole locations were selected to coincide with the end points of the fastest flow paths modeled, which represents an unlikely worst-case condition. Although the Atoka is primarily a gas-bearing unit, Wallace (1996a) assumed that the unit is brine saturated. This assumption is conservative because it prevents two-phase flow from occurring in the Culebra, which would decrease the water permeability and thereby increase transport times. It was conservatively assumed that the pressure in the Atoka would not have been depleted by production before the well was plugged and abandoned. Furthermore, it was conservatively assumed that all flow from the Atoka would enter the Culebra and not intermediate or shallower units, and that flow from the Culebra could somehow enter the Strawn despite intermediate zones having higher pressures than the Culebra. The fluid flux through each borehole was determined using Darcy's Law, assuming a borehole hydraulic conductivity of 10^{-4} m/s (for a permeability of about 10^{-11} m^2 [1.1×10^{-10} ft^2]) representing silty sand, a borehole radius of 0.25 m (.82 ft), and a fluid pressure in the Culebra of 0.88 MPa (132 psi) at a depth of about 200 m (650 ft). With these parameters, the Atoka was calculated to transmit water to the Culebra at about 1.4×10^{-5} m^3/s (0.22 gpm), and the Strawn was calculated to receive water from the Culebra at about 1.5×10^{-6} m^3/s (0.024 gpm).

Travel times through the Culebra to the accessible environment were calculated using the SECOFL2D velocity fields for particles released to the Culebra above the waste panels, assuming no retardation by sorption or diffusion into the rock matrix. Mean Darcy velocities were then determined from the distance each radionuclide traveled, the time taken to reach the accessible environment, and the effective Culebra porosity. The results show that, at worst, interconnections between the Culebra and deep units under the unrealistically conservative assumptions listed above could cause less than a factor of two increase in the largest mean Darcy velocity expected in the Culebra in the absence of such interconnections.

The gradient differential can be compared to the potential effects of climate change on gradients and flow velocities through the Culebra. As discussed in the CCA, Chapter 6.0, Section 6.4.9 (and Corbet and Knupp 1996), the maximum effect of a future, wetter, climate would be to raise the water table to near the ground surface. This would raise heads and alter gradients in all units above the Salado. For the Culebra, the maximum change in gradient was estimated to be about a factor of 2.1. The effect of climate change is incorporated in compliance calculations through the Climate Index, which is used as a multiplier for Culebra groundwater velocities. The Climate Index has a bimodal distribution, with the range from 1.00 to 1.25 having a 75% probability, and the range from 1.50 to 2.25 having a 25% probability. Because implementation of the Climate Index leads to radionuclide releases through the Culebra that are orders of magnitude lower than the regulatory limits, the effects of flow between the Culebra and deeper units through abandoned boreholes can be screened out on the basis of low consequence.

SCR-5.2.1.7.3.4 Connections Between the Culebra and Shallower Units

Abandoned boreholes could also provide interconnections for long-term fluid flow between units (overlying the Salado). Abandoned boreholes could provide pathways for downward flow of water from the Dewey Lake and/or Magenta to the Culebra because the Culebra hydraulic head can be lower than the hydraulic heads of these units. Magenta freshwater heads are as much as 45 m (148 ft) higher than Culebra freshwater heads. Because the Culebra is generally at least one order of magnitude more transmissive than the Magenta at any location, a connection between the Magenta and Culebra would cause proportionally more drawdown in the Magenta head than rise in the Culebra head. For example, for a one-order-of-magnitude difference in transmissivity and a 45 m (148 ft) difference in head, the Magenta head would decrease by approximately 40 m (131 ft) while the Culebra head increased by 5 m (16 ft). This head increase in the Culebra would also be a localized effect, decreasing with radial distance from the leaking borehole. The primary flow direction in the Culebra across the WIPP site is from north to south, with the Culebra head decreasing by approximately 20 m (66 ft) across this distance. A 5 m (16 ft) increase in Culebra head at the northern WIPP boundary would, therefore, increase gradients by at most 25%.

The Dewey Lake freshwater head at the WQSP-6 pad is 55 m (180 ft) higher than the Culebra freshwater head, and the Dewey Lake is two orders of magnitude more transmissive than the Culebra (Beauheim and Ruskaauff 1998) at this location. Leakage from the Dewey Lake could

have a greater effect on Culebra head than leakage from the Magenta if the difference in transmissivity between the Dewey Lake and Culebra observed at the WQSP-6 pad persists over a wide region. However, the saturated, highly transmissive zone in the Dewey Lake has only been observed south of the WIPP disposal panels. A connection between the Dewey Lake and the Culebra south of the panels would tend to decrease the north-south gradient in the Culebra across the site, not increase it.

In any case, leakage of water from overlying units into the Culebra could not increase Culebra gradients as much as the maximum prediction from climate change, discussed above. Because implementation of the Climate Index leads to radionuclide releases through the Culebra that are orders of magnitude lower than the regulatory limits, the effects of flow between the Culebra and shallower units through abandoned boreholes can be screened out on the basis of low consequence.

SCR-5.2.1.7.3.5 Changes in Fluid Density Resulting from Flow Through Abandoned Boreholes

Leakage from historical, current, and near-future abandoned boreholes that penetrate pressurized brine pockets in the Castile could give rise to fluid density changes in affected units. Wilmot and Galson (1996) showed that brine density changes in the Culebra resulting from leakage through an abandoned borehole would not have a significant effect on the Culebra flow field. A localized increase in fluid density in the Culebra resulting from leakage from an abandoned borehole would rotate the flow vector towards the downdip direction (towards the east). A comparison of the relative magnitudes of the freshwater head gradient and the gravitational gradient, based on an analysis similar to that presented in Section SCR-5.2.1.4 (FEPs H27, H28, and H29), shows that the density effect is of low consequence to the performance of the disposal system.

SCR-5.2.1.7.3.6 Future Human EPs

The EPA provides criteria for analysis of the consequences of future drilling events in 40 CFR 194.33(c). Consistent with these criteria, it is assumed that after drilling is complete, the borehole is plugged according to current practice in the Delaware Basin (see U.S. DOE 2025a, Section 2.7, and Appendix PA-1.1.19 and PA-3.2.4). Degradation of casing and/or plugs may result in connections for fluid flow and, potentially, contaminant transport between connected hydraulically conductive zones. The long-term consequences of boreholes drilled and abandoned in the future will primarily depend on the location of the borehole and the borehole casing and plugging methods used.

SCR-5.2.1.7.3.7 Hydraulic Effects of Flow Through Abandoned Boreholes

A future borehole that penetrates a Castile brine reservoir could provide a connection for brine flow from the reservoir to the waste panel, thus increasing fluid pressure and brine volume in the waste panel. Long-term natural borehole fluid flow through such a borehole is accounted for in PA (see the CCA, Chapter 6.0, Section 6.4.8).

Deep, abandoned boreholes that intersect the Salado interbeds near the waste disposal panels could provide pathways for long-term radionuclide transport from the waste panels to the land surface or to overlying units. The potential significance of such events were assessed by the WIPP PA Department (1991, B-26 to B-27), which examined single-phase flow and transport between the waste panels and a borehole intersecting MB 139 outside the DRZ. The analysis assumed an in situ pressure of 11 MPa in MB 139, a borehole pressure of 6.5 MPa (975 psi) (hydrostatic) at MB 139, and a constant pressure of 18 MPa (2,700 psi) as a source term in the waste panels representing gas generation. Also, MB 139 was assigned a permeability of approximately 2.87×10^{-20} m^2 (3.09×10^{-19} ft^2) and a porosity of 1%. The disturbed zone was assumed to exist in MB 139 directly beneath the repository only and was assigned a permeability of 1.0×10^{-17} m^2 (1.1×10^{-16} ft^2) and a porosity of 5.5%. Results showed that the rate of flow through a borehole located just 0.25 m (0.8 ft) outside the DRZ would be more than two orders of magnitude less than the rate of flow through a borehole located within the DRZ because of the contrast in permeability. Thus, any releases of radionuclides to the accessible environment through deep boreholes that do not intersect waste panels would be insignificant compared to the releases that would result from transport through boreholes that intersect waste panels. Thus, radionuclide transport through deep boreholes that do not intersect waste panels has been eliminated from PA calculations on the basis of low consequence to the performance of the disposal system.

SCR-5.2.1.7.3.8 Fluid Flow and Radionuclide Transport in the Culebra

Fluid flow and radionuclide transport within the Culebra could be affected if future boreholes result in hydraulic connections between the Culebra and either deeper or shallower units. Over the 10,000-yr regulatory period, a large number of deep boreholes could be drilled within and around the controlled area (see the CCA, Chapter 6.0, Section 6.4.12.2). The effects on the performance of the disposal system of long-term hydraulic connections between the Culebra and deeper or shallower units would be the same as those discussed above for historic, current, and near-future conditions. Thus, the effects of flow between the Culebra and deeper or shallower units through abandoned future boreholes can be screened out on the basis of low consequence.

SCR-5.2.1.7.3.9 Changes in Fluid Density Resulting from Flow Through Abandoned Boreholes

A future borehole that intersects a pressurized brine reservoir in the Castile could also provide a source for brine flow to the Culebra in the event of borehole casing leakage, with a consequent localized increase in fluid density in the Culebra. This change in fluid density would increase any density-driven component of groundwater flow. If the downdip direction, along which the density-driven component would be directed, is different from the direction of the groundwater pressure gradient, there would be a slight rotation of the flow vector towards the downdip direction. The groundwater modeling presented by Davies (1989, p. 50) indicates that a borehole that intersects a pressurized brine pocket and causes a localized increase in fluid density in the Culebra above the waste panels would result in a rotation of the flow vector slightly towards the east. However, the magnitude of this effect would be small in comparison

to the magnitude of the pressure gradient (see screening argument for FEPs H27, H28, and H29, Section SCR-5.2.1.4, where this effect is screened out on the basis of low consequence).

SCR-5.2.1.7.4 FEP Implementation in PA

Natural Borehole Fluid Flow from future boreholes that intersect the waste panels is implemented in the Exploratory Boreholes and Repository Fluid Flow conceptual models. This fluid flow is implemented in the PA code BRAGFLO.

SCR-5.2.1.8 **FEP Number: H32**
FEP Title: Waste-Induced Borehole Flow

SCR-5.2.1.8.1 Screening Decision: SO-R (HCN)
DP (Future)

Waste-induced flow through boreholes drilled in the near future has been eliminated from PA calculations on regulatory grounds. *Waste-Induced Borehole Flow* through a future borehole that intersects a waste panel is accounted for in PA.

SCR-5.2.1.8.2 Summary of New Information

Since the CRA-2019, the target area for reporting borehole plugging has been changed to the nine-township area. This change was made based on information provided in EPA's TSD for Section 194.33 (U.S. EPA 2022a), Day (2023), and Santillan (2023). Probabilities for the various borehole plug types have been updated for use in PA (King 2025). This is an implementation change within PA and does not affect the screening argument or decision for this FEP.

SCR-5.2.1.8.3 Screening Argument

Abandoned boreholes could provide pathways for fluid flow and, potentially, contaminant transport between any intersected zones. For example, such boreholes could provide pathways for vertical flow between transmissive units in the Rustler, or between the Culebra and units below the Salado, which could affect fluid densities, flow rates, and flow directions.

Continued resource exploration and production in the near future will result in the occurrence of many more abandoned boreholes in the vicinity of the controlled area. Institutional controls will prevent drilling (other than that associated with the WIPP development) from taking place within the controlled area in the near future. Therefore, no boreholes will intersect the waste disposal region in the near future, and waste-induced borehole flow in the near future has been eliminated from PA calculations on regulatory grounds.

SCR-5.2.1.8.3.1 Future Human EPs

The EPA provides criteria concerning analysis of the consequences of future drilling events in 40 CFR 194.33(c). Consistent with these criteria, it is assumed that after drilling is complete, the borehole is plugged according to current practice in the Delaware Basin (see U.S. DOE 2025a,

Section 2.7, and Appendix PA-1.1.19 and PA-3.2.4). Degradation of casing and/or plugs may result in connections for fluid flow and, potentially, contaminant transport between connected hydraulically conductive zones. The long-term consequences of boreholes drilled and abandoned in the future will primarily depend on the location of the borehole and the borehole casing and plugging methods used.

SCR-5.2.1.8.3.2 Hydraulic Effects of Flow Through Abandoned Boreholes

An abandoned future borehole that intersects a waste panel could provide a connection for contaminant transport away from the repository horizon. If the borehole has degraded casing and/or plugs, and the fluid pressure within the waste panel is sufficient, radionuclides could be transported to the land surface. Additionally, if brine flows through the borehole to overlying units, such as the Culebra, it may carry dissolved and colloidal actinides that can be transported laterally to the accessible environment by natural groundwater flow in the overlying units. Long-term waste-induced borehole flow is accounted for in PA (see Appendix PA-2.4.4.2).

SCR-5.2.1.8.4 FEP Implementation in PA

Waste-Induced Borehole Fluid Flow from future boreholes that intersect the waste panels is implemented in the Exploratory Boreholes and Repository Fluid Flow conceptual models. This fluid flow is implemented in the PA code BRAGFLO.

SCR-5.2.1.9 FEP Number: H34
FEP Title: Borehole-Induced Solution and Subsidence

SCR-5.2.1.9.1 Screening Decision: SO-C (HCN)
SO-C (Future)

The effects of *Borehole-Induced Solution and Subsidence* associated with existing, near-future, and future abandoned boreholes have been eliminated from PA calculations on the basis of low consequence to the performance of the disposal system.

SCR-5.2.1.9.2 Summary of New Information

Discussion related to solution mining has been added to the screening argument (Land 2013). This new information does not affect the screening argument or decision for this FEP.

SCR-5.2.1.9.3 Screening Argument

Potentially, boreholes could provide pathways for surface-derived water or groundwater to percolate through low-permeability strata and into formations containing soluble minerals. Solution and subsidence requires that water unsaturated with halite flows through evaporite-bearing formations. Without ongoing throughflow, minor amounts of halite might be dissolved in the immediate vicinity of a borehole, but percolating water would become saturated with

respect to halite and stagnant in the bottom of the drillhole, preventing further dissolution. Large-scale dissolution through this mechanism could lead to subsidence and to changes in groundwater flow patterns. Also, fluid flow between hydraulically conductive horizons through a borehole may result in changes in permeability in the affected units through mineral precipitation.

Land describes additional subsidence and collapse features in the region, including two sinkhole events in northern Eddy County, New Mexico, and a third near Denver City, Texas, that resulted from solution mining (2013). Solution mining is described separately in FEPs H58 *Solution Mining for Potash* and H59 *Solution Mining for Other Resources*.

SCR-5.2.1.9.3.1 Historical, Current, and Near-Future Human EPs

SCR-5.2.1.9.3.1.1 Borehole-Induced Solution and Subsidence

During the period covered by HCN, drilling within the land withdrawn for the WIPP will be controlled, and boreholes will be plugged according to existing regulations. Under these circumstances and during this time period, borehole-induced solution and subsidence at the WIPP is eliminated from PA calculations on the basis of no consequence to the disposal system. Drilling has been regulated outside the area withdrawn for the WIPP, but conditions of historical and existing boreholes are highly variable. Borehole-induced solution and subsidence may occur in these areas, although it is expected to be limited and should not affect the disposal system, as discussed in the following paragraphs.

At, and in the vicinity of the WIPP site, drillholes partially penetrating the evaporite-bearing formations have little potential for dissolution. Brines coming from the Salado and Castile, for example, have high total dissolved solids and are likely to precipitate halite, not dissolve more halite during passage through the borehole. Water infiltrating from the surface or near-surface units may not be saturated with halite. For drillholes with a terminal depth in halite-bearing formations, there is little potential for dissolution because the halite-bearing units have very low permeability and provide little outlet for the brine created as the infiltrating water fills the drillhole. ERDA-9 is the deepest drillhole in the immediate vicinity of the waste panels at the WIPP; the bottom of the drillhole is in the uppermost Castile, with no known outlet for brine at the bottom.

However, drillholes penetrating through the evaporite-bearing formations provide possible pathways for circulation of water. Underlying units in the vicinity of the WIPP site with sufficient potentiometric levels or pressures to reach or move upward through the halite units generally have one of two characteristics: (1) high-salinity brines, which limit or eliminate the potential for dissolution of evaporites, or (2) are gas producers. Wood et al. (1982) analyzed natural processes of dissolution of the evaporites by water from the underlying Bell Canyon. They concluded that brine removal in the Bell Canyon is slow, limiting the movement of dissolution fronts or the creation of natural collapse features. Existing drillholes that are within the boundaries of the withdrawn land and also penetrate through the evaporites are not located in the immediate vicinity of the waste panels or WIPP workings.

There are three examples in the region that appear to demonstrate the process for borehole-induced solution and subsidence; all differ in their geohydrologic setting and drillhole completions from those at or near the WIPP.

Two examples of borehole-induced solution and subsidence occurred about 160 km (100 mi) southeast of the WIPP site (outside the Delaware Basin). The first occurred in 1980 at the Wink Sink (Baumgardner et al. 1982; Johnson 1989), where percolation of shallow groundwater through abandoned boreholes, dissolution of the Salado, and subsidence of overlying units led to a surface collapse feature 110 m (360 ft) in width and 34 m (110 ft) deep. At the Wink Sink, the Salado is underlain by the Tansill, Yates, and Capitan Formations, which contain vugs and solution cavities through which brine could migrate. Also, the hydraulic head of the Santa Rosa (the uppermost aquifer) is greater than those of the deep aquifers (Tansill, Yates, and Capitan), suggesting downward flow if a connection were established. A second sink (Wink Sink 2) formed in May 2002, near the earlier sink (Johnson et al. 2003). Its origin is similar to the earlier sink. By February 2003, Wink Sink 2 had enlarged by surface collapse to a length of about 305 m (1,000 ft) and a width of about 198 m (650 ft).

A similar, though smaller, surface collapse occurred in 1998 northwest of Jal, New Mexico (Powers 2003b). The most likely cause of collapse appears to be dissolution of Rustler, and possibly Salado, halite as relatively low salinity water from the Capitan Reef circulated through breaks in the casing of a deep water supply well. Much of the annulus behind the casing through the evaporite section was uncemented, and work in the well at one time indicated bent and ruptured casing. The surface collapse occurred quickly, and the sink was initially about 23 m (75 ft) across and a little more than 30 m (100 ft) deep. By 2001, the surface diameter was about 37 m (120 ft), and the sink was filled with collapse debris to about 18 m (60 ft) below the ground level (Powers 2003b).

The sinkholes near Wink, Texas and Jal, New Mexico occurred above the Capitan Reef (which is by definition outside the Delaware Basin), and the low-salinity water and relatively high potentiometric levels of the Capitan Reef appear to be integral parts of the process that formed these sinkholes. They are reviewed as examples of the process of evaporite dissolution and subsidence related to circulation in drillholes. Nevertheless, the factors of significant low salinity water and high potentiometric levels in units below the evaporites do not appear to apply at the WIPP site.

Beauheim (1986) considered the direction of natural fluid flow through boreholes in the vicinity of the WIPP. Beauheim (1986, p. 72) examined hydraulic heads measured using drill stem tests in the Bell Canyon and the Culebra at well DOE-2 and concluded that the direction of flow in a cased borehole open only to the Bell Canyon and the Culebra would be upward. Bell Canyon waters in the vicinity of the WIPP site are saline brines (e.g., Lambert 1978; Beauheim et al. 1983; Mercer et al. 1987), limiting the potential for dissolution of the overlying evaporites. However, dissolution of halite in the Castile and the Salado would increase the relative density of the fluid in an open borehole, causing a reduction in the rate of upward flow. The direction of borehole fluid flow could potentially reverse, but such a flow could be sustained only if

sufficient driving pressure, porosity, and permeability exist for fluid to flow laterally within the Bell Canyon. A further potential sink for Salado-derived brine is the Capitan Limestone. However, the subsurface extent of the Capitan Reef is approximately 16 km (10 mi) from the WIPP at its closest point, and this unit will not provide a sink for brine derived from boreholes in the vicinity of the controlled area. A similar screening argument is made for natural deep dissolution in the vicinity of the WIPP (see N16 and N18, Section SCR-4.2.4.1 and Section SCR-4.2.4.2).

The effects of borehole-induced solution and subsidence through a waste panel are considered below. The principal effects of borehole-induced solution and subsidence in the remaining parts of the disposal system should be to change the hydraulic properties of the Culebra and other rocks in the system. The features are local (limited lateral dimensions) and commonly nearly circular. If subsidence occurs along the expected travel path and the transmissivity of the Culebra is increased, as in the calculations conducted by Wallace (1996c), the travel times should increase. If the transmissivity along the expected flow path decreased locally as a result of such a feature, the flow path should be lengthened by travel around the feature. Thus, the effects of borehole-induced solution and subsidence around existing abandoned boreholes, and boreholes drilled and abandoned in the near-future, have been eliminated from PA calculations on the basis of low consequence to the performance of the disposal system.

SCR-5.2.1.9.3.2 Future Human EPs

The EPA provides criteria concerning analysis of the consequences of future drilling events in 40 CFR 194.33(c). Consistent with these criteria, it is assumed that after drilling is complete the borehole is plugged according to current practice in the Delaware Basin (see U.S. DOE 2025a, Section 2.7, and Appendix PA-1.1.19 and PA-3.2.4). Degradation of casing and/or plugs may result in connections for fluid flow and, potentially, contaminant transport between connected hydraulically conductive zones. The long-term consequences of boreholes drilled and abandoned in the future will primarily depend on the location of the borehole and the borehole casing and plugging methods used.

SCR-5.2.1.9.3.2.1 Borehole-Induced Solution and Subsidence

Future boreholes that do not intersect the WIPP excavation do not differ in long-term behavior or consequences from existing boreholes and can be eliminated from PA on the basis of low consequence to the performance of the disposal system.

The condition of more apparent concern is a future borehole that intersects the WIPP excavation. Seals and casings are assumed to degrade, connecting the excavation to various units. For a drillhole intersecting the excavation, but not connecting to a brine reservoir or to formations below the evaporites, downward flow is limited by the open volume of the disposal room(s), which is dependent with time, gas generation, or brine inflow to the disposal system from the Salado.

Maximum dissolution, and maximum increase in borehole diameter, will occur at the top of the Salado; dissolution will decrease with depth as the percolating water becomes salt saturated.

Eventually, degraded casing and concrete plug products, clays, and other materials will fill the borehole. Long-term flow through a borehole that intersects a waste panel is accounted for in DP calculations by assuming that the borehole is eventually filled by such materials, which have the properties of a silty sand (see Appendix PA-2.4.4.2). However, these calculations assume that the borehole diameter does not increase with time. Under the conditions assumed in the CCA for an E2 drilling event at 1,000 yrs, about 1,000 m^3 (35,316 ft^3) would be dissolved from the lower Rustler and upper Salado. If the dissolved area is approximately cylindrical or conical around the borehole, and the collapse/subsidence propagates upward as occurred in breccia pipes (e.g., Snyder and Gard 1982), the diameter of the collapsed or subsided area through the Culebra and other units would be a few tens of meters across. Changes in hydraulic parameters for this small zone should slow travel times for any hypothesized radionuclide release, as discussed for HCN occurrences. This does not change the argument for low consequence due to borehole-induced solution and subsidence for these circumstances.

If a borehole through a waste panel and into deeper evaporites intercepts a Castile brine reservoir, the brine has little or no capability of dissolving additional halite. The Castile brine flow is considered elsewhere as part of DP. There is, however, no Borehole-Induced Solution and *Subsidence* under this circumstance, and therefore there is no effect on performance because of this EP.

If a borehole intersects a waste panel and also interconnects with formations below the evaporite section, fluid flow up or down is determined by several conditions and may change over a period of time (e.g., as dissolution increases the fluid density in the borehole). Fluid flow downward is not a concern for performance, as fluid velocities in units such as the Bell Canyon are slow and should not be of concern for performance (Wilson et al. 1996). As with boreholes considered for HCN, the local change in hydraulic parameters, if it occurs along the expected flow path, would be expected to cause little change in travel time and should increase the travel time.

In summary, the effects of borehole-induced solution and subsidence around future abandoned boreholes have been eliminated from PA calculations on the basis of low consequence to the performance of the disposal system.

SCR-5.2.1.10 **FEP Number: H35**
FEP Title: Borehole-Induced Mineralization

SCR-5.2.1.10.1 Screening Decision: SO-C (HCN)
SO-C (Future)

The effects of *Borehole-Induced Mineralization*, associated with existing, near-future, and future abandoned boreholes, have been eliminated from PA calculations on the basis of low consequence to the performance of the disposal system.

SCR-5.2.1.10.2 Summary of New Information

Since the CRA-2019, the target area for reporting borehole plugging has been changed to the nine-township area. This change was made based on information provided in EPA's TSD for Section 194.33 (U.S. EPA 2022a), Day (2023), and Santillan (2023). Probabilities for the various borehole plug types have been updated for use in PA (King 2025). This is an implementation change within PA and does not affect the screening argument or decision for this FEP.

SCR-5.2.1.10.3 Screening Argument

Abandoned boreholes could provide pathways for fluid flow and, potentially, contaminant transport between any intersected zones. For example, such boreholes could provide pathways for vertical flow between transmissive units in the Rustler, or between the Culebra and units below the Salado, which could affect fluid densities, flow rates, and flow directions.

Movement of fluids through abandoned boreholes could result in borehole-induced geochemical changes in the receiving units, such as the Salado interbeds or Culebra, and thus alter radionuclide migration rates in these units.

Potentially, boreholes could provide pathways for surface-derived water or groundwater to percolate through low-permeability strata and into formations containing soluble minerals. Large-scale dissolution through this mechanism could lead to subsidence and to changes in groundwater flow patterns. Also, fluid flow between hydraulically conductive horizons through a borehole may result in changes in permeability in the affected units through mineral precipitation.

SCR-5.2.1.10.3.1 Borehole-Induced Mineralization

Fluid flow between hydraulically conductive horizons through a borehole may result in changes in permeability in the affected units through mineral precipitation. For example:

- Limited calcite precipitation may occur as the waters mix in the Culebra immediately surrounding the borehole, and calcite dissolution may occur as the brines migrate away from the borehole as a result of variations in water chemistry along the flow path.

- Gypsum may be dissolved as the waters mix in the Culebra immediately surrounding the borehole but may precipitate as the waters migrate through the Culebra.

The effects of these mass transfer processes on groundwater flow depend on the original permeability structure of the Culebra rocks and the location of the mass transfer. The volumes of minerals that may precipitate or dissolve in the Culebra as a result of the injection of Castile or Salado brine through a borehole will not affect the existing spatial variability in the permeability field significantly.

Predicted radionuclide transport rates in the Culebra assume that the dolomite matrix is diffusively accessed by the contaminants. The possible inhibition of matrix diffusion by

secondary mineral precipitation on fracture walls as a result of mixing between brines and Culebra porewater was addressed by Wang (1998). Wang showed that the volume of secondary minerals precipitated because of this mechanism was too small to significantly affect matrix porosity and accessibility.

Consequently, the effects of borehole-induced mineralization on permeability and groundwater flow within the Culebra, as a result of brines introduced via any existing abandoned boreholes and boreholes drilled and abandoned in the near future, have been eliminated from PA calculations on the basis of low consequence to the performance of the disposal system.

SCR-5.2.1.10.4 Future Human EPs

The EPA provides criteria concerning analysis of the consequences of future drilling events in 40 CFR 194.33(c). Consistent with these criteria, it is assumed that after drilling is complete the borehole is plugged according to current practice in the Delaware Basin (see U.S. DOE 2025a, Section 2.7, and Appendix PA-1.1.19 and PA-3.2.4). Degradation of casing and/or plugs may result in connections for fluid flow and, potentially, contaminant transport between connected hydraulically conductive zones. The long-term consequences of boreholes drilled and abandoned in the future will primarily depend on the location of the borehole and the borehole casing and plugging methods used.

SCR-5.2.1.10.4.1 Borehole-Induced Mineralization

Fluid flow between hydraulically conductive horizons through a future borehole may result in changes in permeability in the affected units through mineral precipitation. However, the effects of mineral precipitation as a result of flow through a future borehole in the controlled area will be similar to the effects of mineral precipitation as a result of flow through an existing or near-future borehole (see FEP H32, Section SCR-5.2.1.8). Thus, borehole-induced mineralization associated with flow through a future borehole has been eliminated from PA calculations on the basis of low consequence to the performance of the disposal system.

SCR-5.2.1.11 **FEP Number: H36**
FEP Title: Borehole-Induced Geochemical Changes

SCR-5.2.1.11.1 Screening Decision: UP (HCN)
DP (Future)
SO-C – Beneficial for units other than the Culebra

Geochemical changes that occur inside the controlled area as a result of long-term flow associated with HCN and future abandoned boreholes are accounted for in PA.

SCR-5.2.1.11.2 Summary of New Information

Since the CRA-2019, the target area for reporting borehole plugging has been changed to the nine-township area. This change was made based on information provided in EPA's TSD for Section 194.33 (U.S. EPA 2022a), Day (2023), and Santillan (2023). Probabilities for the various

borehole plug types have been updated for use in PA (King 2025). This is an implementation change within PA and does not affect the screening argument or decision for this FEP.

SCR-5.2.1.11.3 Screening Argument

Abandoned boreholes could provide pathways for fluid flow and, potentially, contaminant transport between any intersected zones. For example, such boreholes could provide pathways for vertical flow between transmissive units in the Rustler, or between the Culebra and units below the Salado, which could affect fluid densities, flow rates, and flow directions.

Movement of fluids through abandoned boreholes could result in borehole-induced geochemical changes in the receiving units such as the Salado interbeds or Culebra, and thus alter radionuclide migration rates in these units.

SCR-5.2.1.11.3.1 Geochemical Effects of Borehole Flow

Movement of fluids through abandoned boreholes could result in borehole-induced geochemical changes in the receiving units such as the Salado interbeds or Culebra. Such geochemical changes could alter radionuclide migration rates within the disposal system in the affected units if they occur sufficiently close to the edge of the controlled area, or if they occur as a result of flow through existing boreholes within the controlled area through their effects on colloid transport and sorption.

The contents of the waste disposal panels provide the main source of colloids in the disposal system. Thus, consistent with the discussion in Section SCR-5.2.1.2 (*Drilling-Induced Geochemical Changes* [H24]), colloid transport as a result of flow through existing and near-future abandoned boreholes has been eliminated from PA calculations on the basis of low consequence to the performance of the disposal system.

As discussed in H24, sorption within the Culebra is accounted for in PA. The sorption model used accounts for the effects of changes in sorption in the Culebra as a result of flow through existing and near-future abandoned boreholes.

Consistent with the screening discussion in Section SCR-5.2.1.2, the effects of changes in sorption in the Dewey Lake inside the controlled area as a result of flow through existing and near-future abandoned boreholes have been eliminated from PA calculations on the basis of low consequence to the performance of the disposal system. Sorption within other geological units of the disposal system has been eliminated from PA calculations on the basis of beneficial consequence to the performance of the disposal system.

SCR-5.2.1.11.4 Future Human EPs

The EPA provides criteria concerning analysis of the consequences of future drilling events in 40 CFR 194.33(c). Consistent with these criteria, it is assumed that after drilling is complete the borehole is plugged according to current practice in the Delaware Basin (see U.S. DOE 2025a, Section 2.7, and Appendix PA-1.1.19 and PA-3.2.4). Degradation of casing and/or plugs may

result in connections for fluid flow and, potentially, contaminant transport between connected hydraulically conductive zones. The long-term consequences of boreholes drilled and abandoned in the future will primarily depend on the location of the borehole and the borehole casing and plugging methods used.

SCR-5.2.1.11.4.1 Geochemical Effects of Flow Through Abandoned Boreholes

Movement of fluids through abandoned boreholes could result in borehole-induced geochemical changes in the receiving units, such as the Salado interbeds or Culebra. Such geochemical changes could alter radionuclide migration rates within the disposal system in the affected units through their effects on colloid transport and sorption.

The waste disposal panels provide the main source of colloids in the disposal system. Colloid transport within the Culebra as a result of long-term flow associated with future abandoned boreholes that intersect the waste disposal region are accounted for in PA, as described in the CCA, Chapter 6.0, Section 6.4.3.6 and Section 6.4.6.2.1. Consistent with the discussion in Section SCR-5.2.1.2, colloid transport as a result of flow through future abandoned boreholes that do not intersect the waste disposal region has been eliminated from PA calculations on the basis of low consequence to the performance of the disposal system. The Culebra is the most transmissive unit in the disposal system, and it is the most likely unit through which significant radionuclide transport could occur. Therefore, colloid transport in units other than the Culebra, as a result of flow through future abandoned boreholes, has been eliminated from PA calculations on the basis of low consequence to the performance of the disposal system.

As discussed in Section SCR-5.2.1.2, sorption within the Culebra is accounted for in PA. The sorption model accounts for the effects of changes in sorption in the Culebra as a result of flow through future abandoned boreholes.

Consistent with the screening discussion in Section SCR-5.2.1.2, the effects of changes in sorption in the Dewey Lake within the controlled area as a result of flow through future abandoned boreholes have been eliminated from PA calculations on the basis of low consequence to the performance of the disposal system. Sorption within other geological units of the disposal system has been eliminated from PA calculations on the basis of beneficial consequence to the performance of the disposal system.

SCR-5.2.1.11.5 FEP Implementation in PA

The FEP *Borehole-Induced Geochemical Changes* is incorporated in the WIPP conceptual models *Transport of Dissolved Actinides in the Culebra* and *Transport of Colloidal Actinides in the Culebra* and is implemented through uncertain sorption parameters for the matrix distribution coefficient in the SECOTP2D radionuclide transport model of the Culebra. Fluid discharge to the Culebra through future boreholes that intersect the waste panels is implemented in the *Exploratory Boreholes* and *Repository Fluid Flow* conceptual models. This fluid flow is implemented in the PA code BRAGFLO.

SCR-5.2.2 Excavation-Induced Flow

SCR-5.2.2.1 **FEP Number: H37**
FEP Title: Changes in Groundwater Flow Due to Mining

SCR-5.2.2.1.1 Screening Decision: UP (HCN)
DP (Future)

Changes in Groundwater Flow due to *Mining* (HCN and future) are accounted for in PA.

SCR-5.2.2.1.2 Summary of New Information

The screening argument was updated with the McNutt Potash mining leases in the vicinity of the WIPP site shown in the 2024 Delaware Basin Monitoring Annual Report (Figure 9, U.S. DOE, 2025a). An explanation of the implementation of this FEP within PA is also provided.

SCR-5.2.2.1.3 Screening Argument

Excavation activities may result in hydrological disturbances of the disposal system. Subsidence associated with excavations may affect groundwater flow patterns through increased hydraulic conductivity within and between units. Fluid flow associated with excavation activities may also result in changes in brine density and geochemistry in the disposal system.

SCR-5.2.2.1.3.1 Historical, Current, and Near-Future Human EPs

Currently, potash mining is the only excavation activity currently taking place in the vicinity of the WIPP that could affect hydrogeological or geochemical conditions in the disposal system. Potash is mined in the region east of Carlsbad from land leases extending to the boundaries of the controlled area. Mining of the McNutt Potash Zone in the Salado is expected to continue in the vicinity of the WIPP (see the CCA, Chapter 2.0, Section 2.3.1.1): it is assumed that all economically recoverable potash in the vicinity of the WIPP (outside the controlled area) will be extracted in the near future.

SCR-5.2.2.1.3.2 Hydrogeological Effects of Mining

Potash mining in the Delaware Basin typically involves constructing vertical shafts to the elevation of the ore zone and then extracting the minerals in an excavation that follows the trend of the ore body. Potash has been extracted using conventional room-and-pillar mining, secondary mining where pillars are removed, and modified long-wall mining methods. Mining techniques used include drilling and blasting (used for mining langbeinite) and continuous mining (commonly used for mining sylvite). Investigations of subsidence associated with potash mining operations located near the WIPP were reported (Westinghouse 1994, pp. 2-17 to 2-19). The reported maximum total subsidence at potash mines is about 1.5 m (5 ft), representing up to 66% of initial excavation height, with an observed angle of draw from the vertical at the edge

of the excavation of 58 degrees. No evidence was found that subsidence over local potash mines had caused fracturing sufficient to connect the mining horizon to water-bearing units or the surface (Westinghouse 1994 pp. 2-22 to 2-23). However, subsidence and fracturing associated with mining in the McNutt in the vicinity of the WIPP may allow increased recharge to the Rustler units and affect the lateral hydraulic conductivity of overlying units, such as the Culebra, which could influence the direction and magnitude of fluid flow within the disposal system. Such changes in groundwater flow due to mining are accounted for in calculations of UP of the disposal system. The effects of any increased recharge that may be occurring are, in effect, included by using the hydraulic heads measured to calibrate Culebra transmissivity fields (T-fields) and calculate transport through those fields (Appendix TFIELD-2026).

Potash mining, and the associated processing outside the controlled area, have changed fluid densities within the Culebra, as demonstrated by the areas of higher densities around boreholes WIPP-27 and WIPP-29 (Davies 1989, p. 43). Transient groundwater flow calculations (Davies 1989, pp. 77–81) show that brine density variations to the west of the WIPP site caused by historical and current potash processing operations will not persist because the rate of groundwater flow in this area is fast enough to flush the high-density groundwaters to the Pecos River. These calculations also show that accounting for the existing brine density variations in the region east of the WIPP site, where hydraulic conductivities are low, would have little effect on the direction or rate of groundwater flow. Therefore, changes in fluid densities from historical and current human EPs have been eliminated from PA calculations on the basis of low consequence to the performance of the disposal system.

The distribution of existing leases and potash grades suggests that near-future mining will take place primarily to the north, west, and south of the controlled area (U.S. DOE 2025a). A localized increase in fluid density in the Culebra, in the mined region or elsewhere outside the controlled area, would rotate the flow vector towards the downdip direction (towards the east). A comparison of the relative magnitudes of the pressure gradient and the density gradient (based on an analysis identical to that presented for fluid leakage to the Culebra through boreholes) shows that the density effect is of low consequence to the performance of the disposal system.

SCR-5.2.2.1.4 Future Human EPs

Consistent with 40 CFR 194.32(b), consideration of future mining may be limited to potash mining within the disposal system. Within the controlled area, the McNutt provides the only potash of appropriate quality. The extent of possible future potash mining within the controlled area is discussed in the CCA, Chapter 2.0, Section 2.3.1.1. Criteria concerning the consequence modeling of future mining are provided in section 194.32(b): the effects of future mining may be limited to changes in the hydraulic conductivity of the hydrogeologic units of the disposal system. Thus, consistent with 40 CFR 194.32(b), changes in groundwater flow due to mining within the controlled area are accounted for in calculations of the DP of the disposal system (see Appendix PA-4.9).

SCR-5.2.2.1.5 FEP Implementation in PA

The Culebra hydrogeology conceptual model accounts for localized increases in Culebra horizontal transmissivity due to mining underlying potash reserves. The impacts of potash mining are implemented in PA by applying the sampled parameter CULEBRA:MINP_FAC as a multiplier on the transmissivity values of MODFLOW Culebra flow model cells that are determined to be disturbed by potash mining. The areas disturbed by mining activities in the Culebra are larger than mined areas due to angle-of-draw effects; the subsidence effects propagate up and out at 45° angles between horizontal and vertical. To accommodate the angle of draw, the mining zone boundaries, as overlaid on the current model grid, are extended outward three model cells (300 meters) in the x- and y-directions, and two model cells (283 meters) in the diagonal directions.

Mining impacts are included in two scenarios, the partial mining scenario in which only potash reserves outside of the LWB are assumed to be mined, and the full mining scenario in which potash reserves are assumed to be mined wherever they are present throughout the model domain. It is assumed that all potash reserves outside of the land withdrawal boundary will be mined by the time of repository closure. Thereafter, the assumption is made that the probability that full mining conditions will occur is 1% every 100 years.

SCR-5.2.2.2 **FEP Number: H38**
FEP Title: Changes in Geochemistry Due to Mining

SCR-5.2.2.2.1 Screening Decision: SO-C (HCN)
SO-R (Future)

Changes in Geochemistry due to Mining (HCN) have been eliminated from PA calculations on the basis of low consequence to the performance of the disposal system. Future *Changes in Geochemistry due to Mining* have been eliminated from PA calculations on regulatory grounds.

SCR-5.2.2.2.2 Summary of New Information

No new information that affects the screening of this FEP has been identified since the CRA-2019. The screening argument has been edited for clarity.

SCR-5.2.2.2.3 Screening Argument

This section discusses surface activities that could affect the geomorphological characteristics of the disposal system and result in changes in infiltration and recharge conditions. The potential effects of water use and control on disposal system performance are discussed in FEPs H42 through H46 (Section SCR-5.4.1.1, Section SCR-5.4.1.2, and Section SCR-5.4.1.3).

SCR-5.2.2.2.3.1 Historical, Current, and Near-Future Human EPs

Potash mining is the only excavation activity currently taking place in the vicinity of the WIPP that could affect hydrogeological or geochemical conditions in the disposal system. Potash is mined in the region east of Carlsbad and up to 5 km (1.5 mi) from the boundaries of the controlled area. Mining of the McNutt in the Salado is expected to continue in the vicinity of the WIPP (see the CCA, Chapter 2.0, Section 2.3.1.1): it is assumed that all economically recoverable potash in the vicinity of the WIPP (outside the controlled area) will be extracted in the near future.

SCR-5.2.2.2.3.2 Geochemical Effects of Mining

Fluid flow associated with excavation activities may result in geochemical disturbances of the disposal system. Some waters from the Culebra reflect the influence of current potash mining, having elevated potassium to sodium ratios. However, conventional potash mining has had no significant effect on the geochemical characteristics of the disposal system. Solution mining, which involves the injection of freshwater to dissolve the ore body, can be used for extracting sylvite. Solution mining has taken place outside of the Delaware Basin (see discussion in SCR-5.2.2.3 (*Solution Mining for Potash*), but there are no current plans for the practice in the vicinity of the WIPP. Thus, changes in geochemistry due to mining (HCN) have been eliminated from PA calculations on the basis of low consequence to the performance of the disposal system.

SCR-5.2.2.2.3.3 Future Human EPs

Consistent with 40 CFR 194.32(b), consideration of future mining may be limited to potash mining within the disposal system. Within the controlled area, the McNutt provides the only potash of appropriate quality. The extent of possible future potash mining within the controlled area is discussed in the CCA, Chapter 2.0, Section 2.3.1.1. Criteria concerning the consequence modeling of future mining are provided in 40 CFR 194.32(b): the effects of future mining may be limited to changes in the hydraulic conductivity of the hydrogeologic units of the disposal system. Thus, consistent with 40 CFR 194.32(b), changes in groundwater flow as a result of mining within the controlled area are accounted for in calculations of the DP of the disposal system (see Appendix PA-4.9). Other potential effects, such as changes in geochemistry due to mining, have been eliminated from PA calculations on regulatory grounds.

SCR-5.2.2.3 **FEP Number H58**
FEP Title: Solution Mining for Potash

SCR-5.2.2.3.1 Screening Decision: SO-R (HCN)
SO-R (Future)

HCN and future *Solution Mining for Potash* has been eliminated from PA calculations on regulatory grounds.

SCR-5.2.2.3.2 Summary of New Information

No new information has been identified that pertains to the screening of this FEP since the CRA-2019.

SCR-5.2.2.3.3 Screening Argument

In August of 2012, Intrepid Potash, Inc., began flooding the abandoned mine workings of the old Eddy Potash mine in an effort to extract residual potash (sylvite) from the mine pillars. Intrepid Potash states that this potash is unrecoverable through conventional methods due to mine stability issues as discussed below. Once saturated, the injected water is pumped to the surface evaporation ponds. Potash ore is harvested from the evaporation ponds once a year and taken through the normal refining process to produce marketable forms of sylvite. Intrepid has indicated that based on the success of the Eddy mine solution project, the abandoned Amax Chemical mine may be a future solution mining target. The Amax site is located approximately 10 miles north of the Eddy mine. Both the Eddy and the Amax sites are north of the Delaware Basin boundary and are therefore beyond the region of interest for the WIPP Project. The existence of the Eddy solution project does not invalidate current screening arguments and decisions, because the actual solution activity is outside the Delaware Basin. If implemented, the Amax site is even further beyond the basinal boundary.

The potash reserves evaluated by Griswold and Griswold (1999) and New Mexico Bureau of Mines and Mineral Resources (1995) at the WIPP are of economic importance in only two ore zones; the 4th and the 10th contain two minerals of economic importance, langbeinite and sylvite. The ore in the 10th ore zone is primarily sylvite with some langbeinite and the ore in the 4th zone is langbeinite with some sylvite. Langbeinite falls between gypsum and polyhalite in solubility and dissolves at a rate 1,000 times slower than sylvite (Heyn 1997). Halite, the predominant gangue mineral present, is much more soluble than the langbeinite. Because of the insolubility of langbeinite, sylvite is the only potash ore in the WIPP vicinity that could be mined using a solution mining process. Mining for sylvite by solutioning would cause the langbeinite to be lost because conventional mining could not be done in conjunction with a solution mining process.

Typically, solution mining is used for potash:

- When deposits are at depths in excess of 914 m (3,000 ft) and rock temperatures are high, or are geologically too complex to mine profitably using conventional underground mining techniques
- To recover the potash pillars at the end of a mine's life
- When a mine is unintentionally flooded with waters from underlying or overlying rock strata and conventional mining is no longer feasible

Communiqués with IMC Global (Heyn 1997; Prichard 2003) indicated that rock temperature is critical to the success of a solution-mining endeavor. Mosaic Potash's (previously IMC Global) solution mines in Michigan and Saskatchewan are at depths of around 914 m (3,000 ft) or greater, at which rock temperatures are higher. The ore zones at the WIPP are shallow, at depths of 457 to 549 m (1,500 to 1,800 ft), with fairly cool rock temperatures. Prichard (2003) states that solution mining is energy intensive and the cool temperature of the rock would add to the energy costs. In addition, variable concentrations of confounding minerals (such as kainite and leonite) will cause problems with the brine chemistry.

Douglas W. Heyn (chief chemist of IMC Kalium) provided written testimony to the EPA related to the Agency's rulemaking activities on the CCA. Heyn concluded that "the rational choice for extracting WIPP potash ore reserves would be by conventional room and pillar mechanical means" (Heyn 1997). It is the opinion of IMC Global that no company will ever attempt solution mining of the ores in or near the WIPP (Heyn 1997; Prichard 2003).

The impact on the WIPP of neighboring potash mines and the possible effects of solution mining for potash or other evaporite minerals were examined in detail by D'Appolonia (1982). According to D'Appolonia (1982), and in agreement with Heyn (1997) of IMC Global, Inc., solution mining of langbeinite is not technically feasible because the ore is less soluble than the surrounding evaporite minerals. Serious technical and economic obstacles exist that render solution mining for potash very unlikely in the immediate vicinity of the WIPP. Expectedly, no operational example of this technology exists within the Delaware Basin; that is, solution mining for potash is not considered a current practice in the area. For this reason, consideration of solution mining on the disposal system in the future may be excluded on regulatory grounds. For example, the EPA stated in their Response to Comments, Section 8, Issue GG (U.S. EPA 1998d):

> …However, the Agency emphasizes that, in accordance with the WIPP compliance criteria, solution mining does not need to be included in the PA. As previously discussed, potash solution mining is not an ongoing activity in the Delaware Basin. Section 194.32(b) of the rule limits assessment of mining effects to excavation mining. Thus, the solution mining scenarios proposed are excluded on regulatory grounds after repository closure. Prior to or soon after disposal, solution mining is an activity that could be considered under Section 194.32(c). However, DOE found that potash solution mining is not an ongoing activity in the Delaware Basin; and one pilot project examining solution mining in the Basin is not substantive evidence that such mining is expected to occur in the near future. (Even if mining were assumed to occur in the near future, the proposed scenarios would not be possible because, even though solution mining might occur, there would be no intruding borehole to provide a pathway into the repository: active institutional controls would preclude such drilling during the first 100 years after disposal.) Furthermore, Section 194.33(d) states that PA need not analyze the effects of techniques used for resource recovery (e.g. solution mining) after a borehole is drilled in the future.

Conventional mining activities will continue to be incorporated into the WIPP PA as directed by the EPA CAG (U.S. EPA 1996b). Because the potash mines in the vicinity of the WIPP are in their mature (declining) stages of production, solution mining may be used in the future for extraction of remaining pillars, as is being done in the Intrepid Potash, Inc. project just outside the Delaware Basin. Nonetheless, at the time of this FEP reassessment, this technology is not

being employed within the Delaware Basin and a screening based on the future states assumption at 40 CFR 194.25(a) is appropriate for this mining technique at this time. While a regulatory screening (SO-R) is currently appropriate, if a potash solution mining project were to exist within the vicinity of the WIPP (within the Delaware Basin), the DOE has effectively argued that the consequences of such activity would be of low consequence and addressed by conventional mining FEPs. In a response to the Environmental Evaluation Group comment, the DOE effectively argued that, "If solution mining for potash were undertaken in the vicinity of the WIPP it could result in subsidence. However, performance assessment calculations already assume that widespread subsidence will occur as a result of potash mining in the near future. The assumed extent of subsidence and its effects on the hydraulic conductivity of Culebra are independent of the mining methods used (underground excavation or solution mining)." (U.S. EPA 1998d).

SCR-5.2.2.4 **FEP Number: H59**
FEP Title: Solution Mining for Other Resources

SCR-5.2.2.4.1 Screening Decision: SO-C (HCN)
SO-C (Future)

HCN and future *Solution Mining for Other Resources* have been eliminated from PA calculations on the basis of low consequence to the performance of the disposal system.

SCR-5.2.2.4.2 Summary of New Information

Brine well information provided in Table SCR-4 has been updated based on new information from the DBDSP (U.S. DOE 2025a).

SCR-5.2.2.4.3 Screening Argument

Brine wells (solution mining for brine) exist within the Delaware Basin, although none within the vicinity of the WIPP. Sulfur extraction using the Frasch process began in 1969 and continued for three decades at the Culberson County Rustler Springs mine near Orla, Texas. Solution mining for the purposes of creating a storage cavity has not occurred within the New Mexico portion of the Delaware Basin.

SCR-5.2.2.4.4 Solution Mining for Brine

Oil and gas reserves in the Delaware Basin are located in structures within the Delaware Mountain Group and lower stratigraphic units. Boreholes drilled to reach these horizons pass through the Salado and Castile that comprise thick halite and other evaporite units. To avoid dissolution of the halite units during drilling and prior to casing of the borehole, the fluid used for lubrication, rotating the drilling-bit cutters, and transporting cuttings (drilling mud) must be saturated with respect to halite. Most oil- and gas-field drilling operations in the Delaware Basin therefore use saturated brine (10 to 10.5 pounds per gallon [lb/gal]) as a drilling fluid until reaching the Bell Canyon, where intermediate casing is set.

One method of providing saturated brine for drilling operations is solution mining, whereby fresh water is pumped into the Salado, allowed to reach saturation with respect to halite, and then recovered. This manufactured brine is then transported to the drilling site by water tanker.

Two principal techniques are used for solution mining: single-borehole operations and doublet or two-borehole operations. In single-borehole operations, a borehole is drilled into the upper part of the halite unit. After casing and cementing this portion of the borehole, the borehole is deepened (uncased) into the upper part of the halite formation. An inner pipe is installed from the surface to the base of this uncased portion of the borehole. During operation, fresh water is pumped down the annulus of the borehole. This dissolves halite over the uncased portion of the borehole, and saturated brine is forced up the inner tube to the surface.

In doublet operations, a pair of boreholes is drilled, cased, and cemented into the upper part of the halite unit. The base of the production well is set some feet below the base of the injection well. In the absence of natural fractures or other connections between the boreholes, hydrofracturing is used to induce fractures around the injection well. During operation, fresh water is pumped down the injection well. This initially dissolves halite from the walls of the fractures and the resulting brine is then pumped from the production well. After a period of operation, a cavity develops between the boreholes as the halite between fractures is removed. Because of its lower density, fresh water injected into this cavity will rise to the top and dissolve halite from the roof of the cavity. As the brine density increases it sinks within the cavern and saturated brine is extracted from the production well.

Table SCR-4. Delaware Basin Brine Well Status

County	Location	API[b] №	Well Name and Number	Operator	Status/Type
Eddy	22S-27E-17	30-015-22574	Eugenie #1	I & W Inc.	Plugged Brine Well
Eddy	22S-27E-17	30-015-23031	Eugenie #2	I & W Inc.	Plugged Brine Well
Eddy	22S-27E-23	30-015-28083	Dunaway #001	Permian Water Solutions, LLC	Plugged Brine Well
Eddy	22S-27E-23	30-015-28084	Dunaway #2	Permian Water Solutions, LLC	Plugged Brine Well
Eddy	22S-26E-36	30-015-21842	City Of Carlsbad # 1	Key Energy Services, LLC	Plugged Brine Well
Eddy	22S-27E-03	30-015-20331	Tracy #3	Ray Westall	Plugged Brine Well

b American Petroleum Institute

SCR-5.2.2.4.4.1 Current Brine Wells within the Delaware Basin

Brine wells are classified as Class II injection wells. In the Delaware Basin, the process includes injecting fresh water into a salt formation to create a saturated brine solution which is then extracted and utilized as a drilling agent. Table SCR-4 provides information on brine wells within the New Mexico portion of the Delaware Basin, however none of these wells remain in use at this time. Additionally, while these wells are within the Delaware Basin, none are within the vicinity (9-township surrounding area) of the WIPP.

SCR-5.2.2.4.5 Solution Mining for Other Minerals

Currently, there are no ongoing solution mining activities within the vicinity of the WIPP. The Rustler Springs sulfur mine located in Culberson County, Texas, began operations in 1969 and continued until it was officially closed in 1999. This mine used the Frasch process (superheated water injection) to extract molten sulfur (Cunningham 1999).

SCR-5.2.2.4.6 Solution Mining for Gas Storage

No gas storage cavities have been solution mined within the New Mexico portion of the Delaware Basin. Five gas storage facilities exist within the general vicinity of the WIPP; however, only one is within the Delaware basin. This one New Mexico Delaware Basin facility uses a depleted gas reservoir for storage and containment; it was not solution mined (see Appendix DATA-2004, Attachment A, Section DATA-A-5.4).

SCR-5.2.2.4.7 Solution Mining for Disposal

Solution mining can be used to create a disposal cavity in bedded salt. Such disposal cavities can be used for the disposal of naturally occurring radioactive material or other wastes. No such cavities have been mined or operated within the vicinity of the WIPP.

SCR-5.2.2.4.8 Effects of Solution Mining

SCR-5.2.2.4.8.1 Subsidence

Regardless of whether the single-borehole or two-borehole technique is used for solution mining, the result is a subsurface cavity which could collapse and lead to subsidence of overlying strata. In a response to the Environmental Evaluation Group comment, the DOE effectively argued that, “If solution mining for potash were undertaken in the vicinity of the WIPP it could result in subsidence. However, performance assessment calculations already assume that widespread subsidence will occur as a result of potash mining in the near future. The assumed extent of subsidence and its effects on the hydraulic conductivity of Culebra are independent of the mining methods used (underground excavation or solution mining).” (U.S. EPA 1998d). While this FEP is primarily concerned with solution mining for other minerals (not potash), this argument holds for the removal of any mineral via the solution process (i.e., brine production).

SCR-5.2.2.4.8.2 Hydrogeological Effects

In regions where solution mining takes place, the hydrogeology could be affected in a number of ways:

- Subsidence above a large dissolution cavity could change the vertical and lateral hydraulic conductivity of overlying units.
- Extraction of fresh water from aquifers for solution mining could cause local changes in pressure gradients.
- Loss of injected fresh water or extracted brine to overlying units could cause local changes in pressure gradients.

The potential for subsidence to take place above solution mining operations in the region of Carlsbad, New Mexico, is discussed above. Some subsidence could occur in the future if brine operations continue at existing wells. Resulting fracturing may change permeabilities locally in overlying formations. However, because of the restricted scale of the solution mining at a particular site, and the distances between such wells, such fracturing will have no significant effect on hydrogeology near the WIPP.

Solution mining operations in the Delaware Basin extract water from shallow aquifers so that, even if large drawdowns are permitted, the effects on the hydrogeology will be limited to a relatively small area around the operation. Since all the active operations are more than 32 km (20 mi) from the WIPP, there will be no significant effects on the hydrogeology near the WIPP.

Discharge plans for solution mining operations typically include provision for annual mechanical integrity tests at one and one-half the normal operating pressure for four hours (New Mexico Oil Conservation Division 1994). Thus, the potential for loss of integrity and consequent leakage of freshwater or brine to overlying formations is low. If, despite these annual tests, large water losses did take place from either injection or production wells, the result would be low brine yields and remedial actions would most likely be taken by the operators.

SCR-5.2.2.4.8.3 Geochemical Effects

Solution mining operations could affect the geochemistry of surface or subsurface water near the operation if there were brine leakage from storage tanks or production wells. Discharge plans for solution mining operations specify the measures to be taken to prevent leakage and to mitigate the effects of any that do take place. These measures include berms around tanks and annual mechanical integrity testing of wells (New Mexico Oil Conservation Division 1994). The potential for changes in geochemistry is therefore low, and any brine losses that did take place would be limited by remedial actions taken by the operator. In the event of leakage from a production well, the effect on geochemistry of overlying formation waters would be localized and given the distance of such wells from the WIPP site, such leakage would have no significant effect on geochemistry near the WIPP.

SCR-5.2.2.4.9 Conclusion of Low Consequence

Brine production through solution mining takes place in the Delaware Basin, and the DOE assumes it will continue in the near future. Because of the existence of these solution operations, it is not possible to screen this activity based on the provisions of 40 CFR 194.25(a). However, despite oil and gas exploration and production taking place in the vicinity of the WIPP site, the nearest operating solution mine is more than 32 km (20 mi) from the WIPP site. It is assumed that these locations are too far from the WIPP site for any changes in hydrogeology or geochemistry, from subsidence or fresh water or brine leakage, to affect the performance of the disposal system. Thus, the effects of HCN and future solution mining for other resources in the Delaware Basin can be eliminated from PA calculations on the basis of low consequence to the performance of the disposal system.

SCR-5.2.3 Explosion-Induced Flow

SCR-5.2.3.1 **FEP Number: H39**
FEPs Title: Changes in Groundwater Flow Due to Explosions

SCR-5.2.3.1.1 Screening Decision: SO-C (HCN)
SO-R (Future)

Changes in Groundwater Flow due to Explosions (HCN) have been eliminated from PA calculations on the basis of low consequence to the performance of the disposal system. Changes in groundwater flow that may be caused by future explosions have been eliminated from PA calculations on regulatory grounds.

SCR-5.2.3.1.2 Summary of New Information

No new information that affects the screening of this FEP has been identified since the CRA-2019.

SCR-5.2.3.1.3 Screening Argument

SCR-5.2.3.1.3.1 Historical, Current, and Near-Future Human EPs

The small-scale explosions that have been used in the Delaware Basin to fracture oil- and natural-gas-bearing units to enhance resource recovery have been too deep to have disturbed the hydrology of the disposal system (see FEP H19, Section SCR-5.1.3.1).

Also, as discussed in Section SCR-5.1.3.2 (*Underground Nuclear Device Testing* [H20]), the Delaware Basin has been used for an isolated nuclear test (Project Gnome), approximately 13 km (8 mi) southwest of the WIPP waste disposal region. An induced zone of increased permeability was observed to extend 46 m (150 ft) laterally from the point of the explosion. The increase in permeability was primarily associated with motions and separations along bedding planes, the major preexisting weaknesses in the rock. This region of increased permeability is too far from the WIPP site to have had a significant effect on the hydrological characteristics of the disposal system. Thus, changes in groundwater flow due to explosions in the past have been eliminated from PA calculations on the basis of low consequence to the performance of the disposal system.

SCR-5.2.3.1.3.2 Future Human EPs

The criterion in 40 CFR 194.32(a) relating to the scope of PAs limits the consideration of future human actions to mining and drilling. Also, consistent with 40 CFR 194.33(d), PAs need not analyze the effects of techniques used for resource recovery subsequent to the drilling of a future borehole. Therefore, changes in groundwater flow due to explosions in the future have been eliminated from PA calculations on regulatory grounds.

SCR-5.3 Geomorphological EPs

SCR-5.3.1 Land Use Changes

SCR-5.3.1.1 **FEP Number: H40**
FEP Title: Land Use Changes

SCR-5.3.1.1.1 Screening Decision: SO-R (HCN)
SO-R (Future)

Land Use Changes have been eliminated from PA calculations on regulatory grounds.

SCR-5.3.1.1.2 Summary of New Information

This FEP screening argument has been updated with new information. The screening decision has not changed.

SCR-5.3.1.1.3 Screening Argument

This section discusses surface activities that could affect the geomorphological characteristics of the disposal system and result in changes in infiltration and recharge conditions. The potential effects of water use and control on disposal system performance are discussed in FEPs H42 through H46 (Section SCR-5.4.1.1, Section SCR-5.4.1.2, and Section SCR-5.4.1.3).

SCR-5.3.1.1.4 Historical, Current, and Near-Future Human EPs

Surface activities that take place at present in the vicinity of the WIPP site include those associated with potash mining, oil and gas reservoir development, water extraction, and grazing. Additionally, a number of archaeological investigations have taken place within the controlled area that were aimed at protecting and preserving cultural resources. Elsewhere in the Delaware Basin, sand, gravel, and caliche are produced through surface quarrying. The only surface activity that has the potential to affect the disposal system is potash tailings, salt tailings (both potash and WIPP), and effluent disposal. Potash tailings ponds may act as sources of focused recharge to the Dewey Lake and Rustler units.

Three potash tailings piles/ponds are in operation that might be influencing groundwater flow at the WIPP site. These are the Mississippi Potash Inc. (MPI) East tailings pile, approximately 10 km (6 mi) due north of the WIPP, the MPI West tailings pile in the northwest arm of Nash Draw, and the IMC Kalium tailings pile, approximately 10 km (6 mi) due west of the WIPP in Nash Draw. These tailings piles have been in operation for decades—disposal at the MPI East site, the youngest of the piles, began in 1965. Brine disposal at these locations affects Rustler groundwaters in Nash Draw, as shown by the hydrochemical facies D waters described by Siegel et al. (1991, p. 2-61). Brine disposal also affects heads in Nash Draw, and these head effects likely propagate to the WIPP site as well. These effects, however, predate water-level monitoring for the WIPP and have been implicitly included when defining boundary heads for

Culebra flow models. The CRA-2026 Culebra T-fields were calibrated using Culebra groundwater level observations collected since 2000 (Appendix TFIELD-2026). Thus, the effects of brine disposal at the tailings piles can be considered to be included in PA calculations. These effects are expected to continue in the near future.

The Delaware Basin monitoring program monitors land use activities in the WIPP vicinity. This program has not identified new planned uses for land in the vicinity of the WIPP (U.S. DOE 2025a). Therefore, consistent with the criteria in section 194.32(c) and section 194.54(b) (U.S. EPA 1996a), land use changes in the near future in the vicinity of the WIPP have been eliminated from PA calculations on regulatory grounds.

SCR-5.3.1.1.5 Future Human EPs

The criterion in 40 CFR 194.25(a), concerned with predictions of the future states of society, requires that compliance assessments and PAs "shall assume that characteristics of the future remain what they are at the time the compliance application is prepared, provided that such characteristics are not related to hydrogeologic, geologic or climatic conditions." Therefore, no future land use changes need be considered in the vicinity of the WIPP, and they have been eliminated from PA calculations on regulatory grounds.

SCR-5.3.1.2 **FEP Number: H41**
FEP Title: Surface Disruptions

SCR-5.3.1.2.1 Screening Decision: UP (HCN)
SO-C (Future)

The effects of HCN *Surface Disruptions* are accounted for in PA. The effects of future *Surface Disruptions* have been eliminated from PA calculations on the basis of low consequence.

SCR-5.3.1.2.2 Summary of New Information

This FEP has been updated to reference new data used in calibrating Culebra T-fields. Otherwise, the screening argument and screening decision for this FEP has not changed. Additional information on FEP implementation in PA has been provided, including related conceptual models implementing PA codes.

SCR-5.3.1.2.3 Screening Argument

This section discusses surface activities that could affect the geomorphological characteristics of the disposal system and result in changes in infiltration and recharge conditions. The potential effects of water use and control on disposal system performance are discussed in FEPs H42 through H46.

SCR-5.3.1.2.4 Historical, Current, and Near-Future Human EPs

Most surface activities have no potential to affect the disposal system and are, therefore, screened out on the basis of low consequence (e.g., archaeological excavations and arable farming). However, the effects of activities capable of altering the disposal system (disposal of potash effluent) are included in the modeling of current conditions (i.e., heads) at and around the site. Discussion regarding these anthropogenic effects is found in the CRA-2004, Chapter 2.0, Section 2.2.1.4.2.2.

Surface activities that take place at present in the vicinity of the WIPP site include those associated with potash mining, oil and gas reservoir development, water extraction, and grazing. Additionally, a number of archaeological investigations have taken place within the controlled area that were aimed at protecting and preserving cultural resources. Elsewhere in the Delaware Basin, sand, gravel, and caliche are produced through surface quarrying. The only surface activity that has the potential to affect the disposal system is potash tailings, salt tailings (both potash and WIPP), and effluent disposal. Potash tailings ponds may act as sources of focused recharge to the Dewey Lake and Rustler units.

Three potash tailings piles/ponds are in operation that might be influencing groundwater flow at the WIPP site. These are the MPI East tailings pile, approximately 10 km (6 mi) due north of the WIPP, the MPI West tailings pile in the northwest arm of Nash Draw, and the IMC Kalium tailings pile, approximately 10 km (6 mi) due west of the WIPP in Nash Draw. These tailings piles have been in operation for decades—disposal at the MPI East site, the youngest of the piles, began in 1965. Brine disposal at these locations affects Rustler groundwaters in Nash Draw, as shown by the hydrochemical facies D waters described by Siegel et al. (1991, p. 2-61). Brine disposal also affects heads in Nash Draw, and these head effects likely propagate to the WIPP site as well. These effects, however, predate water-level monitoring for the WIPP and have been implicitly included when defining boundary heads for Culebra flow models. The Culebra T-fields developed for the CRA-2026 (Appendix TFIELD-2026) include data gathered since 2000 to define model boundary conditions. Thus, the effects of brine disposal at the tailings piles can be considered to be included in PA calculations. These effects are expected to continue in the near future.

SCR-5.3.1.2.5 Future Human EPs

Future tailings ponds, if situated in Nash Draw, are expected to change Culebra (and Magenta) heads, similar to existing ones. Future tailings ponds outside of Nash Draw would not be expected to alter Culebra heads because leakage from the ponds would not be able to propagate through the low-permeability lower Dewey Lake clastics and Rustler anhydrites overlying the Culebra during the 100 yrs or less that such a pond might be in operation. Because PA calculations already include the present-day effects of tailings ponds in Nash Draw on heads, as well as the effects of future potash mining on the permeability of the Culebra (which has much greater potential to alter flow than changes in head), future surface disruptions affecting hydrologic or geologic conditions (such as potash tailings ponds) may be screened out on the basis of low consequence.

SCR-5.3.1.2.6 FEP Implementation in PA

H41 *Surface Disruptions* is included in the UP scenario and is associated with the Culebra Hydrology conceptual model and implemented by the groundwater flow code MODFLOW and parameter calibration code PEST. The effect surface disruptions may have on groundwater flow is captured by calibrating the Culebra flow model using water-level data collected in the Culebra monitoring program.

SCR-5.4 Surface Hydrological EPs

SCR-5.4.1 Water Control and Use

SCR-5.4.1.1 **FEP Numbers: H42, H43, and H44**
FEP Titles: Damming of Streams and Rivers (H42)
Reservoirs (H43)
Irrigation (H44)

SCR-5.4.1.1.1 Screening Decision: SO-C (HCN)
SO-R (Future)

The effects of HCN *Damming of Streams and Rivers*, *Reservoirs*, and *Irrigation* have been eliminated from PA calculations on the basis of low consequence to the performance of the disposal system. Future *Damming of Streams and Rivers*, *Reservoirs*, and *Irrigation* have been eliminated from PA calculations on regulatory grounds.

SCR-5.4.1.1.2 Summary of New Information

No new information that affects the screening of this FEP has been identified since the CRA-2019.

SCR-5.4.1.1.3 Screening Argument

Irrigation and damming, as well as other forms of water control and use, could lead to localized changes in recharge, possibly leading to increased heads locally, thereby affecting flow directions and velocities in the Rustler and Dewey Lake.

SCR-5.4.1.1.4 Historical, Current, and Near-Future Human EPs

In the WIPP area, two topographically low features, the Pecos River and Nash Draw, are sufficiently large to warrant consideration for damming. Dams and reservoirs already exist along the Pecos River. However, the Pecos River is far enough from the waste panels (19 km [12 mi]) that the effects of damming of streams and rivers and reservoirs can be eliminated from PA calculations on the basis of low consequence to the performance of the disposal system. Nash Draw is not currently dammed, and based on current hydrological and climatic conditions, there is no reason to believe it will be dammed in the near future.

Irrigation uses water from rivers, lakes, impoundments, and wells to supplement the rainfall in an area to grow crops. Irrigation in arid environments needs to be efficient and involves the spreading of a relatively thin layer of water for uptake by plants, so little water would be expected to infiltrate beyond the root zone. However, some water added to the surface may infiltrate and reach the water table, affecting groundwater flow patterns. Irrigation currently takes place on a small scale within the Delaware Basin but not in the vicinity of the WIPP, and the extent of irrigation is not expected to change in the near future. Such irrigation has no significant effect on the characteristics of the disposal system. Thus, the effects of irrigation have been eliminated from PA calculations on the basis of low consequence to the performance of the disposal system.

SCR-5.4.1.1.5 Future Human EPs

The EPA has provided criteria relating to future human activities in 40 CFR 194.32(a) that limit the scope of consideration of future human actions in PAs to mining and drilling. Therefore, the effects of future damming of streams and rivers, reservoirs, and irrigation have been eliminated from PA calculations on regulatory grounds.

SCR-5.4.1.2 **FEP Number: H45**
FEP Title: Lake Usage

SCR-5.4.1.2.1 Screening Decision: SO-R (HCN)
SO-R (Future)

The effects of *Lake Usage* have been eliminated from PA calculations on regulatory grounds.

SCR-5.4.1.2.2 Summary of New Information

No new information that affects the screening of this FEP has been identified since the CRA-2019.

SCR-5.4.1.2.3 Screening Argument

Irrigation and damming, as well as other forms of water control and use, could lead to localized changes in recharge, possibly leading to increased heads locally, thereby affecting flow directions and velocities in the Rustler and Dewey Lake. Surface activities, such as those associated with potash mining, could also affect soil and surface water chemistry. Note that the potential effects of geomorphological changes through land use are discussed in Section SCR-5.3.1.1 and Section SCR-5.3.1.2.

SCR-5.4.1.2.4 Historical, Current, and Near-Future Human EPs

As discussed in the CCA, Chapter 2.0, Section 2.2.2, there are no major natural lakes or ponds within 8 km (5 mi) of the site. To the northwest, west, and southwest, Red Lake, Lindsey Lake, and Laguna Grande de la Sal are more than 8 km (5 mi) from the site, at elevations of 914 to

1,006 m (3,000 to 3,300 ft). Laguna Gatuña, Laguna Tonto, Laguna Plata, and Laguna Toston are playas more than 16 km (10 mi) north and are at elevations of 1,050 m (3,450 ft) or higher.

Waters from these lakes are of limited use. Therefore, human activities associated with lakes have been screened out of PA calculations based on regulatory grounds supported by 40 CFR 194.32(c) and 40 CFR 194.54(b).

SCR-5.4.1.2.5 Future Human EPs

The EPA has provided criteria relating to future human activities in 40 CFR 194.32(a) that limit the scope of consideration of future human actions in PAs to mining and drilling. Therefore, the effects of future lake usage have been eliminated from PA calculations on regulatory grounds.

SCR-5.4.1.3 **FEP Number: H46**
FEP Title: Altered Soil or Surface Water Chemistry by Human Activities

SCR-5.4.1.3.1 Screening Decision: SO-C (HCN)
SO-R (Future)

The effects of HCN *Altered Soil or Surface Water Chemistry by Human Activities* have been eliminated from PA calculations on the basis of low consequence to the performance of the disposal system. Future *Altered Soil or Surface Water Chemistry by Human Activities* have been eliminated from PA calculations on regulatory grounds.

SCR-5.4.1.3.2 Summary of New Information

No new information that affects the screening of this FEP has been identified since the CRA-2019.

SCR-5.4.1.3.3 Screening Argument

Irrigation and damming, as well as other forms of water control and use, could lead to localized changes in recharge, possibly leading to increased heads locally, thereby affecting flow directions and velocities in the Rustler and Dewey Lake. Surface activities, such as those associated with potash mining, could also affect soil and surface water chemistry.

SCR-5.4.1.3.4 Historical, Current, and Near-Future Human EPs

Potash mining effluent and runoff from oil fields have altered soil and surface water chemistry in the vicinity of the WIPP. However, the performance of the disposal system will not be sensitive to soil and surface water chemistry. Therefore, altered soil or surface water chemistry by human activities has been eliminated from PA calculations on the basis of low consequence to the performance of the disposal system. The effects of effluent from potash processing on groundwater flow are discussed in H37 (Section SCR-5.2.2.1).

SCR-5.4.1.3.5 Future Human EPs

The EPA has provided criteria relating to future human activities in 40 CFR 194.32(a) that limit the scope of consideration of future human actions in PAs to mining and drilling. Therefore, the effects of future altered soil or surface water chemistry by human activities have been eliminated from PA calculations on regulatory grounds.

SCR-5.5 Climatic EPs

SCR-5.5.1 Anthropogenic Climate Change

SCR-5.5.1.1 **FEP Numbers: H47, H48, and H49**
FEP Titles: Greenhouse Gas Effects (H47)
Acid Rain (H48)
Damage to the Ozone Layer (N49)

SCR-5.5.1.1.1 Screening Decision: SO-R (HCN)
SO-R (Future)

The effects of anthropogenic climate change (*Acid Rain*, *Greenhouse Gas Effects*, and *Damage to the Ozone Layer*) have been eliminated from PA calculations on regulatory grounds.

SCR-5.5.1.1.2 Summary of New Information

No new information that affects the screening of this FEP has been identified since the CRA-2019.

SCR-5.5.1.1.3 Anthropogenic Climate Change

The effects of the current climate and natural climatic change are accounted for in PA, as discussed in the CCA, Chapter 6.0, Section 6.4.9, and Appendix PA-4.9. However, human activities may also affect the future climate and thereby influence groundwater recharge in the WIPP region. The effects of anthropogenic climate change may be on a local to regional scale (acid rain) or on a regional to global scale (greenhouse gas effects and damage to the ozone layer). Of these anthropogenic effects, only the greenhouse gas effect could influence groundwater recharge in the WIPP region. However, consistent with the future states assumptions in 40 CFR 194.25, compliance assessments and PAs need not consider indirect anthropogenic effects on disposal system performance. Therefore, the effects of anthropogenic climate change have been eliminated from PA calculations on regulatory grounds.

SCR-5.6 Marine EPs

SCR-5.6.1 Marine Activities

SCR-5.6.1.1 **FEP Numbers: H50, H51, and H52**
FEP Titles: Coastal Water Use (H50)
Seawater Use (H51)
Estuarine Water Use (H52)

SCR-5.6.1.1.1 Screening Decision: SO-R (HCN)
SO-R (Future)

HCN, and future *Coastal Water Use*, *Seawater Use*, and *Estuarine Water Use* have been eliminated from PA calculations on regulatory grounds.

SCR-5.6.1.1.2 Summary of New Information

No new information that affects the screening of this FEP has been identified since the CRA-2019.

SCR-5.6.1.1.3 Screening Argument

This section discusses the potential for human EPs related to marine activities to affect infiltration and recharge conditions in the vicinity of the WIPP.

SCR-5.6.1.1.4 Historical, Current, and Near-Future Human EPs

The WIPP site is more than 800 km (480 mi) from the nearest seas, and hydrological conditions in the vicinity of the WIPP have not been affected by marine activities. Furthermore, consistent with the criteria in 40 CFR 194.32(c) and 40 CFR 194.54(b), consideration of HCN human activities is limited to those activities that have occurred or are expected to occur in the vicinity of the disposal system. Therefore, Human EPs related to marine activities (such as coastal water use, seawater use, and estuarine water use) have been eliminated from PA calculations on regulatory grounds.

SCR-5.6.1.1.5 Future Human EPs

The EPA has provided criteria relating to future human activities in 40 CFR 194.32(a) that limit the scope of consideration of future human actions in PAs to mining and drilling. Therefore, the effects of future marine activities (such as coastal water use, seawater use, and estuarine water use) have been eliminated from PA calculations on regulatory grounds.

SCR-5.7 Ecological EPs

SCR-5.7.1 Agricultural Activities

SCR-5.7.1.1 **FEP Numbers: H53, H54, and H55**
FEP Titles: Arable Farming (H53)
Ranching (H54)
Fish Farming (H55)

SCR-5.7.1.1.1 Screening Decision: **SO-C (HCN) (H53, H54)**
SO-R (HCN) (H55)
SO-R (Future) (H53, H54, H55)

The effects of HCN *Ranching* and *Arable Farming* have been eliminated from PA calculations on the basis of low consequence to the performance of the disposal system. The effects of changes in future *Ranching* and *Arable Farming* practices have been eliminated from PA calculations on regulatory grounds. *Fish Farming* has been eliminated from PA calculations on regulatory grounds.

SCR-5.7.1.1.2 Summary of New Information

No new information that affects the screening of this FEP has been identified since the CRA-2019.

SCR-5.7.1.1.3 Screening Argument

Agricultural activities could affect infiltration and recharge conditions in the vicinity of the WIPP. Also, application of acids, oxidants, and nitrates during agricultural practice could alter groundwater geochemistry.

SCR-5.7.1.1.4 Historical, Current, and Near-Future Human EPs

Grazing leases exist for all land sections immediately surrounding the WIPP and grazing occurs within the controlled area (see the CCA, Chapter 2.0, Section 2.3.2.2). Although grazing and related crop production have had some control on the vegetation at the WIPP site, these activities are unlikely to have affected subsurface hydrological or geochemical conditions. The climate, soil quality, and lack of suitable water sources all mitigate against agricultural development of the region in the near future. Therefore, the effects of HCN ranching and arable farming have been eliminated from PA calculations on the basis of low consequence to the performance of the disposal system. Consistent with the criteria in 40 CFR 194.32(c) and 40 CFR 194.54(b), agricultural activities, such as fish farming, that have not taken place and are not expected to take place in the near future in the vicinity of the WIPP have been eliminated from PA calculations on regulatory grounds.

SCR-5.7.1.1.5 Future Human EPs

The EPA has provided criteria relating to future human activities in 40 CFR 194.32(a) that limit the scope of consideration of future human activities in PAs to mining and drilling. Also, the criterion in 40 CFR 194.25(a) concerned with predictions of the future states of society requires that compliance assessments and PAs "shall assume that characteristics of the future remain what they are at the time the compliance application is prepared." Therefore, the effects of changes in future agricultural practices (such as ranching, arable farming, and fish farming) have been eliminated from PA calculations on regulatory grounds.

SCR-5.7.2 Social and Technological Development

SCR-5.7.2.1 **FEP Number: H56**
FEP Title: Demographic Change and Urban Development

SCR-5.7.2.1.1 Screening Decision: SO-R (HCN)
SO-R (Future)

Demographic Change and Urban Development in the near future and in the future have been eliminated from PA calculations on regulatory grounds.

SCR-5.7.2.1.2 Summary of New Information

No new information that affects the screening of this FEP has been identified since the CRA-2019.

SCR-5.7.2.1.3 Screening Argument

Social and technological changes in the future could result in the development of new communities and new activities in the vicinity of the WIPP that could have an impact on the performance of the disposal system.

Demography in the WIPP vicinity is discussed in the CCA, Chapter 2.0, Section 2.3.2.1. The community nearest to the WIPP site is the town of Loving, 29 km (18 mi) west-southwest of the site center. There are no existing plans for urban developments in the vicinity of the WIPP in the near future. Furthermore, the criterion in 40 CFR 194.25(a), concerned with predictions of the future states of society, requires that compliance assessments and PAs "shall assume that characteristics of the future remain what they are at the time the compliance application is prepared." Therefore, demographic change and urban development in the vicinity of the WIPP and technological developments have been eliminated from PA calculations on regulatory grounds.

SCR-5.7.2.2 **FEP Number: H57**
FEP Title: Loss of Records

SCR-5.7.2.2.1 Screening Decision: Not Applicable (N/A) (HCN)
DP (Future)

Loss of Records in the future is accounted for in PA.

SCR-5.7.2.2.2 Summary of New Information

The screening argument and screening decision for this FEP has not changed. Additional information on FEP implementation in PA has been provided, including related conceptual models implementing PA codes.

SCR-5.7.2.2.3 Screening Argument

Because the DOE will maintain control for the current period throughout the active institutional period (100 yrs after closure), inadvertent drilling intrusion resulting from the loss of records is not applicable during the HCN period. However, PAs must consider the potential effects of human activities that might take place within the controlled area at a time when institutional controls cannot be assumed to eliminate completely the possibility of human intrusion. Consistent with 40 CFR 194.41(b) (U.S. EPA 1996a), the DOE assumes no credit for AICs for more than 100 yrs after disposal. Also, consistent with 40 CFR 194.43(c) (U.S. EPA 1996a), the DOE originally assumed in the CCA that passive institutional controls (PICs) do not eliminate the likelihood of future human intrusion entirely. The provisions at 40 CFR 194.43(c) allow credit for PICs by reducing the likelihood of human intrusions for several hundred yrs. In U.S. DOE 1996a, the DOE took credit for these controls that include records retention by reducing the probability of intrusion for the first 600 yrs after active controls cease. The EPA disallowed this credit during the original certification (U.S. EPA 1998a). The DOE no longer takes credit for PICs in PA, effectively assuming that all public records and archives relating to the repository are lost 100 yrs after closure. Therefore, the DOE continues to include the loss of records FEP within PA and does not include credit for PICs.

SCR-5.7.2.2.4 FEP Implementation in PA

FEP H57 *Loss of Records* is broadly implemented in PA through the assumption of inadvertent and intermittent human intrusion, as required by 40 CFR 194.33. Therefore, Loss of Records is directly related to DP scenarios and is associated with the following conceptual models: Exploration Boreholes, Cuttings and Cavings, Spallings, Castile and Brine Reservoir, Multiple Intrusions, Direct Brine Release, and Multiple Intrusions. The PA code that implements these conceptual models as they relate to *Loss of Records* is CCDFGF.

SCR-6.0 WASTE AND REPOSITORY-INDUCED FEPS

The following section presents screening arguments and decisions for waste- and repository-induced FEPs. Table SCR-1 provides summary information regarding changes to waste- and repository-induced FEPs since the CRA-2019. There are 114 waste- and repository-induced FEPs used in the CRA-2026. Of these, 29 remain unchanged since the CRA-2019 and 85 were updated with new information. Four FEPs had changes to screening decisions.

SCR-6.1 Waste and Repository Characteristics

SCR-6.1.1 Repository Characteristics

SCR-6.1.1.1 **FEP Number: W1**
FEP Title: Disposal Geometry

SCR-6.1.1.1.1 Screening Decision: UP

The WIPP repository *Disposal Geometry* is accounted for in PA.

SCR-6.1.1.1.2 Summary of New Information

The CRA-2026 will consider a repository design comprising of the 10 original panels and two replacement panels. This configuration represents the certified repository design at the submittal of CRA-2026.

The addition of the new panels was a change to the disposal system geometry conceptual model as well as the related repository fluid flow conceptual model. These conceptual model updates were reviewed and found adequate by a peer review panel (Falta et al. 2021).

During the review of CRA-2019, the EPA raised questions of whether the shafts and concrete monolith plugs extending below the repository were properly accounted for in the PA model (comment CC1-34-8, U.S. EPA 2020a). An analysis was done to show the shaft and concrete monolith extending below the disturbed rock zone were not impactful to the flow solution in the PA calculation (U.S. DOE 2020c). The EPA found this response adequately demonstrated a negligible impact of only modeling the shaft to the top of MB-139 (page A-29, U.S. EPA 2022b).

SCR-6.1.1.1.3 Screening Argument

Disposal geometry is a key element of modeling the performance of the repository over the regulatory period. As such, the appropriate elements of the disposal system geometry are included in WIPP models and their assumptions. Details on implementation of the disposal system geometry can be found in Appendix MASS-3.1.

SCR-6.1.1.1.4 FEP Implementation in PA

FEP W1 Disposal Geometry, which is an UP FEP, is associated with the Disposal System Geometry conceptual model. This is closely tied to the Repository Fluid Flow conceptual model. Both of these conceptual models are implemented in the PA code BRAGFLO for the Salado Flow computation in the PA calculation. The Salado Transport model in the PA code PANEL uses the Salado Flow model geometry and results (Appendix PA-4.2).

SCR-6.1.2 Waste Characteristics

SCR-6.1.2.1 **FEP Number: W2 and W3**
FEP Title: Waste Inventory (W2)
Heterogeneity of Waste Forms (W3)

SCR-6.1.2.1.1 Screening Decision: UP (W2)
DP (W3)

The *Waste Inventory* and *Heterogeneity of Waste Forms* are accounted for in PA.

SCR-6.1.2.1.2 Summary of New Information

The waste inventory used for the CRA-2026 PA calculations has been updated as provided in Van Soest (2025) and in Kicker (2025). The screening argument has not changed. Additional information on FEP implementation in PA has been provided, including conceptual models and related parameters associated with these FEPs. The screening decisions have not changed and these FEPs are represented in PA calculations.

SCR-6.1.2.1.3 Screening Argument

Waste characteristics, comprising the waste inventory and heterogeneity of waste forms, are described in the CCA, Appendix BIR. The waste inventory is accounted for in PA in deriving the dissolved actinide source term and gas generation rates. The distribution of contact-handled transuranic (CH-TRU) and remote-handled transuranic (RH-TRU) waste within the repository leads to room-scale heterogeneity of the waste forms, which is accounted for in PA when considering the potential activity of waste material encountered during inadvertent borehole intrusion (Appendix PA-3.2.5). The DOE implements waste heterogeneity in waste forms through the assumption of random placement of TRU waste in the repository. This assumption is consistent with EPA's certification criteria at 40 CFR 194.24(d) where it states that the DOE must provide a waste loading scheme or assume random emplacement of waste in the repository. This assumption includes all waste container forms and types. Details regarding the implementation of this assumption are provided in Appendix MASS-18.0.

SCR-6.1.2.1.4 FEP Implementation in PA

FEP W2 Waste Inventory, which is an UP FEP, is associated with the following conceptual models:

- Chemical Conditions (implemented in EQ3/6 and PANEL)
- Gas Generation (implemented in BRAGFLO)
- Dissolved actinide source term (implemented in EQ3/6 and PANEL)
- Colloidal actinide source term (implemented in EQ3/6 and PANEL).

FEP W3 Heterogeneity of Waste Forms, which is a DP FEP, is associated with the following conceptual models:

- Exploration Boreholes (implemented in CCDFGF)
- Cuttings and Cavings (implemented in CUTTINGS_S and EPAUNI).

Three of the WIPP PA codes use the radionuclide inventories directly: PANEL, NUTS, and EPAUNI. PANEL provides the radionuclide source for direct brine release to the surface via a borehole, the lumped radionuclide solubility limits for NUTS, and it provides the radionuclide source for releases via a borehole to the Culebra member of the Rustler Formation. PANEL performs the decay and solubility limit calculations on 30 individual radionuclides and on the lumped radionuclides. PANEL performs mass transport calculations on the lumped radionuclides. NUTS, as a simplification and for computational economy, performs decay and transport calculations using only the lumped radionuclides. NUTS calculates radionuclide releases via Salado formation to the accessible boundary. In the Salado Flow calculation, inventory primarily impacts gas generation from iron corrosion, the biodegradation of cellulose, plastic, and rubber (CPR), and brine radiolysis. Actinide mobilization potentials are calculated through time by the PANEL code using the solubility limits and uncertainties from the thermodynamic model in EQ3/6. The Salado Transport process model calculated by the NUTS code builds a radionuclide transport solution on top of the flow solution found by BRAGFLO and the mobilization potentials found by PANEL.

The WIPP PA code EPAUNI reports the volume and decayed activity of each waste stream through time for input into CCDFGF. CCDFGF is used to assemble results obtained from calculations performed with a number of different codes (e.g., BRAGFLO, PANEL, NUTS, SECOTP2D, CUTTINGS_S, and EPAUNI) to produce complementary cumulative distribution functions. CCDFGF uses the inventory information from EPAUNI to assign actinide concentrations to the solids volumes from CUTTINGS_S to calculate direct solid releases to the surface due to drilling activities.

Parameters related to waste characteristics are provided by Kicker (2025) and include the following:

- Waste unit factor (Kicker 2025, Table 26)
- Radionuclide parameters (Kicker 2025, Table 27)
- Lumped radionuclide parameters (Kicker 2025, Table 28)
- Waste material parameters (Kicker 2025, Table 29)
- Oxyanion parameters (Kicker 2025, Table 30)
- Radiolysis and decay parameters for gas generation (Kicker 2025, Table 13)

SCR-6.1.3 Container Characteristics

SCR-6.1.3.1 **FEP Numbers: W4 and W34**
FEP Titles: Container Form (W4)
Container Integrity (W34)

SCR-6.1.3.1.1 Screening Decision: SO-C – Beneficial

Container Form and *Container Integrity* has been excluded from PA calculations on the basis of beneficial consequence to the performance of the disposal system.

SCR-6.1.3.1.2 Summary of New Information

Container Form (W4) and Container Integrity (W34) have been screened together for CRA-2026 as a result of similarities in screening arguments and effects on repository performance.

The screening argument for these FEPs has been updated to provide new container material masses as reported in Van Soest (2025). The screening argument has been streamlined to remove any discussion regarding chemical interactions that relate to container materials. These FEPs are primarily focused on the containment aspects of disposal containers in the repository. Chemical interactions of waste container materials are addressed in FEPs W49, "Gases from Metal Corrosion" and W51, "Chemical Effects of Corrosion."

SCR-6.1.3.1.3 Screening Argument

Container Form has been eliminated from PA calculations on the basis of its beneficial effect on retarding radionuclide release. The chemical aspects of container materials (e.g., steel, cellulosics, plastic, etc.) are accounted for in PA through various inventory-related FEPs; however, this FEP is concerned with the physical containment capability of the container, not its chemical composition. The PA assumes instantaneous container failure and waste dissolution consistent with the source-term model, even though WIPP performance calculations typically show that a significant fraction of steel and other Fe-base materials will remain undegraded over 10,000 yrs (see Helton et al. 1998). Any undegraded container materials associated with containers that have retained confinement integrity will (1) reduce contact between brine and radionuclides; (2) decrease the rate and extent of radionuclide transport because of high tortuosity along the flow pathways. The inventory used for the CRA-2026 contains 4.78×10^7 kg of steel in packaging (includes containers) materials (Van Soest 2025). This value is up from 4.77×10^7 kg reported in 2018 (Van Soest 2018). Current waste containers accepted at WIPP include: the 55-gal drum, the 85-gal drum, the 100-gal drum, the standard waste box, the pipe overpack container (POC), the 72-B canister, the ten-drum overpack, the standard large box, the neutron-shielded canister, the shielded container assembly, and the criticality control overpack. Super-compacted waste is also placed in 100-gal overpack drums.

Integrity of a TRU waste container is required for transportation to the WIPP facility and for safe handling during operations. Container integrity can also facilitate waste recovery prior to

WIPP closure, but it is not required. The TRU waste container is not an engineered barrier and is not required to isolate the waste for any period after WIPP closure. Any undegraded container materials will reduce radionuclide mobilization by (1) slowing contact between brine and radionuclides; and (2) beneficially reducing the oxidation state of actinides, which reduces solubility (except for Pu^{+IV} to Pu^{+III}). Therefore, container integrity can be excluded on the basis of its beneficial effect on isolating radionuclides and reducing actinide solubility.

SCR-6.1.3.2 **FEP Number: W5**
FEP Title: Container Material Inventory

SCR-6.1.3.2.1 Screening Decision: UP

The effects of *Container Material Inventory* is accounted for in PA.

SCR-6.1.3.2.2 Summary of New Information

The masses of container materials associated with the waste inventory for the CRA-2026 have been updated as detailed in Van Soest (2025) (steel, CPR, and lead). The methodology for approximating the initial iron surface area of the waste and containers has been updated to tie the surface area to the inventory mass (King 2021). In the CRA-2019 completeness comment CC5-SCR-9 response, it was shown that gas generation from lead corrosion could be screened out of the WIPP PA calculation based on low consequence (U.S. DOE 2021a). EPA concurred with this response (U.S. EPA 2022d).

Four new shielded container variants were added as potential payload containers with the updated inventory (U.S. DOE 2023). The use of these containers is accounted for by the masses of their component materials in the inventory. The new containers do not require any changes to the existing WIPP PA methodology. While the CC5-SCR-9 did not consider the new shielded container variants, given that the lead in the new shielded container will have lower surface area per kilogram, and the mass of lead in the inventory has not increased, the CC5-SCR-9 response can be considered bounding in screening lead corrosion out of the WIPP PA based on low consequence.

SCR-6.1.3.2.3 Screening Argument

The *Container Material Inventory* is provided in Van Soest (2025) and is accounted for in PA through the Gas Generation model (Appendix PA-4.2.5; Appendix GEOCHEM-2.0). The inventory used for the CRA-2026 contains 5.10×10^7 kg of steel in packaging materials, including containers (Van Soest 2025). This value is up from 4.77×10^7 kg reported in CRA-2019 (Van Soest 2018). The increase in iron mass in the inventory and the new methodology for calculating iron surface area have increased the iron surface area and therefore the iron corrosion rate.

The lead inventory has gone down slightly from 1.38×10^7 kg in CRA-2019 (Van Soest 2018) to 2.43×10^6 kg in CRA-2026 (Van Soest 2025). The CRA-2019 completeness comment CC5-SCR-9 response (U.S. DOE 2021a) showed the amount of $H_2(g)$ generated from lead corrosion is less than 0.5% of total gas generated from iron corrosion, biodegradation, and brine radiolysis

combined. Thus, gas generation from lead corrosion can be screened out of the WIPP PA based on low consequence. The CC5-SCR-9 response calculation assumed all lead was in the original SC-30G1 shielded containers. Lead surface area per kilogram, and therefore corrosion rate, would be lower in the new shielded containers variants. With the decrease in lead mass in the inventory the CC5-SCR-9 response calculation can still be considered bounding. Gas generation from lead corrosion remains screened out of WIPP PA based on low consequence.

The CPR material in the packaging materials is increased from 4.85×10^6 kg in CRA-2019 (Van Soest 2018) to 9.52×10^6 kg in CRA-2026 (Van Soest 2025). Biodegradation of CPR material is included in the gas generation models (Appendix GEOCHEM-2.1.5; Appendix PA-4.2.5).

The *Container Material Inventory* reported by Van Soest (2025) also impacts the Chemical Conditions models (Appendix GEOCHEM-2026, Section GEOCHEM-3.2). In the CCA, Appendix WCL, a quantity of metallic Fe was included that would ensure sufficient reactants to reduce radionuclides to lower oxidation states. This requirement is met as long as there are no substantial changes in container materials. With the current iron inventory, the WCL quantity of metallic Fe that provides adequate reductant is satisfied in both the existing south half of the repository and new west half of the repository independently.

Carbon budget in the repository is assessed from the CPR inventory. The amount of carbon in the inventory controls the MgO inventory through the MgO excess factor (1.2 in CRA-2019 and CRA-2026). The MgO inventory is assumed to exist in the forms of brucite and hydromagnesite for the chemical conditions model. Brucite and hydromagnesite together with iron and lead corrosion products are used as input for predicting the dissolved actinide source term.

SCR-6.1.3.2.4 FEP Implementation in PA

The *Container Material Inventory* has been incorporated into Gas Generation conceptual model through iron corrosion and CPR biodegradation as implemented in the WIPP PA code BRAGFLO. Gas and brine generation contribute to repository conditions which impact several radionuclide release pathways.

The *Container Material Inventory* has also been incorporated into the Chemical Conditions conceptual model, which is closely related to the Dissolved Actinide Source Term and Colloidal Actinide Source Term conceptual models. The Chemical Conditions conceptual model is implemented by the EQ3/6 code.

SCR-6.1.4 Seal Characteristics

SCR-6.1.4.1

FEP Numbers: W6, W7, W109, and W110
FEP Titles: Shaft Seal Geometry (W6)
Shaft Seal Physical Properties (W7)
Panel Closure Geometry (W109)

Panel Closure Physical Properties (W110)

SCR-6.1.4.1.1 Screening Decision: UP

The *Shaft Seal Geometry*, *Shaft Seal Physical Properties*, *Panel Closure Geometry*, and *Panel Closure Properties* are accounted for in PA.

SCR-6.1.4.1.2 Summary of New Information

The DOE requested permission from the EPA to locate the panel closures in alternate locations for Panels 1 and 2 due to impacts from the 2014 incidents (U. S. DOE 2020b). The EPA approved this request (U.S. EPA 2021).

SCR-6.1.4.1.3 Screening Argument

Shaft seal characteristics, including shaft seal geometry, and physical properties are described in the CCA, Chapter 3.0, Section 3.3.2. The run-of-mine panel closure system (ROMPCS) geometry and physical properties are described in Camphouse et al. (2012). These repository elements are accounted for in PA (see Appendix PA-4.2.7 and PA-4.2.8).

SCR-6.1.4.1.4 FEP Implementation in PA

W6, W7, W109, W110 are included in the UP scenario and are accounted for in PA by the Disposal System Geometry conceptual model and implemented through the representation of the seal system and panel closures in BRAGFLO and the parameters assigned to the shaft seal and panel closure materials (see Appendix PA, Table PA-22).

SCR-6.1.4.2 FEP Number: W8
FEP Title: Shaft Seal Chemical Composition (W8)

SCR-6.1.4.2.1 Screening Decision: SO-C

The *Shaft Seal Chemical Composition* has been eliminated from PA calculations on the basis of low consequence to the performance of the disposal system.

SCR-6.1.4.2.2 Summary of New Information

This FEP was previously screened jointly with FEP W111, *Panel Closure Chemical Composition*. Because panel closures now consist of run-of-mine (ROM) salt (no concrete elements) (U.S. EPA 2014), their similarity with shaft seals no longer exists, thus combined screening of these two FEPs is no longer appropriate. The screening argument for this FEP has been refined to specifically address the lower shaft seal components. Because of the limited movement of brine in contact with the lower shaft seal components and resulting minimal impact on pH, the screening decision for this FEP has been changed from “SO-C Beneficial” to “SO-C.” No beneficial consequence is assumed to occur.

SCR-6.1.4.2.3 Screening Argument

When in contact with brine, cementitious materials can elevate pH to a highly alkaline condition. At high pH, calcium ions, hydroxide ions, and isosaccharinic acid could increase the solubility of actinides with the +III and +IV oxidation state. An assessment (U.S. DOE 2021c) concluded that the shaft seal system including cementitious materials could limit the transport of brine through the shaft. A small amount of brine is expected to flow through the shaft seals. An inconsequentially small volume of brine with a high pH is not expected to affect the bulk brine chemistry in the repository. There is no expectation that brine, which has reacted with shaft seal cement, will have an effect on actinide solubility (U.S. DOE 2021b). Therefore, there is no significant change in actinide speciation or solubility expected. Chemical conditions at the WIPP are not cement-dominated because the presence of MgO greatly minimizes pH excursions.

SCR-6.1.4.2.3.1 Repository Shaft Seals

Several publications describe strong actinide (or actinide analog) sorption by cement (Altenheinhaese et al. 1994; Wierczinski et al. 1998; Pointeau et al. 2001). Cementitious materials have the potential to interact with groundwater and significantly alter the chemical speciation of any radionuclides present. In particular, cementitious materials in the shaft seals may have the capacity to buffer groundwaters to extremely high pH (for example, Bennett et al. 1992, pp. 315 – 325). At high pH values, dissolved concentrations of many radionuclides could be reduced in comparison with near-neutral waters. This effect reduces the migration of radionuclides in mobilized form, which encompasses the dissolved (speciated and complexed with organic ligands) form plus dispersed (with colloids) form. However, there was no significant impact of portlandite [$Ca(OH)_2(s)$], as surrogate for Portland cement (in the WIPP waste and in the repository seals), on actinide solubility calculation outputs (U.S. DOE 2021b).

Chemical interactions between the cement seals and brine will be of low consequence to the performance of the disposal system. The effects of cementitious materials in shaft seals on groundwater chemistry have been eliminated from PA calculations on the basis of low consequence to the performance of the disposal system.

SCR-6.1.5 Backfill Characteristics

SCR-6.1.5.1 **FEP Number: W9**
FEP Title: Backfill Physical Properties

SCR-6.1.5.1.1 Screening Decision: SO-C

Backfill Physical Properties have been eliminated from PA calculations on the basis of low consequence to the performance of the disposal system.

SCR-6.1.5.1.2 Summary of New Information

Discussion in FEP W9 *Backfill Physical Properties* has been updated to include the mass of MgO that has been placed in the repository panels. The new information does not change the decision for this FEP.

SCR-6.1.5.1.3 Related FEPs

The screening argument in FEP W9 *Backfill Physical Properties* is supported by the excluded FEPs W35 *Mechanical Effects of Backfill* and W72 *Exothermic Reactions*. It is also indirectly related to the included FEPs W10 *Backfill Chemical Composition*, W40 *Brine Inflow,* and W44 *Degradation of Organic Material.*

SCR-6.1.5.1.4 Screening Argument

MgO also has several minor physical effects that include (1) thermal influence through the chemical reactions of MgO hydration and MgO carbonation, (2) mechanical influence on room closure, and (3) influence on fluid flow through MgO permeability and porosity. The minor thermal influence of MgO on repository temperature is excluded as explained in FEP W72 *Exothermic Reactions*. The minor mechanical influence of MgO on room closure through salt creep is excluded as explained in FEP W35 *Mechanical Effects of Backfill*. The influence of MgO porosity and permeability on fluid flow is also excluded as follows.

SCR-6.1.5.1.4.1 Exclusion of MgO Porosity

In fluid flow calculations, the room porosity determines the void volume available to accommodate gas generated from iron corrosion and biodegradation of cellulose, plastic, and rubber. In turn, the void volume not occupied by gas can accommodate brine produced/consumed in chemical reactions or brine seeping into/out of a disposal room.

Simulations of brine inflow use the original room volume (i.e., the simulations do not use a deformed grid from salt creep). Hence, MgO porosity has a minor role on fluid flow for two reasons (as described in FEP W35 *Mechanical Effects of Backfill*): (1) when no gas is generated, the room porosity is small regardless of whether the MgO volume is included because a large volume of salt creeps into the room, which has practically zero porosity; and (2) when the maximum amount of gas is generated, the MgO volume is small relative to the large gas-filled volume in the room.

SCR-6.1.5.1.4.2 Exclusion of MgO Permeability

In fluid flow calculations, the room permeability determines the difficulty and the pathway that gas or brine takes in moving (1) about the room; (2) into a hypothetical intruding borehole; and (3) into adjacent natural features such as disturbed rock zone, anhydrite layers sandwiched between the halite, and the halite itself. The absolute values of permeability of the waste in the room, the borehole, and adjacent features determine the difficulty in moving gas or brine. The permeability of features relative to other features determines the pathway taken by the fluid.

The MgO is not a continuous layer of the disposal room (since it is typically placed on every other stack of containers) but rather it is a component of the emplaced waste and eventually corroded containers.

Currently, seven of the 12 panels are filled[c] and provide sufficient experience on the average mass of MgO placed in the rooms of each panel (Table SCR-5). The first panel did not fill all rooms and so the MgO mass is less, but generally the average MgO mass in a room has steadily decreased from Panel 2 to Panel 8 as the safety factor has decreased and less equivalent cellulose is included in the containers. Therefore, any effects of the MgO backfill on fluid flow have continued to decrease since CCA-1996.

Table SCR-5. MgO Mass Already Placed in WIPP Panels

	Full Room MgO Mass[d] (Metric tons--t)		
Panel	**Ave**	**Max**	**Min**
1	640	1,128	223
2	952	1,029	692
3	919	1,023	663
4	926	1,050	669
5	752	937	486
6	470	744	235
7	269	555	58
8	326	435	94
Overall	704	1,128	58
Panels 5,6,7	497	937	58

The solid MgO would occupy an average overall volume of 196 m^3 per room assuming a solid MgO density of 3,600 kg/m^3 (Ropp 2013) and a bulk density of Martin Marietta MgO of 1,400 kg/m^3 (Wall 2005). The MgO has approximately 61% porosity upon emplacement, meaning that the volume of solid MgO emplaced represents only 3% of the initial room volume of 6,585 m^3 on average, and 5% at maximum since WIPP opened in 1999. The bulk MgO volume is 8% of the initial room volume on average, and 12% at maximum, which is smaller than the typical error in evaluating waste and container volumes. This small percentage is insufficient to alter the absolute permeability value of the waste and, consequently, its permeability relative to other features.

[c]As of January 10, 2025, Panel 8 is approximately 50% filled. MgO emplacement data from Panel 8 are included in this screening argument for completeness but is not included in the calculation of the average overall volume calculated.

d Table SCR-5 produced from query of the WIPP Waste Data System (WDS) on January 10, 2025.

Therefore, physical properties of the MgO backfill have been excluded from PA calculations based on low consequence to the performance of the disposal system.

SCR-6.1.5.2 **FEP Number: W10**
FEP Title: Backfill Chemical Composition

SCR-6.1.5.2.1 Screening Decision: UP

The *Backfill Chemical Composition* is accounted for in PA.

SCR-6.1.5.2.2 Summary of New Information

No new information that affects the screening of this FEP has been identified since the CRA-2019. However, a summary of the implementation of backfill chemical composition in PA has been added to SCR-6.1.5.2.4.

SCR-6.1.5.2.3 Screening Argument

A chemical backfill is added to the disposal room to buffer the chemical environment. The backfill characteristics are described in Appendix MgO-2009, Section MgO-3.0. The mechanical and thermal effects of backfill are discussed in W35 (Section SCR-6.3.5.3) and W72 (Section SCR-6.3.4.1), respectively, where they have been eliminated from PA calculations on the basis of low consequence to the performance of the disposal system. Backfill chemical composition is accounted for in PA in deriving the dissolved and colloidal actinide source terms (see Appendix SOTERM-6.1.1, SOTERM-6.1.2, SOTERM-6.2, and SOTERM-6.6, Appendix MgO-4.0), and in the production of gas within the repository.

SCR-6.1.5.2.4 FEP Implementation in PA

Backfill chemical composition is incorporated into the MgO Excess Factor (EF) calculation. The EF is defined as the ratio of total moles of emplaced MgO to maximum possible number of moles of CO_2(g), generated by microbial consumption of all carbon in the CPR. The EF parameter value of 1.2 has been used since CRA-2014. In CRA-2026 the EF value is utilized to assess amounts of brucite and hydromagnesite that are used as EQ3/6 input for predicting baseline solubilities of actinides. The PANEL and BRAGFLO codes predict the dissolved and colloidal actinide source terms from the baseline solubilities.

SCR-6.1.6 Post-Closure Monitoring Characteristics

SCR-6.1.6.1 **FEP Number: W11**
FEP Title: Post-Closure Monitoring

SCR-6.1.6.1.1 Screening Decision: SO-C

The potential effects of *Post-Closure Monitoring* have been eliminated from PA calculations on the basis of low consequence to the performance of the disposal system.

SCR-6.1.6.1.2 Summary of New Information

No new information that affects the screening of this FEP has been identified since the CRA-2019.

SCR-6.1.6.1.3 Screening Argument

Post-closure monitorin*g* is required by 40 CFR 191.14(b) (U.S. EPA 1993) as an assurance requirement to "detect substantial and detrimental deviations from expected performance." The DOE has designed the monitoring program (see the CCA, Appendix MON) so that the monitoring methods employed are not detrimental to the performance of the disposal system (40 CFR 194.42(d)) (U.S. EPA 1996a). Nonintrusive monitoring techniques are used so that post-closure monitoring would not impact containment or require remedial activities. In summary, the effects of monitoring have been eliminated from PA calculations on the basis of low consequence to the performance of the disposal system.

SCR-6.2 Radiological FEPs

SCR-6.2.1 Radioactive Decay and Heat

SCR-6.2.1.1 **FEP Number: W12**
FEP Title: Radionuclide Decay and Ingrowth

SCR-6.2.1.1.1 Screening Decision: UP

Radionuclide decay and ingrowth are accounted for in PA.

SCR-6.2.1.1.2 Summary of New Information

No new information that affects the screening of this FEP has been identified since the CRA-2019. However, a summary of the implementation of *Radionuclide Decay and Ingrowth* in PA has been added to SCR-6.2.1.1.4.

SCR-6.2.1.1.3 Screening Argument

Radionuclide decay and ingrowth are accounted for in PA (see Appendix PA-4.3).

SCR-6.2.1.1.4 FEP Implementation in PA

***Radionuclide Decay and Ingrowth* is incorporated into inventory masses and concentrations of actinide radionuclides as implemented by the PANEL, NUTS, SECOTP2D, EPAUNI, and CUTTINGS_S codes.**

SCR-6.2.1.2 **FEP Number: W13**
FEP Title: Heat From Radioactive Decay

SCR-6.2.1.2.1 Screening Decision: SO-C

The effects of temperature increases as a result of *Heat From Radioactive Decay* have been eliminated from PA calculations on the basis of low consequence to the performance of the disposal system.

SCR-6.2.1.2.2 Summary of New Information

The inventory of TRU radionuclides that produce some heat in CRA-2026 PA calculations (Van Soest 2025; Kicker 2025) has increased from that in the original CCA-1996 (U.S. DOE 1996a). However, the initial thermal power is far less than the initial thermal power assumed when evaluating regional effects of radioactive decay heat in the WIPP 1980 Environmental Impact Statement (U.S. DOE 1980; Thorne and Rudeen 1981).

SCR-6.2.1.2.3 Related FEPs

Related FEPs that produce some heat include W72 *Exothermic Reactions* (including MgO hydration, MgO carbonation, microbial degradation, and aluminum corrosion) and W73 *Concrete Hydration* but have been excluded on the basis of low consequence. Potential heat generated from W14 *Heat from Nuclear Criticality* is excluded from PA calculations on the basis of low probability of occurrence.

The influence of the small temperature increases on processes is discussed in related FEPs: (1) geomechanical processes (W29 *Thermal Effects on Material Properties*, W30 *Thermally-Induced Stress Changes*, W31 *Differing Thermal Expansion of Repository Components*, W33 *Movement of Containers*), (2) diffusion (W93 *Soret Effect*), and (3) fluid flow processes (W43 Convection). This set of FEPs have been excluded from PA calculations on the basis of low consequence to the performance of the disposal system. FEP W45 *Effects of Temperature on Microbial Gas Generation* has been included through the uncertainty range assigned to two parameters of microbial gas generation under (a) fully saturated conditions, and (b) partially saturated conditions.

SCR-6.2.1.2.4 Screening Argument

Radioactive decay of transuranic waste emplaced in the WIPP repository will not generate much heat. The modeled maximum small temperature increase of ~3 °C (5.4 °F) in the repository region, as described below in Section SCR-6.2.1.2.4.3, does not change the behavior

of the components in the engineered or geologic barrier and so FEP *W13 Heat from Radioactive Decay* is excluded from PA calculations on the basis of low consequence. Further discussion of the reasoning is described below.

SCR-6.2.1.2.4.1 WIPP Package Design Basis Limit Heat Producing Radionuclides

The WIPP Waste Acceptance Criteria (U.S. DOE 2022c) enforces the receipt of only approved waste streams of TRU waste, which by their nature do not produce much decay heat. In addition, the U.S. Nuclear Regulatory Commission (NRC)-approved Contact-Handled Transuranic Waste Authorized Methods for Payload Control (CH-TRAMPAC) and Remote-Handled Transuranic Waste Authorized Methods for Payload Control (RH-TRAMPAC) documents specify thermal power limits for each waste stream to limit hydrogen gas generation during transportation but the limits indirectly limit overall thermal power: 40 W for some CH-TRU wastes with limited potential to produce hydrogen gas (U.S. DOE 2022d, Table 5.2-1). Also, the Certificate for Compliance for the RH-TRU 72-B canisters and accompanying RH-TRAMPAC specifies payload limits: 90 W for payloads with low density, such as paper wastes, and 270 W payloads with higher density (>192 kg/m^3), such as metals (U.S. NRC 2019, 5(b)(2); U.S. DOE 2015a, §5.3.1; U.S. DOE 2015b, §3.4 and §3.5).

One other limit is applicable to the RH-TRU 72-B canister: the maximum permissible surface dose at the surface shall not exceed 1,000 rem/h (U.S. DOE 2022c, p. 38). Sanchez and Trellue (1996) show (through inverse shielding calculations) that this maximum surface dose limit of 1,000 rem/h constrains the maximum thermal load in an RH-TRU 72-B canister to ~51.1 W (if waste is placed in 3 drums with 0.208 m^3/drum and then inside the canister)[e] or ~63.5 W (if the waste is placed directly inside a 0.89 m^3 canister)[f,g] (Sanchez and Trellue 1996, Table 12. Entry 5). Hence, current 90 W and 270 W limits for the RH-TRU 72-B canister will not be exceeded because of the constraint provided by the maximum surface-dose limit.

SCR-6.2.1.2.4.2 Estimated Disposal Area Temperature Rise is Low in 1980 Environmental Impact Statement

For the 1980 Environmental Impact Statement (EIS-1980) for WIPP, DOE estimated the regional influence of the radionuclide decay heat based on the following assumptions (DOE 1980, p. 9-149; Thorne and Rudeen 1981):

[e] The 0.208 m^3 volume for a drum was used for CCA-1996; the current more accurate drum volume is 0.216 m^3 (Day 2013).
[f] The 63.5 W heat load is the product of the 71.33 W/m^3 in Table 12, Entry 5 and the assumed 0.89 m^3 volume of RH-TRU 72-B payload canister (Sanchez and Trellue 1996).
[g] The 0.89 m^3 volume for an RH-TRU 72-B canister was used for the calculations in CCA-1996 (Sanchez and Trellue 1996). The current more accurate volume is either 0.906 m^3 for welded lid canister or 0.939 m^3 for removable lid canister (Day 2013).

- Plutonium content for CH-TRU waste containers is 200 ^{239}Pu fissile gram equivalents (FGE) per 0.208 m^3 (7.1 oz per 7.3 ft^3) for drum[h] and 325 FGE[i] per 1.88 m^3 (11.5 oz per 66.4 ft^3) for standard waste box (SWB).[j] This assumed maximum fissile content has generally been a conservative assumption at WIPP because the average container content has been only 14.4 FGE (NA/NRC 2020, Table S-1 & Section 5.2.1).
- About 3.7×10^5 m^3 (1.3×10^7 ft^3) of CH-TRU waste is distributed within a repository area of 7.3×10^5 m^2 (180 acre). This assumed waste volume is larger than eventually approved in the Waste Isolation Pilot Plant Land Withdrawal Act (i.e., maximum capacity of 1.756×10^5 m^3—6.2×10^6 ft^3).
- The CH-TRU waste consists of a weapons-grade mixture of 90% ^{239}Pu and 10% ^{240}Pu; thus, the thermal power is 0.0024 watts per gram (W/g). Consequently, the maximum thermal power of a drum is 0.48 watts per drum (W/drum), and that of a standard waste box is 0.78 W/box.
- Half of the CH-TRU waste volume is placed in drums and half in standard waste boxes; thus, the calculated thermal power areal density is 2.8 killowatts per acre (kW/acre) (0.69 W/m^2) (i.e., ((0.48 W/0.208 m^3+ 0.78 W/1.88 m^3)/(2*1,000 W/kW))* (3.7×10^5 m^3/180 acre)).
- Insufficient RH-TRU waste is emplaced to influence the total thermal load.

Under the assumptions of the WIPP EIS-1980 with initial power density of 2.8 kW/acre (0.69 W/m^2) that decreases over time, the maximum rise in temperature at the center of the WIPP repository area was 1.6 °C (2.9 °F) at 80 years after waste emplacement (Thorne and Rudeen 1981).

For a heat load of 0.69 W/m^2 (2.8 kW/acre), the total initial power of CH-TRU is 500 kW, based on repository area of 7.3×10^5 m^2 (Thorne and Rudeen 1981). The anticipated initial power load of TRU waste disposed at WIPP has always been less (Fig. SCR-1). Furthermore, the total RH-TRU thermal load is more than 1.5 orders of magnitude less than the total heat load in the WIPP. Thus, the total thermal load of RH-TRU waste does not affect the average rise in temperature in the repository caused by the decay of radionuclides in CH-TRU waste.

[h] Thorne and Rudeen (1981) used a heat load of 2.8 kW/acre in the analysis. If the current drum volume is used, the heat load would have been 0.676 W/m^2 or 27.4 W/acre.

[i] 1980 EIS used 350 FGE per box (U.S. DOE 1980, p. 9-149), but by CCA-1996 the limit was 325 FGE per box (U.S. DOE 2022b, Table 3.1-1).

[j] Several sizes of steel boxes (2.3 m^3, 9.5 m^3, and 4.1 m^3) and one plywood box (3.17 m^3) had been used to store TRU waste at sites within the DOE complex in the 1970s and early 1980s (Rechard et al. 1991, Table 3.1-2) A standard waste box (1.88 m^3—Day 2013) was developed for CCA-1996 for shipping waste to WIPP in TRUPACT-II. In recreating the reasoning for the 2.8 kW/acre heat load (Thorne and Rudeen 1981), the standard waste box is used.

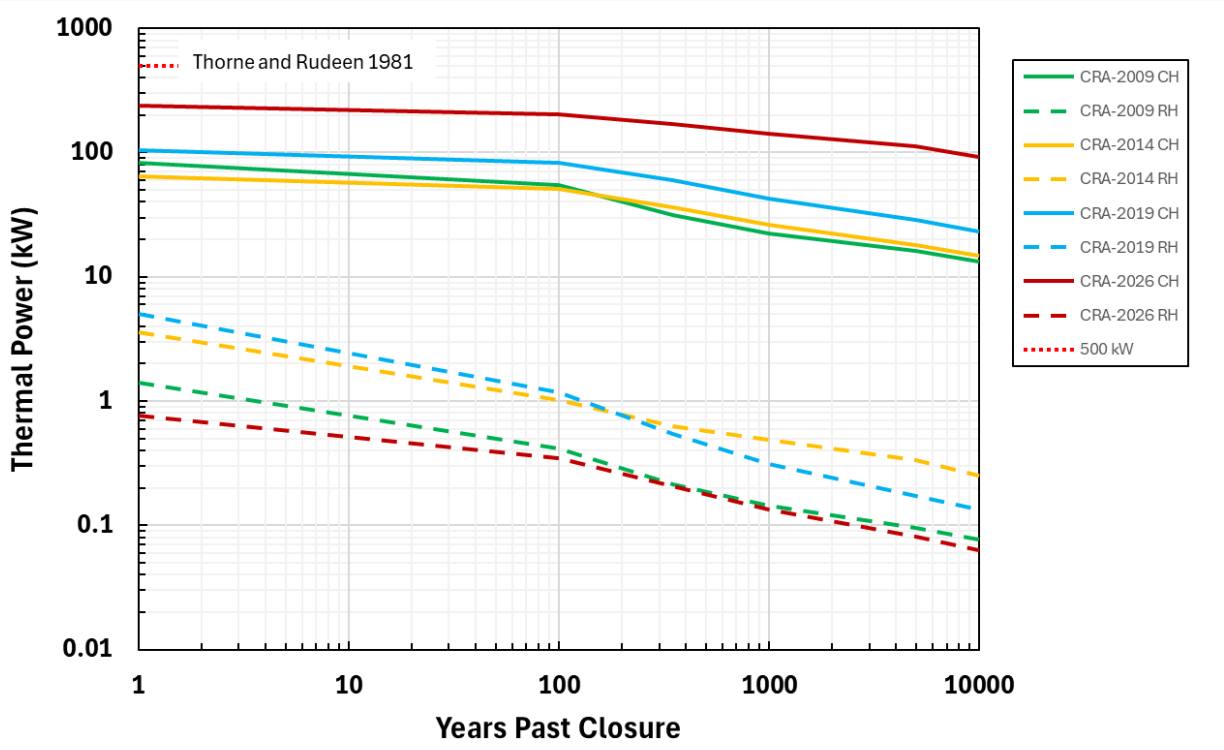

Figure SCR-1. Thermal power for CRA-2026 and past performance assessment derives primarily from Pu isotopes and is less than the assumed 500 kW initial thermal power that resulted in a maximum ~2 °C temperature rise in the entire repository region (Kicker 2025/Van Soest 2025; Van Soest 2018; Van Soest 2012; Crawford et al. 2009; Thorne and Rudeen 1981).

SCR-6.2.1.2.4.3 Estimated Temperature Rise for RH-TRU Waste Canister

The averaging of the 3.7×10^5 m^3 of CH-TRU waste within a repository area of 7.3×10^5 m^2 (180 acre) reduces the peak calculated temperature (i.e., "This averaging effect causes the peak calculated temperature to be much lower than would be expected in a drift of the repository"—Thorne and Rudeen 1981). Hence, an estimate of the maximum temperature rise at the surface of an RH-TRU canister is used as a reasonable estimate of temperature increase in a local area of the drift (Sanchez and Trellue 1996), since much RH-TRU will now be distributed with CH-TRU in shielded containers.

To estimate the temperature increase, Sanchez and Trellue (1996) analytically solved the differential equation of steady-state thermal conduction with non-decaying 63.5-W heat load. A non-decaying heat load is conservative because the thermal load will decrease with time as the radioactive waste decays. Recall, 63.5 W is the maximum heat load that maintains a surface dose less than 1,000 rem/h. A maximum temperature increase of ~3 °C (5.4 °F) occurs at the surface of a 0.89-m^3 RH-TRU 72-B container (Sanchez and Trellue 1996, Table 12, Entry 5).

SCR-6.2.1.2.5 Summary

A temperature rise of ~3 °C (5.4 °F) from radioactive decay within a local region of the disposal area will not cause thermal stresses that enhance existing pathways or create new pathways for groundwater flow in the disturbed rock zone, in the anhydrite layers and marker beds, and through seals (W29 *Thermal Effects on Material Properties* and W31 *Differing Thermal Expansion of Repository Components*), nor create thermal buoyancy forces that could lift the waste upward in the salt rock (W33 *Movement of Containers*), nor noticeably accelerate the rate of salt creep (Arguello and Torres 1988), nor reach temperatures that could cause thermally-induced solute diffusion (W93 *Soret Effect*), nor cause thermal expansion that results in noticeable uplift of the ground surface overlying the repository (1.0 cm uplift estimated at 200 years—Thorne and Rudeen 1981).

Therefore, FEP *W13 Heat from Radioactive Decay* of TRU radionuclides has been excluded from PA calculations on the basis of low consequence to the performance of the disposal system.

SCR-6.2.1.3 FEPs Number: W14
FEPs Title: Nuclear Criticality: Heat

SCR-6.2.1.3.1 Screening Decision: SO-P

FEP W14 *Nuclear Criticality* has been eliminated from PA calculations on the basis of low probability of occurrence.

SCR-6.2.1.3.2 Summary of New Information

The argument for screening this FEP has been updated based on added WIPP waste streams associated with criticality control overpacks (CCOs) that allow disposal of surplus plutonium as contact-handled TRU waste (Rechard 2025a; Rechard et al. 2025a; Rechard et al. 2025b; Rechard 2025b; and Rechard and Brady 2025). The CCOs allow a higher fissile loading of up to 380 ^{239}Pu fissile gram equivalent per container. For CRA-2026, the CCO waste acceptance criteria incorporates additional options for waste content controls on moderation, diluent, and fissile poisons and incorporates a more detailed analysis of rockfall and detailed evaluation of the mechanical compaction from salt creep (Rechard et al. 2025b). Nuclear criticality continues to be excluded because of the low probability of occurrence. A summary of the updated analysis is provided below.

SCR-6.2.1.3.3 Related FEP

FEP W14 *Nuclear Criticality Heat* is directly related to FEP W28 *Nuclear Explosions* (SCR-6.3.3.2), which is also excluded because of the low probability of occurrence.

SCR-6.2.1.3.4 Screening Argument

Nuclear criticality refers to a self-sustained neutron chain reaction that may occur if fissile radionuclides are assembled with sufficiently high concentration and mass. In the subsurface, an important consequence of criticality is the production of heat.

More specifically, whether a fissile assembly is critical depends upon the interaction of neutrons with matter within and outside the assembly, which depends upon four general categories of parameters (Rechard et al. 2025b) (1) type (e.g., plutonium or uranium), enrichment, mass, and form of fissile material (e.g., metal or oxide); (2) shape including array configuration of fissile assembly (and thereby neutron leakage); (3) nearby material and its concentration outside the fissile assembly, and (4) material mixed with the fissile material and its overall concentration (such as a moderator).

The neutron multiplication factor (k_{eff}) is a measure of this neutron interaction with surrounding material. The k_{eff} is conceptually the ratio of the number of neutrons in one generation in a fissile assembly to the number of neutrons present in the previous generation. The fissile assembly is critical when k_{eff} is unity. Here, a subcriticality limit of 0.95 rather 1.0 is used because acceptable knowledge, rather than a measurement, is used to define container contents and configuration of fissile material inside CCO.

The absence or presence of sufficient moderator is one condition used to organize the screening argument (Fig. SCR-2). An effective moderator reduces the neutron energy to the thermal range (i.e., slows down the neutrons) and thereby increases the probability of absorption by nearby fissile material; and thus criticality. The presence of sufficient moderation can be further subdivided into the abundance of moderation from brine inundation of the disposal room or presence of other hydrogenous material (such as plastics) inside the WIPP disposal container. This FEP W14 *Nuclear Criticality Heat* addresses conditions with moderated, slow neutrons. The potential of criticality with unmoderated, fast neutrons is discussed and screened out in FEP W28 *Nuclear Explosions* (SCR-6.3.3.2).

A second condition for organizing the screening argument is the speed of assembling the fissile material into a critical configuration (Fig. SCR-2). Two speeds of assembly are considered here: Slow refers to assembly processes that occur over geologic time, such as slow geomechanical closure of a WIPP disposal room from salt creep or slow assembly through precipitation of fissile minerals. Fast refers to assembly processes that occur over a short time, such as gravity-driven rock fall in a room or rapid transport of fissile material from a disposal room after inadvertent intrusion and deposition somewhere else in the intruded panel.

Assembly of the fissile material is required because insufficient fissile material exists in any individual container to cause criticality. This condition is enforced to ensure safety during transportation and WIPP operations (U.S. DOE 2022c). Hence, a critical configuration must be assembled to cause criticality after WIPP closure: either (1) the array of containers in the disposal room must be compacted such that fissile separation is no longer maintained, or (2) fissile material in each container must be mobilized, transported, and deposited at another location in a sufficient mass with a favorable geometry (through precipitation, adsorption, or colloid aggregation).

The organization of the arguments does not preclude the combination of slow mechanical assembly followed by slow hydrologic/geochemical assembly after brine inundation. Indeed, this situation will likely occur. However, as apparent in the discussion below, the physical conditions and locations are very different such that probability of criticality does not increase. For example, when brine is added to the fissile material assembled by slow, salt creep the chlorine in brine makes criticality less probable. To potentially enhance reactivity beyond that of the slow mechanical configuration, the brine must physically transport and deposit the fissile material to another location with enhanced mass and geometry but without the chloride neutron poison.

As discussed below, the probability of criticality is low in each of four branches (Fig. SCR-2). The two branches with fast assembly are discussed first followed by the two branches with slow assembly in the following sections.

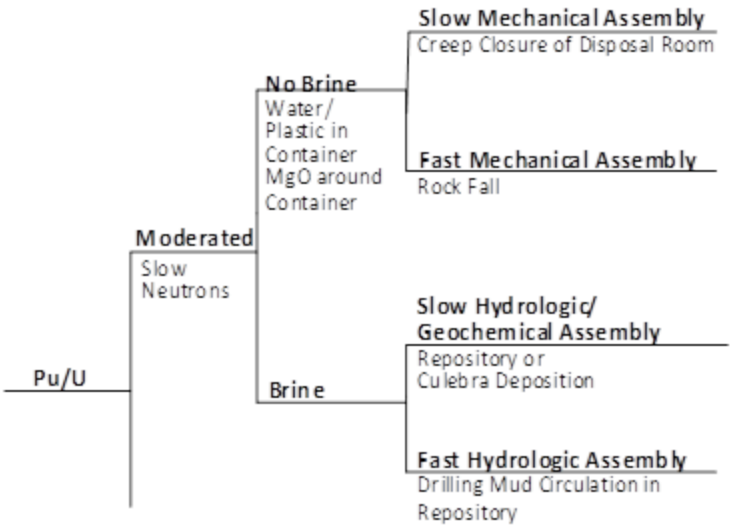

Figure SCR-2. Categories of criticality for organizing arguments based on fast or slow assembly speed for a fissile configuration moderated by brine and hydrogenous material (Rechard et al. 1997, Fig. 7).

SCR-6.2.1.3.4.1 Fast Hydrologic Assembly from Brine Inundation

Fast fissile assembly with brine moderated neutrons (Fig. SCR-2) might conceivably be the result of inadvertent drilling intrusion that causes vigorous mixing of a slurry of fissile material (and possibly suspended colloidal particles) in the repository or in the drilling mud. This type of criticality excursion would be similar to critical accidents of aqueous fissile solutions in nuclear fuel processing plants that involved vigorous mixing. However, a solution of dissolved plutonium or uranium and colloid particles that forms under repository conditions is far from critical (Rechard and Brady 2025) and vigorous mixing with consolidated fissile solids would decrease rather than increase the fissile concentration of the slurry. Rather, to enhance reactivity the solution must be concentrated through a geochemical process (not simple settling of the slurry solution) as included in the branch with assembly by slow hydrologic/geochemical processes, described below in Section SCR-6.2.1.3.4.4.

SCR-6.2.1.3.4.2 Fast Mechanical Assembly

Rockfall in a WIPP disposal room in which an array of containers is compacted sufficiently such that fissile separation between containers is not maintained potentially results in a fast assembly of fissile material. Detailed analysis of rockfall on to a room full of POCs or CCOs was conducted. POCs or CCOs were selected since each container can have a maximum 200 or 380 239Pu gram equivalents, respectively, unlike other WIPP containers.

The POC and CCO analysis used several conservatisms (Reedlunn and Bean 2019; Reedlunn et al. 2023). One large salt block fell onto an array of POCs or CCOs (with weak material strength and without any contents) that were stacked three high. Each layer was offset 2.54 cm from the

layer below to increase the instability of the array. The bags of MgO on top of the stacks were omitted and the rockfall initiated before room closure from salt creep had occurred in order to maximize the fall distance and, thus, the velocity of the salt block. The salt block was not allowed to fracture. The size of the salt block was the largest that had been observed at WIPP. The observed salt block had separated at a clay layer above the disposal room such that larger salt blocks were unlikely.

Neither a block that uniformly released from the ceiling and impacted containers mostly flat or a block that unzipped from the ceiling and thus had more rotation at impact caused the POCs or CCOs to buckle, crush, or cluster together (Fig. SCR-3) (Reedlunn and Bean 2019; Reedlunn et al. 2023). Because the separation of fissile material between each POC or CCO was maintained, rockfall does not promote a critical configuration, whether the container is moderated or not.

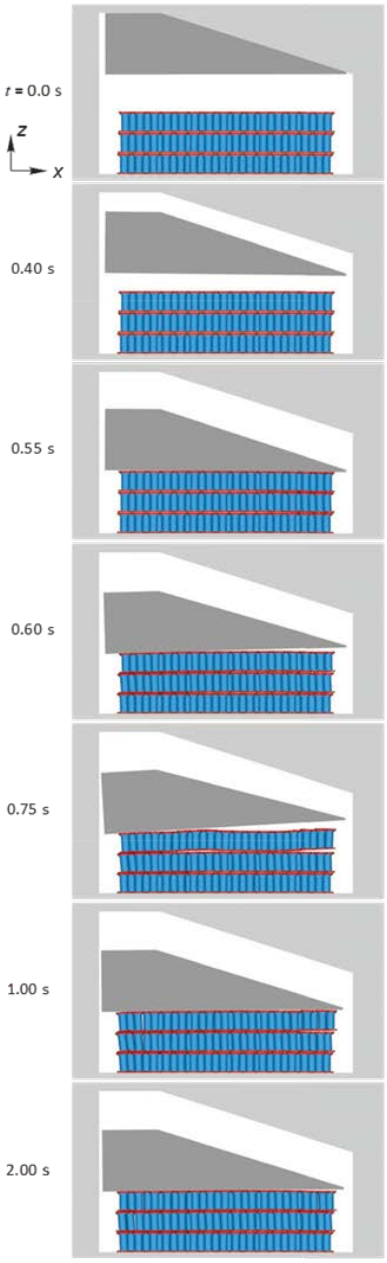

(a) 12-inch POCs with uniform release

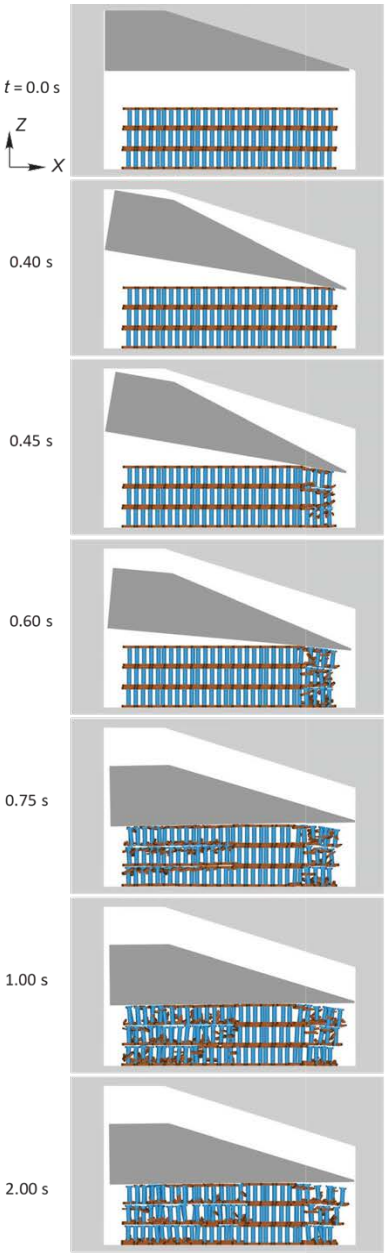

(b) CCOs with enhanced block rotation

Figure SCR-3. Roof falls onto 3 tiers of POCs and CCOs emplaced in a WIPP disposal room does not significantly disrupt the array nor cause clustering or sorting of containers. Red and brown discs represent the top and bottom plywood stabilizer for the blue 12-inch inner pipe

or 6-inch criticality control container inside the 55-gallon shell (which is hidden for visualization) (Rechard et al. 2025a, Fig. 12b; Rechard et al. 2025b, Fig. 3b).

SCR-6.2.1.3.4.3 Slow Mechanical Assembly with Moderation from Internal Hydrogenous Material and Surrounding MgO

Gradual room closure from salt creep and subsequent container compaction represents a slow geomechanical assembly (Fig. SCR-2). The room closure was evaluated with high-fidelity geomechanical models of a disposal room filled with POCs or CCOs (Reedlunn and Bean 2019; Reedlunn et al. 2023). Although brine can conceivably seep into the room over time, only hydrogenous material inside the container was modeled. The presence of brine promotes generation of gas by metal corrosion and, thus, reduces the amount of room closure from the gas pressure. Furthermore, chlorine in brine reduces the likelihood of criticality.

The geomechanical models predicted that most closure occurred within the first 200 years prior to any extensive container corrosion, which could spill container contents (Fig. SCR-4). However, the coordinate positions of the POCs or CCOs used in subsequent criticality analysis were at 1,000 years, when room closure had asymptotically approached maximum compaction. At 1,000 years, the inner 12-inch POC shell buckles but POCs remain mostly upright in two layers in the room center. At 1,000 years, clearly most inner containers of the CCOs are on their side. For CCOs, the room center is mostly a single layer.

The geomechanical compaction analysis evaluated the influence of changes in (Rechard et al. 2025a; Rechard et al. 2025b) (1) repository horizon and, thereby, changes arrangement of clay strata; (2) clay friction coefficient; (3) emplacement configuration (triangular and hexagonal); (4) strength of container (a) directly through increase of yield strength and (b) indirectly through differences in POC and CCO mass and diameter. The variations produced a wide variety of deformed spacing between containers (as evident in Fig. SCR-4), but the final distribution shape and range of several measures of container concentration remained stable at 1,000 years (Rechard et al. 2025a; Rechard et al. 2025b). Consequently, the coordinate positions of the POCs and CCOs reasonably represented conditions in the WIPP disposal room for subsequent criticality analysis.

Neutron/photon transport models placed spheres of 200 fissile gram equivalent of plutonium (as oxide—PuO2) at the predicted irregular spacing of the POC centroids demonstrated that an array of POCs was not critical when surrounded by salt and magnesium oxide (Fig. SCR-4). The probability of criticality in POCs bounds the probability of criticality in other containers except CCOs (Rechard et al. 2025a). That is, POCs can transport 200 fissile gram equivalent per container and 1400 g in a bundle of seven POCs disposed in a room. In comparison, other containers transport less fissile material in bundle of seven containers because of fissile limits on transportation. For example, a bundle of seven 55-gallon drums disposed in a room contains a maximum equivalent plutonium content of 325 fissile gram equivalent (Rechard et al. 2025a).

Criticality models of spheres composed of the maximum 380 fissile gram equivalent of plutonium for CCOs (with 2,660 g in a bundle of seven CCOs) at the predicted irregular spacing

(Fig. SCR-4) are also not critical provided the mass of hydrogenous material shipped in the CCO (usually water and plastics) is controlled (i.e., $k_{eff} < 0.95$ if hydrogenous mass inside container is < 1.3 kg—Fig. SCR-5) or boron carbide (a neutron poison) is mixed with the fissile contents ($k_{eff} < 0.95$ if boron carbide > 10 g—Fig. SCR-6), as specified in the WIPP Waste Acceptance Criteria (WAC) (U.S. DOE 2022c; Rechard et al. 2025b).

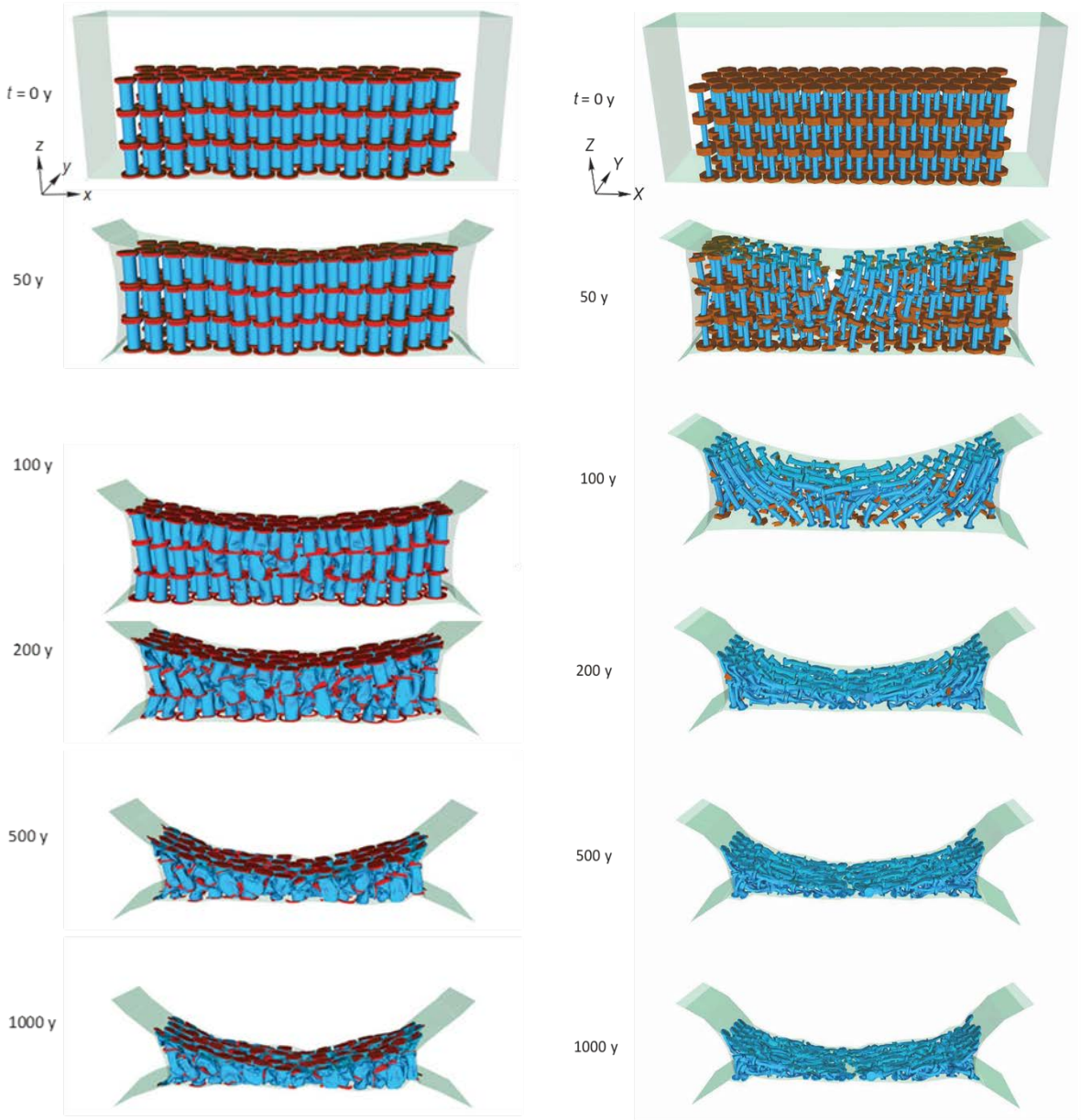

(a) 12” POC (b) CCO

Figure SCR-4. Compacted arrays of POCs and CCOs in disposal room buckle and tip over but groups of containers are not critical (Rechard et al. 2025a, Fig. 14b; Rechard et al. 2025b. Fig. 7b).

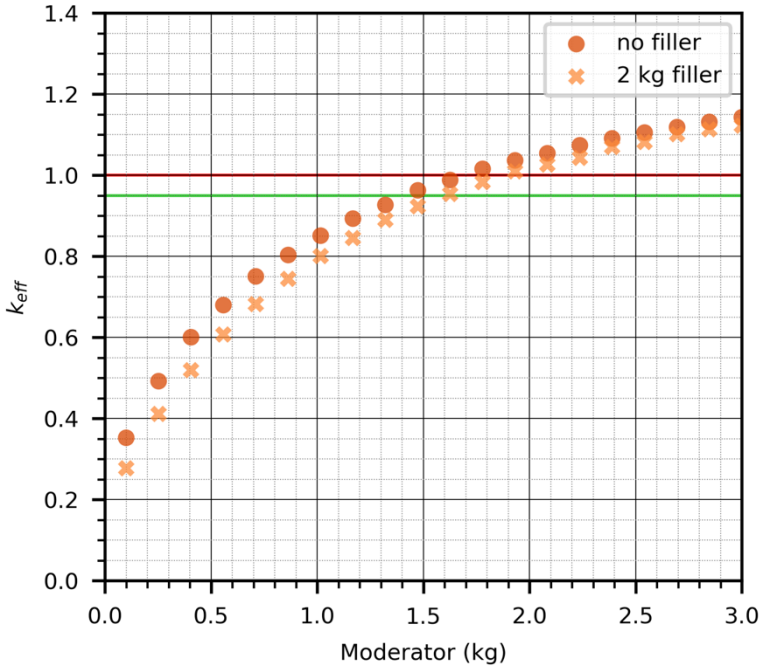

Figure SCR-5. Limiting hydrogenous material to less than 1.3 kg prevents criticality in CCOs (i.e., assembly is safely subcritical if k_{eff}<0.95—green line—if moderator mass inside CCO < 1.3 kg); reactivity decreases further if at least 2 kg miscellaneous filler present (based on Rechard et al. 2025b, Fig. 19b).

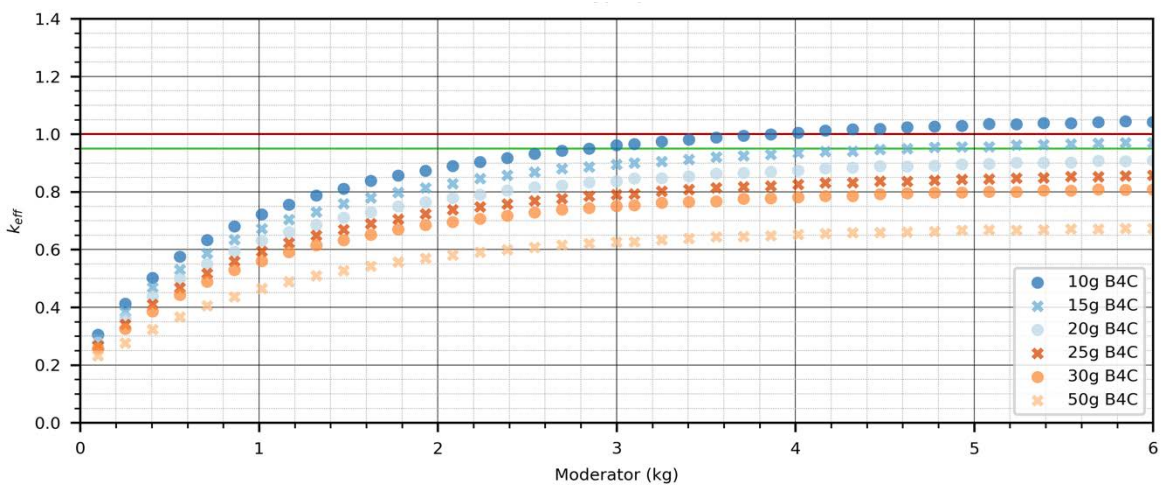

Figure SCR-6. Ten grams boron carbide sufficient to prevent criticality even with large mass of hydrogenous material (i.e., assembly is safely subcritical if k_{eff}<0.95—green line—if moderator mass inside CCO < 2.8 kg) (Rechard et al. 2025b, Fig. 39b).

SCR-6.2.1.3.4.4 Slow Hydrologic/Geochemical Assembly after Brine Inundation

Mobilization of fissile material in a container, transport, and deposition in another location represents slow hydrologic/geochemical assembly (Fig. SCR-2). The dissolution, precipitation, adsorption, or colloid aggregation is only possible after brine inundation of a disposal room.

Neither deposition in the underground facility nor deposition in the strata of the geologic barrier is likely to form a critical assembly (Rechard et al. 2001).

Specifically, the probability for criticality within the repository is low because concentration of fissile material under repository conditions is at least three orders of magnitude below the critical concentration. Mechanisms for concentrating fissile radionuclides such as the reducing agent iron (FeO) from containers, and added MgO are well distributed, on a macroscopic scale, throughout the waste and repository. Also, substrates for colloidal formation, such as rust particles, are also well distributed throughout the repository (Rechard and Brady 2025). Thus, simple gravitational settling following destabilization of mobile colloids causes limited colloid aggregation (like dust settling in a closed room). Furthermore, molecular diffusion is sufficient to mix brine chemistry (FEP W67 Localized Reducing Zones). Consequently, the brine chemistry remains fairly uniform with no preferential location for precipitation, adsorption, and colloidal aggregation.

After human intrusion, brine flow may move fissile solution and colloids about the repository. However, the addition of copious amounts of Castile brine from a hypothetical brine reservoir below the WIPP does not substantially change pH, ionic strength, or the reduction-oxidation potential within the repository and promote sufficient precipitation, adsorption, or colloidal aggregation to cause criticality.

Rechard and Brady (2025) re-evaluated previous analyses regarding criticality in geologic media once transported away from the repository. This new analysis considered previous depositional processes while considering higher fissile content associated with waste streams associated with POC and CCO waste packages. Yet, these new conditions do not promote criticality in the natural geologic barrier. Hydrologic conditions constrain the deposition location of fissile material released outside of the repository through an intrusion borehole. The relatively greater permeability favors movement of fissile material to the Culebra Dolomite Member of the Rustler Formation above the repository rather than to other strata. Furthermore, fluids tend to flow into rather than out of Culebra dolomite; thus, little likelihood exists for deposition in adjacent strata.

Within the Culebra dolomite, the probability of criticality is low because of unfavorable deposition conditions that include (Rechard and Brady 2025) (1) usually low masses of fissile material transported from the repository because of the low solubility of 239Pu and U fissile material under reducing geochemical conditions; (2) a mixing zone in Culebra dolomite too large to reach critical limits for 239Pu and for 5% enriched UO2 for situations when vast amounts of brine are available to transport low-soluble fissile material (Rechard 2025b); (3) a wide, spread-out mixing zone in the Culebra dolomite because of the wide variation of brine flux up the intrusion borehole (i.e., the natural tendency is for transported material to disperse); (4) general absence of uranium ore deposits in evaporates, such as dolomite, because carbonate tends to increase rather than decrease solubility; (5) general inability of uranium to deposit at critical concentrations in Culebra dolomite, since concentrations found in most economically mineable uranium ores are far less (Rechard et al. 2001; Adler 1974); (6)

general inability of plutonium to deposit at a critical density since higher than normally occurs in uranium ore bodies; (7) absence of strong reductants (or oxidants) in Culebra to promote precipitation; (8) minimal projected precipitation of any minerals, including fissile minerals, as Castile brines mix with Culebra brines (FEP H35 Borehole-Induced Mineralization); (9) the necessity of fissile material to dislodge abundant metal cations in brine (such as Ca+2 and Mg+2) on any potentially adsorptive matrix in Culebra dolomite; and (10) control of much adsorption by solution concentration (i.e., equilibrium thermodynamics), which cannot exceed critical limits for 239Pu and 235U since filterable mineral and microbial colloids adsorb fissile material externally.

Conceptually, two types of assemblies may form from slow hydrologic and geochemical processes mobilizing, transporting, and depositing the fissile material: (1) a critical assembly with predominately negative feedback as the criticality heats the fissile material and vaporizes the water moderator such that the neutron chain reaction rapidly shuts down, and (2) a critical assembly with positive feedback as water is driven from surrounding fractures such that the neutron chain reaction continues for a long enough period that the material surrounding the fissile material melts. Importantly, however, both a critical configuration with negative feedback and one with positive feedback must be assembled with the same natural processes (such as precipitation, adsorption, or colloidal aggregation) that are unfavorable in the WIPP disposal system, as mentioned above.

A moderated, slow rate of assembly with negative feedback is represented by the Oklo natural reactors in uranium ore deposits in Gabon, Africa. The critical assembly formed when massive amounts of dissolved uranium in fresh water flowed through the porous sandstone, was reduced by trapped oil, and precipitated as lenticular deposits (Gauthier-Lafaye et al. 1989). These conditions are very different from the WIPP disposal system. While WIPP contains reductants such as iron and radiolytic hydrogen, it lacks the massive, concentrated amounts of dissolved fissile material and the specific geological transport mechanisms (freshwater flow through porous sandstone) that enabled the lenticular precipitation seen at Oklo. Furthermore, the presence of carbonate dolomite at WIPP tends to increase actinide solubility, hindering the localized concentration of fissile material required for a self-sustaining chain reaction. Although thought to be a possible common occurrence soon after their discovery (Cowan 1976), the Oklo natural reactors remain unusual; no other uranium deposits of the Proterozoic System of the Precambrian Era show evidence of forming natural reactors.

In late 1994, Bowman and Venneri (Bowman and Venneri 1996) hypothesized several situations of Pu deposited in an unsaturated fracture system in volcanic tuff that could release substantial energy through positive feedback that melted the surrounding tuff (i.e., autocatalytic behavior) (Bowman and Venneri 1996; Rechard et al. 1997). In general, the initial configurations were either dry and under moderated with water or wet and over moderated with water. However, even the wet over moderated configuration required a theoretical step that dried out the fractures of the assembly to setup autocatalytic behavior (Kastenberg et al. 1996). Neither the initially dry fissile configuration nor the theoretical drying of the fissile region is possible in the saturated environment at WIPP.

SCR-6.2.1.3.4.5 Summary

The probability of criticality is low in each of the four discussed modes of assembling fissile material. Hence, FEP W14 *Nuclear Criticality: Heat* has been excluded from PA calculations on the basis of low probability of occurrence.

SCR-6.2.2 Radiological Effects on Material Properties

SCR-6.2.2.1 **FEP Numbers: W15, W16, W17, and W112**
FEP Titles: Radiological Effects on Waste (W15)
Radiological Effects on Containers (W16)
Radiological Effects on Shaft Seals (W17)
Radiological Effects on Panel Closures (W112)

SCR-6.2.2.1.1 Screening Decision: SO-C

Radiological Effects on the properties of the *Waste*, *Containers*, *Shaft Seals*, and *Panel Closures* have been eliminated from PA calculations on the basis of low consequence to the performance of the disposal system.

SCR-6.2.2.1.2 Summary of New Information

The screening arguments for these FEPs have been updated to include references to the radionuclide inventory used for CRA-2026 PA calculations (Kicker 2025; Van Soest 2025).

SCR-6.2.2.1.3 Related FEP

FEP W15 *Radiological Effects on Waste* is related to FEP W56 *Speciation* (SCR-6.5.2.1), which includes consideration of the radiological effects on waste due to radiolysis within the disposal room affecting the mobile actinide source term.

SCR-6.2.2.1.4 Screening Argument

Ionizing radiation can change the physical properties of many materials. Strong radiation fields could lead to damage of waste matrices, brittleness of metal containers, and disruption of the crystalline structure in the seals. However, the TRU waste at WIPP primarily releases alpha radiation that does not penetrate far into materials and is of low activity such that it can be safely handled directly by humans (contact-handled TRU waste or CH-TRU). The activity at WIPP closure for alpha-emitting TRU radionuclides with half-lives greater than 20 years, as represented by the EPA waste unit factor, has remained fairly constant (i.e., $f_{actvty} = \sum_{n_r} W_r/10^6$ Ci where W_r is the TRU waste initial activity of n_r radionuclides regulated by EPA) until this CRA-2026 where the activity has more than doubled due to the addition of a large plutonium oxide waste stream (Van Soest 2025; 2018; 2012; Kicker 2025; Crawford et al. 2009; DOE 1996a, App. BIR) (Table SCR-6).

Table SCR-6. Initial Inventory Activity as Represented by EPA Waste Unit Factor

PA	Waste Unit Factor (f_{actvty})
CCA-1996	3.44
CRA-2004	2.48
CRA-2009	2.32
CRA-2014	2.06
CRA-2019	3.30
CRA-2026	7.37

Nonetheless, the low activity of the TRU waste is unlikely to generate a radiation field strong enough to damage repository components. Furthermore, the activity of TRU waste at WIPP through the first 100 years is less than spent nuclear fuel and high-level waste, which is also not likely to damage repository components.

More importantly, the source-term model in the PA calculations has assumed instantaneous failure of the containers and instantaneous dissolution of radionuclides in the waste since CCA-1996 (U.S. DOE 1996a; Section 6.4.3.4). Hence, radiation cannot enhance container failure or radionuclide dissolution.

Furthermore, shaft seals are far from the disposal area. The intervening salt sufficiently attenuates alpha and neutron radiation. Finally, panel closures are primary constructed of ROM salt whose radionuclide isolation properties are not degraded by low alpha radiation. Therefore, radiological effects on the properties of the waste, container, shaft seals, and panel closures have been excluded from PA calculations on the basis of low consequence to the performance of the disposal system.

SCR-6.3 Geological and Mechanical FEPs

SCR-6.3.1 Excavation-Induced Changes

SCR-6.3.1.1 **FEP Numbers: W18 and W19**
FEP Titles: Disturbed Rock Zone (W18)
Excavation-Induced Change in Stress (W19)

SCR-6.3.1.1.1 Screening Decision: UP

Excavation-induced host rock fracturing through formation of a *Disturbed Rock Zone* and *Changes in Stress* are accounted for in PA.

SCR-6.3.1.1.2 Summary of New Information

With new panels to the west of the existing repository, additional excavation regions are included in the CRA-2026 PA repository model. This additional excavation will induce changes in stress resulting in the formation of a DRZ surrounding these excavations. The new excavation regions included in the CRA-2026 model are encompassed by a DRZ in the same manner as the existing excavated regions. No changes are necessary to the screening argument or screening decision of these FEPs. They remain classified UP.

SCR-6.3.1.1.3 Screening Argument

Construction of the repository has caused local excavation-induced changes in stress in the surrounding rock as discussed in the CCA, Chapter 3.0, Section 3.3.1.5. Excavation-induced changes in stress has led to failure of intact rock around the opening, creating a DRZ of fractures. On completion of the WIPP excavation, the extent of the induced stress field perturbation will be sufficient to have caused dilation and fracturing in the anhydrite layers “a” and “b,” MB 139, and, possibly, MB 138. The creation of the DRZ around the excavation and the disturbance of the anhydrite layers and MBs will alter the permeability and effective porosity of the rock around the repository, providing enhanced pathways for flow of gas and brine between the waste-filled rooms and the nearby interbeds. Where emplaced, the ROM salt PCS will initially have higher permeability until creep closure processes cause the back and ribs to contact and compress the PCS. These compressive forces will help to consolidate the ROM salt PCS as well as heal the surrounding DRZ. Excavation-induced, host-rock fracturing is accounted for in PA (the CCA, Chapter 6.0, Section 6.4.5.3). Updates to the treatment of the DRZ near panel closures is described in Appendix PA-4.2.8.

SCR-6.3.1.1.4 FEP Implementation in PA

FEP W18 *Disturbed Rock Zone* and FEP W19 *Excavation-Induced Change in Stress*, which are UP FEPs, are associated with the *Disturbed Rock Zone* conceptual model. This conceptual model is implemented in the PA code BRAGFLO for the Salado Flow computation in the PA calculation (Appendix PA-4.2). The DRZ conceptual model is implemented by assigning different DRZ material properties to the host rock immediately surrounding the repository excavation. The DRZ material properties include increased porosity and permeability from the intact Salado Halite. The DRZ material also allows for a further increase in porosity and permeability above specified brine pressures to account for fracture openings.

SCR-6.3.1.2 FEP Numbers: W20 and W21
FEP Titles: Salt Creep (W20)
Change in the Stress Field (W21)

SCR-6.3.1.2.1 Screening Decision: UP

Salt Creep in the Salado and any resultant *Changes in the Stress Field* are accounted for in PA.

SCR-6.3.1.2.2 Summary of New Information

An updated disposal room porosity surface used in the BRAGFLO Salado Flow code has been developed based on the model improvements documented in Vignes et al. (2023) and in Appendix PORSURF-2026. The new porosity surface model replaces the original Stone (1997) disposal room porosity surface used in previous CRAs and the CCA. It should be emphasized that these updates do not constitute a departure from the original *Creep Closure* conceptual model. The same general concepts are involved. No changes are necessary to the screening argument or screening decision of this FEP. It remains classified UP.

SCR-6.3.1.2.3 Screening Argument

Salt creep will lead to changes in the stress field, compaction of the waste and containers, and consolidation of the long-term components of the sealing system. It will also tend to close fractures in the DRZ, leading to reductions in porosity and permeability, increases in pore fluid pressure, and reductions in fluid flow rates in the repository. Salt creep in the Salado is accounted for in PA (the CCA, Chapter 6.0, Section 6.4.3.1).

The long-term repository seal system relies on the consolidation of the crushed-salt seal material and healing of the DRZ around the shaft seals and in and around the panel closures to achieve a low permeability under stresses induced by salt creep. Initially it is expected that the DRZ around the PCS will be no different from that around the disposal rooms since there will be very little back stress from the consolidating ROM salt PCS (Herrick 2012). In a few hundred years after repository closure, calculations demonstrate that back stress will have built up such that fractures in the DRZ and porosity in the panel closure will heal and close rapidly (Camphouse et al. 2012).

Shaft seal and panel closure performance is discussed further in Section SCR-6.3.5.1 (FEPs W36, W37, W113, and W114).

SCR-6.3.1.2.4 FEP Implementation in PA

FEPs W20 *Salt Creep* and W21 *Change in Stress Field a*re associated with the *Creep Closure* conceptual model. This conceptual model is implemented in the PA code BRAGFLO for the Salado Flow computation in the PA calculation (Appendix PA-4.2). In BRAGFLO, the porosity of the waste filled regions is determined from the porosity surface data using a look-up table where the porosity is a function of the time and the pressure computed in the grid cell.

For the ROM PCS regions included in the PA calculations, the regulatory time interval 0-10,000 years is broken up into 3 sub-intervals: 0-100 years, 100-200 years, and 200-10,000 years. The porosity and permeability in the ROM PCS regions will decrease during each successive interval to represent the compaction of the ROM PCS due to the creep of the host rock salt. During the first time period, 0-100 years both the permeability and porosity are treated as uncertain variables and sampled from specified distributions. During the second and third time periods, the porosity is sampled and the permeability is computed using an analytic function. The

distributions used for the porosity and permeability variables are available in Feng and Kicker 2025.

Non-waste-filled areas, which include the experimental and operational regions, the abandoned panel closures, and the new excavations going west to access the new replacement and additional panels, are conservatively modeled as permanently "open" with a high porosity and high permeability of $\phi = 0.18$ and $k = 10^{-11}\ m^2$, respectively (Feng and Kicker 2025).

SCR-6.3.1.3 **FEP Number: W22**
FEP Title: Roof Falls

SCR-6.3.1.3.1 Screening Decision: UP

The potential effects of *Roof Falls* on flow paths are accounted for in PA.

SCR-6.3.1.3.2 Summary of New Information

Additional excavation regions are included in the CRA-2026 PA repository model to account for the new panels to the west of the existing repository, a new utility shaft, and associated access drifts. These additional excavations induce stresses in the surrounding rock salt that cause the formation of a DRZ. The new excavation regions included in the CRA-2026 model are encompassed by a DRZ in the same manner as the existing excavated regions. No changes are necessary to the screening argument or screening decision for this FEP. It remains classified UP.

SCR-6.3.1.3.3 Screening Argument

Cracks form in the DRZ, near rooms at the WIPP, due to the lack of stiff support (confining pressure). These cracks can lead to blocks of salt detaching from the surrounding rock formation. If the room is filled with waste or crushed salt, the room contents will likely support these salt blocks such that they will partially mate up with the surrounding rock formation as the room closes. If surfaces mate up well, healing of fissures may happen relatively rapidly. When blocks detach around empty rooms, however, the blocks can fall several meters, land on the floor, and likely break into smaller pieces. This rubble pile will almost certainly not mate up with the surrounding rock formation, meaning the surrounding rock must apply sufficient pressure to rearrange, break up, and heal the rubble pile. If fluid pressures in the repository are low enough, the flow channels within the DRZ and rubble will eventually be squeezed out. If fluid pressures are substantial, then larger flow channels could persist for longer before they become hydraulically isolated voids. The time required for the permeability and porosity to reach their end states, nevertheless, is not precisely known. Considering this uncertainty, the PA flow model uses wide ranges for DRZ permeability and DRZ porosity and bounding values for the permeability and porosity of empty rooms than are expected to remain in the long term.

The addition of new panels to the west of the repository, a new utility shaft, and associated access drifts will not affect this screening argument or decision for this FEP. The effects of post-closure roof falls in these areas will be similar to the effects in other underground workings.

SCR-6.3.1.3.4 FEP Implementation in PA

FEP W22 *Roof Falls* is associated with the *Disturbed Rock Zone* conceptual model and is closely related to the *Repository Fluid Flow* conceptual model. These conceptual models are implemented in the PA code BRAGFLO for the Salado Flow computation in the PA calculation (Appendix PA-4.2). The DRZ conceptual model is implemented by assigning different DRZ material properties to the host rock immediately surrounding the repository excavation. The DRZ material properties include increased porosity and permeability from the intact Salado Halite. The DRZ material also allows for a further increase in porosity and permeability above specified brine pressures to account for fracture openings.

SCR-6.3.1.4

FEP Numbers: W23 and W24
FEP Titles: Subsidence (W23)
Large-Scale Rock Fracturing (W24)

SCR-6.3.1.4.1 Screening Decision:

SO-C (W23)
SO-P (W24)

FEPS W23 and W24 are concerned with subsidence and the potential large-scale fracturing of the geologic regions above the WIPP. Fracturing within units overlying the Salado and ground surface displacement (*Subsidence)* associated with excavated areas undergoing creep closure have been eliminated from PA calculations on the basis of low consequence to the performance of the disposal system. The potential for excavation- or repository-induced *Subsidence* to create *Large Scale Rock Fracturing* and fluid flow paths between the repository and units overlying the Salado has been eliminated from PA calculations on the basis of the low probability of occurrence over 10,000 yrs.

SCR-6.3.1.4.2 Summary of New Information

The additional new panels located to the west of the existing repository have been included in the CRA-2026 PA repository model. The rock extraction ratio for the new panels will be equal to or less than in the original repository design because the isolation pillars between the rooms will be greater for the new panels than in the original panel design. Thus, the subsidence over these new panels shouldn't be greater than over the original repository layout. These additional excavated panels are expected to create approximately the same deformation in the immediate vicinity of the excavations (DRZ) and similar fracture openings in the formations above the Salado as in CRA-2019.

The impact of subsidence due to potash mining has historically been accounted for in PA using transmissivity field modification in the Culebra. Potential mining-affected areas are identified

and random transmissivity multipliers are applied to the transmissivity field in those areas as described in Appendix TFIELD-2026. However, as noted in the 2019 FEPs Technical Support Document (U.S. EPA 2022d), the additional impact on the Culebra transmissivity fields due to repository excavation has not been treated in a similar manner. To address this concern, recent analyses by Bethune (2023a) examined the influence of subsidence-induced vertical strain on the horizontal fracture aperture opening on radionuclide transport in the Culebra. A constant one-order of magnitude increase in transmissivity was applied to all of the computational cells in the Culebra flow model directly above the original waste region (panels 1-10), the replacement panels (11 and 12), and the additional panel region (panels 13-19). Simulations accounting for full and partial mining conditions, radionuclide transport processes in the Culebra, and CCDFGF probabilistic release calculations were also performed. This analysis showed that releases through the Culebra remain small compared to the other release mechanisms and there was no discernable difference with the total release curve from the RPPCR PA.

SCR-6.3.1.4.3 Screening Argument

Instability of the DRZ due to salt fracturing could lead to localized roof falls in the first few hundred years. If instability of the DRZ causes roof falls, development of the DRZ may be sufficient to disrupt the anhydrite layers above the repository, which may create a zone of rock containing anhydrite extending from the interbeds toward a waste-filled room. Fracture development is most likely to be induced as the rock stress and strain distributions evolve because of creep and the local lithologies. In the long term, the effects of roof falls in the repository are likely to be minor because salt creep will reduce the void space and the potential for roof falls as well as promote healing of any roof material that has fallen into the rooms. Because of uncertainty in the complex process by which the disposal room DRZ heals and the rubble pile resulting from roof falls compacts, the flow model used in PA assumed that a higher-permeability zone remained for the long term. The CCA Performance Assessment Verification Test (PAVT) modified the DRZ permeability to a sampled range. Thus, the potential effects of roof falls on flow paths are accounted for in PA through appropriate ranges of the parameters describing the DRZ. The FEPs associated with the treatment of the DRZ and roof falls are W18 and W22 respectively.

The amount of subsidence that can occur as a result of salt creep closure or roof collapse in the WIPP excavation depends primarily on the volume of excavated rock, the initial and compressed porosities of the various emplaced materials (waste, backfill, panel and drift closures, and seals), the amount of inward creep of the repository walls, and the gas and fluid pressures within the repository. There was an analysis of the potential excavation-induced subsidence completed with the primary objective of determining the geomechanical advantage of backfilling the WIPP excavation (Westinghouse 1994). Mass conservation calculations, the influence function method, the National Coal Board empirical method, and the two-dimensional, finite-difference-code, Fast Lagrangian Analysis of Continua (FLAC) were used to estimate subsidence for conditions ranging from no backfill to emplacement of a highly compacted crushed-salt backfill (Westinghouse 1994, pp. 3-4 through 3-23). Subsidence at

potash mines located near the WIPP site was also investigated to gain insight into the expected subsidence conditions at the WIPP and to calibrate the subsidence calculation methods (Westinghouse 1994, pp. 2-17 to 2-23).

Subsidence over potash mines will be much greater than subsidence over the WIPP because of the significant differences in stratigraphic position, depth, extraction ratio, and layout. The WIPP site is located stratigraphically lower than the lowest potash mine, which is near the base of the McNutt. At the WIPP site, the base of the McNutt is about 150 m (490 ft) above the repository horizon. The WIPP rock extraction ratio in the waste disposal region will be about 22%, as compared to 65% for the lowest extraction ratios within potash mines investigated (Westinghouse 1994, p. 2-17).

The maximum total subsidence at potash mines was reported to be about 1.5 m (5 ft) (Westinghouse 1994, p. 2-22). This level of subsidence has been observed to have caused surface fractures. However, no evidence was found that subsidence over potash mines had caused fracturing sufficient to connect the mining horizon to water-bearing units or the land surface (Westinghouse 1994, p. 2-23). The level of disturbance caused by subsidence above the WIPP repository will be less than that associated with potash mining and thus, by analogy, will not create fluid flow paths between the repository and the overlying units.

The various subsidence calculation methods used provided similar and consistent results, which support the premise that subsidence over the WIPP will be less than subsidence over potash mines (Westinghouse 1994, pp. 3-4 to 3-23). Estimates of maximum subsidence at the land surface for the cases of no backfill and highly compacted backfill are 0.62 m (2 ft) and 0.52 m (1.7 ft), respectively. The mass conservation method gave the upper bound estimate of subsidence in each case. The surface topography in the WIPP area varies by more than 3 m (10 ft), so the expected amount of repository-induced subsidence will not create a basin and will not affect surface hydrology significantly. Subsidence was also estimated at the depth of the Culebra using the FLAC model for the case of an empty repository (containing no waste or backfill) (Westinghouse 1994, Table 3-13). The FLAC analysis assumed the Salado to be halite and the Culebra to have anhydrite material parameters. The 2-dimensional plane strain FLAC simulations essentially represent the disposal room excavations as having infinite length when they are actually 91 m (300 ft) in length. These types of 2-dimensional calculations likely provide a conservative over-estimate of the subsidence in the Culebra.

Maximum subsidence at the Culebra was estimated to be 0.56 m (1.8 ft) (Westinghouse 1994, Table 3-13). The vertical strain was concentrated in the Salado above the repository. Vertical tensile strain was less than 0.01% in units overlying the Salado and was very small (0.0034%) in the Culebra (Westinghouse 1994, Table 3-13). The maximum horizontal displacement in the Culebra was estimated to be 0.024 m (0.08 ft), with a maximum tensile horizontal strain of 0.007%. It was concluded that the induced strains in the Culebra will be uniformly distributed because no large- scale faults or discontinuities are present in the vicinity of the WIPP (Westinghouse 1994, pp. 4-1 to 4-2). Furthermore, strains of this magnitude would not be expected to cause extensive fracturing.

At the WIPP site, the Culebra transmissivity varies spatially over approximately five orders of magnitude (see Appendix TFIELD, Figure TFIELD-27). Where transmissive horizontal fractures exist, hydraulic conductivity in the Culebra is dominated by flow through the fractures. An induced tensile vertical strain may result in an increase in fracture aperture and corresponding increases in hydraulic conductivity. The magnitude of increase in hydraulic conductivity can be estimated by approximating the hydrological behavior of the Culebra with a simple conceptual model of fluid flow through a series of parallel fractures with uniform properties. A conservative estimate of the change in hydraulic conductivity can be made by assuming that all the vertical strain is translated to fracture opening (and none to rock expansion). This method for evaluating changes in hydraulic conductivity is similar to that used by the EPA in estimating the effects of subsidence caused by potash mining (Peake 1996; U.S. EPA 1996c).

The equivalent porous medium hydraulic conductivity, K (m/s), of a system of parallel fractures can be calculated assuming the cubic law for fluid flow (Witherspoon et al. 1980):

$$K = \frac{w^3 \rho g N}{12 \mu D} \qquad \text{(SCR.10)}$$

where w is the fracture aperture, ρ is the fluid density (taken to be 1,000 kg/m^3), g is the acceleration due to gravity (9.81m/s^2 (32 ft/sec^2)), μ is the fluid viscosity (taken as 0.001 Pa-sec), D is the effective Culebra thickness (7.7 m (26.3 ft)), and N is the number of fractures. For 10 fractures with a fracture aperture, w, of 6 x 10^{-5} m (2 x 10^{-4} ft), the Culebra hydraulic conductivity, K, is approximately 7 m/yr (2.3 x 10^{-7}m/sec (7.5 x 10^{-7} ft/sec)). The values of the parameters used in this calculation are within the range of those expected for the Culebra at the WIPP site (Appendix TFIELD).

The amount of opening of each fracture as a result of subsidence-induced tensile vertical strain, ε, (assuming rigid rock), is $D\varepsilon/N$ meters. Thus, for a vertical strain of 0.0001, which is approximately 3 times the value computed in the FLAC simulations (Westinghouse 1994, Table 3-13), the fracture aperture, w, becomes approximately 1.4 x 10^{-4} m. The Culebra hydraulic conductivity, K, then increases to approximately 85 m/yr (279 ft/yr) (2.7 x 10^{-6} m/sec (8.9 x 10^{-6} ft/sec)). Thus, for 10 fractures and a conservative estimate of vertical strain, the hydraulic conductivity of the Culebra may increase by an order of magnitude.

Recent simulations by Bethune (2023a) using the order of magnitude increase in hydraulic conductivity (or transmissivity) in regions above the current, replacement, and new panels showed that while there is an order of magnitude increase in releases at the LWB, the actual impact on mean total releases is minimal because the Culebra releases are an insignificant portion of the total releases[k]. Thus, changes in the horizontal component of Culebra hydraulic

[k] Bethune (2023a) results show that radionuclide releases from the Culebra are more than 3 orders of magnitude smaller than other release mechanisms (direct brine, cuttings, cavings, and spallings).

conductivity resulting from repository-induced subsidence have been eliminated from PA calculations on the basis of low consequence.

A similar calculation can be performed to estimate the change in vertical hydraulic conductivity in the Culebra as a result of a horizontal strain of 0.00007 m/m (Westinghouse 1994, p. 3-20). Assuming this strain is to be distributed over about 1,000 fractures (neglecting rock expansion), with zero initial aperture, in a lateral extent of the Culebra of about 800 m (2,625 ft) (Westinghouse 1994, Figure 3-39), then the subsidence-induced fracture aperture is approximately 6×10^{-5} m (1.9×10^{-4} ft). Using the values for ρ, g, and μ, above, the vertical hydraulic conductivity of the Culebra can then be calculated, through an equation similar to above, to be 7 m/yr (23 ft/yr) (2×10^{-7} m/sec (6.5×10^{-7} ft/sec)). Thus, vertical hydraulic conductivity in the Culebra may be created as a result of repository-induced subsidence, although this is expected to be insignificant.

Plans for the addition of new panels to the west of the existing repository will not affect this screening argument or decision for this FEP. Post-closure subsidence and large scale rock fracturing associated with these new panels will be largely unchanged since salt extraction ratios within the new panel regions will be kept within current design basis limits.

In summary, as a result of observations of subsidence associated with potash mines in the vicinity of the WIPP, the potential for subsidence to create fluid flow paths between the repository and units overlying the Salado has been eliminated from PA calculations on the basis of low probability. The effects of repository-induced subsidence on hydraulic conductivity in the Culebra have been eliminated from PA calculations on the basis of low consequence to the performance of the disposal system.

SCR-6.3.2 Effects of Fluid Pressure Changes

SCR-6.3.2.1 **FEP Numbers: W25 and W26**
FEP Titles: Disruption Due to Gas Effects (W25)
Pressurization (W26)

SCR-6.3.2.1.1 Screening Decision: UP

The mechanical effects of gas generation through *Pressurization* and *Disruption Due to Gas Effects* flow are accounted for in PA.

SCR-6.3.2.1.2 Summary of New Information

Several improvements to the disposal room porosity model have been made. The improvements pertain to three sub-models: the geomechanical model, the waste compaction model, and the gas pressurization model. The improvements to the disposal room porosity

model have been used to generate a new porosity response surface for use in the performance assessment calculation (Vignes et al. 2023).

SCR-6.3.2.1.3 Screening Argument

The mechanical effects of gas generation, including the slowing creep closure of the repository because of gas pressurization and the fracturing of interbeds in the Salado through disruption due to gas effects, are accounted for in PA (the CCA, Chapter 6.0, Section 6.4.5.2 and Section 6.4.3.1). Gas pressurization effects are not expected to affect consolidation of the ROM salt PCS because physical (creep) closure and complete consolidation are expected to occur before significant gas pressures can develop. The screening decisions have not changed and these FEPs are represented in the PA calculations.

SCR-6.3.2.1.4 FEP Implementation in PA

FEPs W25 *Disruption Due to Gas Effects* and W26 *Pressurization*, which are UP FEPs, are associated with the Repository Fluid Flow, Creep Closure, and Gas Generation conceptual models. These conceptual models are implemented in the PA code BRAGFLO for the Salado Flow computation in the PA calculation.

SCR-6.3.3 Effects of Explosions

SCR-6.3.3.1 **FEP Number: W27**
FEP Title: Gas Explosions

SCR-6.3.3.1.1 Screening Decision: UP

The potential effects of *W27 Gas Explosions* are accounted for in the design of panel closures during operations and by a disturbed rock zone in post-closure PA calculations.

SCR-6.3.3.1.2 Summary of New Information

The screening argument for this FEP has been updated for completeness and a summary of the implementation of this FEP within PA has been provided.

SCR-6.3.3.1.3 Screening Argument

Explosive gas mixtures could collect in the head space above the waste in a closed panel. The most explosive gas mixture potentially generated will be a mixture of hydrogen (H_2), methane (CH_4), and oxygen (O_2), which will convert to carbon dioxide (CO_2) and water (H_2O) on ignition. There is little likelihood of a gas explosion in the long term because the rooms and panels are expected to become oxygen depleted. Analysis suggests that the most explosive mixture of hydrogen, methane, and oxygen will be present in the void space ~20 years after emplacement of the panel closures (U.S. DOE 2004, Appendix BARRIERS-2004, Attachment PCS). The possibility of an explosion prior to anoxic conditions is considered in the design of the operational panel closure.

The effect of a room explosion on the disposal system after closure is expected to be no more severe than roof fall in a disposal room. In turn, the influence of disposal room rock fall is included in PA calculations through the designation of a DRZ feature. The DRZ feature is discussed in the included FEPs W18 *Disturbed Rock Zone* and W22 *Rock Falls* and described in the Disturbed Rock Zone Conceptual Model. The conceptual model of the DRZ about a disposal room is as follows (U.S. DOE 1996a, Appendix PEER 1, Section 3.7.1):

> …For the waste room, the DRZ model is incorporated by assuming a high permeability and low porosity, with the result that the DRZ is unable to act as a constraint to brine or gas flow from the repository rooms and is unable to store brine. A primary reason for this approach is the uncertain behavior of the rock zone, which is dependent on many uncontrollable factors.

SCR-6.3.3.1.4 FEP Implementation in PA

The DRZ Conceptual Model for the disposal area is implemented in PA calculations by designating a DRZ region adjacent to the intruded waste panel, south rest-of-repository, north rest-of-repository in the BRAGFLO code (Appendix PA -4.2; WIPP Performance Assessment 2025). The current parameter values in the DRZ are as follows: (1) sampled permeability between $10^{-19.4}$ and $10^{-12.5}$ m^2, which is high relative to intact halite permeability but low relative to waste permeability of 10^{-13} m^2; and (2) sampled porosity between 0.39% and 5.48%, which is consistently 0.29% higher than the sampled intact halite porosity. The DRZ porosity and permeability may increase beyond sampled values if the room pressure exceeds a threshold value to account for fracture openings.

SCR-6.3.3.2 FEP Number: W28
FEP Title: Nuclear Explosions

SCR-6.3.3.2.1 Screening Decision: SO-P

Nuclear Explosions have been eliminated from PA calculations on the basis of low probability of occurrence.

SCR-6.3.3.2.2 Summary of New Information

FEP W28 *Nuclear Explosions* has been updated to recognize the updated criticality screening assessment for FEP W14 *Nuclear Criticality Heat*. This new information does not change the screening decision for this FEP.

SCR-6.3.3.2.3 Screening Argument

Nuclear criticality refers to a self-sustained neutron chain reaction. Whether an assembly of fissile material is critical depends upon the interaction of neutrons with matter within and outside the assembly. The neutron multiplication factor (k_{eff}) is a measure of this interaction. The k_{eff} is conceptually the ratio of the number of neutrons in one generation in a fissile assembly to the number of neutrons present in the previous generation. The fissile assembly is critical when k_{eff} is unity.

Two conditions are used to organize the screening arguments of FEPs W28 *Nuclear Explosions* and W14 *Nuclear Criticality* (Fig. *1z*) (Rechard et al. 1997, Fig. 7): (1) speed of assembly, and (2) presence of a moderator to reduce neutron energy (i.e., slow down neutrons) and thereby probability of interaction with fissile material. Three speeds of assembly are considered here: (a) slow refers to assembly processes that occur over geologic time; (b) fast refers to assembly processes that occur over a short time; and (c) explosive refers to assembly processes that occur in microseconds.

Assembly of the fissile material is required because insufficient fissile material exists in any individual container disposed at WIPP to cause criticality. This condition is enforced to ensure safety during transportation and WIPP operations (U.S. DOE 2022c). Hence, to cause criticality after WIPP closure, a critical configuration must be assembled: either (1) the array of containers in the disposal room must be compacted such that fissile separation is no longer maintained, or (2) fissile material in each container must be mobilized, transported, and deposited in another location at a critical concentration and mass.

The second condition used to organize the criticality arguments is presence or absence of a moderator. The potential of criticality with moderated, slow neutrons is discussed and screened out in FEP W14 *Nuclear Criticality* (SCR-6.2.1.3). This FEP W28 *Nuclear Explosions* addresses conditions with unmoderated, fast neutrons.

Criticality involving little or no moderation in the WIPP disposal system is improbable (Rechard et al. 2001). All WIPP containers have some hydrogenous material such as organic material in the form of polyethylene plastic bagging to prevent external contamination when loading containers. The containers also often have inorganic material with absorbed moisture, water of hydration (e.g., clay), or hydrated metal ions. Furthermore, MgO acts as a moderator and is used throughout the disposal region. Finally, the WIPP disposal system is currently or eventually saturated with brine (currently, as the Culebra dolomite, or eventually, as brine seeps into a room). Further discussion of the improbability of each branch in Fig. SCR-7 is discussed below.

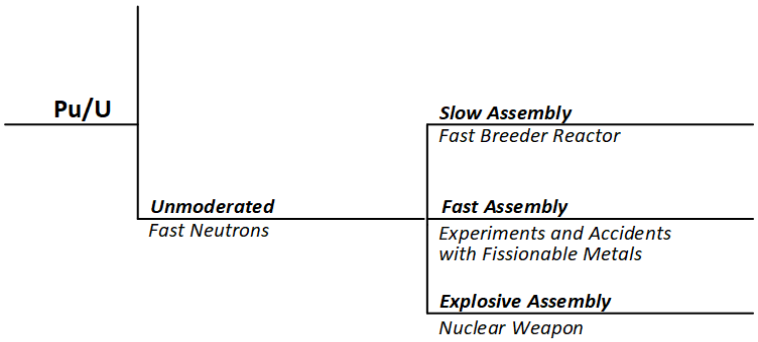

Figure SCR-7. Categories of criticality for organizing arguments based on explosive, fast, or slow fissile assembly speed for fissile assembly with unmoderated, fast neutrons (Rechard et al. 1997, Fig. 7).

SCR-6.3.3.2.3.1 Unmoderated Explosive Assembly

An unmoderated, explosive assembly is a nuclear weapon, which requires special design features; it is a situation that cannot occur by accident or natural processes in the saturated environment at WIPP (Rechard et al. 1997, Fig. 7; Rechard et al. 2001). k_{eff} greater than unity is a necessary condition for an atomic explosion, but it alone is not sufficient. Special conditions must exist such that the rate of increase in k_{eff} is very rapid. To obtain a rapid increase in k_{eff} requires, in turn, that sufficient energy be added to the system such that the fissile mass is assembled through rapid compression to allow for many generations of neutrons (each uranium fission and thus each generation requiring about 10 nanoseconds) to produce massive numbers of fissions and thereby sufficient heat and kinetic energy before negative feedback, such as material thermal expansion, changes the configuration density and limits the number of neutron generations. For ^{239}Pu, an atomic explosion is typically produced by imploding a sphere of fissile mass by detonating surrounding explosives to rapidly increase the ^{239}Pu density.

For ^{235}U, a somewhat simpler design is possible for an atomic explosion in which two subcritical amounts of ^{235}U are explosively brought together with a velocity between 300 and 1,000 m/s to form a supercritical mass (Serber 1992). This velocity is 300 to 1,000 times faster than the fast assembly caused by the acceleration of gravity over ~2 m in the WIPP disposal room. Furthermore, the average uranium enrichment of WIPP TRU waste is <20%, which is far below the theoretical minimum enrichment of 35% required for nuclear explosion (Murray 1957 p. 182).

SCR-6.3.3.2.3.2 Unmoderated Fast Rate of Assembly

Rockfall in a WIPP disposal room in which an array of containers is compacted sufficiently such that fissile separation between containers is not maintained potentially results in a fast assembly of fissile material. Thus, detailed analysis of rockfall on to a room full of POCs or CCOs was conducted (Reedlunn and Bean 2019; Reedlunn et al. 2023; Rechard et al. 2025b).

Neither a block that fell mostly flat or one that unzipped from the ceiling in order to impart rotation caused the POCs or CCOs to buckle, crush, or cluster together (Reedlunn and Bean 2019; Reedlunn et al. 2023; Rechard et al. 2025b). Because the separation of fissile material between each POC or CCO was maintained in the analysis, rockfall does not promote a critical configuration, whether the container is moderated or not. The situation without moderation would roughly correspond to experiments and accidents with fissile metals (Rechard et al. 1997; Stratton and Smith 1989). Yet, rooms filled with containers without hydrogenous material and rooms without MgO are improbable in the WIPP disposal system. Fast assembly with moderation is considered in FEP W14 *Nuclear Criticality* (SCR-6.2.1.3).

SCR-6.3.3.2.3.3 Unmoderated Slow Rate of Assembly

No credible method exists to mobilize, transport, and slowly assembly fissile material beyond a disposal room without brine in the saturated environment of WIPP (Rechard and Brady 2025) (Rechard et al. 2001). Certainly, gradual closure from salt creep and subsequent container compaction represents a slow assembly inside a disposal room. Yet, rooms filled with containers without hydrogenous material and rooms without MgO, which acts as a moderator, are improbable in the WIPP disposal system.

SCR-6.3.3.2.3.4 Summary

Because each branch in Figure SCR-7 is improbable, FEP W28 *Nuclear Explosions* has been excluded from PA calculations on the basis of low probability of occurrence.

SCR-6.3.4 Thermal Effects

SCR-6.3.4.1 **FEP Numbers: W29, W30, W31, W72, and W73**
FEP Titles: Thermal Effects on Material Properties (W29)
Thermally-Induced Stress Changes (W30)
Differing Thermal Expansion of Repository Components (W31)
Exothermic Reactions (W72)
Concrete Hydration (W73)

SCR-6.3.4.1.1 Screening Decision: SO-C

The effects of *Thermally-Induced Stress*, *Differing Thermal Expansion of Repository Components*, *Thermal Effects on Material Properties, Exothermic Reactions,* and *Concrete Hydration* have been eliminated from PA calculations on the basis of low consequence to performance of the disposal system.

SCR-6.3.4.1.2 Summary of New Information

The most recent inventory of potential reactants for CRA-2026 have been used in the screening argument (Van Soest 2025; Kicker 2025). In addition, maximum recorded amounts of potential reactants deposited in the first seven panels has been incorporated. The potential temperature increases have been recalculated with these updated reactant quantities.

SCR-6.3.4.1.3 Related FEPs

In addition to heat from W72 *Exothermic Reactions* and W73 *Concrete Hydration*, directly considered, related FEPs are W13 *Heat from Radioactive Decay* (Section SCR-6.2.1.2) and W14 *Nuclear Criticality Heat* (Section SCR-6.2.1.3). W13 *Heat from Radioactive Decay* was excluded because of low consequence. W14 *Nuclear Criticality Heat* was excluded because of low probability.

Other FEPs that reference and exclude processes because of small temperature increase include W33 *Movement of Containers*, W43 *Convection*, and W93 *Soret Effect*.

SCR-6.3.4.1.4 Screening Argument

Material properties (such as viscosity, permeability, and porosity) are influenced by temperature changes (W29 *Thermal Effects on Material Properties*). Although elevated temperatures will accelerate the rate of salt creep and mitigate fracture development in the host halite, thermally-induced stress (W30 *Thermally-Induced Stress Changes*) could enhance existing pathways or create new pathways for groundwater flow in the disturbed rock zone (as discussed in FEP W18 *Disturbed Rock Zone (DRZ)*), in the anhydrite layers and marker beds, and through seals. Thermal expansion could result in uplift of the rock and ground surface overlying the repository (W31 *Differing Thermal Expansion of Repository Components*), and thermal buoyancy forces could lift the waste upward in the salt rock (as discussed in related FEP W33 *Movement of Containers*). Finally, temperature gradients could promote convection and thermal-chemical diffusion (as discussed in the related FEPs W43 *Convection* and W93 *Soret Effect*).

The potential for these effects to be significant depends upon the temperature changes anticipated from FEPs W72 *Exothermic Reactions* and W73 *Concrete Hydration*. In CCA-1996, a combined temperature increase of ~8 °C above an ambient 27 °C repository temperature was estimated from aluminum corrosion of aluminum foils and hydration of cement in the waste over a time scale of ~2 years (Bennett et al. 1996). The combined temperature increase for a combination of short-duration reactions occurring simultaneously for CRA-2026 is smaller at ~4 °C, based on the aluminum and cement reactants anticipated in the WIPP repository, as discussed in following sections. Further, combining temperature increases from all reactions for CRA-2026 results in a maximum increase of ~11 °C by W72 *Exothermic Reactions* and W73 *Concrete Hydration* that which is too low to meaningfully impact WIPP material properties or transport pathways. Therefore, W29 *Thermal Effects on Material Properties*, W30 *Thermally-Induced Stress Changes*, from W72 *Exothermic Reactions*, and W73 *Concrete Hydration* have

been excluded from WIPP performance assessments on the basis of low consequence to the performance of the disposal system.

SCR-6.3.4.1.4.1 Potential Reactants Associated with Waste

Exothermic reactions expected in the WIPP repository include MgO hydration, MgO carbonation, microbial degradation, aluminum corrosion, and cement hydration (Bennett et al. 1996). MgO hydration, MgO carbonation, and microbial degradation, in turn, depend upon the amount of cellulose, plastic, and rubber placed in the repository. In general, the mass of rubber and cement reactants have not changed much from CCA-1996. Cellulose and plastic mass have increased substantially while aluminum alloy mass has decreased substantially (Table SCR-7).

Although rubber and plastic are more difficult to biodegrade, they may do so under some circumstances. The equivalent quantity of cellulose (m_{equiv}^{cell}) by (Wang and Brush 1996a; Wang and Brush 1996b) was estimated using:

$$m_{equiv} = m_{cell} + m_{rub} + 1.7m_{plstc} \quad \text{(SCR.11)}$$

where m_{cell} is mass of carbon in waste as cellulose, m_{rub} is mass of rubber, and a factor of 1.7 times mass of plastics (m_{plstc}). Hence, the amount of equivalent cellulose in CCA-1996 and CRA-2026 is respectively 1.34×10^4 t and 3.10×10^4 t based on mass of cellulose, rubber, and plastics in Table SCR-7.

The MgO mass (m_{MgO}) emplaced is adjusted for every batch of containers that is disposed. The m_{MgO} is calculated assuming a one-to-one correspondence between CO_2 produced and six times mass of carbon in equivalent cellulose (m_{equiv}) ($C_6H_{10}O_5$—see Eq. SCR-17) (Wang and Brush 1996a; Wang and Brush 1996b):

$$m_{MgO} = \left(6 f_{safety} \frac{m_{equiv}}{162 \text{ g/mole cellulose}}\right)(40.3 \text{ g/mole MgO}) \quad \text{(SCR.12)}$$

Between 1996 and 2000, the requirement was to maintain f_{safety} at 1.95 (Panel 1). Between 2001 and until February 2008, f_{safety} was 1.67 (Panels 2, 3, and 4) (U.S. EPA 2001). After February 2008, f_{safety} is 1.2 (Reyes 2008).

Table SCR-7. Potential Reactants in Disposal Area Associated with Waste for CCA-1996, and CRA-2026.

Inventory	CCA-1996	CRA-2026
MgO (t)	85,600[a]	63,841[d]
Equivalent Cellulose (t)	13,398[b]	30,994[b]
Cellulose (t)	5,940[c]	9,709[e]
Plastics (t)	3,740[c]	11,849[e]
Rubber (t)	1,100[c]	1,142[e]
Aluminum alloys (t)	1,980[c]	387[e]
Cement in waste (t)	8,540[c]	8,546[e]

[a] U.S. DOE 2000

[b] Based on Eq. SCR-11

[c] U.S. DOE 1996b. Only CH-TRU wastes were included; total volume of CH-TRU wastes was 1.1×10^5 m^3, which was not scaled to WIPP disposal volume.

[d] Estimate based on Eq. SCR-12. The safety factor is derived based on Panel 1 with a MgO safety factor of 1.95, three panels with a 1.67 safety factor, and the remaining 8 panels with a 1.2 safety factor, resulting in a 1.38 projected safety factor for 12-panel repository.

[e] From Van Soest 2025 for CH, RH, packaging, and emplacement materials; cement value includes current and future estimates of both reacted and unreacted cements.

In CRA-2026, 12 panels are anticipated for the interim repository. This results in the average mass of material per panel being much lower than calculated for the 9.5 panels originally planned in WIPP.[l] Currently, however, 7 of the original 10 panels are filled and provide sufficient experience to determine maximums of material that often exceed the average panel masses determined from the repository masses divided by number of panels (Table SCR-8).

[l] The WIPP disposal region initially considered 10 panels: 8 standard panels, and two smaller panels (9) south equivalent panel, and (10) north equivalent panel. The combined disposal volume of panels 9 and 10 is ~1.5 times the volume of the 8 standard panels; hence, the average panel mass is the total disposed repository mass divided by 9.5 (Schreiber 1991; WIPP PA Department 1992, Table 3.1-1).

Table SCR-8. Waste Material Mass Already Placed in WIPP Panels[a]

Panel	MgO	Equivalent Cellulose	Cellulose	Plastic	Rubber	Aluminum
1	4,482	1,604	706	523	8.9	5.5
2	6,664	2,043	477	877	74.5	17.7
3	6,435	2,158	548	891	95.2	9.9
4	6,483	2,744	833	1,065	100.1	9.4
5	5,263	2,168	647	864	52.4	7.6
6	3,290	1,489	599	503	34.7	11.0
7	1,881	884	248	360	24.5	5.5
Ave	4,928	1,870	580	726	55.8	9.5
Max	6,664	2,744	833	1,065	100.1	17.7

[a]Table SCR-8 produced from query of the WIPP Waste Data System (WDS) on January 10, 2025 in units of metric ton - t.

SCR-6.3.4.1.4.2 Estimated Temperature Increase from Exothermic Reactions in Panel

Wang (1996a; 1996b) estimated the temperature increase from an exothermic reaction in a panel based on assumptions that (1) heat loss occurs by conduction through the salt roof and floor of the panel; (2) negligible heat loss occurs through the side wall (i.e., two-dimensional heat loss); and (3) heat from chemical reactions occurs uniformly through the panel. Based on these assumptions the temperature increase (ΔT) is proportional to the $(RM)^{1/2}$ where R is the reactant reaction rate (mole/y) and often controlled by the influx of brine into the panel, M is the reactant mass in the panel (mole). To elaborate (Wang 1996a; Wang 1996b),

$$\Delta T = \frac{\Delta H_f^o}{S}\left(\frac{1}{\pi c_p \rho \kappa}\right)^{\frac{1}{2}} R t^{\frac{1}{2}} \qquad \text{(SCR.13)}$$

where ΔH_f^o is the standard enthalpy of the reaction, S is the horizontal surface area of panel drifts (~1.16×10^4 m^2 for CCA-1996 and ~1.18×10^4 m^2 for CRA-2026), c_p is the specific heat capacity of the surrounding halite at constant pressure (50 J/mole-K), ρ is the density of the surrounding halite (3.7×10^4 mole/m^3), and κ is the thermal conductivity of the surrounding halite (6 W/m-K or 1.88×10^8 J/y-m-K).

The time (t) when the reactant is depleted is M/R so Eq. SCR.13 reduces to

$$\Delta T = 2.56 \times 10^{-12} \Delta H_f^o (RM)^{\frac{1}{2}}. \qquad \text{(SCR.14)}$$

SCR-6.3.4.1.4.3 MgO Backfill Hydration

If the reaction goes to completion to form brucite ($Mg(OH)_2$), hydration of MgO backfill occurs by

$$\begin{array}{cccc} & MgO & + H_2O & \rightarrow Mg(OH)_2 \\ \Delta H_f^o & -601.7 & -285.8 & -925.5 \end{array} \quad \text{(SCR.15)}$$

which has an enthalpy of formation ΔH_f^o of -38 kJ/mole (Bennet et al. 1996, Table 1). It is reasonable to assume that MgO reaction occurs instantaneous compared to the rate of brine inflow such that brine inflow controls the reaction rate (*R*). In WIPP PAs, the maximum brine flow through a panel occurs after a drilling intrusion into the repository that continues down to a hypothetical brine reservoir in the Castile Formation below the repository (E1 intrusion—Scenario S2-BF).

In CCA-1996, the panel brine inflow was assumed at 200 m^3/y or 1.1×10^7 mole/y with water density of 5.56×10^4 mole/m^3. In CCA, the bounding temperature rise from MgO hydration was 4.5 °C after ~19 years (Table SCR-9), based on 9.5 panels with equal mass in each panel (Table SCR-7).

For CRA-2026, the maximum rate of MgO hydration in an E1 intrusion into a panel (Scenario S2-BF) is used to estimate the heat production directly. The maximum rate of MgO hydration after intrusion observed in one simulation is 4.75×10^5 kg/y (Figure SCR-8b).[m] The maximum MgO mass placed in the intruded panel is 6664 metric tons (1.65×10^8 moles) (Table SCR-8), which results in a maximum temperature rise of 4.3 °C after 14 years (Table SCR-9).

[m] Most simulations prior to inadvertent drilling intrusion do not have sufficient brine inflow to hydrate all the MgO; however, several simulations do, in which case the maximum hydration rate prior to intrusion is similar at 2.56×10^5 kg/y (Figure SCR-8a).

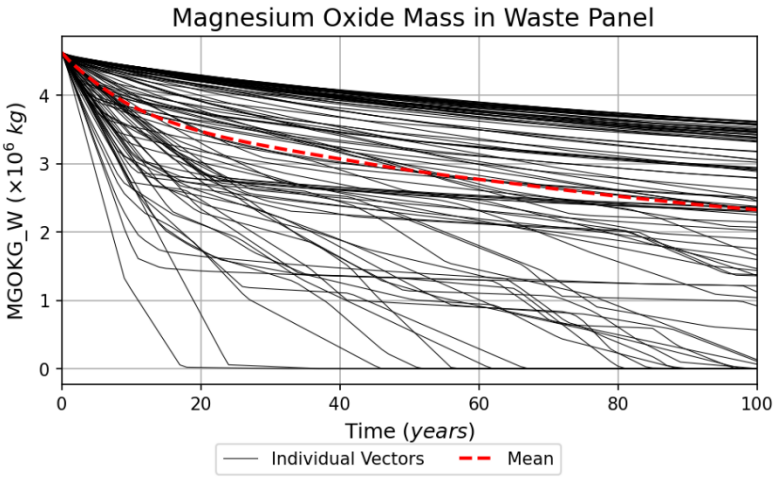

(a) Early time prior to inadvertent human intrusion (undisturbed conditions) with maximum hydration rate of 2.56×10^5 kg/y.

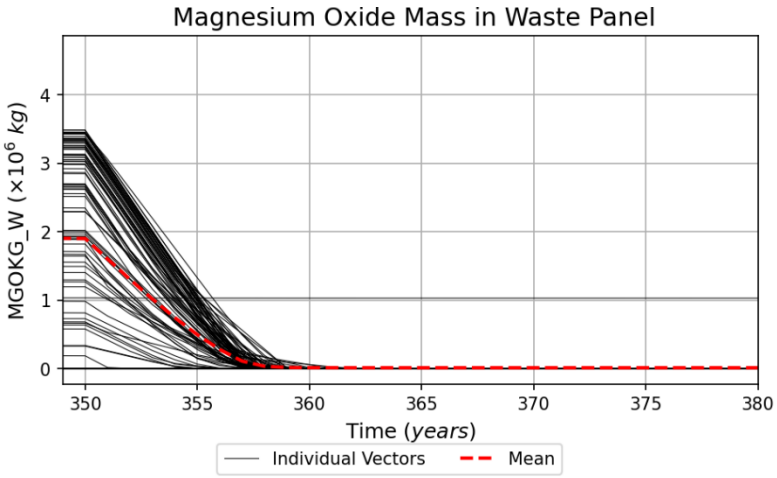

(b) E1 intrusion at 350 years with maximum hydration rate of 4.75×10^5 kg/y.

Figure SCR-8. Mass of magnesium oxide remaining in waste panel (MGOKG_W) for E1 intrusion, Replicate 1, CRA-2026 (Scenario S2-BF-t350-r1).

SCR-6.3.4.1.4.4 Microbial Degradation

In CCA-1996, Wang (1996a) assumed microbial degradation of cellulose occurred by methanogenesis:

$$\begin{array}{cccccc} C_6H_{10}O_5 & + H_2O & \rightarrow & 3CH_4 & + 3CO_2 \\ \Delta H_f^o & \text{-805.5} & & \text{-285.83} & 3(\text{-74.6}) & 3(\text{-393.5}) \end{array} \qquad \text{(SCR.16)}$$

which has an ΔH_f^o of -312 kJ/mole, based on ΔH_f^o of 805.5 kJ/mole for $C_6H_{10}O_5$ (Bennet et al. 1996, Table 1). However, methanogenesis (Eq. SCR-16) does not occur in highly saline solutions and, thus, has not been included since CRA-2009 (U.S. DOE 2009, Appendix SOTERM-2009, Section SOTERM-4.2). Rather 96% of microbial degradation is now thought to

potentially occur through sulfate-reducing bacteria because of the abundance of sulfate available in Salado brine that flows through the anhydrite marker beds (included FEP *W44 Degradation of Organic Material*) The reaction ΔH_f^o is -2983 kJ/mole:

$$\begin{array}{cccccc} C_6H_{10}O_5 + 3H_2SO_4 & \rightarrow & 5H_2O & + 6CO_2 & + 3H_2S \\ \Delta H_f^o \quad -805.5 & & 3(\text{-}20.6) & 5(\text{-}285.8) \quad 6(\text{-}393.1) & 3(\text{-}21) \end{array} \qquad \text{(SCR.17)}$$

For CRA-2026, the maximum rate of microbial degradation in an E1 intrusion into a panel (Scenario S2-BF) is used to estimate the heat production directly. The maximum degradation rate of equivalent cellulose after intrusion observed in one simulation is 6,780 mole/y (Figure SCR-9). The maximum equivalent cellulose mass placed in the intruded panel in CRA-2026 is 2,744 metric tons (1.69×10^7 moles) (Table SCR-8), which results in a maximum temperature rise of 2.6 °C after 2,500 years (Table SCR-9). In comparison, the temperature rise in CCA-1996 was 0.8 °C from methanogenesis after 120 years (Table SCR-9).

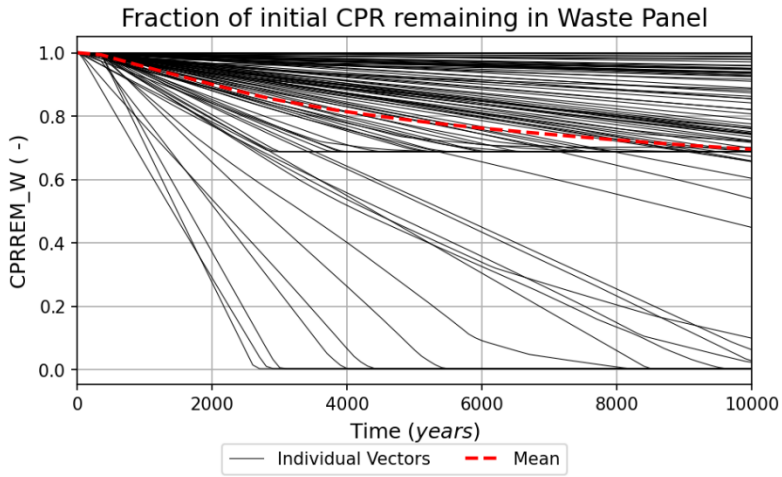

Figure SCR-9. Fraction of initial cellulose, plastic, and rubber remaining in waste panel (CPRREM_W) for E1 intrusion with intrusion at 350 years, Replicate 1, CRA-2026 (Scenario S2-BF-t350-r1).

SCR-6.3.4.1.4.5 Capture of CO_2 by MgO Backfill

Capture of CO_2 by the hydrated MgO (i.e., brucite ($Mg(OH)_2$) to form magnesite ($MgCO_3$) occurs by

$$\begin{array}{cccccc} Mg(OH)_2 + CO_2 & \rightarrow & MgCO_3 + H_2O \\ \Delta H_f^o \quad \text{-}925.4 & & \text{-}393.1 \quad \text{-}1110.3 & & \text{-}285.8 \end{array} \qquad \text{(SCR.18)}$$

which has ΔH_f^o of -77 kJ/mole (Bennet et al. 1996, Table 1). Wang (1996b) reasonably assumed that carbonization of the MgO backfill was limited by production of microbial CO_2 estimated by Eq. SCR-18 above.

For CRA-2026, the maximum rate of gas generation from microbial biodegradation in an E1 intrusion into a panel (Scenario S2-BF) is used to estimate the heat production directly. The maximum rate of gas generation from microbial biodegradation is 1.76×10^{4} mole/y (Figure SCR-10). The maximum equivalent cellulose mass placed in the intruded panel in CRA-2026 is 2,744 metric tons (1.69×10^{7} moles) (Table SCR-8). The corresponding maximum temperature rise from MgO capture of 1.02×10^{8} moles (6 times 1.69×10^{7} moles, Eq. SCR-17) of CO_2 is 0.3 °C after 5,770 years (Table SCR-9). In comparison, the maximum temperature rise was estimated at twice as large at 0.6 °C after 124 years in CCA-1996 (Table SCR-9).

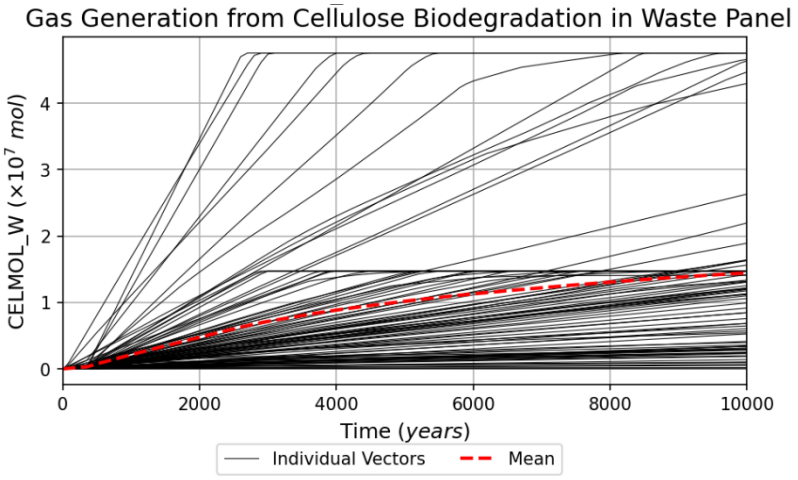

Figure SCR-10. Mass of gas generated from equivalent cellulose biodegradation in waste panel (CELMOL_W) for E1 intrusion at 350 years, Replicate 1, CRA-2026 (Scenario S2-BF-t350-r1).

SCR-6.3.4.1.4.6 Aluminum Corrosion

Aluminum corrosion occurs by

$$\begin{array}{cccccc} Al & + & 3H_2O & \rightarrow & Al(OH)_3 & + 1.5H_2 \\ \Delta H_f^o & 0 & 3(\text{-}285.8) & & \text{-}1291.9 & 0 \end{array} \qquad \text{(SCR.19)}$$

which has ΔH_f^o of -434 kJ/mole (Bennet et al. 1996, Table 1).

Aluminum is mostly present as foil in the waste with a thickness of 2.54×10^{-4} cm, which will rapidly corrode. Hence, aluminum corrosion is controlled by brine inflow into a panel. In CCA-1996, the brine flow was set at 200 m^3/y or 1.1×10^{7}mole/y. The corresponding aluminum reaction consumption was then 3.7×10^{6} mole/y (i.e., 1/3rd of 1.1×10^{7}mole/y), assuming a zero-order reaction rate. In the CCA, the bounding temperature rise from aluminum corrosion was 6 °C after 2.2 years (Table SCR-9).

For CRA-2026, the aluminum corrosion rate is controlled by brine flow into the panel and so is 1/3rd the rate of MgO hydration (3.93×10^{6} mole/y). The maximum aluminum mass placed in the intruded panel in CRA-2026 is 17.7 metric tons (6.57×10^{5} moles) (Table SCR-8), which results in a maximum temperature rise of 1.8 °C after 0.2 years (Table SCR-9).

SCR-6.3.4.1.4.7 Cement Hydration

Generally, cement is added to absorb/react with water in the waste and, thereby, solidify the waste for shipping and disposal since greater than 1% free liquid is prohibited. Hence, most cement that comes to WIPP will already be hydrated. Nonetheless, excess cement may be added to ensure any water is bound and not free; thus, we conservatively consider the possibility that all cement added to containers is unreacted.

The primary cement component, calcium oxide (CaO), hydrates as follows:

$$\begin{array}{ccccc} CaO & + & H_2O & \rightarrow & Ca(OH)_2 \\ \Delta H_f^o & -635.1 & -285.8 & & -986.1 \end{array} \quad \text{(SCR.20)}$$

which has ΔH_f^o of -65.2 kJ/mole (Bennet et al. 1996, Table 1).

For CRA-2026, brine flow acts as the limiting factor for cement reactivity, constraining it to the established MgO hydration rate (1.18×10^7 mole/y). The amount of cement either unreacted or reacted placed in the disposal area is not tracked for the repository. Hence, for CRA-2026, the maximum cement mass of 1.60×10^7 moles placed in the intruded panel is based on the projected 8,546 metric tons (Table SCR-7) of cement divided by 9.5 panels (Table SCR-9). Although the repository in CRA-2026 has 12 panels, the first 8 panels will have greater amounts of cement and so we still estimate the panel average using 9.5 panels. Cement hydration results in a maximum temperature rise of 2.3 °C after 1.4 years for CRA-2026 (Table SCR-9). In comparison, the bounding temperature rise from cement in the waste panel was 2 °C after 1.4 years in CCA-1996 (Table SCR-9).

Emplacement of structural or sealing concrete in the repository (e.g., shaft seals) will be completed by repository closure. Hence, any temperature increase because of concrete hydration of shaft seals or closure elements will have abated by the time active institutional controls are assumed to no longer prevent drilling into the repository 100 years after closure. Furthermore, the overall mass of concrete emplaced within the repository is significantly decreased from that anticipated in CCA-1996 because new panel closures are to be constructed of mined salt. Consequently, hydration of concrete components in the repository (not intrinsic to the TRU waste) is not considered because any related thermal rise will be short-term and only exist during the operational period, or at the very earliest part of the post-closure disposal period.

Table SCR-9. Temperature Increase from Exothermic Reactions in CCA-1996 and CRA-2026

Reactant	CCA-1996[a,b] DT (˚C)	CCA-1996 Min Time[c] (y)	CRA-2026 DT (˚C)	CRA-2026 Min Time (y)
MgO Hydration	4.5	19	4.3	14
Microbial Degradation	0.8	120	2.6	2,500
CO_2 Capture by $Mg(OH)_2$	0.6	124	0.3	5,770
Aluminum Corrosion	6	2.2	1.8	0.2
Cement Hydration	2	1.4	2.3	1.4

[a]Wang 1996a
[b]Bennet et al. 1996, Table 1
[c]Minimum time after ample brine inflow is available, which usually occurs after inadvertent drilling intrusion (Figure SCR-8b) but occasionally occurs prior to intrusion (undisturbed conditions—Figure SCR-8a).

SCR-6.3.4.1.4.8 Summary

Exothermic reactions and cement hydration in the repository only cause small temperature increases. Furthermore, the small temperature increases generally do not occur simultaneously but are spread out over the regulatory 10,000-year period (Table SCR-9). Hence, ~4 ˚C is a reasonable maximum temperature increase from W72 *Exothermic Reactions* and W73 *Concrete Hydration* based on combined temperature contributions from aluminum corrosion and cement hydration over a ~2 year timeframe and too low to meaningfully impact WIPP material properties or transport pathways. Temperature increases from MgO hydration are also ~4 ˚C over 14 years with long duration reactions (<2,500 yr) from microbial degradation and CO_2 capture capable of minimally further increasing temperature beyond ~4 ˚C. Therefore, W29 *Thermal Effects on Material Properties*, W30 *Thermally-Induced Stress Changes*, from W72 *Exothermic Reactions* and W73 *Concrete Hydration* have been excluded from WIPP performance assessments on the basis of low consequence to the performance of the disposal system.

SCR-6.3.5 Mechanical Effects on Material Properties

SCR-6.3.5.1 **FEP Numbers: W32, W36, W37, W39, W113, and W114**
FEP Titles: Consolidation of Waste (W32)
Consolidation of Shaft Seals (W36)
Mechanical Degradation of Shaft Seals (W37)
Underground Boreholes (W39)
Consolidation of Panel Closures (W113)
Mechanical Degradation of Panel Closures (W114)

SCR-6.3.5.1.1 Screening Decision: UP (W32, W36, W37, W39, W113)
SO-P (W114)

Consolidation of Waste is accounted for in PA. *Consolidation of Shaft Seals* and *Panel Closures* and *Mechanical Degradation of Shaft Seals* are accounted for in PA. Flow through isolated, unsealed *Underground Boreholes* is also accounted for in PA. *Mechanical Degradation of Panel Closures* is screened out based on low probability of occurrence (SO-P).

SCR-6.3.5.1.2 Summary of New Information

FEP W32, *Consolidation of Waste* is now implemented by an updated disposal room porosity surface as documented in Vignes et al. (2023) and in Appendix PORSURF-2026. The new porosity surface model, which accounts for the consolidation of the waste, replaces the original Stone (1997) disposal room porosity surface used in previous CRAs and the CCA. It should be emphasized that these updates do not constitute a departure from the original *Creep Closure* conceptual model. The same general concepts are involved. No changes are necessary to the screening argument or screening decision of this FEP and it remains classified UP.

FEPs W36, W37, W39, W113 and W114 remain unchanged from the CRA-2019. No changes are necessary for the screening arguments or screening decision for these FEPs.

SCR-6.3.5.1.3 Screening Argument

Consolidation of waste is accounted for in PA in the modeling of creep closure of the disposal room (Appendix PA-4.2.3).

The long-term repository seal system relies on the consolidation of the crushed-salt seal material and healing of the DRZ around the shaft seals and in and around the ROM salt PCS to achieve a low permeability under stresses induced by salt creep. Initially it is expected that the DRZ around the ROM salt PCS will be no different from that around the disposal rooms, since there will be only very small back stress from the consolidating ROM salt PCS (Herrick 2012). In a few hundred years after repository closure, calculations demonstrate that back stress will

have built up such that fractures in the DRZ and porosity in the panel closure will heal and close rapidly (Camphouse et al. 2012).

Consolidation of shaft seals, consolidation of the ROM salt PCS, and mechanical degradation of shaft seals are accounted for in PA through the permeability ranges assumed for the seal and closure systems (Appendix PA-4.2.7 and PA-4.2.8).

The site investigation program has also involved the drilling of boreholes from within the excavated part of the repository. Following their use for monitoring or other purposes, these underground boreholes will be sealed where practical, and salt creep will also serve to consolidate the seals and to close the boreholes. Any boreholes that remain unsealed will connect the repository to anhydrite interbeds within the Salado, and thus provide potential pathways for radionuclide transport. PA calculations account for fluid flow to and from the interbeds by assuming that the DRZ has a permanently enhanced permeability that allows flow of repository brines into specific anhydrite layers and interbeds. This treatment is also considered to account for the effects of any unsealed boreholes.

Mechanical degradation of panel closures is not expected to occur due to their ROM salt composition. Further, because of the healing nature of salt, the permeability and porosity within the ROM salt PCS are expected to reach that similar to intact halite. Therefore, mechanical degradation of panel closures is screened out of PA calculations due to low probability.

SCR-6.3.5.1.4 FEP Implementation in PA

Consolidation of Waste (W32) is associated with the Creep Closure conceptual model. This conceptual model is implemented in the PA code BRAGFLO for the Salado Flow computation in the PA calculation (Appendix PA-4.2). In BRAGFLO, the porosity of the waste filled regions is determined from the porosity surface data using a look-up table where the porosity is a function of the time and the pressure computed in the grid cell.

Consolidation of Shaft Seals (W36) and *Mechanical Degradation of Shaft Seals* (W37) are accounted for in the Salado Flow PA calculations through the permeability ranges assumed for the shaft seal systems (Appendix PA-4.2.7. The current model divides the shaft into three sections: an upper section (shaft seal above the Salado), a lower section (within the Salado), and a concrete monolith section within the repository horizon. The permeabilities of the upper and lower sections are treated as uncertain variables (sampled from a distribution). The upper shaft seal uses the sampled permeability for the entire 10,000 year regulatory period while the lower section of the shaft experiences a reduction in permeability at 200 years. This change simulates the consolidation of shaft seal materials within the Salado. The transition at 200 years was chosen as a conservative overestimate of the amount of time expected for this section of the shaft to become consolidated. To account for the mechanical degradation of the shaft seal system, the concrete monolith section of the shaft is represented as being highly permeable ($k = 10^{-14}$ m^2) for the entire 10,000 years to ensure that fluids can access the north end (OPS and

EXP areas) in the model. The parameter d0istributions used for the permeability in the upper and lower shaft seals are available in Feng and Kicker (2025).

Consolidation of Panel Closures (W113) is accounted for in the Salado Flow PA calculations by adjusting the permeability and porosity of the regions representing the ROM PCS (Appendix PA-4.2.8). For the ROM PCS regions, the regulatory time interval 0-10,000 years is broken up into 3 sub-intervals: 0-100 years, 100-200 years, and 200-10,000 years. The porosity and permeability in the ROM PCS regions will decrease during each successive interval to represent the compaction of the ROM PCS due to the creep of the host rock salt. During the first time period, 0-100 years both the permeability and porosity are treated as uncertain variables and sampled from specified distributions. During the second and third time periods the porosity is sampled and the permeability is computed using an analytic function. The parameter distributions used for the porosity and permeability variables are available in Feng and Kicker (2025).

Underground Boreholes (W39) are accounted for in the DRZ around the disposal rooms in the Salado Flow PA calculations (Appendix PA-4.2). The DRZ conceptual model is implemented by assigning different DRZ material properties to the host rock immediately surrounding the repository excavation. The DRZ material properties include increased porosity and permeability from the intact Salado Halite. The DRZ material also allows for a further increase in porosity and permeability above specified brine pressures to account for fracture openings. The parameter distributions used for the porosity and permeability variables are available in Feng and Kicker (2025).

SCR-6.3.5.2 **FEP Number: W33**
FEP Title: Movement of Containers

SCR-6.3.5.2.1 Screening Decision: SO-C

Movement of Containers has been eliminated from PA calculations on the basis of low consequence to the performance of the disposal system.

SCR-6.3.5.2.2 Summary of New Information

The FEP screening argument has been updated in the CRA-2026 to include references to other FEPs that address container movements due to room closure and roof falls[n], as well as to revise the analysis of density-driven container movement. The density-driven container movement analysis now includes pressure solution creep, uses a wider range of container densities, and considers clusters of compacted containers moving together. These changes have no impact upon the screening decision for this FEP.

[n] In their review of the CRA-2014 and CRA-2019, the EPA (2017c, 2022d) commented that FEP W33 should be modified to address "container movement associated with salt creep and roof falls."

SCR-6.3.5.2.3 Screening Argument

Waste container movements after the operational period can be divided into two types. One type consists of container deformations and rearrangements due to roof falls and/or room closure. Roof falls and room closure will only cause small container movements within the disposal room. The second type consists of density-driven container movements that have the potential to transport containers far from the disposal room in which they were emplaced. The first movement type is addressed in FEPs W14, W28, and W32 (see Sections SCR-6.2.1.3, SCR-6.3.3.2, and SCR-6.3.5.1, respectively), while the second movement type is addressed in this FEP screening argument.

Waste containers placed in the WIPP may move because of density contrasts between the waste containers and the surrounding salt. When the density of a waste container is greater than the density of the surrounding salt, the container will sink relative to the salt, whereas when the container density is less than the salt density, the container will rise relative to the salt. One could also consider density contrasts between a finite volume of heated salt surrounding a hot container and the unheated far-field salt (Dawson and Tillerson [1978]), but the transient temperature rises due to radioactive decay and exothermic reactions at the WIPP are expected to be only 3.5 °C or less (see Section SCR-6.3.4.1), so these thermal effects are neglected herein.

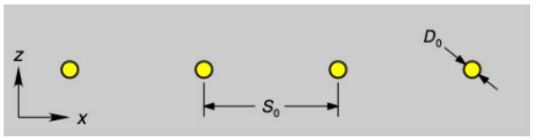

Figure SCR-11. Four infinitely long cylindrical containers within a single-layer infinite array. (Gravity acts in the negative z-direction.).

Previous studies on density-driven container movement (Dawson and Tillerson [1978], Clayton et al. [2014], Hardin et al. [2014], and Tounsi et al. [2023]) used numerical methods, such as the finite element method, to consider complex scenarios, such as heat generating waste and consolidating crushed salt around the containers. The Hardin et al. (2014) and Tounsi et al. (2023) studies are most relevant because they included both pressure solution creep and dislocation creep, while the other studies only considered dislocation creep. These two studies considered an array of cylindrical containers lying on their side, as shown in Figure SCR-11. Gravity acted in the z-direction, the containers were infinitely long in the y-direction, the array was infinite in the x-direction, and the array spacings were significant ($S_0 = 30$ m and 50 m). The containers were made of solid steel, had relatively large diameters ($D_0 = 2$ m and 1.6 m), and were encased in salt. Hardin et al. (2014) used a uniform temperature of 27°C, while Tounsi et al. (2023) used a temperature of 100°C within 30 m of each container and used the undisturbed temperature further away. They also used different material parameters for the salt's behavior. The spliced power-law in Hardin et al. (2014, Figure 7b) predicted a steady-state container velocity of $v \approx -0.95\ \mathrm{m}/10^4\ \mathrm{yr}$, while the combined law in Tounsi et al. (2023, Figure 15b) predicted $v \approx -0.31\ \mathrm{m}/10^4\ \mathrm{yr}$ (Negative velocities indicate container sinking).

Although such detailed studies are useful, one can also estimate WIPP container movement with a simple analytical calculation of v. An analytical form allows one to quickly observe how a different container density, container volume, container spacing, and/or salt viscosity affects the steady-state velocity, provided the following conditions are met. Each condition is followed by a supporting argument.

1. The salt behaves as a Newtonian fluid, in which the engineering shear stress τ is related to the dynamic shear viscosity η and engineering shear strain rate $\dot{\gamma}$ as $\tau = \eta\,\dot{\gamma}$.

    a. Berest et al. (2019) and Lüdeling et al. (2022) demonstrated that salt's behavior at room temperature and low stresses (< 4 MPa) is consistent with a Newtonian fluid. This low stress behavior in salt is often referred to as pressure solution creep. The salt stresses are above 4 MPa as the room closes in around the salt but they should drop below 4 MPa for nearly all the regulatory period when the room contents supply sufficient resistance to balance salt's lithostatic pressure. Tounsi et al. (2023, Figure 16a), for example, reported von Mises stresses no higher than 0.024 MPa after 10^4 years.

2. The containers within a room can be idealized as an infinitely long waste cylinder of diameter D and density ρ_{w}.

    a. Although this condition is only loosely satisfied, it is conservative. Reedlunn et al. (2025, Figure 2-7) showed that, in the first 200 years after waste emplacement, the room closes before the fluid pressure can build to substantial values. This means the containers are tightly compacted together, such that it is reasonable to assume they remain bonded together as the container cluster moves through the salt during the remainder of the 10^4-year regulatory period. It is possible that the containers could disaggregate as they move through the salt, but this would increase the total drag force, so it is conservative to assume they remain bonded. Similarly, the compacted container cluster in Figure SCR-13 more closely resembles a flat plate than a cylinder, but a cylinder has less drag per unit length than a flat plate (Leith [1987, Figure 6]), so a cylinder is used herein. Finally, the disposal rooms at the WIPP are far from infinitely long, but it is conservative to make the waste cylinders infinitely long. Long and slender bodies fall faster through highly viscous media than short bodies because the weight and buoyancy scale linearly with length, while the drag force scales sub-linearly with length (Batchelor [1970]).

3. The Reynolds number is smaller than unity.

    a. The Reynolds number is defined as $Re = \rho_{\mathrm{s}}\, v\, D\, /\, \eta$, where $\rho_{\mathrm{s}} = 2170\ \mathrm{kg/m^3}$ is the density of salt. The velocity v is expected to be very small, and η is very large, so $Re \ll 1$.

4. The waste cylinder movement, as it speeds up to reach steady-state velocity, is negligible compared to the motion during the thousands of years at steady-state velocity, or negligible compared to thickness of the salt formation.

    a. Hardin et al. (2014) and Tounsi et al. (2023) found that one of these two cases held when they included pressure solution creep in their numerical simulations.

5. The salt is spatially uniform.

    a. Although the Salado is not spatially uniform, it is conservative to ignore anhydrite strata that would serve to slow down or halt waste cylinder movement, and a conservatively small viscosity η is utilized below to roughly incorporate strata-to-strata variations in salt creep rates. The small amount of localized heating due to exothermic reactions and radioactive decay (see Section SCR-6.3.4.1), is again considered negligible.

6. The interactions between the viscous flow fields in the infinite array sufficiently capture the more complex interactions at the WIPP.

    a. The WIPP repository is a lattice of drifts, so it is appropriate to include interactions between the viscous flow fields. Although the two-dimensional infinite array cannot capture the true three-dimensional interactions at the WIPP, the two-dimensional simplification is conservative. Cross-drifts running in the x-direction in Figure SCR-11 would create a grid for the salt to flow through, which would increase the drag on each cylinder. In addition, the spacing between neighboring drifts spatially varies within the repository, yet a given infinite array can only have one waste cylinder spacing S_0. The analysis below, therefore, varies S_0 to visualize the sensitivity.

Under the conditions above, one can use the relations in Tamada and Fujikawa (1957, Equations 6, 12, 17a, 18) to compute the drag force per unit length on each waste cylinder as

$$f_{\mathrm{d}} = \frac{8\,\pi\,\eta\,v}{1 - 2\ln(\pi\,D/S_0) + (\pi\,D/S_0)^2/6} \qquad \text{(SCR.22)}$$

where fourth and higher order terms of $\pi\,D/S_0$ have been neglected. A simple force balance between the drag, buoyancy, and gravitational forces yields the following expression for the steady-state velocity:

$$v = \frac{g\,(\rho_s - \rho_w)\,D^2}{32\,\eta}\left[1 - 2\ln(\pi\,D/S_0) + (\pi\,D/S_0)^2/6\right] \qquad \text{(SCR.23)}$$

where $g = 9.79\ \mathrm{m/s^2}$ is the acceleration due to gravity after adjustment to account for the latitude and elevation at the WIPP repository (32.37° and 381 m) (Hofmann-Wellenhof and Moritz [2006, Equations 2-146 and 3-26]).

The analytical expression in Equation SCR.23 appears to be consistent with the numerical results in Hardin et al. (2014) and Tounsi et al. (2023). For the scenario in Hardin et al. (2014)[o], Equation SCR.23 gives $v = -0.93\ \mathrm{m}/10^4\ \mathrm{yr}$, which underpredicts their numerical result by only 0.98X. Equation SCR.23 is not directly applicable to the scenario in Tounsi et al. (2023) because they used a spatially varying temperature field. If, however, one uses a single value of η, corresponding to 100°C, in the Tounsi et al. (2023) scenario, then Equation SCR.23 gives $v = -0.32\ \mathrm{m}/10^4\ \mathrm{yr}$, which overpredicts their numerical result by only 1.03X.

To estimate waste cylinder movements with Equation SCR.23, one must select a value for η, but the dynamic viscosity is a difficult quantity to precisely measure for a variety of reasons (Berest et al. [2019] and Lüdeling et al. [2022]). Nevertheless, Berest et al. (2019, Section 7), Lüdeling et al. (2022, Figure 1), and Tounsi et al. (2023, Eqn. 7, Table 1, New Calibration) independently analyzed[p] a similar set of experiments on natural rock salt and obtained $\eta \approx 10^{17}\ \mathrm{Pa \cdot s}$ at a temperature of 300 K. To roughly bound the uncertainty in η, Tounsi et al. (2023, Figure 18) reduced the Lux-Wolters-Lerche model's pressure solution viscosity by 10X. The analysis herein, therefore, adopts the same 10X reduction and utilizes $\eta = 10^{16}\ \mathrm{Pa \cdot s}$ as a conservative lower bound.

Three steady-state velocity scenarios are now considered: a nominal scenario, a lower bound, and an upper bound. All three scenarios employ the homogenization discussed in Vignes (2023, Section 2.2.2), where the undeformed containers within an infinitely long disposal room are assembled into an infinitely long waste block of width $W_{\mathrm{x0}} = 7.35\ \mathrm{m}$ and height $W_{\mathrm{z0}} = 2.676\ \mathrm{m}$. This block has an undeformed cross-sectional area of $A_0 = W_{\mathrm{x0}}\ W_{\mathrm{z0}}$, which is converted into a waste cylinder with undeformed diameter $D_0 = \sqrt{4\ A_0/\pi} = 5.00\ \mathrm{m}$. The details of the three scenarios are as follows:

1. The nominal scenario considers one of the most common containers at the WIPP, a standard 55-gallon drum filled with a typical composition of contaminated debris. After compaction within a disposal room, the cross-sectional area of the waste block becomes $A = 4.82\ \mathrm{m}^2$ (Vignes et al. [2023, Figure 3-3]). The typical initial density of one of these containers is $\rho_{\mathrm{w0}} = 505.5\ \mathrm{kg/m}^3$(Jensen et al. [2023, Table 2-3]), so the compacted density is $\rho_{\mathrm{w}} = \rho_{\mathrm{w0}}\ A_0\ /\ A = 2062\ \mathrm{kg/m}^3$. Insertion of these values into Equation SCR.23 yields the v_{nom} curve in Figure SCR-12.

2. The lower bound scenario considers the possibility of extremely strong and dense containers. The waste cylinder is, therefore, made rigid ($D_0 = D = 5.00\ m$) and

[o] Hardin et al. (2014, Sections 2.2, 3.1, and 3.4) mentions both $\eta = 1.6 \times 10^{16}\ Pa \cdot s$ and $1 \times 10^{16}\ Pa \cdot s$, but it is not clear which value they used in their spliced power-law container movement simulation. The latter value of $\eta = 1 \times 10^{16}\ Pa \cdot s$ was used herein in Equation SCR.23.

[p] Berest et al. (2019), Lüdeling et al. (2022), and Tounsi et al. (2023) used a pressure solution strain rate of the form $\dot{\varepsilon} = \sigma/c$, where $\dot{\varepsilon}$ was the equivalent (axial) strain rate, σ was the equivalent (axial) stress, and $c \approx 3.0 \times 10^{17}\ \mathrm{Pa \cdot s}$, while this analysis requires a pressure solution strain rate of the form $\dot{\gamma} = \tau/\eta$. Recognizing that $\sigma = 2\tau$ and $\dot{\varepsilon} = 2\ \dot{\gamma}/3$ under isochoric axisymmetric compression allows one to compute the dynamic shear viscosity as $\eta = c/3 = 1.0 \times 10^{17}\ \mathrm{Pa \cdot s}$.

assigned the density of solid carbon steel ($\rho_{w0} = \rho_w = 7850\ \mathrm{kg/m^3}$). Insertion of these values into Equation SCR.23 yields the v_{lo} curve in Figure SCR-12.

3. The upper bound scenario considers the possibility of extremely strong and light containers. The waste cylinder is again made rigid ($D_0 = D = 5.00\ m$), yet made empty ($\rho_{w0} = \rho_w = 0\ \mathrm{kg/m^3}$). Insertion of these values into Equation SCR.23 yields v_{hi} curve in Figure SCR-12.

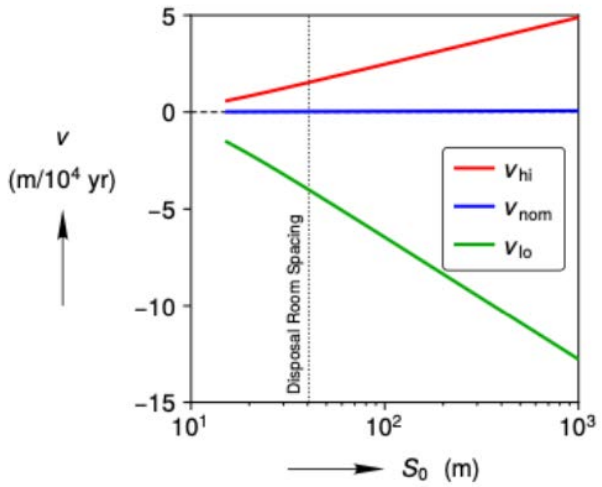

Figure SCR-12 Waste cylinder movement velocities as a function of cylinder spacing for the lower bound, nominal, and upper bound scenarios.

The waste cylinder velocities from each of the three scenarios are compared over a range of S_0 values in Figure SCR-12. The velocity v_{nom} is virtually zero because the density contrast between the compacted waste and the salt is nearly zero ($\rho_s - \rho_w \approx 0$). The velocities v_{lo} and v_{hi} are more significant because the waste cylinder diameter is larger and the density contrasts are larger. As one might expect from the magnitude of the density contrasts, v_{lo} is the largest magnitude velocity at a given S_0.

Figure SCR-12 also shows the impact of the interactions between neighboring cylinders. The three v versus $\log_{10}(S_0)$ curves are virtually straight because the $2\ln(\pi\ D/S_0)$ term in Equation SCR.23 dominates. This logarithmic decay means the waste movement is not highly sensitive to the waste cylinder spacing. Considering this mild sensitivity and all the other conservatisms embedded in Equation SCR.23, it seems appropriate to adopt the spacing between the disposal rooms within a waste panel $S_0 = 40.54\ \mathrm{m}$ for further analysis.

At $S_0 = 40.54\ \mathrm{m}$, the waste velocity is expected to be $-4.00\ \mathrm{m/10^4\ yr} \leq v \leq 1.53\ \mathrm{m/10^4\ yr}$. Any velocity within this range is negligible compared to the roughly 206 m and 243 m distances to the respective bottom and top of the Salado Formation. Therefore, movement of waste containers has been eliminated from PA calculations based on low consequence to the performance of the disposal system.

SCR-6.3.5.3 **FEP Number: W35**
FEP Title: Mechanical Effects of Backfill

SCR-6.3.5.3.1 Screening Decision: SO-C

The *Mechanical Effects of Backfill* have been eliminated from PA calculations on the basis of low consequence to the performance of the disposal system.

SCR-6.3.5.3.2 Summary of New Information

Discussion in FEP W35 *Mechanical Effects of Backfill* has been updated to include the development of a new porosity response surface for evaluating the influence of disposal room closure from salt creep on two phase brine and gas flow in and about the disposal area for CRA-2026 (Vignes et al. 2023). The new information does not change the decision for this FEP.

SCR-6.3.5.3.3 Screening Argument

The MgO backfill is granular and, thus, cannot prop up the room during initial room closure from salt creep. Rather, it is expected that the grains of MgO will sift into the voids between containers because the volume of MgO emplaced is of the same order of magnitude as estimates of the initial space available between containers. Thus, MgO has little or no impact on the porosity predictions in the first ~125 years. After substantial closure in ~125 years, MgO will also have a minor role for two reasons: (1) when no gas is generated, the room porosity is small regardless of whether one included the MgO because a large volume of salt creeps into the room, which has practically zero porosity; and (2) when the maximum amount of gas is generated, the solid volume of MgO is so small in comparison to the large gas-filled volume in the room. Furthermore, the volume of MgO emplaced in individual panels of the disposal area has continued to decrease from CCA-1996 to CRA-2026. Therefore, the mechanical effects of the MgO are omitted in the room porosity simulations. Further background on the justification for omitting the MgO are as follows.

SCR-6.3.5.3.3.1 Room Porosity Simulations

Closure of a disposal room mined 650 m underground in the Salado Formation occurs naturally as the viscoplastic halite responds to deviatoric stresses caused by ~14.7 MPa lithostatic pressure on the excavated room (included FEP W20 *Salt Creep*) (Vignes et al. 2023). Countering this lithostatic pressure are (a) mechanical strength of the various containers and waste as it compacts (included FEP W32 *Consolidation of Waste*) (b) gas pressures produced as the iron contents of the containers and waste anoxically corrode to produce hydrogen gas (as described in included FEP W49 *Gases from Metal Corrosion*), (c) gas pressures produced as the organic material in the containers and waste microbial degraded to produce CO2, which is sequestered by MgO, and hydrogen sulfide (as described in included FEP W44 *Degradation of Organic Material*), and (d) gas pressures from brine radiolysis (as described in included FEP W52 *Radiolysis of Brine*—Day 2019b). In turn, the change in room volume influences the brine and gas flow in and about the repository excavations, which also counteracts the lithostatic pressure (as described in included FEP W40 *Brine Inflow*).

To represent the phenomena resisting the room closure from salt creep, a porosity response function ϕ_{room}^{matrix} is developed. The ϕ_{room}^{matrix} represents the change is porosity of the initial volume of a disposal room as a function of the mass of gas present and elapsed time since the repository closed (Vignes et al. 2023; Stone 1997). In turn, the mass of gas present is a function of the combined gas generation rate from corrosion of metal, degradation of organic material, and radiolysis of brine $\Gamma_{combine}^{gas}(t,x)$ at time t and grid location x. (i.e., $\phi_{room}^{matrix}\{\Gamma_{combine}^{gas}(t,x)\}$)

The ϕ_{room}^{matrix} represents a Lagrangian room porosity, which is the ratio of the calculated void volume at a specified time to the *initial* volume of the room. The Lagrangian porosity is used because fluid flow simulations do not use a deformed room grid, but rather the initial grid. In contrast, the porosity of the only room contents is a Eulerian porosity, which is the ratio of the calculated void volume to the calculated room volume at a specified time.

When developing ϕ_{room}^{matrix} for CCA-1996 through CRA-2026 (Stone 1997; Vignes et al. 2023), the volume occupied by the MgO backfill is omitted.

SCR-6.3.5.3.3.2 MgO Backfill Volume

The MgO mass emplaced in a disposal room is adjusted for every batch of containers that is disposed. The mass (m_{MgO}) is calculated based on the room mass of cellulose (m_{cell}), rubber (m_{rub}), and plastics (m_{plstc}) in the following manner

$$m_{MgO} = \left(6 f_{MgO}^{safety} \frac{m_{cell}+m_{rub}+1.7 m_{plstc}}{162\ g/mole\ cellulose}\right) \times 40.3\ g/mole\ MgO \qquad \text{(SCR.24)}$$

where f_{MgO}^{safety} is a safety factor. Between 1996 and until 2001, the requirement was to maintain f_{MgO}^{safety} at 1.95. Between 2001and until February 2008, f_{MgO}^{safety} was set at 1.67 (U.S. EPA 2001). After February 2008, f_{MgO}^{safety} is set at 1.2 (Reyes 2008). Equation SCR.24 assumes rubber produces the same amount of CO_2 per unit mass as cellulose, but it uses an equivalence factor of 1.7 for plastic waste in order to assume a one-to-one correspondence between CO_2 produced and 6 carbon atoms in waste cellulose ($C_6H_{10}O_5$) (Wang and Brush 1996b).

Currently, 7 of the original 10 panels are filled and provide sufficient experience on the average mass and volume MgO placed in the rooms of each panel (Table SCR-5). The first panel did not fill all rooms and so the MgO mass is less, but generally the average MgO mass in a room has steadily decreased from Panel 2 to Panel 7 as the safety factor has decreased and less equivalent cellulose is included in the containers. Therefore, any mechanical effects of the MgO backfill have continued to decrease since CCA-1996.

The solid MgO, if it were fully compacted, would occupy an overall average of 108 m^3 per room segment (Table SCR-5). The MgO, however, has 61 % porosity upon emplacement, so it occupies an overall average initial 278 m^3 per room (8% of the initial room volume). This bulk average MgO volume is smaller than the typical error in evaluating waste volume and container

volume. Specifically, for a room segment 3.96-m high, 10.06-m wide, and 91.44-m long with 6804 drums, the inner drum volumes occupy 1470 m^3 or 40.4% of the initial room segment volume (based on 0.216 m^3 inner drum volume—Day 2013). The homogeneous block considered by Stone (1997) and Vignes et al. (2023), when calculating ϕ_{room}^{matrix}, occupies 1728 m^3, based on 0.254 m^3 outer volume to drum rims or 47.4% of initial room segment volume (7% difference). The steel in the drum is ~0.00257 m^3 or 17.5 m^3 in a room segment, thus, the empty space between drums is 240.5 m^3 if all drums were initially placed rim to rim. Hence, the bulk MgO volume emplaced is of the same order of magnitude as estimates of the initial space available between containers (i.e., the average bulk volume of MgO of 278 m^3 can fit within this empty space). Consequently, for the first ~125 years (Vignes et al. 2023, Fig. 3-14), the granular MgO has negligible impact on room closure, because the grains of MgO may easily sift into the voids between containers.

Even after ~125 years during the final compaction, the MgO will still not have much influence. When small amounts of gas are generated (Fig. SCR-13), the Lagrangian porosity is very small because the Lagrangian porosity is the volume average of (1) the compressed waste porosity (with small waste volume because most TRU waste is somewhat compressible), and (2) the practically zero salt porosity (with large volume of salt that creeps into the room) (Vignes et al. 2023, Fig. 3-15).

Specifically, the calculated variation in Lagrangian room porosity φ_{room}^{matrix} at 10,000 years is between 0.038 at f^{gas}=0 and 0.84 at f^{gas}=1, which corresponds to a room segment void volume between 138 m^3 and 3060 m^3 (i.e., 0.84*3642 m^2) (Vignes et al. 2023, Fig. 3-5, Table D-2). When no gas is generated, the Lagrangian porosity will remain small even if the 302.4-m^3 solid volume of the room segment is increased by an average of 36% by adding the 108-m^3 solid volume of MgO (Table SCR-10), because of the large volume of practically zero salt porosity.

Conversely, when large amounts of gas are generated, the Lagrangian porosity is large because the porosity is the volume average of the (1) the small volume of compressed waste porosity, (2) the large empty space as the room inflates (because the host salt geology is somewhat yielding), and (3) an amount of salt with practically zero porosity (Vignes et al. 2023, Fig. 3-6). With moderate amounts of gas generation both the salt porosity and the empty space will dominate over the volume of waste.

Specifically, at the maximum gas generation rate, adding the 108-m^3 average solid MgO volume to the 302.4-m^3 room segment solid volume will conservatively decrease the Lagrangian porosity. However, the decrease will not be much. The 108 m^3 is only 3% of the initial room segment volume (Table SCR-10). Even accounting for the chemical expansion of MgO into brucite (~237 m3) or magnesite (~269 m3), this represents only ~8-9% of the final room segment void volume at maximum gas generation on average (i.e., 269 m^3/ 3060 m^3). With moderate amounts of gas generation both the salt porosity and the empty void space will dominate over the volume of waste.

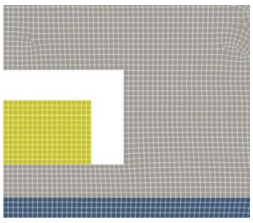

Initial Condition

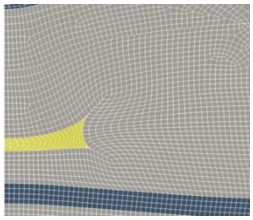

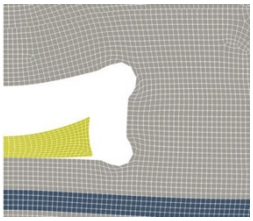

No Gas Generation Maximum Gas Generation

10,000 years

Figure SCR-13. Lagrangian porosity (based on initial room volume) is very small because of practically zero salt porosity that creeps into room when no gas is generated and is very large because of empty volume of expanded room when maximum gas is generated (Vignes et al. 2023, Fig. 3-6).

Table SCR-10. Volumes of MgO in Full and Room Segment (in m^3)

Condition	Average	Maximum	Minimum
Solid MgO Volume[a]	-	-	-
Full Room	196	313	16
Segment[b]	108	173	9
Percent of Initial Room Volume	3%	5%	0.2%
Percent of CCA-1996 Solid Waste Volume[c]	20%	31%	2%
Percent of CRA-2026 Solid Waste Volume[d]	36%	57%	3%
Percent of Final Room Void Volume[e]	4%	6%	0.3%
Bulk MgO Volume[f]	-	-	-
Full Room	503	806	41
Segment[b]	278	446	23
Percent of Initial Room Volume	8%	12%	0.6%

[a] Assumes MgO grain density of 3600 kg/m^3 of overall average, maximum, and minimum of Table SCR-5.
[b] Ratio of full volume to straight segment volume for modeling is 6585m^3/3642 m^3
[c] CCA-1996 solid waste volume in a room segment is 551.2 m^3, based on an initial waste porosity of 0.681 (Vignes et al. 2023, p. 24).
[d] CRA-2026 solid waste volume in a room segment is 302.4 m^3, based on an initial waste porosity of 0.825 (Vignes et al. 2023, p. 24).
[e] CRA-2026 void volume in a room segment is 3060 m^3, based on a Lagrangian porosity of 0.84 when f^{gas} =1 (Vignes et al. 2023).
[f] Assumes MgO initial bulk density of 1400 kg/m^3 of overall average, maximum, and minimum values shown in Table SCR-5.

SCR-6.3.5.3.3.3 Summary

In the first ~125 years, the mechanical effects of the MgO are omitted in porosity surface calculations because the grains of MgO may sift into the voids between containers since the volume of MgO emplaced is of the same order of magnitude as estimates of the initial space available between containers. After substantial closure at ~125 years, the mechanical effects of the MgO are also omitted because the Lagrangian porosity is strongly influenced by the practically zero porosity of the salt creeping into the waste when no gas is generated and the size of the inflated void volume when at the maximum theoretical gas generation, rather than the presence/absence of MgO.

SCR-6.4 Subsurface Hydrological and Fluid Dynamic FEPs

SCR-6.4.1 Repository-Induced Flow

SCR-6.4.1.1 **FEP Numbers: W40 and W41**
FEP Titles: Brine Inflow (W40)
Wicking (W41)

SCR-6.4.1.1.1 Screening Decision: UP

WIPP PA analysis includes two-phase brine/gas flow and capillary behavior (wicking) in the repository and surrounding Salado Formation.

SCR-6.4.1.1.2 Summary of New Information

These FEPs have been updated to include a discussion of repository conditions and to add a summary of implementation in PA.

SCR-6.4.1.1.3 Screening Argument

Several mechanisms for releasing radionuclides from the disposal area are dependent on repository conditions (Appendix PA-4.1, Eq. PA.17). An important aspect of establishing repository conditions is two-phase brine/gas flow in the repository and surrounding Salado Formation. Hence, W40 *Brine Inflow* and W41 *Wicking* are included in PA calculations.

SCR-6.4.1.1.4 FEP Implementation in PA

SCR-6.4.1.1.4.1 Brine Inflow
Two-phase brine/gas flow and capillary behavior process is part of the Repository Fluid Flow conceptual model (U.S. DOE 1996a, Appendix PEER, Section 2.1.1), one of 24 major conceptual models included in PA calculations.[q] The Repository Fluid Flow conceptual model is included in the BRAGFLO Salado Flow model to calculation repository conditions in the WIPP PA (WIPP Performance Assessment 2025).

[q] Other conceptual models related to Repository Fluid Flow include (DOE 1996a, Appendix PEER, Section 2.1.1) (1) Salado: simplification of Salado Formation stratigraphy to impure halite and anhydrite; (2) Impure Halite: conceptualization of Salado Formation layers of pure halite, polyhalite, clay, and minor anhydrite as single impure halite; (3) Salado Interbeds: conceptualization of the transmission of brines through and dilatation/fracture of 3 anhydrite interbeds in Salado Formation; (4) Disturbed Rock Zone: conceptualization of disturbed rock zone as fixed geometry unable to constrain brine and gas flow; (5) Shafts & Shaft Seals: conceptualization of 5 shafts and 1 and simplified seal geometry and permeability; (6) Creep Closure: conceptualization of creep closure as porosity surface; (7) Disposal System Geometry: conceptual of repository as two dimensional; (8) Disposal Room Geometry; (9) Gas Generation: conceptualization of gas generation from (b) anoxic iron corrosion to produce hydrogen gas and consume water, and (b) microbial degradation (but not pressurization); (10) Exploration Boreholes: simplification of intrusion boreholes to one single borehole; (11) Multiple Intrusions: simplified geometry for multiple intrusions into disposal area; and (12) Castile & Brine Reservoir: conceptualization of brine reservoir potentially underlying repository and probability of intersecting the brine reservoir.

The partial differential equation for the conservation of brine flow in and out of computational cells that make up the repository and surrounding Salado Formation, as solved by BRAGFLO, is (Appendix PA-4.2, Eq. PA.19)

$$\nabla\left[\Delta z\rho_{brn}^{dnsty}\frac{k^{perm}k_{brn}^{relative}}{\mu_{brn}^{visco}}(\nabla P_{brn}^{Press}+\rho_{brn}^{dnsty}g\nabla h^{head})\right]+\Delta zq_{brn}^{inject}+\Delta zq_{brn}^{rxn}=\Delta z\frac{\partial(\varphi\rho_{brn}^{dnsty}S_{brn}^{sat})}{\partial t} \quad \text{(SCR.25)}$$

where Δz is the spatial dimension perpendicular to flow; ρ_{brn}^{dnsty} is brine density; k^{perm} is the intrinsic permeability of the numerous materials in and around the disposal area (e.g., Salado halite, disturbed rock zone, TRU waste, panel salt closures, etc.); $k_{brn}^{relative}$ is the relative permeability; μ_{brn}^{visco} is the brine viscosity; P_{brn}^{Press} is the brine pressure variable solved for, g is gravity acceleration; ∇h^{head} is the cell vertical distance relative to center of anhydrite Marker Bed 139; q_{brn}^{inject} is brine injected into or removed from specified cells in repository; q_{brn}^{rxn} is consumption or production of water from chemical reactions in specified computational cells of disposal area (e.g., magnesium-oxide hydration or carbonization of magnesium hydroxide); ϕ is material porosity, and S_{brn}^{sat} is brine saturation.

Pressurization of the repository through gas generation (evaluated through the partial differential equation for conservation of gas—Appendix PA-4.2, Eq. PA.18) can limit the amount of brine that flows into the rooms and drifts. The influence of gas pressure P_{gas}^{press} on Eq. SCR.25 is through a saturation constraint: $S_{brn}^{sat}+S_{gas}^{sat}=1$ where S_{gas}^{sat} is gas saturation.

SCR-6.4.1.1.4.2 Wicking

Capillary behavior (or wicking) is the ability to move brine by capillary forces. Wicking is also incorporated into the Repository Fluid Flow conceptual model implemented in BRAGLO (WIPP Performance Assessment 2025). Capillary pressure enters Eq. SCR.25 through a constraint between gas and brine pressure, P_{gas}^{press} and P_{brn}^{press} (Eq. SCR.26) and is expressed by the Brooks-Corey model (Eq. SCR.27):

$$P_{cap}^{press}=P_{gas}^{press}-P_{brn}^{press} \quad \text{(SCR.26)}$$

$$=B_{cap}^{Brooks}(\lambda^{pore},P_{cap}^{threshold},S_{brn}^{sat},S_{brn}^{rsdual},S_{gas}^{rsdual}) \quad \text{(SCR.27)}$$

where B_{cap}^{Brooks} in Eq. SCR.26 is the Brooks-Corey model for capillary pressure (Appendix PA -4.2, Eq. PA.36); λ^{pore} is the material pore distribution, $P_{cap}^{threshold}$ is the capillary threshold pressure; S_{brn}^{rsdual} is the residual brine saturation; and S_{gas}^{rsdual} is the residual gas saturation.

Capillary behavior is also included when evaluating geochemical reaction rates in the disposal area (i.e., iron corrosion and microbial degradation). Specifically, an effective saturation (S_{brn}^{eff}) in each grid block of the disposal area is used that is greater than S_{brn}^{sat} calculated by BRAGFLO (Appendix PA-4.2; Appendix PA -4.2.7, Eq. PA.57)

$$S_{brn}^{eff} = \begin{cases} S_{brn}^{sat} - S_{brn}^{min} + S_{brn}^{wick}\left(1 - \exp\left(200\alpha\left(MAX\left[S_{brn}^{sat} - S_{brn}^{min}, 0\right]\right)^2\right)\right) if\ 0 < S_{brn}^{sat} \leq 1 - S_{brn}^{wick} + S_{brn}^{min} \\ 0\ if\ S_{brn}^{sat} \leq S_{brn}^{min} \\ 1\ if\ S_{brn}^{sat} > 1 - S_{brn}^{wick} + S_{brn}^{min} \end{cases} \quad \text{(SCR.28)}$$

where the new parameters introduced in Eq. SCR.28 are S_{brn}^{min}, which is a minimum saturation to prevent numerical problems; S_{brn}^{wick}, which is the added but uncertain wicking saturation; and the exponential term is a smoothing function with parameter α.

SCR-6.4.2 Effects of Gas Generation

SCR-6.4.2.1 **FEP Number: W42**
FEP Title: Fluid Flow Due to Gas Production

SCR-6.4.2.1.1 Screening Decision: UP

Fluid Flow Due to Gas Production in the repository and the Salado is accounted for in PA.

SCR-6.4.2.1.2 Summary of New Information

As discussed in FEP W52 (Section SCR-6.5.1.7) radiolysis of brine from dissolved, colloidal, and wetted solid radionuclides is modeled in the PA calculations (Day 2019b). During the EPA review of the CRA-2019, the EPA questioned if radiolysis of adsorbed water on non-wetted solid radionuclides should also be accounted for (U.S. EPA 2022c). King et al. (2023) argued the gas generation from adsorbed water on non-wetted solids would have minimal impact and can be ignored in the PA calculations.

As discussed in FEP W49 (Section SCR-6.5.1.5) the calculation of iron-based metal surface area has been updated (Hansen et al. 2023). No changes are necessary to this FEP. It remains classified UP.

SCR-6.4.2.1.3 Screening Argument

Pressurization of the repository through gas generation could limit the amount of brine that flows into the rooms and drifts. Gas may flow from the repository through the DRZ, impure halite, anhydrite layers, or clay layers. The amount of water available for reactions and microbial activity will impact the amounts and types of gases produced (W44 through W55, Section SCR-6.5.1.1, Section SCR-6.5.1.2, Section SCR-6.5.1.3, Section SCR-6.5.1.4, Section SCR-6.5.1.5, Section SCR-6.5.1.6, Section SCR-6.5.1.7, Section SCR-6.5.1.8, Section SCR-6.5.1.9 and Section SCR-6.5.1.10). Updates to the probability of intercepting pressurized brine may increase brine availability in the repository to aid these reactions. Gas generation rates, and therefore repository pressure, may change as the water content of the repository changes. Pressure changes and fluid flow due to gas production in the repository and the Salado are accounted for in PA through modeling the two-phase flow (Appendix PA-2026, Section PA-4.2).

SCR-6.4.2.1.4 FEP Implementation in PA

FEP W42 *Fluid Flow Due to Gas Production*, which is an UP FEP, is associated with the Gas Generation and Repository Fluid Flow conceptual models. These conceptual models are implemented in the PA code BRAGFLO for the Salado Flow computation in the PA calculation (Appendix PA-4.2).

SCR-6.4.3 Thermal Effects

SCR-6.4.3.1 **FEP Number: W43**
FEP Title: Convection

SCR-6.4.3.1.1 Screening Decision: SO-C

Convection has been eliminated from PA calculations on the basis of low consequence to the performance of the disposal system.

SCR-6.4.3.1.2 Summary of New Information

FEP W43 *Convection* has been updated with new estimates of heat produced from inventory data for CRA-2026 (Van Soest 2025; Kicker 2025). The screening argument and decision for this FEP is unchanged by the inventory update.

SCR-6.4.3.1.3 Related FEPs

Convection depends upon temperature gradients; which, in turn, depends upon heat producing reactions discussed in W13 *Heat from Radioactive Decay* (Section SCR-6.2.1.2); and W72 *Exothermic Reactions* (including MgO hydration, MgO carbonation, microbial degradation, and aluminum corrosion) and W73 *Concrete Hydration* (Section SCR-6.3.4). These two FEPs have been excluded because of low consequence. An additional FEP, W14 *Nuclear Criticality Heat* (Section SCR-6.2.1.3), has been excluded because of low probability.

SCR-6.4.3.1.4 Screening Argument

Temperature gradients in the disposal rooms could initiate convection in brine and contribute to contaminant transport. Thermal gradients in the disposal rooms could potentially drive the movement of water vapor. For example, temperature increases around waste located at the edges of the rooms could cause evaporation of water entering from the DRZ. This water vapor could condense on cooler waste containers in the rooms and could contribute to iron corrosion and, thus, gas generation. However, heat producing reactions in the disposal area only produce small temperature increases. Therefore, temperature gradients in the WIPP repository are small such that convection will not contribute to contaminant transport or gas generation. Consequently, FEP W43 *Convection* has been excluded because of low consequence to the performance of the disposal system, as elaborated below.

SCR-6.4.3.1.4.1 Rayleigh-Darcy Number for Porous Media

The potential significance of thermal convection in a porous media can be determined from the Rayleigh-Darcy number (Hicks 1996; de Marsily 1986, p. 283):

$$\Re a_{fluid}^{pore} = \frac{k_{pore}^{perm}\alpha_{fluid}^{expand} cp_{fluid}^{heat}\rho_{fluid}^{2} g L^{char}}{\kappa_{pore}^{conduct}\mu_{fluid}^{viscosity}}\Delta T \qquad \text{(SCR.29)}$$

Where k_{pore}^{perm} is intrinsic permeability of porous medium (10^{-13} m^2 for waste and $10^{-19.4}$< k_{pore}^{perm}<$10^{-12.4}$ m^2 for disturbed rock zone); α_{fluid}^{expand} is fluid coefficient of thermal expansion (2.07×10^{-4} K^{-1} for water and 3×10^{-4} K^{-1} for air); cp_{fluid}^{heat} is fluid specific heat capacity at constant pressure (4×10^{3} J/kg-K for brine and 0.7×10^{3} J/kg-K for gas); ρ_{fluid} is fluid density (1.23×10^{3} kg/m^3 for Salado brine and 1 kg/m^3 for air); g is acceleration due to gravity (9.8 m/s^2); L^{char} is a characteristic length over which thermal convection acts (here assumed to be width of disposal room—10 m); $\kappa_{pore}^{conduct}$ is thermal conductivity of halite porous medium (5 W/m-K); $\mu_{fluid}^{viscosity}$ is fluid viscosity (1.8×10^{-3} Pa-s for Salado brine; 9.2×10^{-3} Pa-s for H_2 gas) and ΔT is change in temperature.

SCR-6.4.3.1.4.2 Rayleigh-Darcy Number in DRZ

Radioactive decay and exothermic reactions are two possible sources of heat in the WIPP repository. As discussed in FEP W13 *Heat from Radioactive Decay*, temperature increases of about 3 °C (5.4 °F) may occur on the surface of RH-TRU containers over 100 to 300 years. Temperature increases resulting from exothermic reactions are discussed in FEP W72 *Exothermic Reactions*. Temperature increase resulting from cement hydration is discussed in FEP W73 *Cement Hydration*. The maximum temperature rise in the disposal panels due to exothermic reactions and cement hydration, conservatively assuming all sources contribute simultaneously, will be less than 11.2 °C (20 °F) Thus, a combined increase of 14.2 °C from radioactive decay, exothermic reactions, and cement hydration is conservatively bounded by a 20 °C temperature increase used here.

For a temperature increase of 20 °C and the highest DRZ permeability of $10^{-12.5}$ m^2, the Rayleigh-Darcy number is much less than unity for both the brine and gas phase (i.e., $\Re a_{brine}^{pore}$ is ~10^{-1} and $\Re a_{air}^{pore}$ is ~4×10^{-5}). When the $\Re a_{fluid}^{pore}$ is less than unity, heat transfer is solely by conduction (Hicks 1996; de Marsily 1986, p. 283). Consequently, temperature gradients in the disposal system will not cause significant thermal convection in brine or gas in the porous media of the closed repository. Therefore, FEP W43 *Convection* has been excluded because of low consequence to the performance of the WIPP disposal system.

SCR-6.5 Geochemical and Chemical FEPs

SCR-6.5.1 Gas Generation

SCR-6.5.1.1 **FEP Number: W44**
FEP Title: Degradation of Organic Material

SCR-6.5.1.1.1 Screening Decision: UP

Microbial degradation of cellulosic material, and possibly plastics and rubber may produce carbon dioxide and hydrogen sulfide, and minor amounts of nitrogen (N_2). Hence, microbial gas generation from W44 *Degradation of Organic Material* is included in PA calculations.

SCR-6.5.1.1.2 Summary of New Information

The most recent inventory of potential reactants for CRA-2026 is indirectly used in the screening argument (Van Soest 2025; Kicker 2025). The new information does not change the decision for FEP W44 *Degradation of Organic Material.* In the CRA-2019, FEP W44 *Degradation of Organic Material*, was screened jointly with FEPs W45 and W48. It is now screened separately.

SCR-6.5.1.1.3 Related FEPs

FEP W49 *Gases for Metal Corrosion* is directly related to FEP W44 *Degradation of Organic Material.* Also, FEPs W45 *Effects of Temperature on Microbial Gas Generation, W46 Effects of Pressure on Microbial Gas Generation,* W47 *Effects of Radiation on Microbial Gas Generation,* and W48 *Effects of Biofilm Formation on Microbial Gas Generation* are considered in defining the uncertainty in the gas generation rates used.

SCR-6.5.1.1.4 Screening Argument

Microbial gas generation from W44 *Degradation of Organic Material* is included in PA calculations because of the ubiquitous presence of microbial communities throughout nature. However, microbial activity and subsequent gas production will be severely constrained under WIPP conditions as more fully described in Appendix SOTERM-4.0 and Swanson and Reed (2018) (and referred to FEPs W45 *Effects of Temperature on Microbial Gas Generation, W46 Effects of Pressure on Microbial Gas Generation,* W47 *Effects of Radiation on Microbial Gas Generation,* and W48 *Effects of Biofilm Formation on Microbial Gas Generation*). The severe conditions include high ionic strength brine, low water activity, high concentrations of magnesium and calcium (chaotropicity), anoxic conditions, high pH, radioactivity, lack of nutrients, and lack of suitable substrates.

The conceivable microbial degradation of cellulosic material, and possibly plastics and rubber, has been narrowed to production of carbon dioxide (CO_2) and hydrogen sulfide (H_2S), through

sulfate reduction (FEP W72 *Exothermic Reactions*), and minor amounts of nitrogen (N_2), through denitrification (Wang and Brush 1996a).

SCR-6.5.1.1.5 FEP Implementation in PA

The implementation of microbial gas generation from FEP W44 *Degradation of Organic Material* is part of the Gas Generation Conceptual Model and implemented in PA calculations by the BRAGFLO code (WIPP Performance Assessment 2025). The portion of the Gas Generation Conceptual Model related to microbial gas generation is described below.

SCR-6.5.1.1.5.1 Conceptual Model of Microbial Gas Generation

The PA calculation includes production of H_2O and the gases CO_2, H_2S, N_2 from microbes degrading cellulose ($C_6H_{10}O_5$), based on the following sequence of two reactions (Appendix GEOCHEM-2.1.5):[r]

$$\text{Denitrification } C_6H_{10}O_5 + 4.8HNO_3 \rightarrow 7.4H_2O + 6CO_2 + 2.4N_2 \quad \text{(SCR.30)}$$

$$\text{Sulfate reduction } C_6H_{10}O_5 + 3H_2SO_4 \rightarrow 5H_2O + 6CO_2 + 3H_2S \quad \text{(SCR.31)}$$

Denitrification will be minor because of low nitrate levels in the waste, the only source of nitrate. Sulfate reduction will dominate as abundant sulfate is available from the Salado (Appendix GEOCHEM-2019, Section GEOCHEM-2.1.5).

The PA calculation implements these reactions as an average stoichiometry model:

$$\frac{1}{6}C_6H_{10}O_5 + \text{microbes} \rightarrow \mathrm{X}_{H_2}^{micro}\ \text{moles}\ \mathrm{H_2}\ \text{gas} + \mathrm{X}_{water}^{micro}\ \text{moles}\ \mathrm{H_2}O \quad \text{(SCR.32)}$$

where the reaction rates are not dependent upon the concentration of the reactants and products (zero-order reaction rate). The stoichiometric parameters $\mathrm{X}_{H_2}^{micro}$ and $\mathrm{X}_{water}^{micro}$ are solved from Eq. SCR.30 and Eq. SCR.31 (further assuming all CO_2 gas reacts with the MgO backfill and, thus, does not contribute to gas generation):

$$X_{H_2}^{micro} = \frac{2.4}{6} f_{NO_3}^{carbon} + \frac{3}{6}(1 - f_{NO_3}^{carbon}) \quad \text{(SCR.33)}$$

where $f_{NO_3}^{carbon}$ is the fraction of carbon consumed by denitrification and $1 - f_{NO_3}^{carbon}$ is the fraction of carbon consumed by sulfate reduction. The microbial reaction stops when the carbon in the cellulose is consumed, as defined by the inventory for CRA-2026 (Van Soest 2025; Kicker 2025).

Brine must also be available. Specifically, the microbial gas generations rates are dependent upon the portion of the disposal area that is saturated, partially saturated (humid conditions), or below a saturation threshold (S_{brn}^{min}) after which the microbial (and corrosion) reaction ceases. The microbial gas generation rate, $\Gamma_{microb}^{gas}(t, x)$, is expressed as

[r] In CCA-1996, Wang (1996a) assumed microbial degradation of cellulose occurred by methanogenesis. However, methanogenesis does not occur in highly saline solutions and, thus, has not been included since CRA-2009 (U.S. DOE 2009, Appendix SOTERM-2009, Section SOTERM-4.2)

$$\Gamma_{microb}^{gas}(t,x) = \begin{cases} [r_{sat}^{microb} S_{brn}^{eff}(t,x) + r_{humid}^{microb}(1 - S_{brn}^{eff}(t,x)] \frac{m_{cell}^{equiv}}{V_{room}} X_{H_2}^{microb} M_{H_2}^{weight} & \text{if } S_{brn}^{eff}(t,x) > 0 \\ 0 & \text{if } S_{brn}^{eff}(t,x) = 0 \end{cases} \quad \text{(SCR.34)}$$

where V_{room} is the volume of a room in the disposal area (3644 m^3), and $M_{H_2}^{weight}$ is the molecular weight of H_2 (2.02 ×10^{-3} kg/mol). Only H_2 gas in assumed in the repository to simplify computations since much more H_2 is produced from anoxic corrosion of iron and iron alloys (as described in FEP W49 *Gases from Metal Corrosion*) than microbial gases.

The $S_{brn}^{eff}(t,x)$of Eq. SCR-33 is the effective brine saturation at time *t* and grid location *x* in the disposal area. The $S_{brn}^{eff}(t,x)$is an adjustment to the brine saturation, $S_{brn}^{sat}(t,x)$, calculated by Repository Fluid Flow conceptual model implemented by BRAGLO (WIPP Performance Assessment 2025), in order to include capillary action in the waste materials, S_{brn}^{wick}, and define a minimum saturation threshold, S_{brn}^{min}, as described in FEPs W40 *Brine Inflow* and W41 *Wicking.*

The $m_{cell}^{equiv}$of Eq. SCR-33 is the equivalent mass of cellulose in the disposal area. For CRA-2009 and afterwards (U.S. DOE, 2009, Appendix PA Section PA-2.1.1), the probability that only cellulose degradation occurs in the repository has been set to 0.75.[s] For 25% of the time (when rubber and plastic biodegradation occurs in addition to cellulose degradation), the mass inventory of rubber (m_{rub}) is added to the mass of cellulose (m_{cell}) (as provided by Van Soest 2025; Kicker 2025). The mass of plastic (m_{plstc}) is converted to an equivalent amount of cellulose through an equivalence factor of 1.7 (Wang and Brush 1996a):

$$m\frac{equiv}{cell} = \begin{cases} m_{cell} & \text{if } \wp > 0.25 \\ m_{cell} + m_{rub} + 1.7 m_{plstc} & \text{if } \wp \leq 0.25 \end{cases} \quad \text{(SCR.35)}$$

where in Eq. SCR.35, $\wp$is a sampled uncertain probability parameter between 0 and 1.

The $r_{sat}^{micro}$of Eq. SCR.34 is the sampled uncertain microbial gas generation rate under fully saturated conditions and$r_{humid}^{micro}$is the sampled uncertain microbial gas generation rate under humid conditions. The uncertainty range in $r_{sat}^{micro}$and r_{humid}^{micro}implicitly incorporate the uncertainty described in FEPs W45 *Effects of Temperature on Microbial Gas Generation,* W46 *Effects of Pressure on Microbial Gas Generation,* W47 *Effects of Radiation on Microbial Gas Generation,* and W48 *Effects of Biofilm Formation on Microbial Gas Generation.*

SCR-6.5.1.2 **FEP Numbers: W45, and W48**
FEP Titles: Effects of Temperature on Microbial Gas Generation (W45)

[s] In CCA-1996, the PA calculations assumed microbial degradation of cellulose occurred in only half of the simulations because of the uncertainty in the viability of microbial colonies. In half of the simulations with microbial degradation, the PA calculations assumed plastic and rubber was not degraded (U.S. DOE 1996a, App. MASS, Section MASS.8).

Effects of Biofilms on Microbial Gas Generation (W48)

SCR-6.5.1.2.1 Screening Decision: UP

The *Effects of Temperature on Microbial Gas Generation* and the *Effects of Biofilm Formation on Microbial Gas Generation* are included PA calculations through microbial gas generation rate parameters.

SCR-6.5.1.2.2 Summary of New Information

In the CRA-2019, FEP W44 *Degradation of Organic Material*, was screened jointly with FEPs W45 and W48. It is now screened separately (see Section SCR-6.5.1.1). Screening arguments for FEPs W45 *Effects of Temperature on Microbial Gas Generation*, and W48 *Effects of Biofilms on Microbial Gas Generation* have been updated with new thermal increase calculations based on the updated waste inventory data used for CRA-2026 PA calculations (Van Soest 2025; Kicker 2025). Finally, as with all screened-in FEPs, a summary of the implementation of these FEPs has been provided.

SCR-6.5.1.2.3 Screening Argument

Microbial breakdown of cellulosic material, and possibly plastics and other organic materials, will produce mainly carbon dioxide (CO_2) hydrogen sulfide (H_2S), and minor amounts of nitrogen (N_2). The rate of microbial gas production will depend upon the nature of the microbial populations established, the prevailing conditions, and the substrates present. Microbial gas generation from degradation of organic material is accounted for in PA, as described in FEP W44 *Degradation of Organic Material*.

The following subsections discuss the effects of temperature and biofilms on microbial gas production rate parameters.

SCR-6.5.1.2.4 Effects of Temperature on Microbial Gas Generation

The effects of temperature on microbial gas generation are implicitly incorporated in the gas generation rates used given the relatively small potential maximum increase in temperature (< 4˚C) predicted and the wide range of conditions used to establish the gas generation rates used in PA (Appendix PA-4.2.5).

For the WIPP, calculations and experimental studies of induced temperatures from chemical reactions within the repository were undertaken and are described in FEPs W72 *Exothermic Reactions* and W73 *Concrete Hydration* (Section SCR-6.3.4.1). Analysis suggest that the maximum temperature increase in the disposal area caused by chemical reactions is likely less than 4 ºC. Furthermore, analysis suggests that the maximum temperature increase in the disposal area caused by radioactive decay of the emplaced waste is likely to be less than 3 °C (5.4 °F) (FEP W13 *Heat from Radioactive Decay*). Both transient exothermic reactions and radioactive decay can occur simultaneously, but the maximums likely will not. However, the

combined temperature increase of 7 °C (12.6 °F) (based on the maximums) above the ambient temperature of 27 °C (80.6 °F) is still small. The small 7 °C (12.6 °F) temperature increase is not likely to have a negative effect on general microbial activity; rather, the effect could have a positive, transient effect on haloarchaeal growth under aerobic conditions.

Relatively few data exist on the effects of temperature on microbial gas generation under expected WIPP conditions. Molecke (Molecke 1979, p. 4) observed an increase in gas production from cellulosic waste under both aerobic and anaerobic conditions when temperatures increased from ambient up to between 40 °C (104 °F) and 50 °C (122 °F). Above 70 °C (158 °F), gas production decreased. Studies by Francis and Gillow (1994) confirmed the gas generation rates reported by Molecke at 30°C (Molecke 1979). The effects of temperature on microbial gas generation are implicitly incorporated in the uncertain microbial gas generation rates under fully saturated and partially saturated, humid conditions used in PA calculations.

SCR-6.5.1.2.5 Effects of Biofilms on Microbial Gas Generation

Biofilms are the predominant lifestyle exhibited by microorganisms in nature. They comprise aggregates (micro-colonies) of cells within a matrix of extracellular polymeric substances that serves as a protective habitat. Biofilms are also ubiquitous in anthropogenic settings; therefore, it is possible that they will be present at the WIPP, if conditions are conducive to microbial growth.

Whether or not biofilms formed during the gas generation experiments conducted for the CCA is unknown. Regardless, their effects are implicitly incorporated into the gas generation rates used in PA calculations, as these rates are based on laboratory measurements that reflect the net outcome of microbial activity under test conditions, including any influence of biofilm formation.

SCR-6.5.1.2.6 FEP Implementation in PA

FEPs W45 *Effects of Temperature on Microbial Gas Generation* and the W48 *Effects of Biofilm Formation on Microbial Gas Generation* are included through the range of uncertainty defined for microbial gas generation rate parameters under fully saturated and partially saturated, humid conditions of the Gas Generation Conceptual Model implemented in PA calculations by the BRAGFLO code (WIPP Performance Assessment 2025).

SCR-6.5.1.3 **FEP Number: W46**
FEP Title: Effects of Pressure on Microbial Gas Generation

SCR-6.5.1.3.1 Screening Decision: SO-C

The *Effects of Pressure on Microbial Gas Generation* has been eliminated from PA calculations on the basis of low consequence to the performance of the disposal system.

SCR-6.5.1.3.2 Summary of New Information

The screening argument for this FEP has been modified to more directly discuss the effects of pressure on gas generation. This updated screening argument does not affect the screening decision for this FEP; it remains SO-C.

SCR-6.5.1.3.3 Screening Argument

High pressures (e.g., 100-200 MPa) can cause changes in cell membrane permeability and morphology and can affect biochemical reactions and gene expression by altering protein conformation (Sehrawat et al. 2021). In turn, this will negatively affect microbial activity and dependent processes, such as gas generation. The projected pressure at the WIPP is 15 MPa, which is well below the effective threshold mentioned above. Pressures as low as 50 MPa can inhibit growth, but lethality is not typically observed until 180 MPa (Lado and Yousef, 2002). Consequently, the effects of pressure on microbial gas generation have been eliminated from PA calculations on the basis of low consequence to the performance of the disposal system.

Furthermore, the low intracellular water activities found in halophile cells from the coping strategies used for osmoregulation also help to stabilize proteins and maintain membrane fluidity under high pressure. Short-term (1 hour) exposure to 400 MPa was not completely lethal in tests with a haloarchaeon (Kish et al. 2012).

The predicted pressure at WIPP is due to H_2 gas production from corrosion processes. The effects of hydrogen specifically and the consumption of H_2 by microorganisms is beyond the scope of this argument, as this FEPS only addresses pressure in general and not hydrogen overpressure.

SCR-6.5.1.4 FEP Number: W47 FEP Title: Effects of Radiation on Microbial Gas Generation

SCR-6.5.1.4.1 Screening Decision: SO-C

The *Effects of Radiation on Microbial Gas Generation* has been eliminated from PA calculations on the basis of low consequence to the performance of the disposal system.

SCR-6.5.1.4.2 Summary of New Information

This screening argument has been rewritten to provide a stronger and more relevant argument. The screening decision has not changed.

SCR-6.5.1.4.3 Screening Argument

Radiation toxicity could lead to cell inhibition and/or death, which could result in decreased gas generation rates. Experiments investigating microbial gas generation rates measured a 70% reduction in CO_2 generation in the presence of ^{239}Pu (Caldwell et al. 1988). Numbers of

microorganisms in ^{239}Pu-contaminated waste were very low (Most Probable Number between 33-9,500/g), and numbers in contaminated soils were between 10^3-10^5, depending on radioactivity and depth (Barnhart et al. 1980). Studies on WIPP-bound waste found no extractable deoxyribonucleic acid (DNA) in waste containing ~760 nanocuries per gram (nCi/g), but both DNA and cultivable organisms were obtained from waste containing less than 500 nCi/g (Swanson et al. 2015). These data point towards deleterious effects of radiation on microbial activities, such as gas generation, to introduced microorganisms.

However, haloarchaea naturally found in hypersaline settings, possess several traits that make them resistant or tolerant to ionizing radiation: carotenoid pigmentation, polyploidy, selection for amino acids less prone to reactive oxygen species (ROS), high intracellular Mn/Fe ratios, redundancy in genes encoding antioxidants, and differential regulation of genes needed for ROS damage repair (Sharma et al. 2012). Additionally, resistance can develop over time in organisms that are able to survive initially (Siasou et al. 2017). Regardless of their tolerance to radiation, the activity of these organisms will be constrained by other factors, such as anoxia.

These opposing effects are not taken into account in the WIPP PA calculations, on the basis of low consequence to the performance of the disposal system.

SCR-6.5.1.5 **FEP Numbers: W49 and W51**
FEP Titles: Gases from Metal Corrosion (W49)
Chemical Effects of Corrosion (W51)

SCR-6.5.1.5.1 Screening Decision: UP

Gas generation from metal corrosion is accounted for in PA, and the effects of chemical changes from metal corrosion are incorporated in the reducing conditions assumed in WIPP models.

SCR-6.5.1.5.2 Summary of New Information

The screening argument has been updated by referencing new inventory information as presented in Van Soest (2025), including the inventory of metals present in the waste and waste containers. During the EPA review of the CRA-2019, the EPA requested calculations of gas generated by lead corrosion and a comparison to gas generated by iron corrosion (U.S. EPA 2020c). The DOE responded with calculations showing that the omission of lead corrosion could be considered conservative with respect to mean total releases (U.S. DOE 2021a).

The EPA also requested an explanation for why the steel surface area per unit volume had not changed for the CRA-2019 despite an increased number of shielded containers (U. S. EPA 2020c). The DOE responded with a reasoned argument that the currently implemented steel surface area continues to overestimate steel surface area in the repository and that PA calculations continue to overestimate gas generation due to iron corrosion (U.S. DOE 2021c).

The EPA also requested clarification on values used for the humid steel corrosion rates (U.S. EPA 2020c). The DOE responded that the correct values were entered into the PA parameter database (PAPDB) and used in CRA-2019 PA calculations (U.S. DOE 2021c).

The calculation of iron surface area used for gas generation has been updated since the CRA-2019 PA. For CRA-2019, the total surface area of iron-based metals for gas generation was calculated based on an estimated iron surface per drum, and an optimal loading of drums in the repository. For CRA-2026, the total iron surface area is calculated with an estimated surface area per kilogram of iron inventory, as outlined in King (2021).

Additional information on FEP implementation in PA has been provided, including conceptual models and related parameters associated with these FEPs. The screening decisions have not changed and these FEPs are represented in PA calculations.

SCR-6.5.1.5.3 Screening Argument

Oxic corrosion of waste drums and metallic waste will occur at early times following closure of the repository and will deplete its oxygen content. Anoxic corrosion will follow the oxic phase and will produce hydrogen while consuming water. Gases from metal corrosion are accounted for in PA.

The predominant chemical effect of corrosion reactions on the environment of disposal rooms will be to establish and maintain reducing conditions in WIPP.

The inventory of metals present in the waste and waste containers has been updated for the CRA-2026 in Van Soest (2025). Of these updated metal quantities, only the steel (iron) inventory plays a role in PA calculations. The steel corrosion rate for humid and inundated conditions has been most recently updated as described in Zeitler (2018a) and Zeitler (2018b).

Molecke (1979, p. 4) summarized gas generation rates that were observed during a range of experiments. The experiments were conducted over a range of temperatures and chemical conditions representing likely states within the repository. Later experiments reported by Telander and Westerman (1993) support the gas generation rate data reported by Molecke (1979). Their experiments investigated gas generation from corrosion under a wide range of possible conditions in the repository. The studies included corrosion of low-carbon steel waste packaging materials in synthetic brines, representative of intergranular Salado brines at the repository horizon, under anoxic (reducing) conditions.

For the CRA-2014 PA, experimental results from Roselle (2013) were used to determine an updated parameter distribution for CORRMCO2, which represents the anoxic steel corrosion rate for brine-inundated steel in the absence of microbially produced CO_2. After the submittal of the CRA-2014, the EPA requested that the DOE reconsider the subset of the Roselle data to be included in the CORRMCO2 distribution (U.S. EPA 2015). As a result, a new, cumulative distribution for CORRMCO2 was developed (Zeitler and Hansen 2015). Later, in their TSD on chemistry-related issues, the EPA recommended an adjustment of the Zeitler and Hansen

(2015) distribution for the CRA-2019 PA via an increase by a factor of two (U.S. EPA 2017d) and the DOE agreed to the adjustment by a factor of two to accommodate the potential for enhanced corrosion at elevated pressures. The resulting cumulative distribution for CORRMCO2 is described in detail in Zeitler (2018b) and was used in the CRA-2019 PA (Appendix PA-2019).

Gas generation from the corrosion of lead in the waste has never proven to be a significant contributor to overall gas quantities (Bryson 2015). The inventory of lead increased significantly for the CRA-2019 compared to earlier inventories (Van Soest 2018). The DOE has also showed that the omission of lead corrosion could be considered conservative with respect to mean total releases (U.S. DOE 2021a). The lead inventory has since decreased from the level analyzed by Kirkes (2019b) and U.S. DOE (2021a) (Van Soest 2025).

The effects of chemical changes from metal corrosion are, therefore, accounted for in PA.

SCR-6.5.1.5.4 FEP Implementation in PA

FEP W49 *Gases from Metal Corrosion*, which is an UP FEP, is associated with the following conceptual model:

- Gas Generation (implemented in BRAGFLO)

Corrosion reactions generate gases. In the Salado Flow calculation by the BRAGFLO code, iron inventory impacts gas generation from iron corrosion, which impacts repository pressure in the UP scenario. Iron corrosion reactions are described in detail in Appendix GEOCHEM.

FEP W51 *Chemical Effects of Corrosion*, which is an UP FEP, is associated with the following conceptual models:

- Chemical Conditions (implemented in EQ3/6)

Corrosion reactions sustain the assumed reducing condition in the repository. The thermodynamic model in EQ3/6 uses steel (iron) inventory as an input via inclusion of iron corrosion byproduct (Domski 2023, Domski 2025). This model is used to parameterize the radionuclide solubilities that are used to calculate the dissolved and colloidal actinide source terms. Actinide mobilization potentials are calculated across time by the PANEL code, which uses the solubility limits and uncertainties established using the thermodynamic model in EQ3/6.

Input related to chemical conditions (i.e., reducing conditions in the repository) is contained in the EQ3/6 thermodynamic database and inventory PAIR data (Van Soest 2025). Parameters related to gas generation due to iron corrosion include the following:

- Surface area per kilogram of iron inventory (King 2021)
- Mass of iron containers, CH and RH wastes (Kicker 2025, Table 29)
- Mass of iron-based material in CH and RH wastes (Kicker 2025, Table 29)

- Inundated corrosion rate for steel (Zeitler 2018b)
- Humid corrosion rate for steel (Zeitler 2018a)
- Inventory of iron and lead per kg brine (Van Soest 2025, Domski 2025)[t]

SCR-6.5.1.6 **FEP Number: W50**
FEP Title: Galvanic Coupling (within the repository)

SCR-6.5.1.6.1 Screening Decision: SO-C

The effects of *Galvanic Coupling* have been eliminated from PA calculations on the basis of low consequence to the performance of the disposal system.

SCR-6.5.1.6.2 Summary of New Information

This FEP screening argument has been updated to include a discussion of lead in the inventory used for the CRA-2026.

SCR-6.5.1.6.3 Screening Argument

Galvanic coupling (i.e., establishing an electrical current through chemical processes) could lead to the propagation of electric potential gradients between metals in the waste form, canisters, and other metals external to the waste form, potentially influencing corrosion processes, gas generation rates, and chemical migration.

Metallic ore bodies external to the repository are nonexistent (see the CCA, Appendix GCR) and therefore galvanic coupling between the waste and metals external to the repository would not occur. However, a variety of metals will be present within the repository as waste metals and containers, creating a potential for formation of galvanic cells over short distances. As an example, the presence of copper could influence rates of hydrogen gas production resulting from the corrosion of iron. The interactions between metals depend upon their physical disposition and the prevailing solution conditions, including pH and salinity.

Galvanic coupling of metallic iron and lead can be represented by reactions including

$$Pb(m,s) + Fe^{2+} = Fe(m,s) + Pb^{2+}, \quad \text{(SCR.36)}$$

where (m,s) denotes metallic solid. The following discussion assumes no passivation of the metals, which would be considered an upper bound assessment of gas generation due to galvanic corrosion.

Iron is a stronger reducer than lead, thus it is unlikely to expect active oxidation of lead in the presence of iron. Therefore, until the depletion of iron or the isolation of iron by passivation, contribution of lead corrosion to gas generation would be inconsequential. Local environments

[t] Note that these are inputs into the EQ3/6 calculations, but do not exist in the PAPDB.

for active and selective corrosion of lead cannot be excluded within the conceptual model but has not been identified.

Consequently, given the preponderance of iron over other metals within the repository and the limited inventory or inactive corrosion of many nonferrous materials including lead, the influence of these electrochemical interactions on corrosion, and therefore on gas generation, is expected to be minimal. Therefore, the effects of galvanic coupling have been eliminated from PA calculations on the basis of low consequence.

SCR-6.5.1.7 **FEP Number: W52**
FEP Title: Radiolysis of Brine (gas effects)

SCR-6.5.1.7.1 Screening Decision: UP

Gas generation from Radiolysis of Brine has been included in PA calculations for the CRA-2026

SCR-6.5.1.7.2 Summary of New Information

For CRA-2019, the screening decision for the gas effects of the radiolysis of brine was changed to UP from SO-C in previous analyses. With the increase in alpha-emitting radionuclides in the inventory (Van Soest 2025), it is expected that the radiolysis of brine will account for an increased fraction of the total gas generation in the repository, as well as a reduction in brine quantity.

Radiolysis of brine from dissolved, colloidal, and wetted solid radionuclides is modeled in the PA calculations (Day 2019b). During the EPA review of the CRA-2019, the EPA questioned if radiolysis of adsorbed water on non-wetted solid radionuclides should also be accounted for (U.S. EPA 2022c). King et al. (2023) argued the gas generation from adsorbed water on non-wetted solids would have minimal impact and can be ignored in the PA calculations. Additionally, in their TSD (U.S. EPA 2022d), the EPA requested a separate FEP be developed to address the consumption of brine by radiolysis. Since many other repository processes affect brine and gas production and consumption, but do not have discrete FEPs that address them, it was determined that the addition of a separate FEP to address this single process is unnecessary and presents a level of detail inconsistent with most FEP descriptions. Instead, this FEP (W52) acknowledges that brine consumption will occur as a result of radiolysis, and that the explanation of this process is best found in the descriptions of various process models in PA. Details regarding the implementation of brine consumption by radiolysis presented in Day (2019b).

SCR-6.5.1.7.3 Screening Argument

Radiolysis of brine in the WIPP disposal rooms, and of water in the waste, will lead to the production of gases and may contribute to total gas generation in the repository.

The overall reaction for the radiolysis of water in the waste and brine is

$$H_2O \rightarrow H_2 + ½\ O_2 \text{ (generally as aqueous oxidizing species).} \quad \text{(SCR.37)}$$

Ionizing radiation affects the chemistry of aqueous solutions through generation of free radical, ionic, and molecular products. The expected impacts on the brine chemistry are discussed in Appendix SOTERM-2026, Section SOTERM-3.4.1.

The $G(H_2)$ for aqueous brine systems strongly depends on linear energy transfer (LET), increasing by a factor of 3-4 from gamma radiolysis to alpha radiolysis. LET is the rate of energy loss by an ionizing particle traveling through a material, where *E* is energy in megaelectron volts (MeV) and *x* is the distance traveled (μm) as follows:

$$LET = -\frac{dE}{dx} \quad \left(\frac{\text{MeV}}{\mu\text{m}}\right) \quad \text{(SCR.38)}$$

The lower $G(H_2)$ for gamma radiation along with the relatively low gamma radiation field predominant in WIPP (e.g., contact-handled container dose rates less than 200 millirem per hour [mrem/hr]) support consideration of only the alpha radiation in evaluations affecting PA.

Reed et al. (1993) conducted WIPP-relevant radiolytic gas generation experiments lasting between 155 and 182 days. These experiments involved both synthetic Salado and Castile Formation brines (ERDA-6 and Brine A) as well as real brines (DH-36 and G8-B) sampled from the Salado in the repository workings. The brines were spiked with $^{239}Pu(VI)$ at concentrations between 6.9×10^{-9} and 3.4×10^{-4} molal. During these experiments, hydrogen gas was observed as the main gaseous product of radiolysis and, as predicted, no oxygen was observed. In PA, radiolytic gas generation only produces net hydrogen gas (i.e., one mole of gas produced for each net mole of water consumed) as produced oxygen is consumed via oxidation of excess metals in the repository. The WIPP-relevant $G(H_2)$ values experimentally determined by Reed et al. (1993) are summarized in Table SCR-11:

Table SCR-11. WIPP-Relevant G-Values

WIPP Brine	G-Values (molecules per 100 eV)
Brine A	1.4 ± 0.1
ERDA-6	0.9 ± 0.2
DH-36	1.3 ± 0.1
G8-B (GSEEP)	1.3 ± 0.1

The $G(H_2)$ values shown in Table SCR-11 were experimentally determined with ^{239}Pu in solution such that effectively all the alpha disintegration energy associated with the Pu contributed to the dissociation of water and H_2 production. In WIPP, the inventory of alpha-emitting radionuclides is sufficiently large, and the solubility coefficients and brine volumes are sufficiently small, such that only a small fraction of the total alpha-emitting inventory can be dissolved. Although not dissolved, the remaining solid alpha-emitting radionuclide inventory in close-proximity to brine can also contribute to radiolytic gas generation. Only a portion of the

disintegration energy associated with wetted-solid alpha-emitting radionuclides in the inventory will contribute to radiolytic H_2 generation due to several factors, including particle-size distributions and geometric effects influencing self-shielding.

Consideration of the above leads to an implementation in PA (Day 2019b) that quantifies the rate of hydrogen gas generation due to radiolytic decomposition (consumption) of brine in WIPP from radionuclides in solution and a fractional contribution from the wetted solid form of the radionuclides.

SCR-6.5.1.7.4 FEP Implementation in PA

FEP W52 *Radiolysis of Brine*, which is an UP FEP, is associated with the Gas Generation conceptual model, with a strong tie to the Repository Fluid Flow. These conceptual models are implemented in the PA code BRAGFLO for the Salado Flow computation in the PA calculation (Appendix PA-4.2).

SCR-6.5.1.8 **FEP Number: W53**
FEP Title: Radiolysis of Cellulose

SCR-6.5.1.8.1 Screening Decision: SO-C

Gas generation from W53 *Radiolysis of Cellulose*, plastic, and rubber has been excluded from PA calculations on the basis of low consequence to the performance of the disposal system.

SCR-6.5.1.8.2 Summary of New Information

FEP W53 *Radiolysis of Cellulose* has been updated to include discussion of the EPA request for additional information on the CRA-2019 (CC3-GEOCHEM-19b—U.S. EPA 2020d) to perform an analysis with constant gas generation from radiolysis of cellulose, plastics, and rubber and the DOE response (U.S. DOE 2020d).

SCR-6.5.1.8.3 Related FEP

Gas generation from W52 *Radiolysis of Brine* is directly related to W53 *Radiolysis of Cellulose.* W52 *Radiolysis of Brine* was excluded in PA calculations as of low consequence through CRA-2014. In CRA-2019 and afterward, W52 *Radiolysis of Brine* is now included (Day 2019b). However, gas generation from radiolysis of cellulose, plastic, and rubber in the solid waste matrix is still a minor fraction of total gas generation because of matrix depletion.

SCR-6.5.1.8.4 Screening Argument

Not every realization of the WIPP PA results in complete degradation of the CPR matrix by microbes. Therefore, additional hydrogen gas could potentially be generated by radiolysis of CPR in some realizations (Day 2019b). However, radiolytic hydrogen gas generation from a solid waste matrix reaches a plateau and then monotonically decreases over time in direct proportion to cumulative dose deposited from alpha sources due to the low-penetrating nature of alpha-particles. This effect known as “matrix depletion” occurs in a solid waste matrix

because the radiolytic sources are generally spatially fixed with respect to the surrounding hydrogen-bearing material. Over time, less unaltered hydrogen-bearing material is available to be exposed to a short-range alpha-emitting source in the waste matrix; thus, the probability of breaking additional bonds decreases. For most actinide sources, this decline in hydrogen generation rate is not significantly dependent upon the radioactive lifetime of the source (Day 2019b; INEEL 1999).

In the case of TRU waste destined for disposal at WIPP, the dominant source of radiation is plutonium and its daughters, which mostly decay through alpha particle emission. Because relatively little physical movement occurs within the solid waste matrix, alpha particles from plutonium decay are not exposed to new hydrogen bonds. Hence, radiolytic decomposition of the solid waste matrix will effectively cease because of matrix depletion. Granted, some movement of waste occurs as disposal rooms close from salt creep in the first 200 years or so (Reedlunn et al. 2023), but experiments evaluating the effects of vibration and settling of contents within TRU waste containers concluded that there is no appreciable change in depleted radiolytic gas generation rates due to transportation-driven consolidation processes (Day 2019b; Zerwekh et al. 1993).

Over the 10,000-y regulatory period of the WIPP repository, depletion of adjacent hydrogen bonds in the solid CPR waste matrix due to short-ranged alpha radiation and minimal reconfiguration of the waste matrix ensures that radiolytic gas generation from CPR will be insignificant in comparison to other already considered gas generation sources. This conclusion is based on extrapolation of G(gas) values for cellulose and cellulose/plastic/rubber TRU waste mixtures that were experimentally-determined for elapsed times up to 4.9 yr (Day 2019b; Zerwekh 1979). Extrapolating the data, the average G(gas) value for all waste matrices at 100 years is less than 1% of the initial average G(gas) value (Day 2019b, Figure 3).

Therefore, the potential for radiolytic gas generation from CPR for 99% of the repository regulatory period is associated with a $G(H_2)$ value that is less than 1% of the initial $G(H_2)$ value. Consequently, radiolytic gas generation of CPR is an insignificant contributor to total gas generation within WIPP. This conclusion is further bolstered by the fact that other degradation sources will be competing for the solid CPR waste matrix (i.e., microbial degradation) and the fact that many TRU waste containers will have already aged a considerable fraction of the 100-year depletion benchmark by the time of WIPP closure (Day 2019b).

SCR-6.5.1.8.5 Demonstration

In comments on CRA-2019 (CC3-GEOCHEM-19b—U.S. EPA 2020d), EPA requested that DOE perform an analysis with constant gas generation from CPR radiolysis. Constant gas generation ignores matrix depletion, but just as importantly ignores the consumption of CPR from biodegradation by microbes. In response to EPA (U.S. DOE 2020d), a calculation was made that doubled the amount of CPR biodegradation gas generated to bound gas generation from CPR radiolysis. Furthermore, the gas generation continues regardless of whether the CPR inventory is depleted. In the analysis, the increased gas pressure increased brine pressure but decreased brine saturation, which have competing effects on total PA releases. Specifically, increased

brine pressure can increase direct brine releases, but decreased brine saturation can decrease direct brine releases.

A comparison of the complementary cumulative distribution function of releases from CRA-2019 and the bounding analysis that doubles CPR biodegradation gas generation shows very little difference (U.S. DOE 2020c, Figure 18). Hence, gas generation from CPR radiolysis has little impact on PA releases.

SCR-6.5.1.8.6 Additional Support for Screening Argument

The matrix depletion argument relies on a matrix structure to the CPR material, which conflicts with the well-mixed, batch-reactor assumptions made when modeling room chemistry in the WIPP PA (King et al. 2023). There is no reason that a screening argument for excluding a FEP must use the modeling simplifications and assumptions used to represent retained FEPs in the PA calculations. However, CPR radiolysis in a well-mixed system can still be excluded from the PA because the estimate of gas generation from CPR radiolysis using a batch reactor assumption is less than gas generation from CPR radiolysis using a matrix depletion assumption (King et al. 2023, Figure 4 versus U.S. DOE 2020d, Figure 9).

SCR-6.5.1.8.7 Summary

Doubling the gas generation from CPR degradation to bound gas from W53 *Radiolysis of Cellulose*, plastic, and rubber shows little influence on PA releases in CRA-2019. Therefore, W53 *Radiolysis of Cellulose* has been excluded from PA calculations on the basis of low consequence to the performance of the disposal system.

SCR-6.5.1.9 FEP Number: W54
FEP Title: Helium Gas Production

SCR-6.5.1.9.1 Screening Decision: SO-C

Gas generation from helium production has been eliminated from PA calculations on the basis of low consequence to the performance of the disposal system.

SCR-6.5.1.9.2 Summary of New Information

This FEP has been updated with references to the latest inventory information for CRA-2026 (Kicker, 2025; Van Soest 2025).

SCR-6.5.1.9.3 Screening Argument

The updated CH and RH-TRU total activity for CRA-2026 at closure in 2083 is 8.05×10^6 Ci (2.98×10^{17} Bq) (Kicker 2025; Van Soest 2025). This CRA-2026 inventory is somewhat larger than the 4.02×10^6 Ci (1.49×10^{17} Bq) previously estimated for CCA-1996 at closure in 2033 (U.S. DOE 1996a,

Table 4-6).[u] However, helium gas production is still negligible compared to other sources of gas production. Hence, the FEP screening argument and screening decision remains unchanged.

Helium gas ($He_{(g)}$) is produced by the reduction of α-particles (helium nuclei) emitted from the decay of actinides in the TRU waste. The α-particles are converted to helium gas by capturing 2 electrons:

$$^4He^{2+} + 2e^- \rightarrow He(g) \quad \text{(SCR.39)}$$

The maximum amount of helium that could be produced can be calculated from the number of α-particles generated during radioactive decay. Conservatively assuming that the initial inventory continues to yield α-particles at the initial rate throughout the 10,000-year regulatory period,[v] the maximum rate of helium gas produced is

$$R_{\mathrm{He}} = \frac{A^{total} \frac{1 \text{ He atom}}{\alpha \text{ decay}}}{N_A} \quad \text{(SCR.40)}$$

where R_{He} is the rate of helium gas production in the repository (mole/s), A^{total} is the waste activity at repository closure (Bq—where one Bq is equal to one decay per second), and N_A is Avogadro's number (6.022×10^{23} atoms per mole).

For CRA-2026, R_{He} is 4.9×10^{-7} mole/s (15.6 mole/y) for the total activity of 8.05×10^{6} Ci (2.98×10^{17} Bq). This rate is larger but of the same order of magnitude as 2.5×10^{-7} mole/s (7.85 mole/y) produced in CCA-1996, based on the total activity of 4.02×10^{6} Ci (1.49×10^{17} Bq). Over 10,000 years, a maximum of 1.56×10^{5} moles of helium could be produced in the closed repository in CRA-2026.

To provide some perspective, the volume of helium (V) can be estimated from the ideal gas law:

$$V = \frac{nRT}{p} \quad \text{(SCR.41)}$$

Where *n* is number of moles, *R* is universal gas constant (0.0821 L atm/(mol K), *T* is absolute temperature (K), and *p* is pressure (atmospheres). The gas volume production rate is ~2.7 L/y (compared to ~1.3 L/y in CCA-1996) for repository conditions of 30 °C (86 °F) and 14.8 MPa or 146 atmospheres (lithostatic pressure).

In comparison, the maximum combined mass of gas produced by iron corrosion, cellulose biodegradation, and radiolysis in the disposal area of WIPP for CRA-2026 in Scenario S2-BF is ~4 orders of magnitude greater over 10,000 years (i.e., $\sim2\times10^{9}$ moles hydrogen gas); the minimum is ~3 orders of magnitude greater (i.e., 1×10^{8} moles hydrogen gas) (Figure SCR-14). Because the

[u] Time of closure is used since presumably much of the helium produced prior to closure will be removed by ventilation.

[v] This assumption maximizes the estimate of helium production because some radionuclides will decay by beta and gamma emission.

mass of helium gas is so small, helium gas production has been excluded from PA calculation on the basis of low consequence to the performance of the disposal system.

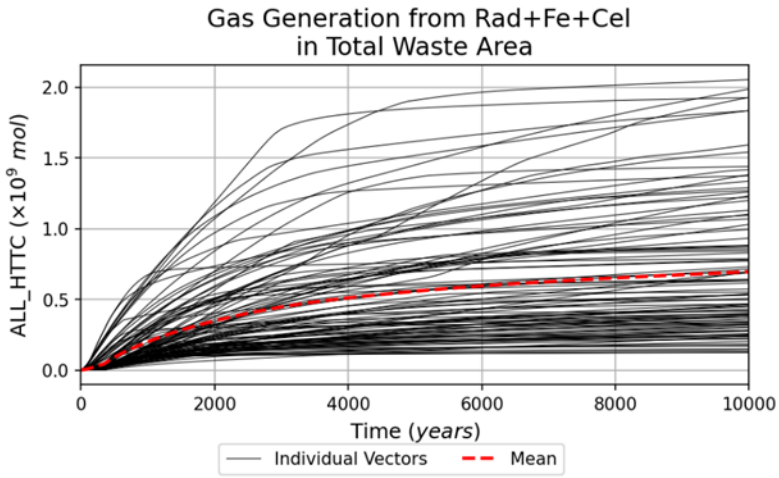

Figure SCR-14. Total repository gas generation from iron corrosion, cellulose biodegradation, and radiolysis (ALL_HTTC) for E1 intrusion with intrusion at 350 years, Replicate 1, CRA-2026 (Scenario S2-BF-t350-r1).

SCR-6.5.1.10 **FEP Number: W55**
FEP Title: Radioactive Gases

SCR-6.5.1.10.1 Screening Decision: SO-C

FEP *W55 Radioactive Gases* is excluded from PA calculations on the basis of low consequence to the performance of the WIPP disposal system.

SCR-6.5.1.10.2 Summary of New Information

FEP *W55 Radioactive Gases* has been updated with references to the latest inventory information (Kicker, 2025; Van Soest 2025).

SCR-6.5.1.10.3 Related FEP

Because of the exclusion of radioactive gases from PA calculations here, FEP *W89 Transport of Radioactive Gases* (Section SCR-6.6.4.1) is also excluded.

SCR-6.5.1.10.4 Screening Argument

Based on the composition of the CRA-2026 anticipated waste inventory (Kicker, 2025; Van Soest 2025), the radioactive gases that will be present in the repository are radon (Rn) and carbon-14 (^{14}C).

SCR-6.5.1.10.5 Carbon-14

The initial activities of 0.15 Ci ^{14}C in CH-TRU waste and 0.12 Ci ^{14}C in RH-TRU) waste anticipated in CRA-2026 (Van Soest 2025, Table 5-3 & Table 5-4) represent only a minute fraction of the total initial activity of 6.43×10^{6} Ci. After 10,000 years, the total decayed ^{14}C inventory of 0.08 Ci continues to represent only a minute fraction of the total activity of 2.96×10^{6} Ci.

Generally, only radionuclides that have an activity of at least 0.001 EPA units at some point during the 10,000-year regulatory period (as adjusted for the total transuranic waste activity) are considered for inclusion in a PA calculation. For CRA-2026, the maximum potential release of ^{14}C is less than 0.0004 EPA units (Kicker 2025, Appendix A-Tables 15 through 20) such that it cannot meaningfully contribute to cumulative releases related to 40 CFR 191.13 and is not retained in the PA calculations.

Furthermore, large quantities of mobile ^{14}C are unlikely. The ^{14}C can partition onto carbon dioxide gas (CO_2) that is formed during biodegradation of organic material in the TRU waste disposed at WIPP.[w] The gaseous $^{14}CO_2$ formed during biodegradation of organic waste in the WIPP will be incorporated into either (a) cementitious material to form a solid calcium carbonate phase as described in Appendix GEOCHEM-5. Hence, ^{14}C will mostly become immobile in solid phases and cannot contribute to dose (as related to the Individual Protection Requirements in 40 CFR 191.15).

SCR-6.5.1.10.6 Radon Gases

Radon gases (i.e., ^{219}Rn, ^{220}Rn, and ^{222}Rn) are produced from decay of $^{239}Pu/^{235}U$ to solid radium-233 (^{223}Ra), $^{240}Pu/^{236}U$ to^{224}Ra, and $^{238}Pu/^{234}U$ to ^{226}Ra, respectively. In turn, the solid radium isotopes are in secular equilibrium with their decay products, radon gas isotopes (i.e., ^{219}Rn, ^{220}Rn, and ^{222}Rn, respectively), which would be produced throughout the 10,000-year regulatory period. However, radon gas is not considered when evaluating cumulative releases related to 40 CFR 191.13 because the radon gas half-lives are all less than 20 years (^{222}Rn has the longest half-live of 3.82 days); thus, radon gas isotopes can be excluded on regulatory grounds as related to cumulative releases.

As regards individual protection requirements of 40 CFR 191.15, only undisturbed conditions are considered. The presence of radon gas at the accessible environment would be dependent on the mobilization of Pu parent since the half-lives of radon gas and even radium are short (^{226}Ra is the longest lived with half live of 1,600 years). The dose to humans would thus be dominated by Pu, particularly, ^{239}Pu, rather than radon gas ^{222}Rn whose initial activity is 4.39 Ci at WIPP closure and still small at 77.5 Ci after 10,000 years in CRA-2026 (Van Soest 2025, Table 5-3 & Table 5-4).

Furthermore and as described in FEP W89 *Transport of Radioactive Gases* (Section SCR-6.6.4.1), CRA-2026 does not have undisturbed releases (Appendix PA-7.2), which solely apply to

[w]Methane ($^{14}CH_4$) is not expected to form in the chemical conditions of the repository. Methonagenesis does not occur in highly saline solutions and, thus, has not been included since CRA-2009 (U.S. Department of Energy 2009, Appendix SOTERM-2019, Section SOTERM-4.2)

individual protection requirements of 40 CFR 191.15. Consequently, gas transport of radon gas is excluded because of low consequence, as regards the individual protection requirements of 40 CFR 191.15.

SCR-6.5.2 Speciation

SCR-6.5.2.1 **FEP Number: W56**
FEP Title: Speciation

SCR-6.5.2.1.1 Screening Decision: **UP – Disposal Room**
UP – Culebra
SO-C – Elsewhere
SO-C – Beneficial (Shaft Seals)

Chemical *Speciation* is accounted for in PA in the estimates of the radionuclide solubilities and colloidal concentrations that comprise the mobile actinide source term in the disposal rooms. In the Culebra, the speciation establishes the degree of chemical retardation estimated during contaminant transport. The effects of cementitious seals on chemical *Speciation* have been eliminated from PA calculations on the basis of beneficial consequence to the performance of the disposal system.

SCR-6.5.2.1.2 Summary of New Information

Actinide solubilities have been recalculated for the CRA-2026 (Domski 2025) based on the latest inventory components as provided by Van Soest (2025). Colloidal contributions are also calculated in PA (Appendix PA-1.1.17) based on project-specific parameters recommended (Kaplan et al. 2025; Appendix SOTERM-3.5; Appendix GEOCHEM-5). New considerations have been taken into account for the shaft seals. The new solubilities and considerations do not affect the screening arguments or overall decisions described below.

SCR-6.5.2.1.3 Screening Argument

Chemical speciation refers to the form in which elements occur under a particular set of chemical or environmental conditions. Conditions affecting chemical speciation include the temperature, pressure, radiolysis, redox conditions, presence/absence of complexants and counterions, degree of aggregation, and salinity (ionic strength) of the brine. The predicted chemical speciation defines the mobile actinide source term which is critical input to release scenarios that impact overall actinide mobilization.

SCR-6.5.2.1.4 Disposal Room

The concentrations of radionuclides that dissolve in any brines present in the disposal rooms after repository closure will depend on the stability of the chemical species that form under the prevailing conditions (for example, temperature, pressure, radiolysis, redox conditions, and ionic strength). The approach used to define the mobile actinide concentration is given in

Appendix PA-2.4.4.1. The underlying approach and model assumptions used to calculate actinide solubilities are described by Domski (Domski 2025). This approach considers the predicted brine composition after reaction with the emplaced waste materials. Key inorganic and organic complexants are also considered. The MgO backfill will buffer pH values in the disposal room to between 9 and 10 and help maintain low concentrations of dissolved carbonate. Thus, chemical speciation is accounted for in PA in the estimates of mobile actinide concentrations used as the actinide source term in the disposal rooms.

SCR-6.5.2.1.5 Repository (Shaft) Seals

Certain repository materials, including the cementitious components of the shaft seals, have the potential to interact with groundwater and significantly alter the chemical speciation of any radionuclides present. In particular, cementitious materials in the shaft seals have the capacity to strongly sorb actinides or actinide analogs (Altenhein-Haese et al. 1994; Wierczinski et al. 1998; Pointeau et al. 2001), and buffer groundwater to high pH (Bennett et al. 1992, pp. 315–25; Kienzler et al., 2016). High alkalinity conditions overwhelmingly lead to reduced concentrations of radionuclides, and consequently to reduced migration of these radionuclides. In very localized conditions, the formation of specific actinide species could be possible (U.S. EPA 2022c), which could increase the solubility of the +III and +IV actinides (Altmaier et al. 2008, Gaona et al. 2008, Tasi et al. 2018). However, those localized conditions do not prevail in the WIPP: the presence of MgO greatly minimizes the pH excursion to extremely high values, and the degradation of cellulosic materials, leading to isosaccharinic acid (ISA), is predicted to be insignificant in the repository (Mijnendonckx et al. 2021, U.S. DOE 2021c). Therefore, there is no significant impact of cementious materials at the repository shafts on actinide speciation or solubility expected (U.S. DOE 2021c). The effects of cementitious seals on actinide speciation have been eliminated from PA calculations on the basis of low consequence to the performance of the disposal system.

SCR-6.5.2.1.6 Culebra

Chemical speciation will affect actinide retardation in the Culebra. The dependence of An retardation on speciation in the Culebra is accounted for in PA by sampling over ranges of K_ds. The ranges of K_ds are based on the range of groundwater compositions and speciation in the Culebra, including consideration of non-radionuclide solutes. The methodology used to simulate sorption in the Culebra is described in Appendix PA-4.10.

SCR-6.5.2.1.7 FEP Implementation in PA

W56 *Speciation* is included in the UP scenario and is associated with the Chemical Conditions and Dissolved Actinide Source Term conceptual models implemented by the EQ3/6 code and with the Transport of Dissolved Actinides in the Culebra conceptual model implemented in the SECOTP2D code.

SCR-6.5.2.2 **FEP Number: W57**
FEP Title: Kinetics of Speciation

SCR-6.5.2.2.1 Screening Decision: SO-C

The effects of reaction kinetics in chemical speciation reactions have been eliminated from PA calculations on the basis of low consequence to the performance of the disposal system.

SCR-6.5.2.2.2 Summary of New Information

No new information has been identified that affects the screening of this FEP since the CRA-2019.

SCR-6.5.2.2.3 Screening Argument

The chemical speciation of an actinide is described by its oxidation state, complexation (organic and inorganic), and aggregation that contributes to its mobile concentration. Conditions affecting chemical speciation include radiolysis, redox conditions, temperature, ionic strength, ligand concentration, extent of aggregation, and pH of the solution. Speciation kinetics is associated with the rate of complex formation, redox changes, and aggregation in WIPP brines.

SCR-6.5.2.2.4 Disposal Room Equilibrium Conditions

The concentrations of radionuclides that can be dissolved in brines within the disposal rooms will depend on the thermodynamic stabilities and solubilities of the respective actinide/radionuclide complexes. Geochemical modeling using the code EQ3/6 to determine the brine solubilities of radionuclides takes into account the expected conditions, including temperature, ionic strength, pH, and ligand concentration. The chemical speciation at equilibrium is accounted for in PA in the estimates of the mobile actinide source term in the disposal rooms.

SCR-6.5.2.2.5 Kinetics of Complex Formation

The waste that is emplaced within the WIPP contains radionuclides, including actinides or An-bearing materials in solid phases, e.g., metal oxides, salts, coprecipitated solids, and contaminated objects. In the event of contact with brine, the solution phase concentration of dissolved radionuclides is controlled both by the solution composition and by the kinetics of dissolution of the solid phases, effectively approaching equilibrium from undersaturation. Solution complexation reactions of most actinide/radionuclide ions with common inorganic ligands, such as carbonate and hydroxide, and with organic ligands such as acetate, citrate, oxalate, and ethylenediaminetetraacetate (EDTA) are kinetically very fast (typically hours or less), an inconsequentially short time on the scale of the 10,000-yr regulatory period. The relatively fast reaction kinetics in aqueous systems has been well understood for some time (Lasaga et al. 1994).

Solid transformation and precipitation can occur relatively slowly in the WIPP (several years), and this could alter the aqueous speciation with time. In WIPP PA the more soluble, initially formed solid phases, are used to conservatively overpredict the aqueous concentrations. In time, the phase transformation will evolve towards more highly crystalline phases that lower solubility and correspondingly aqueous mobile concentrations (Van Santen 1984).

The relatively fast rate at which solution species approach equilibrium is of no consequence to repository performance. Additionally, a conservative approach to account for the potentially slower phase transformations is used in PA. Kinetics of chemical speciation, for this reason, may be eliminated from PA calculations on the basis of no consequence.

SCR-6.5.3 Precipitation and Dissolution

SCR-6.5.3.1 **FEP Numbers: W58, W59, and W60**
FEP Titles: Dissolution of Waste (W58)
Precipitation of Secondary Minerals (W59)
Kinetics of Precipitation and Dissolution (W60)

SCR-6.5.3.1.1 Screening Decision: UP (W58)
SO-C (W59, W60)

Waste dissolution and the release of radionuclides in the disposal rooms are accounted for in PA. The formation of radionuclide-bearing precipitates from groundwaters and brines and the associated retardation of contaminants have been eliminated from PA calculations on the basis of low consequence to the performance of the disposal system. The effect of reaction kinetics in controlling the rate of waste dissolution within the disposal rooms has been eliminated from PA calculations on the basis of low consequence to the performance of the disposal system.

SCR-6.5.3.1.2 Summary of New Information

Precipitation of An-bearing minerals occurs only when the radionuclide inventory exceeds its solubility limit. Since the solubility limit represents the maximum estimated concentration for a radionuclide, the precipitation of An-bearing minerals does not impact the release of the radionuclide. Therefore, the screening decision for W59 has been changed from SO-C Beneficial to SO-C. A summary of the implementation of *Dissolution of Waste* (W58) in PA has been added.

SCR-6.5.3.1.3 Screening Argument

Dissolution of waste and precipitation of An-bearing minerals control the concentrations of radionuclides in brines and can influence rates of contaminant transport. Waste dissolution is accounted for in PA. The formation of radionuclide-bearing precipitates from groundwaters and brines and the associated retardation of contaminants have been eliminated from PA calculations on the basis of low consequence to the performance of the disposal system.

Results of actinide studies that in some cases identify phase formation are provided in Appendix SOTERM-5.0. These results do not affect the screening arguments or decisions.

At low temperatures, precipitation and dissolution reactions are caused by changes in fluid chemistry that result in chemical undersaturation or oversaturation (Bruno and Sandino 1987). Precipitation can be divided into two stages: nucleation and crystal growth. Following nucleation, growth rates depend on the rates of surface processes and the transport of materials to the growth site. Mineral dissolution often depends on whether a surface reaction or transport of material away from the reaction site acts as the rate-controlling process. The former case may cause selective dissolution along crystallographically controlled features, whereas the latter may induce rapid bulk dissolution (Berner 1981). Thus, a range of kinetic behaviors will be exhibited by different mineral precipitation and dissolution reactions in geochemical systems.

SCR-6.5.3.1.4 Disposal Room

The waste that is emplaced within the WIPP contains radionuclides, including actinides or An-bearing materials in solid phases, e.g., metal oxides, salts, coprecipitated solids, and contaminated objects. In the event of contact with brine, the solution phase concentration of dissolved radionuclides is controlled both by the solution composition and the kinetics of dissolution of the solid phases, effectively approaching equilibrium from undersaturation. Solution complexation reactions of most metal ions with common inorganic ligands, such as carbonate and hydroxide, and with organic ligands such as acetate, citrate, oxalate, and EDTA are kinetically very fast, reaching equilibrium in less than 1 s, which is infinitesimally small on the time scale of the 10,000-yr regulatory period. The rate at which thermodynamic equilibrium is approached between solution composition and the solubility-controlling solid phases will be limited by rate of dissolution of the solid materials in the waste. As a result, until equilibrium is reached, the solution concentration of the actinides will be lower than the concentration predicted based upon equilibrium of the solution phase components with the solubility-limiting solid phases. The WIPP An source term model, which describes interactions of the waste and brine, is described in detail in the CCA, Chapter 6.0, Section 6.4.3.5. The assumption of instantaneous equilibrium in waste dissolution reactions is a conservative approach, yielding maximum concentration estimates for radionuclides in the disposal rooms because a time-weighted average resulting from a kinetically accurate estimate of solution compositions would have lower concentrations at early times. Waste dissolution at the thermodynamic equilibrium solubility limit is accounted for in PA. However, the kinetics of dissolution within the disposal rooms has been eliminated from PA calculations on the basis of low consequence to the performance of the disposal system.

SCR-6.5.3.1.5 Geological Units

Brine entering the Culebra will be diluted by the groundwater of the Culebra and the precipitation of the An-bearing phases is unlikely to occur. No credit is given in PA calculations to the occurrence of precipitation of secondary minerals. The formation of radionuclide-bearing precipitates from groundwaters and brines and the associated retardation of contaminants

have been eliminated from PA calculations on the basis of low consequence to disposal system performance. As a result, kinetics of precipitation has also been eliminated from PA calculations because no credit is taken for precipitation reactions.

SCR-6.5.3.1.6 FEP Implementation in PA

Dissolution of Waste (W58) in the disposal rooms is incorporated into concentrations of actinide radionuclides as implemented by the PA codes PANEL, NUTS, and BRAGFLO.

SCR-6.5.4 Sorption

SCR-6.5.4.1 **FEP Numbers: W61, W62, and W63**
FEP Titles: Actinide Sorption (W61)
Kinetics of Sorption (W62)
Changes in Sorptive Surfaces (W63)

SCR-6.5.4.1.1 Screening Decision: **UP (W61, W62) In the Culebra and Dewey Lake**
UP(W63)
SO-C – Beneficial (W61, W62) In the Disposal Room, Shaft Seals, Other Geologic Units

Sorption within the disposal rooms, which would serve to reduce radionuclide concentrations, has been eliminated from PA calculations on the basis of beneficial consequence to the performance of the disposal system. The effects of sorption processes in shaft seals and panel closures have been eliminated from PA calculations on the basis of beneficial consequence to the performance of the disposal system. Sorption within the Culebra and the Dewey Lake is accounted for in PA. Sorption processes within other geological units of the disposal system have been eliminated from PA calculations on the basis of beneficial consequence to the performance of the disposal system. Mobile adsorbents (for example, microbes and humic acids), and the sorption of radionuclides at their surfaces, are accounted for in PA in the estimates of the mobile actinide concentrations that comprise the actinide source term. The potential effects of reaction kinetics in adsorption processes and of *Changes in Sorptive Surfaces* are accounted for in PA.

SCR-6.5.4.1.2 Summary of New Information

The microbial and intrinsic colloid enhancement parameters were updated to those of Kaplan et al. (2025). The speciation, which implicitly impacts sorption, was updated in the solubility calculations (Domski 2025). This new information does not change the screening arguments, decisions, or implementation of these FEPs within PA.

SCR-6.5.4.1.3 Screening Argument

Sorption may be defined as the accumulation of matter at the interface between a solid and an aqueous solution. Within PA calculations, including those made for the WIPP, the use of isotherm representations of An sorption is widely used because of their computational simplicity in comparison with other models (Serne 1992, pp. 238−39). New mineral colloid and biosorption data for colloid formation have been used to update colloidal enhancement factors (see Appendix SOTERM-3.5; Kaplan et al. 2025).

The mechanisms that control the kinetics of sorption processes are, in general, poorly understood. Often, sorption of inorganic ions on mineral surfaces is a two-step process consisting of a short period (typically minutes) of diffusion-controlled, rapid uptake, followed by slower processes (typically weeks to months) including surface rearrangement, aggregation and precipitation, and solid solution formation (Davis and Kent 1990, p. 202). Available data concerning rates of sorption reactions involving the important radionuclides indicate that, in general, a range of kinetic behavior is to be expected.

The relevance to the WIPP of sorption reaction kinetics lies in their effects on chemical transport. Sorption of waste contaminants to static surfaces of the disposal system, such as seals and host rocks, acts to retard chemical transport. Sorption of waste contaminants to potentially mobile surfaces, such as colloids, however, may act to enhance chemical transport, particularly if the kinetics of contaminant desorption are slow or the process is irreversible (nonequilibrium).

The following subsections discuss sorption in the disposal rooms, shaft seals, panel closures, the Culebra, and other geological units of the WIPP disposal system. Sorption on colloids, microbes, and particulate material is also discussed.

SCR-6.5.4.1.4 Disposal Room

The concentrations of actinides/radionuclides that dissolve in brine entering the disposal room will be controlled by a combination of sorption and dissolution/precipitation reactions. With the prevalence of iron oxides and other highly sorptive materials in the disposal room, a significantly high amount of sorption is predicted that would effectively lower the mobile concentrations of inventory-limited actinides/radionuclides. The WIPP PA calculations, however, ignore the potential highly beneficial effects of sorption as a conservatism that overestimates the actinide source term. Sorption, in this context, has been eliminated from PA calculations on the basis of beneficial consequence to the performance of the disposal system.

SCR-6.5.4.1.5 Shaft Seals and Panel Closures

The CCA, Chapter 3.0 and Appendix SEAL (U.S. DOE 1996a) describe the seals that are to be placed at various locations in the access shafts. The materials to be used include crushed salt, bentonite clay, and cementitious grouts. Of these, the latter two in particular possess significant sorption capacities. No credit is given for the influence of sorption processes that

may occur in seal materials and their likely beneficial effects on radionuclide migration rates. The effects of sorption processes in shaft seals have been eliminated from PA calculations on the basis of beneficial consequence to the performance of the disposal system.

SCR-6.5.4.1.6 Culebra

Sorption within the Culebra is accounted for in PA as discussed in the CCA, Chapter 6.0, Section 6.4.6.2. The model used comprises an equilibrium, sorption isotherm approximation, employing constructed CDFs of K_ds applicable to dolomite in the Culebra. The potential effects of reaction kinetics in adsorption processes are encompassed in the ranges of K_ds used. The geochemical speciation of the Culebra groundwaters and the effects of changes in sorptive surfaces are implicitly accounted for in PA for the WIPP in the ranges of K_ds used.

SCR-6.5.4.1.7 Other Geological Units

During groundwater flow, any radionuclide sorption processes that occur between dissolved or colloidal actinides and rock surfaces will lead to reduced rates of contaminant transport. The sorptive capacity of the Dewey Lake is sufficiently large to prevent any radionuclides that enter it from being released to the accessible environment over 10,000 yrs (Wallace et al. 1995). Thus, sorption within the Dewey Lake is accounted for in PA, as discussed in the CCA, Chapter 6.0, Section 6.4.6.6. No credit is given to the potentially beneficial occurrence of sorption in other geological units outside the Culebra. Sorption processes within other geological units of the disposal system have been eliminated from PA calculations on the basis of beneficial consequence to the performance of the disposal system.

SCR-6.5.4.1.8 Sorption on Colloids, Microbes, and Particulate Material

The interactions of sorption processes with colloidal, microbial, or particulate transport are complex (see discussion in Kaplan et al. [2025], Mariner [2025]; Appendix SOTERM-3.5; Appendix GEOCHEM-5). Neglecting sorption of contaminants on immobile surfaces in the repository shafts and Salado (for example, the clays of the Salado interbeds) is a conservative approach because it leads to overestimated transport rates. However, neglecting sorption on potentially mobile adsorbents (for example, microbes and humic acids) cannot be shown to be conservative with respect to potential releases, because mobile adsorbents may act to transport radionuclides sorbed to them. Consequently, the concentrations of actinides that may be carried by mobile adsorbents are accounted for in PA of the mobile actinide concentrations in the actinide source term.

SCR-6.5.4.1.9 FEP Implementation in PA

FEPs *Actinide Sorption* (W61), *Kinetics of Sorption* (W62), and C*hanges in Sorptive Surfaces* (W63) are included in the UP scenario and associated with the Dissolved Actinide Source Term and Colloidal Actinide Source Term conceptual models.

SCR-6.5.5 Reduction-Oxidation Chemistry

SCR-6.5.5.1 **FEP Numbers: W64 and W66**
FEP Titles: Effects of Metal Corrosion (W64)
Reduction-Oxidation Kinetics (W66)

SCR-6.5.5.1.1 Screening Decision: UP

The effects of reduction-oxidation reactions related to metal corrosion on reduction-oxidation conditions are accounted for in PA. Reduction-oxidation reaction kinetics are accounted for in PA.

SCR-6.5.5.1.2 Summary of New Information

No new information has been identified that affects the screening of these FEPs since the CRA-2019. Information has been provided regarding the implementation of these FEPs in PA.

SCR-6.5.5.1.3 Screening Argument

SCR-6.5.5.1.3.1 Reduction-Oxidation Kinetics

In general, investigation of the reduction-oxidation couples present in aqueous geochemical systems suggests that most reduction-oxidation reactions are not in thermodynamic equilibrium (Wolery 1992, p. 27). The lack of data characterizing the rates of reactions among trace element reduction-oxidation couples leads to uncertainty in elemental speciation. This uncertainty in reduction-oxidation kinetics is accounted for in PA in the dissolved An source term model (see Appendix SOTERM-6.4), which estimates the probabilities that particular actinides occur in certain oxidation states. Appendix SOTERM-5.0 evaluates WIPP-relevant experimental results for important actinide species since the CRA-2019.

SCR-6.5.5.1.3.2 Corrosion

Other than gas generation, which is discussed in FEPs W44 through W55, the main effect of metal corrosion will be to influence the chemical conditions that prevail within the repository. Ferrous metals will be the most abundant metals in the WIPP, and these will corrode in humid conditions and on contact with any brines entering the repository. Initially, corrosion will occur under oxic conditions owing to the atmospheric oxygen present in the repository at the time of closure. However, consumption of the available oxygen by corrosion reactions will rapidly lead to anoxic (reducing) conditions. These changes and controls on conditions within the repository will affect the chemical speciation of the brines and may affect the oxidation states of the actinides present. Changes to the oxidation states of the actinides will lead to changes in the concentrations that may be mobilized during brine flow. The oxidation states of the actinides are accounted for in PA by the use of parameters that describe probabilities that the actinides exist in particular oxidation states and, as a result, the likely An concentrations. Therefore, the effects of metal corrosion are accounted for in PA.

SCR-6.5.5.1.4 FEP Implementation in PA

W64 *Effects of Metal Corrosion* and W66 *Reduction-Oxidation Kinetics* are included in the UP scenario and associated with the Chemical Conditions and Dissolved Actinide Source Term conceptual models. FEPs W64 and W66 are implemented by the EQ3/6 code.

SCR-6.5.5.2 FEP Number: W65
FEP Title: Reduction-Oxidation Fronts

SCR-6.5.5.2.1 Screening Decision: SO-P

The migration of *Reduction-Oxidation Fronts* through the repository has been eliminated from PA calculations on the basis of low probability of occurrence over 10,000 yrs.

SCR-6.5.5.2.2 Summary of New Information

No new information has been identified that affects the screening of this FEP since the CRA-2019.

SCR-6.5.5.2.3 Screening Argument

The development of reduction-oxidation fronts in the disposal system may affect the chemistry and migration of radionuclides. Reduction-oxidation fronts separate regions that may be characterized, in broad terms, as having different oxidation potentials. On either side of a reduction-oxidation front, the behavior of reduction-oxidation-sensitive elements may be controlled by different geochemical reactions. Elements that exhibit the greatest range of oxidation states (for example, U, Np, and Pu) will be the most affected by reduction-oxidation front development and migration. The migration of reduction-oxidation fronts may occur as a result of diffusion processes, or in response to groundwater flow, but will be restricted by the occurrence of heterogeneous buffering reactions (for example, mineral dissolution and precipitation reactions) (Waber 1991 and Snelling 1992). Indeed, these buffering reactions cause the typically sharp, distinct nature of reduction-oxidation fronts.

The redox properties of the WIPP repository will be established and maintained by the emplaced waste and materials. Salt creep and self-sealing will essentially isolate the geochemistry of the repository and will eliminate the possible influence of large-scale redox fronts through the repository. Large-scale reduction-oxidation fronts have therefore been eliminated from PA calculations on the basis of low probability of occurrence over 10,000 yrs.

SCR-6.5.5.3 **FEP Number: W67**
FEP Title: Localized Reducing Zones

SCR-6.5.5.3.1 Screening Decision: SO-C

The formation of *Localized Reducing Zones* has been eliminated from PA calculations on the basis of low consequence to the performance of the disposal system.

SCR-6.5.5.3.2 Summary of New Information

No new information has been identified that affects the screening of this FEP since the CRA-2019.

SCR-6.5.5.3.3 Screening Argument

The dominant reduction reactions in the repository include steel corrosion and microbial degradation. The following bounding calculation shows that molecular diffusion alone will be sufficient to mix brine chemistry over a distance of meters and therefore the formation of localized reducing zones in the repository is of low consequence.

The diffusion of a chemical species in a porous medium can be described by Fick's equation (e.g., Richardson and McSween 1989, p.132):

$$\frac{\partial C}{\partial t} = \frac{\partial}{\partial X}\left(D_{eff}\frac{\partial C}{\partial X}\right) \quad \text{(SCR.42)}$$

where C is the concentration of the diffusing chemical species, t is the time, X is the distance, and D_{eff} is the effective diffusivity of the chemical species in a given porous medium. D_{eff} is related to the porosity (ϕ) of the medium by (e.g., Oelkers 1996):

$$D_{eff} = \phi^2 D \quad \text{(SCR.43)}$$

where D is the diffusivity of the species in pure solution. The D values for most aqueous species at room temperatures fall into a narrow range, and 10^{-5} cm^2 (1.5×10^{-6} in.^{2}) per s is a good approximation (e.g., Richardson and McSween 1989, p.138). From the WIPP PA calculations (Bean et al. 1996, p.7-29; WIPP PA Department 1993, Equation B-8), the porosity in the WIPP waste panels after room closure is calculated to be 0.4 to 0.7. From Equation SCR.44, the effective diffusivity D_{eff} in the waste is estimated to be $2 - 5 \times 10^{-6}$ cm^2 (7×10^{-7} in.^{2}) per second ($6 - 16 \times 10^{-3}$ m^2/yr).

Given a time scale of T, the typical diffusion penetration distance (L) can be determined by scaling:

$$L = \sqrt{D_{eff}T} \quad \text{(SCR.44)}$$

Using Equation SCR.44, the diffusion penetration distance in the WIPP can be calculated as a function of diffusion time, as shown in Figure SCR-15.

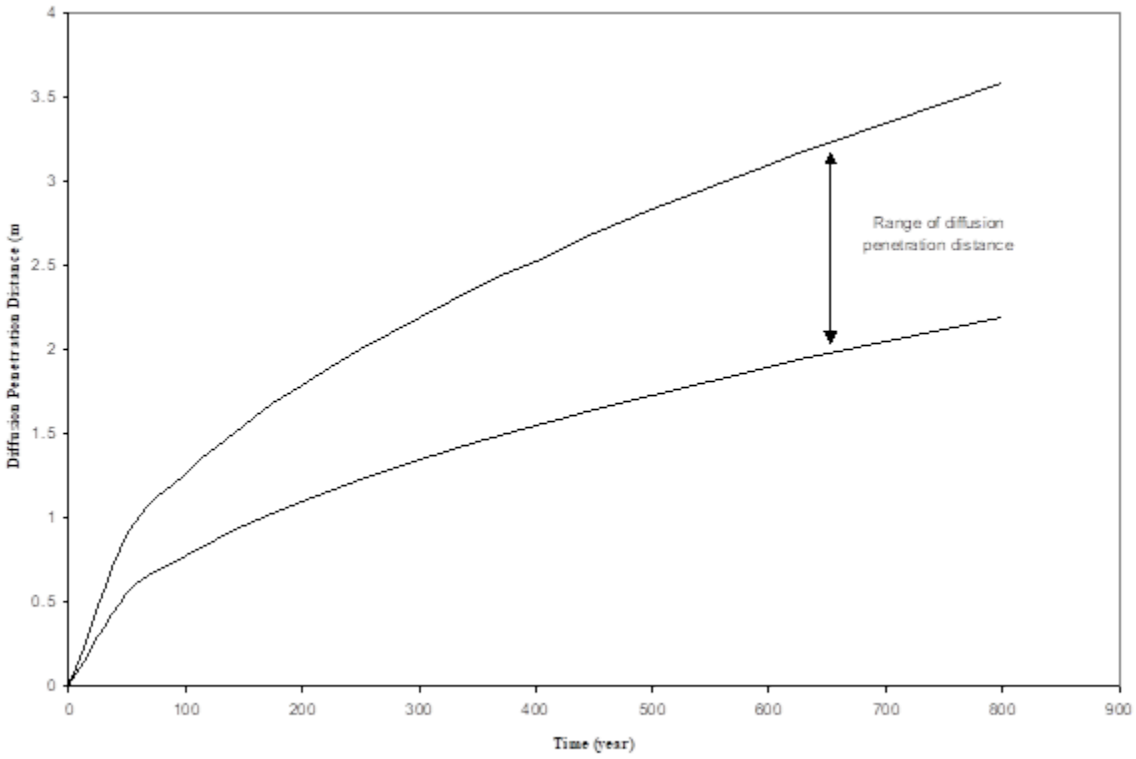

Figure SCR-15. Diffusion Penetration Distance as a Function of Diffusion Time

Direct brine release requires the repository gas pressure to be at least 8 MPa (Stoelzel and O'Brien 1996). The CRA-2026 calculations show that it will take at least 250 yrs for the repository pressure to reach this critical value by gas generation, although mean pressures for the undisturbed case never exceed this value (Brunell et al. 2025). Over this time scale, according to Equation SCR.44 and Figure SCR-15, molecular diffusion alone can mix brine composition effectively at least over a distance of ~ 1 m (3.3 ft).

The above calculation assumes diffusion only through liquid water. This assumption is applicable to steel corrosion. Note that microbial reactions and radiolysis can also release gaseous species. The diffusion of a gaseous species is much faster than an aqueous one. Thus, molecular diffusion can homogenize microbial and radiolysis reactions even at a much larger scale.

The height of waste stacks in the repository after room closure (*h*) can be calculated by:

$$h = \frac{h_0(1-\varphi_0)}{1-\varphi} \quad \text{(SCR.45)}$$

where h_0 and ϕ_0 are the initial height of waste stacks and the initial porosity of wastes, which are assumed to be 3.96 m and 0.848, respectively, in the WIPP PA. For ϕ = 0.4 – 0.7, h is estimated to be 1.0 to 2.0 m. This means that molecular diffusion alone can homogenize redox reaction in the vertical dimension of the repository. Therefore, the formation of localized reducing zones is unlikely. The general repository environment will become reducing shortly after room closure because of metal corrosion and microbial reactions. Therefore, localized reducing zones can be eliminated from PA calculations on the basis of low consequence to the disposal system.

SCR-6.5.6 Organic Complexation

SCR-6.5.6.1 **FEP Numbers: W68, W69, and W71**
FEP Titles: Organic Complexation (W68)
Organic Ligands (W69)
Kinetics of Organic Complexation (W71)

SCR-6.5.6.1.1 Screening Decision: UP (W68 and W69)
SO-C (W71)

The effects of anthropogenic *Organic Complexation* reactions, including the effects of *Organic Ligands*, humic, and fulvic acids, have been incorporated in the PA calculations. The kinetics of organic ligand complexation is screened out because the rate at which organic ligands are complexed to actinide is so fast that it has no consequence to repository performance.

SCR-6.5.6.1.2 Summary of New Information

These FEPs have been updated with references to the newest waste inventory (Van Soest 2025) and the most recent solubility calculations (Domski 2025). FEPs W68 and W69 continue to be screened in as UP.

SCR-6.5.6.1.3 Screening Argument

From a PA standpoint, the most important actinides are Th, U, Np, Pu, and Am (Kicker 2025). Dissolved Th, U, Np, Pu, and Am will essentially speciate entirely as Th(IV), U(IV) or, Np(IV), Pu(III) or Pu(IV), and Am(III) under the strongly reducing conditions expected as a result of the presence of Fe(II) and microbes (see Appendix SOTERM-2026, Section SOTERM-6.4). New WIPP-specific data on the effects of organic complexation on uranium, neptunium, plutonium, and neodymium (as an analog for americium) are summarized in Appendix SOTERM-2026, Section 5.0. This new information does not affect the screening argument or decision for these FEPs.

Some organic ligands can increase the actinide dissolved concentrations. An estimate of masses of the complexing agents in TRU waste scheduled for disposal in the WIPP is presented by Van Soest (Van Soest 2025). Acetate, citrate, oxalate, and EDTA were determined to be the only

water-soluble and actinide-complexing organic ligands present in significant quantities in the inventory. These ligands and their complexation with actinides (Th(IV), U(VI), Np(V), and Am(III)) in a variety of ionic strength media were studied at Florida State University (FSU) (Choppin et al. 2001). The FSU studies showed that acetate, citrate, oxalate, and EDTA are capable of significantly enhancing dissolved An concentrations.

The effects of organic ligands on actinide solubility were not simulated for the CCA, because (1) the thermodynamic database for organic complexation of actinides was not considered adequate at the time, and (2) side-calculations using thermodynamic data for low-ionic-strength NaCl solutions showed that transition metals (in particular iron, nickel, chromium, vanadium, and manganese present in waste drum steel) would compete effectively with the actinides for the binding sites on the organic ligands, thus preventing significant complexation of actinides.

The solubilities of the actinides are calculated using EQ3/6, a software package for calculating actinide concentration limits based on thermodynamic parameters. The parameters for EQ3/6 are derived both from experimental investigations specifically designed to provide parameter values for this model and from the published literature. The CRA-2026 calculations include the effects of organic ligands (acetate, citrate, EDTA, and oxalate) on actinide solubilities in the EQ3/6 calculations (Domski 2025). Competing metal ions (Ca, Mg, and Fe) are included in the thermodynamic database and simulations to account for competitive complexation with these ligands. However, Fe–EDTA complexation is suppressed in the simulations due to its high stability relative to Am–EDTA, which would otherwise dominate the speciation. Fe–citrate complexes are retained, as they do not significantly influence total Am concentrations under the modeled conditions (Domski 2025).

Solution complexation reactions of most metal ions with common inorganic ligands, such as carbonate and hydroxide, and with organic ligands, such as acetate, citrate, oxalate, and EDTA, are kinetically very fast, reaching equilibrium in fractions of a second, an inconsequentially short time increment on the scale of the 10,000-yr regulatory period. Reactions of these types are generally so fast that special techniques must be adopted to measure the reaction rates; as a practical matter, the reaction rate is limited by the mixing rate when metal solutions are combined with ligand solutions (Alimarin, 1973). Furthermore, the conceptual model assumes instantaneous equilibrium, which includes instantaneous complexation reactions.

For that reason, the rate at which organic ligands are complexed to actinide is of no consequence to repository performance. Kinetics of organic complexation may be eliminated from PA calculations on the basis of no consequence.

Organic ligands can also influence potential retardation of radionuclides in geologic materials. Organic ligand concentration in repository brine could reduce K_ds in the Culebra. The impact of organic ligands on K_d ranges used in radionuclide transport calculations was included in PA for the CRA-2009 PABC (Clayton 2009). The CRA-2026 uses these ranges (Wilgus and Bethune 2025).

SCR-6.5.6.1.4 FEP Implementation in PA

W68 *Organic Complexation* and W69 *Organic Ligands* are included in the UP scenario and associated with the Dissolved Actinide Source Term and Colloidal Actinide Source Term conceptual models. W68 and W69 are implemented by the EQ3/6 and PANEL codes.

SCR-6.5.6.2 **FEP Number: W70**
FEP Title: Humic and Fulvic Acids

SCR-6.5.6.2.1 Screening Decision: UP

The presence of *Humic Acids* and *Fulvic Acids* is incorporated in PA calculations.

SCR-6.5.6.2.2 Summary of New Information

No new information has been identified that affects the screening of this FEP since the CRA-2019. A summary of the implementation of this FEP within PA has been provided.

SCR-6.5.6.2.3 Screening Argument

The occurrence of humic acids and fulvic acids is incorporated in PA calculations in the models for radionuclide transport by humic colloids (see Appendix PA-4.3).

SCR-6.5.6.2.4 FEP Implementation in PA

W70 *Humic and Fulvic Acids* is associated with the Colloidal Actinide Source Term and the Transport of Dissolved Actinides in the Culebra conceptual models. W70 is implemented in the PA calculation by the PANEL and SECOTP2D codes.

SCR-6.5.7 Chemical Effects on Material Properties

SCR-6.5.7.1 **FEP Numbers: W74, and W76**
FEP Titles: Chemical Degradation of Shaft Seals (W74)
Microbial Growth on Concrete (W76)

SCR-6.5.7.1.1 Screening Decision: UP (W74 and W76)

The effects of *Chemical Degradation of Shaft Seals*, and *Microbial Growth on Concrete* are accounted for in PA.

SCR-6.5.7.1.2 Summary of New Information

Previously, FEPs W74 and W76 were grouped with FEP W115. FEPs W74 and W76 are now screened in a separate group for clarity. The new grouping does not affect the screening of these FEPs and no new information was identified for these FEPs.

SCR-6.5.7.1.3 Screening Argument

The concrete used in the shaft seal systems will degrade as a result of chemical reaction with the infiltrating groundwater. Degradation could lead to an increase in permeability of the seal system. The main uncertainties with regard to cement degradation rates at the WIPP are the effects of groundwater chemistry, the exact nature of the cementitious phases present, and the rates of brine infiltration. The PA calculations take a conservative approach to these uncertainties by assuming a large increase in permeability of the concrete seals only a few hundred years after closure. These permeability values are based on seal design considerations and consider the potential effects of degradation processes. Therefore, the effects of chemical degradation of shaft seals are accounted for in PA through the CDFs used for seal material permeabilities.

Concrete can be inhabited by alkalophilic bacteria, which could produce acids, thereby accelerating the seal degradation process. Nitrification processes, which will produce nitric acid, tend to be aerobic, and will be further limited at the WIPP by the low availability of ammonium in the brines (Pedersen and Karlsson 1995, p. 75). Because of the limitations on growth caused by the chemical conditions, it is likely that the effects of microbial growth on concrete will be small. The effects of such microbial activity on seal properties are, therefore, implicitly accounted for in PA through the CDFs used for seal material permeabilities.

SCR-6.5.7.1.4 FEP Implementation in PA

Chemical degradation of the Shaft Seals (W74) and *Microbial Growth on Concrete* (W76) are incorporated into the Shaft and Shaft Seals and Repository Fluid Flow conceptual models as implemented by the BRAGFLO code in the PA calculations.

SCR-6.5.7.2 FEP Number: W75
FEP Title: Chemical Degradation of Backfill

SCR-6.5.7.2.1 Screening Decision: SO-C

The effects on material properties of the *Chemical Degradation of Backfill* have been eliminated from PA calculations on the basis of low consequence.

SCR-6.5.7.2.2 Summary of New Information

No new information has been identified that affects the screening of this FEP since the CRA-2019.

SCR-6.5.7.2.3 Screening Argument

Degradation of the chemical conditioners or backfill added to the disposal room is a prerequisite of their function in buffering the chemical environment of the disposal room. However, the chemical reactions (Snider 2001) and dissolution involved will change the physical properties of the material. Because the mechanical and hydraulic characteristics of the backfill have been eliminated from PA calculations on the basis of low consequence to the performance of the disposal system, the effects of the chemical degradation of backfill on material properties have been eliminated from PA calculations on the same basis.

SCR-6.5.7.3 **FEP Numbers: W111**
FEP Title: Panel Closure Chemical Composition (W111)

SCR-6.5.7.3.1 Screening Decision: SO-C

The *Panel Closure Chemical Composition* has been eliminated from PA calculations on the basis of low consequence to the performance of the disposal system.

SCR-6.5.7.3.2 Summary of New Information

This FEP has been updated by separating it from joint screening with FEP W8, *Shaft Seal Chemical Composition*. This separate screening argument best reflects the PCS composition of ROM salt and lack of similarity with shaft seals, which are composed of multiple materials. Additionally, the screening decision has changed from "SO-C Beneficial," to "SO-C."

SCR-6.5.7.3.3 Screening Argument

The primary construction element for panel closures is ROM salt (U.S. EPA 2014). Therefore, from a chemical standpoint, the panel closures are identical to the host rock of the repository. For the ROM salt PCS, choosing to ignore any sorptive properties potentially present in closure is consistent with other modeling assumptions that relate to the repository environment. Radionuclide concentrations in brine are modeled to remain constant throughout each vector and are not reduced through sorption by any closure component, regardless of its composition, even though impurities in the host rock and ROM salt (such as clays) have sorptive properties.

The EPA's panel closure rulemaking (U.S. EPA 2014) stated "the panel closure system will be constructed using a steel bulkhead as a construction aid." This construction aid is not designed as a long-term closure component and is not discussed here. It is acknowledged that due to its steel composition it will corrode like other iron-based repository elements. This corrosion has no impact or effect upon the ROM salt PCS performance. Effects of iron corrosion are discussed in FEPs W49 *Gases from Metal Corrosion*, and W51 *Chemical Effects of Corrosion*.

The effect of *Panel Closure Chemical Composition* on actinide mobilization has been eliminated from PA calculations on the basis of low consequence to the performance of the disposal system.

SCR-6.5.7.4 **FEP Number: W115**
FEP Title: Chemical Degradation of Panel Closures (W115)

SCR-6.5.7.4.1 Screening Decision: SO-P

The Chemical Degradation of Panel Closures has been screened out based on low probability.

SCR-6.5.7.4.2 Summary of New Information

There is no new information relating to FEP W115 *Chemical Degradation of Panel Closures*. However, for the CRA-2026, it has been separated from group screening (formerly screened with W74 *Chemical Degradation of Shaft Seals* and W76 *Microbial Growth on Concrete*) and has been screened independently. This is considered an editorial change and does not affect the technical content of the screening argument or decision.

SCR-6.5.7.4.3 Screening Argument

The panel closures will be constructed of ROM salt. Due to the salt construction, chemical degradation is not expected to occur to the ROM salt PCS. Steel bulkheads are used as a construction aid when emplacing the ROM salt PCS as noted in EPA's panel closure rulemaking (U.S. EPA 2014). These bulkheads are not considered a sealing component of the ROM salt PCS. It is acknowledged that they will corrode, like other steel objects within the repository such as roof bolts, chain link, and other iron-based objects. Effects of metal corrosion are discussed in FEPs W49 *Gases from Metal Corrosion* and W51 *Chemical Effects of Corrosion*. Therefore, the *Chemical Degradation of Panel Closures* (ROM salt element) has been eliminated from consideration based on low probability of occurrence.

SCR-6.6 Contaminant Transport Mode FEPs

SCR-6.6.1 Solute and Colloid Transport

SCR-6.6.1.1 **FEP Number: W77**
FEP Title: Solute Transport

SCR-6.6.1.1.1 Screening Decision: UP

Transport of dissolved radionuclides is accounted for in PA.

SCR-6.6.1.1.2 Summary of New Information

The screening argument for this FEP has been updated for clarity and a summary of the implementation of *Solute Transport* within PA has been added.

SCR-6.6.1.1.3 Screening Argument

Solute transport may occur in the Salado Formation by advection, while in the Culebra member of the Rustler Formation Transport may occur by advection, dispersion, and diffusion down chemical potential gradients, and is accounted for in PA (see Appendix PA-4.4 and PA-4.10).

SCR-6.6.1.1.4 FEP Implementation in PA

Solute Transport is incorporated into the Actinide Transport in the Salado conceptual model as implemented by the PA code NUTS and the Transport of Dissolved Actinides in the Culebra and Transport of Colloidal Actinides in the Culebra conceptual models as implemented by the PA code SECOTP2D. Note that dispersion is included in the SECOTP2D governing equations, however, both the transverse and longitudinal dispersivities are set to 0 in the Culebra model, so the dispersion tensor reduces to molecular diffusion.

SCR-6.6.1.2 FEP Numbers: W78, W79, W80, and W81

FEP Titles:
Colloidal Transport (W78)
Colloidal Formation and Stability (W79)
Colloidal Filtration (W80)
Colloidal Sorption (W81)

SCR-6.6.1.2.1 Screening Decision: UP

Formation of colloids, transport of colloidal radionuclides, and colloid retardation through filtration and sorption are accounted for in PA.

SCR-6.6.1.2.2 Summary of New Information

The colloidal source term is updated by Kaplan et al. (Kaplan et al. 2025) and Mariner (Mariner 2025) based on the updated inventory information presented by Van Soest (Van Soest 2025). These updates do not alter the screening arguments or decisions presented here. A summary of the implementation of these FEPs in PA has been provided.

SCR-6.6.1.2.3 Screening Argument

Colloids typically have sizes of between 1 nm and 1 μm and may form stable dispersions in groundwaters. Colloid formation and stability depend on their composition and the prevailing chemical conditions (for example, salinity). Depending on their size, colloid transport may occur at different rates than those of fully dissolved species. They may be physically excluded from fine porous media, and their migration may be accelerated through fractured media in channels where velocities are greatest. However, they can also interact with the host rocks during

transport and become retarded. These interactions may be of a chemical or physical nature and include electrostatic effects leading to colloid sorption, and sieving leading to colloid filtration and pore blocking. Colloidal formation and stability is accounted for in PA through estimates of colloid numbers in the disposal room based on the prevailing chemical conditions (Appendix SOTERM-2026, Section SOTERM-3.5). Colloidal sorption, colloidal filtration, and colloidal transport in the Culebra are accounted for in PA (Appendix GEOCHEM-2026, Section GEOCHEM-5.0). New WIPP-relevant data regarding colloid formation and transport can be found in Appendix SOTERM-3.5.1. This information does not affect the screening argument or decision for these FEPs.

SCR-6.6.1.2.4 FEP Implementation in PA

W78 *Colloidal Transport* and W80 *Colloidal Filtration* are included in the UP scenario and associated with the Actinide Transport in the Salado and Transport of Colloidal Actinides in the Culebra conceptual models. W78 and W80 are implemented in the PA by the NUTS and SECOTP2D codes. W79 *Colloidal Formation and Stability* and W81 *Colloidal Sorption* are associated with the Colloidal Actinide Source Term conceptual model. W79 and W81 are implemented by the PANEL code.

SCR-6.6.2 Particle Transport

SCR-6.6.2.1 **FEP Numbers: W82, W83, W84, W85, and W86**
FEP Titles: Suspension of Particles (W82)
Rinse (W83)
Cuttings (W84)
Cavings (W85)
Spallings (W86)

SCR-6.6.2.1.1 Screening Decision: DP (W84, W85, W86)
SO-C (W82, W83)

The formation of *Suspended Particles* through *Rinse* and subsequent transport of radionuclides in groundwater and brine has been eliminated from PA calculations for undisturbed conditions on the basis of low consequence to the performance of the disposal system. The transport of radionuclides as part of the waste matrix (cuttings, cavings, and spallings) during penetration of the repository by a borehole, is accounted for in PA.

SCR-6.6.2.1.2 Summary of New Information

The screening decision for FEP W82 has been revised to SO-C to eliminate inconsistencies within the FEPs baseline. This screening designation is consistent with that used in the CCA (DOE 1996a), and places the proper emphasis on dissolved and colloidal actinides as currently implemented in PA. An implementation summary has been provided for those FEPs within this group that are screened into PA calculations.

SCR-6.6.2.1.3 Screening Argument

Suspension of Particles that have sizes larger than colloids are unstable because the particles undergo gravitational settling. It is unlikely that brine flow will be rapid enough within the WIPP disposal rooms to generate particulate suspensions through rinse and transport under undisturbed conditions. Mobilization of suspensions could cause a local and minor redistribution of radionuclides within the room and would not result in increased radionuclide transport from the repository. The formation of particulates through rinse and transport of suspended radionuclides in groundwater and brine have been eliminated from PA calculations for undisturbed conditions on the basis of low consequence to the performance of the disposal system. Transport of dissolved and colloidal actinides are accounted for in PA and are discussed in Sections SCR-6.6.1 and SCR-6.6.2.

Inadvertent human intrusion into the repository by a borehole could result in transport of waste material to the ground surface through drilling-induced flow and blowouts (FEPs H21 and H23, Section SCR-5.2.1.1). This waste could include material intersected by the drill bit (cuttings), material eroded from the borehole wall by circulating drilling fluid (cavings), and material that enters the borehole as the repository depressurizes (spallings). Transport of radionuclides by these materials and in brine is accounted for in PA in DP scenarios.

SCR-6.6.2.1.4 FEP Implementation in PA

Cuttings, and *Cavings,* are represented in the "Cuttings and Cavings" conceptual model and implemented in PA by the CUTTINGS_S code. Releases via *Spallings* are represented by the "Spallings" conceptual model and are calculated by the PA code, DRSPALL. Further implementation details are provided in Appendix PA-4.6 and PA-4.7.

SCR-6.6.3 Microbial Transport

SCR-6.6.3.1 **FEP Number: W87**
FEP Title: Microbial Transport

SCR-6.6.3.1.1 Screening Decision: UP

Transport of radionuclides bound to microbes is accounted for in PA.

SCR-6.6.3.1.2 Summary of New Information

Model parameters for colloidal actinide enhancement (including biocolloids) have been updated for CRA-2026 (Kaplan et al. 2025). New data are from experiments with the +3 analog, neodymium, and several microbial isolates from the WIPP near-field. Results show that bioassociation is variable between organisms but correlates with matrix composition: less association is observed in Generic Weep Brine (GWB) than in Energy Research and Development Administration Well 6 (ERDA-6) brine (Swanson 2025b). This new information does not affect the screening decision for this FEP.

SCR-6.6.3.1.3 Screening Argument

Indigenous or introduced microorganisms can serve as vectors for transport of radionuclides bound to their surfaces or internalized within cells. Radionuclide transport only occurs if the cells themselves are mobile. This transport is accounted for in PA. This information does not affect the screening argument or decision for this FEP.

SCR-6.6.3.1.4 FEP Implementation in PA

W87 *Microbial Transport* is included in the UP scenario and radionuclide transport by microorganisms is accounted for in PA. This FEP is associated with the Colloidal Actinide Source Term and Actinide Transport in the Salado conceptual models. Microbial Transport is implemented in the PANEL and NUTS codes.

SCR-6.6.3.2 FEP Number: W88
FEP Title: Biofilms

SCR-6.6.3.2.1 Screening Decision: SO-C Beneficial

The effects of *Biofilms* on microbial transport have been eliminated from PA calculations on the basis of beneficial consequence to the performance of the disposal system.

SCR-6.6.3.2.2 Summary of New Information

The screening argument for this FEP has been updated based on new information. The screening decision is not affected due to this update.

SCR-6.6.3.2.3 Screening Argument

The formation of biofilms under WIPP repository conditions has not been specifically investigated, and biofilm presence was not documented in the early gas generation experiments. Regardless, a biofilm existence is preferred to a planktonic one in all natural settings (Flemming et al. 2016). Biofilms can protect cells from environmental stressors, such as radionuclide exposure, by sequestering the radionuclides within the extracellular polymeric fraction and away from adhered cells. This results in a radionuclide sink (Van Hullenbusch et al. 2003; Harrison et al. 2007; Flemming et al. 2016). Therefore, this effect has been eliminated from PA calculations on the basis of beneficial consequence to the performance of the disposal system.

SCR-6.6.4 Gas Transport

SCR-6.6.4.1 **FEP Number: W89**
FEP Title: Transport of Radioactive Gases

SCR-6.6.4.1.1 Screening Decision: SO-C

FEP W89 *Transport of Radioactive Gases* has been excluded from PA calculations on the basis of low consequence to the performance of the disposal system.

SCR-6.6.4.1.2 Summary of New Information

FEP W89 *Transport of Radioactive Gases* discussion has been updated to include recent inventory information (Kicker 2025; Van Soest 2025) and the lack of undisturbed releases in CRA-2026 (Appendix PA-7.2). This new information does not affect the screening argument or decision for this FEP.

SCR-6.6.4.1.3 Related FEP

The related FEP, W55 *Radioactive Gas*es (Section SCR-6.5.1.11) has also been excluded from PA calculations on the basis of low consequence.

SCR-6.6.4.1.4 Screening Argument

Transport of radioactive gases have been excluded from PA calculations because the inventory and production of radioactive gases have been excluded on the basis of low consequence to the performance of the disposal system. As described in FEP W55 *Radioactive Gas*, Carbon-14 (^{14}C) and radon gas have an insignificant potential for release from the repository due to their small inventory and short half-lives.

SCR-6.7 Contaminant Transport Processes

SCR-6.7.1 Advection

SCR-6.7.1.1 **FEP Number: W90**
FEP Title: Advection

SCR-6.7.1.1.1 Screening Decision: UP

Advection of contaminants is accounted for in PA.

SCR-6.7.1.1.2 Summary of New Information

This screening argument has been updated to describe how radionuclide release can occur by advection. A summary of the implementation of this FEP has also been provided.

SCR-6.7.1.1.3 Related FEPs

FEPs W78 *Colloid Transport,* W91 *Diffusion* and W92 *Matrix Diffusion* (SCR-6.7.2) are directly related to W90 *Advection* in the fractured Culebra dolomite above the repository and also included in PA calculations.

SCR-6.7.1.1.4 Screening Argument

Radionuclide release to the accessible environment potentially occurs sometime in the future either (1) to the surface immediately after a borehole is inadvertently drilled into the disposal area or (2) to the outer boundary of the disposal system via (a) advection in the disposal area, and (b) leakage through degraded seals of the abandoned intrusion borehole and then advection and diffusion through the fractured Culebra Dolomite Member of the Rustler Formation.[x] Advection is the primary transport process for radionuclides in the second pathway; hence, FEP W90 *Advection* is included in the PA calculations.

SCR-6.7.1.1.5 FEP Implementation in PA

FEP W90 *Advection* is included in three conceptual models, as described in the following sections: *Actinide Transport in the Salado, Transport of Dissolved Actinides in the Culebra,* and *Transport of Colloidal Actinides in the Culebra.*

SCR-6.7.1.1.5.1 Actinide Transport in the Salado

Advective transport of radionuclides in and near the disposal area is part of the *Actinide Transport in the Salado* conceptual model, which is one of 24 conceptual models included in the exposure consequence model for evaluating radionuclide releases from the disposal region (Appendix PA-4.1, Eq. PA.21). The *Actinide Transport in the Salado* conceptual model is implemented by NUTS (WIPP Performance Assessment 2022a), which models advective transport of dissolved radionuclides and colloids carrying radionuclides within the disposal area and up an intrusion borehole.

The partial differential equation for the conservation of radionuclide transport in and out of computational cells that make up the repository and surrounding Salado Formation, as solved by NUTS, is (Appendix PA -4.4.1, Eq. PA.76 and PA.77;)

$$-\nabla \cdot \Delta z \boldsymbol{v}_{brn}^{vel} C_r^{conc} = \Delta z \frac{\partial}{\partial t}\left(\phi_{advect}^{pore} S_{brn}^{sat} C_r^{conc}\right) + \Delta z \phi_{advect}^{pore} S_{brn}^{sat} C_r^{conc} \lambda_r^{decay}$$
$$-\Delta z \phi_{advect}^{pore} S_{brn}^{sat} \sum_p C_p^{conc} \lambda_p^{decay} - \Delta z \Gamma_r^{precip} \quad \text{for } r=1,2,\ldots,n_r \qquad \text{(SCR.46)}$$

where Δz is the spatial dimension perpendicular to flow (m); $\boldsymbol{v}_{brn}^{vel}$ is the Darcy brine flow velocity (or specific discharge) as calculated by BRAGFLO (m/s) (WIPP Performance Assessment 2025); C_r^{conc} and C_p^{conc} are the concentration of radionuclide *r* and its parents *p* in the Culebra brine, respectively (kg/m^3); ϕ_{advect}^{pore} is the material porosity as used by BRAGFLO; S_{brn}^{sat} is the

[x] Although radionuclide releases to the accessible environment through sealed shafts and along marker beds prior to an inadvertent drilling intrusion are plausible, no releases occurred via this pathway in CRA-2019 and CRA-2026 (Appendix PA-2019, Section PA-7.2; Appendix PA-2026, Section PA-7.2).

porous media saturation as calculated by BRAGFLO (dimensionless); λ_r^{decay} and λ_p^{decay} are the decay constant for radionuclide *r* and its parents *p* (s^{-1}); and Γ_r^{precip} is loss/gain from precipitation/redissolution between radionuclide *r* in the brine and solid immobile phase in the disposal area ((kg/s)/m^3). As apparent from Eq. SCR.46, NUTS only models advective transport of radionuclides (i.e., $\boldsymbol{v}^{vel}C_r^{conc}$). Geochemical reactions such as precipitation are also included but only in the disposal area. Sorption retardation, molecular dispersion, and mechanical dispersion are disregarded.

SCR-6.7.1.1.5.2 Transport of Dissolved Actinides in Culebra and Transport of Colloidal Actinides in the Culebra

Advective transport of radionuclides in Culebra dolomite is part of the *Transport of Dissolved Actinides in the Culebra* and *Transport of Colloidal Actinides in the Culebra* conceptual models, which are two of 24 conceptual models included in the exposure consequence model for evaluating radionuclide releases from the disposal region (Appendix PA-4.1, Eq. PA.17). These two conceptual models are implemented by SECOTP2D (WIPP Performance Assessment 2022b) and used to analyze the advective transport of a unit source term of dissolved radionuclides and colloids through the fractured Culebra Dolomite Member of the Rustler Formation (via an abandoned intrusion borehole after plugs fail). The fractional release results from the unit source term analyzed by SECOTP2D are convolved with the NUTS results, described above, to calculate a realized release. SECOTP2D models advective transport (i.e., $\mathbf{v}^{vel}C_r^{conc}$) with sorption retardation, molecular dispersion, and mechanical dispersion in the Culebra dolomite, but SECOTP2D does not model geochemical reactions. SECOTP2D uses a dual porosity (advective/diffusive) formulation. The diffusive transport in the fractures of the Culebra dolomite and diffusion into the Culebra dolomite matrix is described in the related FEPs W91 *Diffusion* and W92 *Matrix Diffusion* (SCR-6.7.2).

The partial differential equation for the conservation of the flux of radionuclide *r* in and out of computational cells that make up the Culebra dolomite, as solved by SECOTP2D, is (Appendix PA-2026, Eq. PA.237; Wilgus and Bethune 2025; WIPP Performance Assessment 2022b)

$$\nabla \cdot \left[\phi_{advect}^{frac}\boldsymbol{D}_r^{disperse}\nabla C_r^{conc} - \boldsymbol{v}_{brn}^{vel}C_r^{conc}\right] = \phi_{advect}^{frac}R_r^{frac}\left(\frac{\partial}{\partial t}C_r^{conc}\right)$$

$$+\phi_{advect}^{pore}R_r^{frac}C_r^{conc}\lambda_r^{decay} - \phi_{advect}^{pore}R_p^{frac}C_p^{conc}\lambda_p^{decay} - Q_r^{inject} - \Gamma_r^{diff} \text{ for } r=1,2\ldots n_r \quad \text{(SCR.47)}$$

where $\phi_{advect}^{pore}\phi_{advect}^{pore}$ is the advective (i.e., fracture) porosity (dimensionless); $\boldsymbol{D}_r^{disperse}$ is the hydrodynamic dispersion tensor (m^2/s); $\boldsymbol{v}_{brn}^{vel}$ is the Darcy velocity (or specific discharge) of Culebra brine is calculated by MODFLOW6 model when implementing the *Culebra Hydrogeology* conceptual model and discussed with FEP N23 *Saturated Groundwater Flow* ((m^3/m^2)/s); C_r^{conc} and C_p^{conc} are the concentration of radionuclide *r* and its parent in the Culebra brine, respectively (kg/m^3); R_r^{frac} and R_p^{frac} are the advective retardation coefficient for

radionuclide *r* and its parent *p* and set to one in PA calculations (dimensionless) λ_r^{decay} and λ_p^{decay} are the decay constant for radionuclide *r* and its parent (s^{-1}); Q_r^{inject} is the injection rate of one unit into the fractures of radionuclide *r* per bulk volume of Culebra dolomite into the fractures ((kg/s)/m^3); and Γ_r^{diff} is the loss/gain of radionuclide *r* from/to the fracture to the matrix via diffusion per bulk volume of Culebra dolomite ((kg/s)/m^3), as described in W92 *Matrix Diffusion* (SCR-6.7.2).

SCR-6.7.2 Diffusion

SCR-6.7.2.1 **FEP Numbers: W91 and W92**
FEP Titles: Diffusion (W91)
Matrix Diffusion (W92)

SCR-6.7.2.1.1 Screening Decision: UP

W91 *Diffusion* of radionuclides and physical retardation of radionuclides by W92 *Matrix Diffusion* are included in PA calculations.

SCR-6.7.2.1.2 Summary of New Information

The screening arguments for these FEPs have been updated for clarity and with new information that relates to their implementation within PA.

SCR-6.7.2.1.3 Related FEP

FEPs W91 *Diffusion* and W92 *Matrix Diffusion* are directly related to FEP W90 *Advection*, which is also included in PA calculations.

SCR-6.7.2.1.4 Screening Argument

Matrix diffusion (i.e., movement of molecules into the surrounding rock matrix transverse to the direction of advective flow within a fracture) provides important physical retardation of radionuclides moving through the geologic barrier, such as the Culebra dolomite, and is included in PA calculations. Diffusion (i.e., the movement of radionuclides parallel to the direction of advection in response to Brownian forces) can be important in regions of slow advective flow in the geologic barrier and is also included in PA calculations.

SCR-6.7.2.1.5 FEP Implementation in PA

The exposure consequence model for evaluating radionuclide releases from the disposal region is a complex composite function (Appendix PA -4.1, Eq. PA.17;). A major submodel of this composite consequence model, SECOTP2D (WIPP Performance Assessment 2022b), implements the dual (advective/diffusive) porosity conceptual model for dissolved radionuclide and colloidal transport through the fractured Culebra Dolomite Member of the Rustler Formation where radionuclides reach the Culebra dolomite via an abandoned intrusion borehole after plugs fail

(i.e., Dissolved Actinides [Culebra] and Colloidal Actinides [Culebra] conceptual models[y] described in CCA-1996) (U.S. DOE 1996a, Appendix PEER, Section 2.1.1).

Specifically, the SECOTP2D implements W91 *Diffusion* and W92 *Matrix Diffusion* as follows. The partial differential equation for the conservation of the flux of radionuclide *r* in and out of computational cells that make up the fractures in the Culebra dolomite of the geologic barrier, as solved by SECOTP2D, is (Appendix PA -4.10, Eq. PA.237;)

$$\nabla\left[\varphi^{frac}\boldsymbol{D}_{\boldsymbol{r}}^{disperse}\nabla C_r^{frac} - \boldsymbol{v}_{brn}^{vel}C_r^{frac}\right] = \varphi^{frac}R_r^{frac}\left(\frac{\partial}{\partial t}C_r^{frac}\right) + \varphi^{frac}R_r^{frac}C_r^{frac}\lambda_r^{decay} - \varphi^{frac}R_p^{frac}C_p^{frac}\lambda_p^{decay} + Q_r^{inject} - \Gamma_r^{diff}$$

for r=1,2…n_r (SCR.48)

where φ^{frac} is the fracture (i.e., advective) porosity (dimensionless); $\boldsymbol{D}_{\boldsymbol{r}}^{disperse}$ is the hydrodynamic dispersion tensor (m^2/s); $\boldsymbol{v}_{brn}^{vel}$ is the Darcy velocity (or specific discharge) of Culebra brine, as calculated by the fluid flow model MODFLOW6 ((m^3/m^2)/s); C_r^{frac} and C_p^{frac} are the fracture concentration of radionuclide *r* and its parent in the Culebra brine, respectively (kg/m^3); R_r^{frac} and R_p^{frac} are the advective fracture retardation coefficient for radionuclide *r* and its parent and set to one in PA calculations (dimensionless) λ_r^{decay} and λ_p^{decay} are the decay constant for radionuclide *r* and its parent (s^{-1}); Q_r^{inject} is the injection rate into the fractures of radionuclide *r* per unit bulk volume of Culebra dolomite into the fractures ((kg/s)/m^3); and Γ_r^{diff} is the loss/gain of radionuclide *r* from the fracture to/from the matrix via diffusion per unit bulk volume of Culebra dolomite ((kg/s)/m^3).

The hydrodynamic dispersion tensor is defined by

$$\boldsymbol{D}_{\boldsymbol{r}}^{disperse} = \frac{1}{\|\boldsymbol{v}\|\boldsymbol{\varphi}^{\boldsymbol{matrix}}}\begin{bmatrix} u & -v \\ v & u \end{bmatrix}\begin{bmatrix} \alpha_L & 0 \\ 0 & \alpha_T \end{bmatrix}\begin{bmatrix} u & v \\ -v & u \end{bmatrix} + \tau^{frac}D_r^*\begin{bmatrix} 1 & 0 \\ 0 & 1 \end{bmatrix} \quad \text{(SCR.49)}$$

where *u* and *v* are the x and y velocity components of **v** (i.e., **v**=[*v*, *u*]). In the WIPP PA, the longitudinal and transverse dispersivity (α_L and α_T) are set to zero and the fracture tortuosity (τ^{frac}) is set to one. Thus, the hydrodynamic dispersion tensor in Eq. (SCR.49) reduces to

$$\boldsymbol{D}_{\boldsymbol{r}}^{disperse} = D_r^*\begin{bmatrix} 1 & 0 \\ 0 & 1 \end{bmatrix} \quad \text{(SCR.50)}$$

[y] Other conceptual models related to Dissolved Actinides (Culebra) and Colloidal Actinides (Culebra) include (DOE 1996a, Appendix PEER, Section 2.1.1) (1) Culebra: simplification of Culebra dolomite stratigraphy, (2) Dissolved Actinide Source Term; in disposal area, and (3) Colloidal Actinides Source Term: in disposal area.

where D_r^* is the molecular free-water diffusion coefficient for radionuclide *r* (m^2s^{-1}). Eqs. SCR.48 and SCR.50 implement W91 *Diffusion* in the PA calculations.

The partial differential equation for the conservation of flux in the matrix surrounding the fractures, as solved by SECOTP2D, is (Appendix PA-4.10, Eq. PA.244)

$$\frac{\partial}{\partial \mathrm{c}}\left(\varphi^{matrix} D_r^{matrix} \frac{\partial C_r^{matrix}}{\partial \mathrm{c}}\right) = \varphi^{matrix} R_r^{matrix} \frac{\partial C_r^{matrix}}{\partial \mathrm{t}} + \varphi^{matrix} R_r^{matrix} \lambda_r^{decay} C_r^{matrix} - \varphi^{matrix} R_p^{matrix} \lambda_p^{decay} C_p^{matrix} \text{ for } r=1,2,\ldots,n_r \quad \text{(SCR.51)}$$

where χ is the spatial coordinate in the matrix perpendicular to the fracture, φ^{matrix} is the matrix porosity (dimensionless); D_r^{matrix} is the matrix diffusion coefficient for radionuclide *r* (m^2s^{-1}); C_r^{matrix} and C_p^{matrix} are the fracture concentration of radionuclide *r* and its parent *p* in the Culebra brine, respectively (kg/m^3); R_r^{matrix} and R_p^{matrix} are the matrix retardation coefficient for radionuclide *r* and its parent *p* (dimensionless); λ_r^{decay} and λ_p^{decay} are the decay constant for radionuclide *r* and its parent *p* (s^{-1}).

The matrix diffusion coefficient D_r^{matrix} in the PA calculations is defined by

$$D_r^{matrix} = \tau^{matrix} D_r^* \quad \text{(SCR.52)}$$

where τ^{matrix} is matrix tortuosity and D_r^* is the molecular free-water diffusion coefficient for radionuclide *r* (m^2s^{-1}). Eqs. SCR.51 and SCR.52 implement *W92 Matrix Diffusion* in the PA calculations.

The coupling between Eq. SCR.48 and Eq. SCR.51 occurs through Γ_r^{diff} at the interface between the fracture and matrix (χ=0); specifically,

$$\Gamma_r^{diff} = -\frac{2\varphi^{frac}}{b}\left(\varphi^{matrix} D_r^{matrix} \frac{\partial C_r^{matrix}}{\partial \mathrm{c}}\Big|_{\mathrm{c}=0}\right) \quad \text{(SCR.53)}$$

where $b = \varphi^{frac} B(1 - \varphi^{frac})$ and *B* is matrix half-block length (m) of the fractured Culebra dolomite ($0 \le \chi \le B$).

SCR-6.7.3 Thermochemical Transport Phenomena

SCR-6.7.3.1 **FEP Number: W93**
FEP Title: Soret Effect

SCR-6.7.3.1.1 Screening Decision: SO-C

The effects of thermochemical transport phenomena (the *Soret Effect*) have been eliminated from PA calculations on the basis of low consequence to the performance of the disposal system.

SCR-6.7.3.1.2 Summary of New Information

FEP W93 *Soret Effect* has been updated to include the discussion of thermal heat produced from radioactive decay and exothermal reactions of aluminum corrosion, cement hydration, microbial degradation, and MgO hydration, based on the latest inventory data (Van Soest 2025; Kicker 2025). Heat from radioactive decay and exothermal reactions is still low and does not affect the screening argument or decision for this FEP.

SCR-6.7.3.1.3 Related FEPs

As discussed in FEP W91 *Diffusion,* all solute diffusion is excluded in the disposal area because of low consequence.

Related FEPs that may produce heat and temperature gradients are discussed in (1) W13 *Heat from Radioactive Decay* (SCR-6.2.1.2), and (2) W72 *Exothermic Reactions* (SCR-6.3.4.1). The heat produced is low; thus, these FEPs have been excluded because of low consequence. Another potential source of heat is W14 *Nuclear Criticality Heat* (SCR-6.2.1.3), which has been excluded because of low probability.

SCR-6.7.3.1.4 Screening Argument

Because temperature gradients are small in the disposal region (as discussed in FEPs W72 *Exothermic Reactions* and W13 *Heat from Radioactive Decay*), radionuclide diffusion from a temperature gradient (Soret diffusion) is much less than diffusion from a concentration gradient (Fickian diffusion). Furthermore, all solute diffusion is excluded in the disposal area when assessing direct releases to the surface after an inadvertent drilling intrusion because of low consequence, as discussed in FEP W91 *Diffusion.* Thus, Soret diffusion is also excluded in the disposal area because of low consequence.

After an inadvertent drilling intrusion, advective transport of radionuclides in fractures is by far the most important transport process for evaluating releases through the Culebra dolomite outside of the disposal area (FEP W90 *Advection*). Although solute diffusion is included in transporting radionuclides in the Culebra dolomite (FEP W91 *Diffusion)*, solute diffusion is most important in moving radionuclides into the Culebra matrix (FEP W92 *Matrix Diffusion*), which retards advective transport of radionuclides. Neglecting any small additional Soret diffusion

would be conservative. Nonetheless, Soret diffusion is less than in the disposal region and thus negligible because temperature gradients along the Culebra dolomite are much less. Consequently, Soret diffusion is also excluded outside the disposal area because of low consequence.

The screening argument is elaborated upon as follows. According to Fick's law, solute diffusion is proportional to the solute concentration gradient. In the presence of a temperature gradient, solute diffusion is also proportional to the temperature gradient (the Soret effect). Thus, the mass conservation equation for solute diffusion in the presence of concentration and temperature gradients in a liquid is

$$\frac{\partial C}{\partial t} = \nabla g(D\nabla C + ND\nabla T) \quad \text{(SCR.54)}$$

where *C* is the solute concentration, *T* is the temperature of the liquid, *D* is the solute diffusion coefficient, and

$$N = S_T C(1 - C) \quad \text{(SCR.55)}$$

in which S_T is the Soret coefficient.

When temperature gradients exist in solutions with both light and heavy solute molecules, the heavier molecules tend to concentrate in the colder regions of the solution. Large temperature gradients are required for Soret diffusion to be significant compared to Fickian diffusion.

Radioactive decay and exothermic reactions are two possible sources of heat in the WIPP repository. As discussed in FEP *W13 Heat from Radioactive Decay*, temperature increases of about 3 °C (5.4 °F) may occur at RH-TRU containers over 100 to 300 years. As discussed in FEP W72 *Exothermic Reactions* and W73 *Concrete Hydration* (Section SCR-6.3.4.1), the temperature rise in the disposal panels will be less than ~4 °C (7 °F) as a consequence of the simultaneous contributions from aluminum corrosion, cement hydration, MgO hydration, microbial degradation or CO_2 capture with some contribution from radioactive decay.

Soret diffusion generated by temperature gradients of this magnitude are negligible compared to Fickian diffusion. Furthermore, all solute diffusion is excluded in the disposal region as discussed in FEP W91 *Diffusion.*

Temperature gradients along the transport pathway through the Culebra dolomite are even less than in the disposal region. Exothermic reactions do not occur because potential reactants that produce heat are not transported in an unreacted state. Only radionuclide decay during transport outside the disposal area can potentially produce small amounts of heat in the Culebra dolomite. However, the earliest time for transport outside the disposal area is 300 years after closure when short-lived radionuclides in RH-TRU waste will have decayed because active institution control prevents intrusion for 100 years and an elapsed time of 200 years is required for borehole seal degradation. Hence, Fickian diffusion will dominate in the Culebra dolomite.

The limited magnitude of temperature gradients in the disposal system suggest that Soret diffusion will be insignificant. Consequently, the effects of thermochemical transport (Soret diffusion) are excluded from PA calculations on the basis of low consequence to the performance of the disposal system.

SCR-6.7.4 Electrochemical Transport Phenomena

SCR-6.7.4.1 **FEP Number: W94**
FEP Title: Electrochemical Effects

SCR-6.7.4.1.1 Screening Decision: SO-C

The effects of electrochemical transport phenomena caused by electrochemical reactions have been eliminated from PA calculations on the basis of low consequence to the performance of the disposal system.

SCR-6.7.4.1.2 Summary of New Information

No new information that affects the screening of this FEP has been identified since the CRA-2019.

SCR-6.7.4.1.3 Screening Argument

The variety of waste metals and metal packaging in the repository may allow galvanic cells spanning short distances to be established. The interactions among the metals depend upon their physical characteristics and the chemical conditions in the repository. For example, good physical and electrical contact, which is critical to the establishment of galvanic cells, may be impeded by electrically nonconductive waste materials. Additionally, in order to establish a galvanic cell, it is necessary that the metals have different values for standard reduction potentials. For example, a galvanic cell is not expected to be formed by contact of two segments of metals with identical compositions. As a result, galvanic cells can only be established by contact of dissimilar metals, as might happen because of contact between a waste drum and the contents, or between contents within a waste package. The localized nature of electrochemical transport is restricted to the size scale over which galvanic cells can develop, i.e., on the order of size of waste packages. Since the possible range of transport is restricted by the physical extent of galvanic activity, electrochemical effects cannot act as long-range transport mechanisms for radionuclides and therefore are of no consequence to the performance of the repository.

SCR-6.7.4.2 **FEP Number: W95**
FEP Title: Galvanic Coupling (outside the repository)

SCR-6.7.4.2.1 Screening Decision: SO-P

The effects of *Galvanic Coupling* between the waste and metals external to the repository on transport have been eliminated from PA calculations on the basis of low probability of occurrence over 10,000 yrs.

SCR-6.7.4.2.2 Summary of New Information

No new information that affects the screening of this FEP has been identified since the CRA-2019.

SCR-6.7.4.2.3 Screening Argument

With regard to the WIPP, galvanic coupling refers to the establishment of galvanic cells between metals in the waste form, canisters, and other metals external to the waste form.

Long-range electric potential gradients may exist in the subsurface as a result of groundwater flow and electrochemical reactions. The development of electric potential gradients may be associated with the weathering of sulfide ore bodies, variations in rock properties at geological contacts, bioelectric activity associated with organic matter, natural corrosion reactions, and temperature gradients in groundwater. With the exception of mineralization potentials associated with metal sulfide ores, the magnitude of electric potentials is usually less than about 100 millivolts (mV) and the potentials tend to average to zero over distances of several thousand feet (Telford et al. 1976). Metals external to the waste form can include natural metallic ore bodies in the host rock. However, metallic ore bodies and metallic sulfide ores do not exist in the region of the repository (the CCA, Appendix GCR). As a result, galvanic coupling between the waste and metallic materials outside the repository cannot occur. Therefore, galvanic coupling is eliminated from PA calculations on the basis of low probability of occurrence over 10,000 yrs.

SCR-6.7.4.3 **FEP Number: W96**
FEP Title: Electrophoresis

SCR-6.7.4.3.1 Screening Decision: SO-C

The effects of electrochemical transport phenomena caused by *Electrophoresis* have been eliminated from PA calculations on the basis of low consequence to the performance of the disposal system.

SCR-6.7.4.3.2 Summary of New Information

No new information that affects the screening of this FEP has been identified since the CRA-2019.

SCR-6.7.4.3.3 Screening Argument

Long range (in terms of distance) electric potential gradients may exist in the subsurface as a result of groundwater flow and electrochemical reactions. The development of potentials may be associated with the weathering of sulfide ore bodies, variations in rock properties at geological contacts, bioelectric activity associated with organic matter, natural corrosion reactions, and temperature gradients in groundwater. With the exception of mineralization potentials associated with metal sulfide ores, the magnitude of such potentials is usually less than about 100 mV and the potentials tend to average to zero over distances of several thousand feet (Telford et al. 1976, p. 458). Short range potential gradients caused by the corrosion of metals within the waste may be set up over distances that are restricted to the size scale of the waste packages.

A variety of metals will be present within the repository as waste metals and metal packaging, which may allow electrochemical cells to be established over short distances. The types of interactions that will occur depend on the metals involved, their physical characteristics, and the prevailing solution conditions. Electrochemical cells that may be established will be small relative to the size of the repository, limiting the extent to which migration of contaminants by electrophoresis can occur. The electric field gradients will be of small magnitude and confined to regions of electrochemical activity in the area immediately surrounding the waste material. As a result, electrophoretic effects on migration behavior caused by both long- and short-range potential gradients have been eliminated from PA calculations on the basis of low consequence to the performance of the disposal system.

SCR-6.7.5 Physiochemical Transport Phenomena

SCR-6.7.5.1 **FEP Number: W97**
FEP Title: Chemical Gradients

SCR-6.7.5.1.1 Screening Decision: SO-C

The effects of enhanced diffusion across *Chemical Gradients* have been eliminated from PAs on the basis of low consequence to the performance of the disposal system.

SCR-6.7.5.1.2 Summary of New Information

This FEP has been updated with new information regarding colloidal enhancement parameters (Kaplan et al. 2025).

SCR-6.7.5.1.3 Screening Argument

Chemical gradients within the disposal system, whether induced naturally or resulting from repository material and waste emplacement, may influence the transport of contaminants. Gradients will exist at interfaces between different repository materials and between repository and geological materials. Distinct chemical regimes will be established within concrete seals and adjoining host rocks. Similarly, chemical gradients will exist between the waste and the surrounding rocks of the Salado. Other chemical gradients may exist because of the juxtaposition of relatively dilute groundwaters and brines or between groundwaters with different compositions. Natural gradients currently exist between different groundwaters in the Culebra.

Enhanced diffusion is a possible consequence of chemical gradients that occur at material boundaries. However, the distances over which enhanced diffusion could occur will be small in comparison to the size of the disposal system (see also Section SCR-6.7.5.4). Processes that may be induced by chemical gradients at material boundaries include the formation or destabilization of colloids. The colloidal enhancement parameters for mineral, intrinsic, and microbial colloids were reassessed for the CRA-2019 PA (Reed et al. 2019) and recently updated for intrinsic and microbial colloids (Kaplan et al. 2025). The most important observations for mineral colloids are: (1) there is no evidence for the formation of significant amounts of magnesium-derived mineral colloid species, and (2) iron oxides can lead to long-term and relatively small plutonium mineral colloids in these brine systems, and the concentrations observed are within the current enhancement parameter values (Reed et al. 2013, Section 4.3). Microbial transport is discussed in FEP W87 (see Section SCR-6.6.3.1). As such, the impact of chemical gradients has been eliminated from PA on the basis of low consequence.

SCR-6.7.5.2 **FEP Number: W98**
FEP Title: Osmotic Processes

SCR-6.7.5.2.1 Screening Decision: SO-C

The effects of *Osmotic Processes* have been eliminated from PA calculations on the basis of beneficial consequence to the performance of the disposal system.

SCR-6.7.5.2.2 Summary of New Information

No new information that affects the screening of this FEP has been identified since the CRA-2019.

SCR-6.7.5.2.3 Screening Argument

Osmotic processes, i.e., diffusion of water through a semipermeable or differentially permeable membrane in response to a concentration gradient, may occur at interfaces between waters of different salinities. Osmotic processes can occur if waters of different salinities and/or compositions exist on either side of a particular lithology such as clay, or a lithological boundary

that behaves as a semipermeable membrane. At the WIPP, clay layers within the Salado may act as semipermeable membranes across which osmotic processes may occur.

In the absence of a semipermeable membrane, water will move from the more dilute water into the more saline water. However, the migration of dissolved contaminants across an interface may be restricted depending upon the nature of the membrane. A hydrological gradient across a semipermeable membrane may either enhance or oppose water movement by osmosis depending on the direction and magnitude of the gradient. Dissolved contaminants that cannot pass through a semipermeable membrane may be moved towards the membrane and concentrated along the interface when advection dominates over osmosis and reverse osmosis occurs. Thus, both osmosis and reverse osmosis can restrict the migration of dissolved contaminants and possibly lead to concentration along interfaces between different water bodies. The effects of osmotic processes have been eliminated from PA calculations on the basis of beneficial consequence to the performance of the disposal system.

SCR-6.7.5.3 **FEP Number: W99**
FEP Title: Alpha Recoil

SCR-6.7.5.3.1 Screening Decision: SO-C

The effects of *Alpha Recoil* processes on radionuclide transport have been eliminated from PA calculations on the basis of low consequence to performance of the disposal system.

SCR-6.7.5.3.2 Summary of New Information

No new information that affects the screening of this FEP has been identified since the CRA-2019.

SCR-6.7.5.3.3 Screening Argument

Alpha particles are emitted with sufficiently high energies that daughter nuclides recoil appreciably to conserve system momentum. For example, ^{238}U decays to ^{234}Th with emission of a 4.1 MeV alpha particle. The law of conservation of momentum requires that the daughter nuclide, ^{234}Th, recoils in the opposite direction with an energy of approximately 0.07 MeV. The energy is great enough to break chemical bonds or cause ^{234}Th to move a short distance through a crystal lattice. If the ^{234}Th is close enough to the surface of the crystal, it will be ejected into the surroundings. ^{234}Th decays to ^{234}Pa which decays to ^{234}U with respective half-lives of 24.1 days and 1.17 minutes. The recoil and decay processes can lead to the apparent preferential dissolution or leaching of ^{234}U relative to ^{238}U from crystal structures and amorphous or adsorbed phases. Preferential leaching may be enhanced because of radiation damage to the host phase resulting from earlier radioactive decay events. Because of apparent preferential dissolution and radiation damage, ^{234}U may exhibit apparent enhanced transport behavior relative to ^{238}U in laboratory settings.

The influence of alpha recoil processes on radionuclide transport through natural geologic media is dependent on many site-specific factors, such as mineralogy, geometry, and microstructure of the rocks, as well as geometrical constraints on the type of groundwater flow, e.g., porous or fracture flow. Studies of natural radionuclide-bearing groundwater systems often fail to discern a measurable effect of alpha-recoil processes on radionuclide transport above the background uncertainty introduced by the spatial heterogeneity of the geological system. Consequently, the effects of the alpha recoil processes that occur on radionuclide transport are thought to be minor. These effects have therefore been eliminated from PA calculations on the basis of low consequence to the performance of the disposal system.

SCR-6.7.5.4 **FEP Number: W100**
FEP Title: Enhanced Diffusion

SCR-6.7.5.4.1 Screening Decision: SO-C

Enhanced diffusion is a possible consequence of chemical gradients that occur at material boundaries. However, the distances over which enhanced diffusion could occur will be small in comparison to the size of the disposal system. Therefore, the effects of *Enhanced Diffusion* across chemical gradients at material boundaries have been eliminated from PAs on the basis of low consequence to the performance of the disposal system.

SCR-6.7.5.4.2 Summary of New Information

No new information that affects the screening of this FEP has been identified since the CRA-2019.

SCR-6.7.5.4.3 Screening Argument

Enhanced diffusion only occurs where there are higher than average chemical gradients. The spatial extent of chemical gradients should be quite limited and as enhanced diffusion occurs, it will tend to reduce the chemical gradient. Thus, the driving force for the enhanced diffusion will be reduced and eventually eliminated as the system approaches steady state or equilibrium conditions. Because of the limited spatial extent of enhanced diffusion, its effect on radionuclide transport should be small.

Processes that may be induced by chemical gradients at material boundaries include the formation or destabilization of colloids. For example, cementitious materials, emplaced in the WIPP as part of the waste and the seals, contain colloidal-sized phases such as calcium-silicate-hydrate gels and alkaline pore fluids. Chemical gradients will exist between the pore fluids in the cementitious materials and the less-alkaline surroundings. Chemical interactions at these interfaces may lead to the generation of colloids of the inorganic, mineral-fragment type. Colloidal compositions may include calcium and MgO, calcium hydroxide, calcium-aluminum silicates, calcium-silicate-hydrate gels, and silica. Concentrations of colloidal suspensions originating from concrete within the repository are considered in PA calculations even though expected to be extremely low.

Distinct interfaces between waters of different salinities and different densities may limit mixing of the water bodies and affect flow and contaminant transport. Such effects have been eliminated from PA calculations on the basis of low consequence to the performance of the disposal system.

The effects of enhanced diffusion across chemical gradients at material boundaries have been eliminated from PAs on the basis of low consequence to the performance of the disposal system.

SCR-6.8 Ecological FEPs

SCR-6.8.1 Plant, Animal, and Soil Uptake

SCR-6.8.1.1 **FEP Numbers: W101, W102, and W103**
FEP Titles: Plant Uptake (W101)
Animal Uptake (W102)
Accumulation in Soils (W103)

SCR-6.8.1.1.1 Screening Decision: **SO-R for section 191.13 (W101, W102)**
SO-C Beneficial for section 191.13 (W103)
SO-C for section 191.15 (W101, W102, W103)

Plant Uptake, *Animal Uptake*, and *Accumulation in Soils* have been excluded from compliance assessment calculations for 40 CFR 191.15, Individual Protection Requirements, on the basis of low consequence. *Plant Uptake* and *Animal Uptake* in the accessible environment have been excluded from PA calculations for 40 CFR 191.13, Containment Requirements, on regulatory grounds. *Accumulation in Soils* within the controlled area has been eliminated from compliance assessment calculations for 40 CFR 191.13, Containment Requirements, on the basis of beneficial consequences.

SCR-6.8.1.1.2 Summary of New Information

As of CRA-2026, no releases occur through either the shaft seals or laterally through the marker beds for the UP scenario (Appendix PA-2026, Section PA-7.2), which is the scenario that applies to 40 CFR 191.15, Individual Protection Requirements. Therefore, FEPs related to plant, animal, and soil uptake are excluded from the WIPP performance assessment.

SCR-6.8.1.1.3 Screening Argument

As described in Section PA-7.2 of CRA-2026, “Radionuclide Transport,” releases to the accessible environment under undisturbed conditions (either through the sealed shafts or laterally through the marker beds at repository depth) do not occur. Thus, for evaluating compliance with the EPA’s Individual Protection Requirements in 40 CFR 191.15, FEPs that relate to plant uptake, animal uptake, and accumulation in soils have been excluded from compliance assessment calculations on the basis of low consequence.

The WIPP PA evaluating compliance with the EPA's Containment Requirements, 40 CFR 191.13, need not consider radionuclide migration in the accessible environment. Therefore, FEPs that relate to plant uptake and animal uptake in the accessible environment have been excluded from PA calculations on regulatory grounds. Accumulation in soils that may occur within the controlled area would reduce releases to the accessible environment and can, therefore, be excluded from PA calculations on the basis of beneficial consequence.

SCR-6.8.2 Human Uptake

SCR-6.8.2.1 **FEP Numbers: W104, W105, W106, W107, and W108**

FEP Titles: Ingestion (W104)
Inhalation (W105)
Irradiation (W106)
Dermal Sorption (W107)
Injection (W108)

SCR-6.8.2.1.1 Screening Decision: SO-R
SO-C for section 191.15

Ingestion, *Inhalation*, *Irradiation*, *Dermal Sorption*, and *Injection* have been excluded from compliance assessment calculations for 40 CFR 191.15, Individual Protection Requirements on the basis of low consequence. FEPs that relate to human uptake in the accessible environment have been excluded from PA calculations for 40 CFR 191.13, Containment Requirements, on regulatory grounds.

SCR-6.8.2.1.2 Summary of New Information

As of CRA-2026, no releases occur through either the shaft seals or laterally through the marker beds for the UP scenario (Appendix PA-2026, Section PA-7.2). The UP scenario is used to assess compliance with 40 CFR 191.15, Individual Protection Requirements. Therefore, the FEPs related to human uptake of radionuclides are excluded from the PA calculations.

SCR-6.8.2.1.3 Screening Argument

As described in Appendix PA-7.2, "Radionuclide Transport," releases to the accessible environment under undisturbed conditions (either through the sealed shafts or laterally through the marker beds at repository depth) do not occur. Thus, for evaluating compliance with the EPA's Individual Protection Requirements, 40 CFR 191.15, FEPs that relate to human uptake have been excluded from compliance assessment calculations on the basis of low consequence.

The performance assessment evaluating compliance with the EPA's Containment Requirements, 40 CFR 191.13 need not consider radionuclide migration in the accessible environment. Therefore, FEPs that relate to human uptake in the accessible environment have been excluded from PA calculations on regulatory grounds.

SCR-7.0 REFERENCES

(*Indicates a reference that has not been previously submitted.)

Adler, H.H. 1974. Concepts of Uranium-Ore Formation in Reducing Environments in Sandstones and Other Sediments, Proceedings of Symposium on Formation of Uranium Ore Deposits, Athens, Greece, May 6-10, 141, STI/PUB/374; IAEA-SM-183/43; Vienna, Austria: International Atomic Energy Agency (1974).*

Alimarin, I.P. 1973. Kinetics of Complex Formation of Metals with Organic Ligands in Analytical Chemistry. Pure and Applied Chemistry 34: 1-11.

Altmaier, M., V. Neck, and T. Fanghänel. 2008. Solubility of Zr(IV), Th(IV) and Pu(IV) Hydrous Oxides in $CaCl_2$ Solutions and the Formation of Ternary Ca-M(IV)-OH Complexes. Radiochimica Acta, vol. 96: 541-550.

Altenheinhaese, C., H., H. Bischoff, L. Fu, J. Mao, and G. Marx. 1994. Adsorption of Actinides on Cement Compounds. Journal of Allows and Compounds, vol. 213: 553–56.

Ams D.A., Swanson J.S., Szymanowski J.E.S., Fein J.B., Richmann M., Reed D.T. 2013. The Effect of High Ionic Strength on Neptunium(V) Adsorption to a Halophilic Bacterium. Geochimica et Cosmochimica Acta 110: 45-57.

Anderson, R.Y. 1978. Deep Dissolution of Salt, Northern Delaware Basin, New Mexico. Report to Sandia National Laboratories. Albuquerque, NM: Sandia National Laboratories. ERMS 229530.

Anderson, R.Y., W.E. Dean, Jr., D.W. Kirkland, and H.I. Snider. 1972. Permian Castile Varved Evaporite Sequence, West Texas and New Mexico. Geological Society of America Bulletin, vol. 83, no. 1: 59–85. ERMS 241261.

Anderson, R.Y., and D.W. Powers. 1978. Salt Anticlines in Castile-Salado Evaporite Sequence, Northern Delaware Basin. Geology and Mineral Deposits of Ochoan Rocks in Delaware Basin and Adjacent Areas: New Mexico Bureau of Mines and Mineral Resources (pp. 79–84), Circular 159. G.S. Austin, ed. ERMS 241419.

Arguello, J.G., and T.M. Torres. 1988. Thermal Effects of RH-TRU Waste Emplacement on WIPP Storage Room Thermal/Structural Response. SAND88-2217. Albuquerque, NM: Sandia National Laboratories.*

Attia, S., M.T. Heizler, and J. Ricci. 2023, Quaternary age of the Gatuña Formation at Livingston Ridge: New Mexico Geological Society Guidebook, 73rd Fall Field Conference.*

Bachman, G.O. 1974. Geologic Processes and Cenozoic History Related to Salt Dissolution in Southeastern New Mexico. Denver, CO: U.S. Geological Survey. Open-File Report 74-194. ERMS 243249.

Bachman, G.O. 1980. Regional Geology and Cenozoic History of Pecos Region, Southeastern New Mexico. Denver, CO: U.S. Geological Survey. Open-File Report 80-1099. ERMS 241268.

Bachman, G.O. 1981. Geology of Nash Draw, Eddy County, New Mexico. Denver, CO: U.S. Geological Survey. Open-File Report 81-31. ERMS 241265.

Bachman, G.O. 1985. Assessment of Near-Surface Dissolution at and Near the Waste Isolation Pilot Plant (WIPP), Southeastern New Mexico. Albuquerque, NM: Sandia National Laboratories. SAND84-7178. ERMS 224609.

Bachman, G.O. 1987a. Stratigraphy and Dissolution of the Rustler Formation. The Rustler Formation at the WIPP Site: Report of a Workshop on the Geology and Hydrology of the Rustler Formation as it Relates to the WIPP Project (pp. 16–25). L. Chaturvedi, ed. Carlsbad, NM, March 1985. Santa Fe, NM: EEG-34, Environmental Evaluation Group. ERMS 249769.

Bachman, G.O. 1987b. Karst in Evaporites in Southeastern New Mexico. Albuquerque, NM: Sandia National Laboratories. SAND86-7078. ERMS 224006.

Barnhart, B.J., R. Hallet, D.E. Caldwell, E. Martinez, and E.W. Campbell. 1980. Potential Microbial Impact on Transuranic Wastes under Conditions Expected in the Waste Isolation Pilot Plant (WIPP): Annual Report, October 1, 1978–September 30, 1979. Los Alamos, NM: Los Alamos Scientific Laboratory. LA-8297-PR. ERMS 241220.

Batchelor, G.K. 1970. Slender-body theory for particles of arbitrary cross-section in Stokes flow. J. Fluid Mech., vol. 44, part 3, pp. 419-440*

Batchelor, G.K. 1973. An Introduction to Fluid Dynamics. Cambridge: Cambridge UP, London, UK. ERMS 243337.

Baumgardner, R.W., Jr., A.D. Hoadley, and A.G. Goldstein. 1982. Formation of the Wink Sink, a Salt Dissolution and Collapse Feature, Winkler County, Texas. Austin, TX: Bureau of Economic Geology. Report of Investigations No. 114.

Bean, J.E., M.E. Lord, D.A. McArthur, R.J. MacKinnon, J.D. Miller, and J.D. Schreiber. 1996. Analysis Package for the Salado Flow Calculations (Task 1) of the Performance Assessment Analysis Supporting the Compliance Certification Application. Albuquerque, NM: Sandia National Laboratories. EPA Air Docket A-93-02, Item II-G-08. ERMS 420238.

Beauheim, R.L. 1986. Hydraulic-Test Interpretations for Well DOE-2 at the Waste Isolation Pilot Plant (WIPP) Site. Albuquerque, NM: Sandia National Laboratories. SAND86-1364. ERMS 227656.

Beauheim, R.L. 2002. Analysis Plan for Evaluation of the Effects of Head Changes on Calibration of Culebra Transmissivity Fields: Analysis Plan AP-088. (Rev. 1). Carlsbad, NM: Sandia National Laboratories. ERMS 522085.

Beauheim, R.L., and R.M. Holt. 1990. Hydrogeology of the WIPP site, in Powers, D.W., Holt, R.M., Beauheim, R.L., and Rempe, N., eds., Geological and Hydrological Studies of Evaporites in the Northern Delaware Basin for the Waste Isolation Pilot Plant (WIPP): Guidebook 14. Geological Society of America (Dallas Geological Society), p. 45-78. ERMS 246378.

Beauheim, R.L., B.W. Hassinger, and J.A. Klaiber. 1983. Basic Data Report for Borehole Cabin Baby-1 Deepening and Hydrologic Testing, Waste Isolation Pilot Plant (WIPP) Project, Southeastern New Mexico. Carlsbad, NM: Westinghouse Electric Corporation. WTSD-TME-020. ERMS 241315.

Beauheim, R.L., and Roberts, R.M., 2002, Hydrology and hydraulic properties of a bedded evaporite formation: Journal of Hydrology, v. 259, p. 66-88.*

Beauheim, R.L., and G.J. Ruskauff. 1998. Analysis of Hydraulic Tests of the Culebra and Magenta Dolomites and Dewey Lake Redbeds Conducted at the Waste Isolation Pilot Plant Site. Albuquerque, NM: Sandia National Laboratories. SAND98-0049. ERMS 251839.

Bennett, D. 1996. Formation and Transport of Radioactive Gases. Summary Memorandum of Record for GG-8 and RNT-26. 16 May 1996. Albuquerque, NM: Sandia National Laboratories. SWCF-A 1.2.07.3: PA: QA: TSK: GG-8, RNT-26. ERMS 415478.

Bennett, D.G., D. Read, M. Atkins, F.P. Glasser. 1992. A Thermodynamic Model for Blended Cements II: Cement Hydrate Phases; Thermodynamic Values and Modeling Studies. Journal of Nuclear Materials, vol. 190: 315–15. ERMS 241221.

Bennett, D., Y. Wang, and T. Hicks. 1996. Memorandum to Distribution (Subject: An Evaluation of Heat Generation Processes for the WIPP). 20 August 1996. Albuquerque, NM: Sandia National Laboratories. ERMS 240635.

Bérest, P., H. Gharbi, B. Brouard, D. Brückner, K. DeVries, G. Hévin, G. Hofer, C. J. Spiers, and J. Urai. 2019. Very slow creep tests on salt samples. Rock Mechanics and Rock Engineering. Vol. 52. No. 9. Pg. 2917-2934. DOI: 10.1007/s00603-019-01778-9.

Berner, R.A. 1981. Kinetics of Weathering and Diagenesis, in Kinetics of Geochemical Processes. A.C. Lasaga, and R.J. Kirkpatrick, eds. Washington, DC: Mineralogical Society of America. Reviews in Mineralogy, vol. 8: 111–33. ERMS 241361.

Bethune, J. 2023a. Screening Calculation for FEP W23 Subsidence. Carlsbad, NM: Sandia National Laboratories. ERMS 580693.*

Bethune, J. 2023b. Analysis Report for Culebra Flow and Transport in the Replacement Panels Planned Change Request (RPPCR) and Compliance Recertification Application Performance Assessment (CRA-2024). Carlsbad, NM: Sandia National Laboratories. ERMS 579725.*

Blackwell, D.D., J.L. Steele, and L.S. Carter. 1991. Heat-Flow Patterns of the North American Continent: A Discussion of the Geothermal Map of North America. D.B. Slemmons, E.R. Engdahl,

M.D. Zoback, and D.D. Blackwell, eds. Boulder, CO: Geological Society of America. Neotectonics of North America (pp. 423-436). ERMS 241460.

Bodine, M.W., Jr., and Lohr, C.A., 1978, Selected investigations of igneous dikes intruding Ochoan sediments in the Carlsbad region, Interim report (Jan. 6, 1978): report to Sandia National Laboratories.*

Borns, D.J. 1987. Structural Development of Evaporites in the Northern Delaware Basin. Guidebook 18: Geology of the Western Delaware Basin, West Texas and Southeastern New Mexico. D.W Powers and W.C. James, eds. El Paso, TX: El Paso Geological Society. (pp. 80–97). ERMS 235759.

Borns, D.J., L.J. Barrows, D.W. Powers, and R.P. Snyder. 1983. Deformation of Evaporites Near the Waste Isolation Pilot Plant (WIPP) Site. Albuquerque, NM: Sandia National Laboratories. SAND82-1069. ERMS 227532.

Borns, D.J., and S.E. Shaffer. 1985. Regional Well-Log Correlation in the New Mexico Portion of the Delaware Basin. Albuquerque, NM: Sandia National Laboratories. SAND83-1798. ERMS 224511.

Bowman, C.D., and F. Venneri. 1996. Underground Supercriticality from Plutonium and Other Fissile Material, Science and Global Security, 5(3), 279-302.

Bowman, D.O., R. Kushnereit, M. Pedrazas, P. Johnson, N. Deeds, and J. Pinkard. 2023. Analysis Report for AP-203: Analysis Report Documenting the Data, Generation, and Calibration of T-Fields for CRA-2024. ERMS 579507. Carlsbad, NM: Sandia National Laboratories.*

Brausch, L.M., Kuhn, A.K., Register, J.K. 1982. Natural Resources Study, Waste Isolation Pilot Plant (WIPP) Project, Southeastern New Mexico. Carlsbad, NM: U.S. Department of Energy. WTSD-TME-3156. ERMS 239094.

Bredehoeft, J.D., F.S. Riley, and E.A. Roeloffs. 1987. Earthquakes and Groundwater. Earthquakes and Volcanoes, vol. 19, no. 4: 138–46. ERMS 241635.

Brickner, B.D. 2019. Post Placement Nuclear Criticality Evaluations Involving 6- and 12-Inch Pipe Overpack TRU Waste Containers at the Waste Isolation Pilot Plant. October 2019. Oak Ridge, TN: Oak Ridge National Laboratory. ORNL/TM-2019/1222.

Brokaw, A.L., C.L. Jones, M.E. Cooley, and W.H. Hays. 1972. Geology and Hydrology of the Carlsbad Potash Area, Eddy and Lea Counties, New Mexico. Denver, CO: U.S. Geological Survey. Open File Report 4339-1. ERMS 243356.

Brookins, D.G., 1980, K-Ar age of lamprophyre dike from the Kerr-McGee potash mine, southeastern New Mexico: Isochron/West, v. 29, p. 27-28.*

Brookins, D.G., 1981 Geochronologic studies near the WIPP site, southeastern New Mexico, *in*, Wells, S.G., Lambert, W., and Callender, J.F., eds., Environmental Geology and Hydrology in New Mexico: Special Publication 10, New Mexico Geological Society, p. 147-152.*

Brunell, S., B. Day, P. Docherty, D. Kicker, S. Kim, S. King, J. Long, J. Wilgus, and T. Zeitler. 2025. Summary Report for the 2026 Compliance Recertification Application Performance Assessment: Interim State Repository. 2026. Carlsbad, NM: Sandia National Laboratories.*

Bruno, J., and A. Sandino. 1987. Radionuclide Co-Precipitation. Stockholm: Swedish Nuclear Fuel and Waste Management Co. SKB Technical Report, no. 87-23. ERMS 241222.

Brush, L.H. 1996. Memorandum to M.S. Tierney (Subject: Ranges and Probability Distributions of K_ds for Dissolved Pu, Am, U, Th, and Np in the Culebra for the PA Calculations to Support the CCA). (June 10, 1996). Albuquerque, NM: Sandia National Laboratories. ERMS 238801.

Brush, L.H., and L.J. Storz. 1996. Memorandum to M.S. Tierney (Subject: Revised Ranges and Probability Distributions of K_ds for Dissolved Pu, Am, U, Th, and Np in the Culebra for the PA Calculations to Support the CCA). (July 24, 1996). Albuquerque, NM: Sandia National Laboratories. ERMS 241561.

Bryson, D. 2015. Letter to Mr. Jonathan D. Edwards, Director, Radiation Protection Division. (Subject: Response to the U.S. Environmental Protection Agency Letters Dated February 27, 2015 and June 5, 2015 Regarding the 2014 Compliance Recertification Application). (September 5, 2015). Carlsbad, NM: Department of Energy, Carlsbad Field Office.

Burton, P.L., J.W. Adams, and C. Engwall. 1993. History of the Washington Ranch, Eddy County, New Mexico. New Mexico Geological Society Guidebook. 44th Field Conference, Carlsbad Region, New Mexico and West Texas. D.W. Love, J.W. Hawley, B.S. Kues, J.W. Adams, G.W. Austin, and J.M. Barker, eds. Roswell, NM: New Mexico Geological Society. ERMS 241273.

Caldwell, D.E., M.A. Molecke, E. Martinez, and B.J. Barnhart. 1988. Rates of CO2 Production from the Microbial Degradation of Transuranic Wastes under Simulated Geologic Isolation Conditions. Sandia National Laboratories: Albuquerque, NM. SAND87-7170

Camphouse, R.C., M. Gross, C.G., Herrick, D.C. Kicker, and B. Thompson. 2012 Memo to WIPP Records Center. (Subject: Recommendations and Justifications of Parameter Values for the Run-of-Mine Salt Panel Closure System Design Modeled in the PCS-2012 PA). (May 3, 2012). Carlsbad, NM. Sandia National Laboratories. ERMS 557396.

Cauffman, T.L., A.M. LaVenue, and J.P. McCord. 1990. Ground-Water Flow Modeling of the Culebra Dolomite, Volume II: Data Base. Albuquerque, NM: Sandia National Laboratories. SAND89-7068/2. ERMS 210551.

Chapman, J.B. 1986. Stable Isotopes in Southeastern New Mexico Groundwater: Implications for Dating Recharge in the WIPP Area, EEG-35, DOE/AL/10752-35. Santa Fe, NM: Environmental Evaluation Group. ERMS 241274.

Chapman, J.B. 1988. Chemical and Radiochemical Characteristics of Groundwater in the Culebra Dolomite, Southeastern New Mexico. EEG-39. Santa Fe, NM: New Mexico Environmental Evaluation Group. ERMS 241223.

Chappell, J., and N.J. Shackleton. 1986. Oxygen Isotopes and Sea Level. Nature, vol. 324, no. 6093: 137–40. ERMS 241275.

Choppin, G.R., A.H. Bond, M. Borkowski, M.G. Bronikowski, J.F. Chen, S. Lis, J. Mizera, O. Pokrovsky, N.A. Wall, Y.X. Xia, and R.C. Moore. 2001. Waste Isolation Pilot Plant Actinide Source Term Test Program: Solubility Studies and Development of Modeling Parameters. Albuquerque, NM: Sandia National Laboratories. SAND99-0943. ERMS 518556.

Cisneros-Dozal, L.M., Y. Huang, J. Heikoop, P. Fawcett, J. Fesenden, R. Anderson, P. Meyers, T. Larson, G. Perkins, J. Toney, J. Werne, F. Goff, G. WoldeGabriel, C. Allen, and M. Berke. 2014. Assessing the strength of the monsoon during the late Pleistocene in southwestern United States: Quaternary Science Reviews, v. 103, p. 81-90.*

Claiborne, H.C., and F. Gera. 1974. Potential Containment Failure Mechanisms and Their Consequences at a Radioactive Waste Repository in Bedded Salt in New Mexico. Oak Ridge, TN: Oak Ridge National Laboratory. ORNL-TM-4639. ERMS 241224.

Clayton, D.J. 2009. Update to the K_d values for the PABC-2009. Carlsbad, NM: Sandia National Laboratories. ERMS 552395.

Clayton, D.J., M. J. Martinez, and E. L. Hardin. 2014. Potential Vertical Movement of Large Heat-Generating Waste Packages in Salt. Sandia National Laboratories. Tech Report SAND2013-3596.

Corbet, T.F., and P.M. Knupp. 1996. The Role of Regional Groundwater Flow in the Hydrogeology of the Culebra Member of the Rustler Formation at the Waste Isolation Pilot Plant (WIPP), Southeastern New Mexico. Albuquerque, NM: Sandia National Laboratories. SAND96-2133. ERMS 243482.

Cowan, G.A. 1976. A Natural Fission Reactor, Scientific American, 235(1), 36 (1976).

Cranwell, R.M., R.V. Guzowski, J.E. Campbell, and N.R. Ortiz. 1990. Risk Methodology for Geologic Disposal of Radioactive Waste: Scenario Selection Procedure. Albuquerque, NM: Sandia National Laboratories. NUREG/CR-1667. SAND80-1429. ERMS 226750.

Crawford, B., D. Guerin, S. Lott, W. McInroy, J. McTaggart, and G.D. Van Soest. 2009. Performance Assessment Inventory Report—2008. INV-PA-08, Revision 0, Los Alamos National Laboratory, Carlsbad Operations.*

Cunningham, C. 1999. End of the Santa Fe Trail. September-October 1999. Sulfur, no. 264 ERMS 530223.

D'Appolonia Consulting Engineers, Inc. 1982. Natural Resources Study - Waste Isolation Pilot Plant (WIPP) Project, Southeastern New Mexico (January). Albuquerque, NM: D'Appolonia Consulting Engineers, Inc. NM78-648-813A.

Davies, P.B. 1983. Assessing the Potential for Deep-Seated Salt Dissolution and Subsidence at the Waste Isolation Pilot Plant (WIPP). State of New Mexico Environmental Evaluation Group Conference, WIPP Site Suitability for Radioactive Waste Disposal, Carlsbad, NM, May 12-13, 1983. Albuquerque, NM: Sandia National Laboratories. ERMS 229533.

Davies, P.B. 1989. Variable Density Ground-Water Flow and Paleohydrology in the Waste Isolation Pilot Plant (WIPP) Region, Southeastern New Mexico Denver, CO: U.S. Geological Survey. Open File Report 88-490. ERMS 238854.

Davis, J.A. and D.B. Kent. 1990. Surface Complexation Modeling in Aqueous Geochemistry. Mineral-Water Interface Geochemistry. ERMS 241473. M.F. Hochella and A.F. White, eds. Washington, DC: Mineralogical Society of America. Reviews in Mineralogy vol. 23: pp. 177–260. ERMS 241473.

Dawson, P.R., and J.R. Tillerson. 1978. Nuclear Waste Canister Thermally Induced Motion. Albuquerque, NM: Sandia National Laboratories. SAND78-0566. ERMS 227328.

Day, B.A. 2013. Calculation of CH and RH Payload Container Waste Volumes. PLD-CAL-0001, Revision 1. Carlsbad, NM: Nuclear Waste Partnership.

Day, B.A. 2019a. Analysis Package for Salado Flow in the 2019 Compliance Recertification Application Performance Assessment (CRA-2019 PA). Carlsbad, NM: Sandia National Laboratories. ERMS 571368.

Day, B.A. 2019b. Reassessment of Need and Parameter Justification for Modeling Gas Generation due to Radiolysis of Brine and Cellulose/Plastic/Rubber in WIPP for CRA-2019. (February 12, 2019). Carlsbad, NM: Sandia National Laboratories. ERMS 570873.

Day, K. 2023. Memo to Steve Wagner. Subject: "Borehole Plugging Practices White Paper". Carlsbad, NM: Los Alamos Technical Associates. ERMS 578970. *

De Marsily, G. 1986. Groundwater Hydrology for Engineers. Quantitative Hydrogeology. London, UK: Academic Press.*

Dence, M.R., R.A.F. Grieve, and P.B. Robertson. 1977. Terrestrial Impact Structures: Principal Characteristics and Energy Considerations. D.J. Roddy, R.O. Pepin, and R.B. Merrill, eds. New York: Permagon. Impact and Explosion Cratering: Planetary and Terrestrial Implications (pp. 247–75).

Dickson, C.L., and F.P. Glasser. 2000. Cerium (III, IV) in Cement–Implications for Actinide (III, IV) Immobilization. Cement and Concrete Research, vol. 30: 1619–23.

Dietz, R.S. 1961. Astroblemes. Scientific American, vol. 205, no. 2: 50–58. ERMS 241226.

Domski, P. 2019. Th(IV), Np(V), and Am(III) Baseline Solubilities and Th(IV) and Am(III) Solubility Uncertainties for the CRA-2019 PA. 2019. Carlsbad, NM: Sandia National Laboratories. ERMS 571169.

Domski, P. and C. Sisk-Scott. 2019. Prediction of Baseline Actinide Solubilities for CRA 2019 with and Updated EQ3/6 Pitzer Thermodynamic Database, DATA0.FM4. Carlsbad, NM: Sandia National Laboratories. ERMS 571178.

Domski, P. 2023. An Update to the WIPP EQ3/6 Database DATA0.FM1 with the Creation of DATA0.FM6. Sandia National Laboratories. Carlsbad, NM. *

Domski, P.S. 2025. Prediction of Baseline Actinide Solubilities for the 2026 WIPP Compliance Recertification Application Performance Assessment Interim-State Analysis (CRA-2026 IS). Carlsbad, NM: Sandia National Laboratories.*

Dowding, C.H., and A. Rozen. 1978. Damage to Rock Tunnels from Earthquake Shaking. Journal of the Geotechnical Engineering Division, American Society of Civil Engineers, vol. 104, No. GT2: 175–91. ERMS 241350.

Dunagan, S.C., G.T. Roselle, E.D. Vugrin, and J.J. Long. 2007. “Analysis Report for the Shielded Container Performance Assessment.” October 31, 2007. Carlsbad, NM: Sandia National Laboratories. ERMS 547197.

Dvory, N.Z., and M.D. Zoback. 2021. Prior oil and gas production can limit the occurrence of injection-induced seismicity: A case study in the Delaware Basin of western Texas and southeastern New Mexico, USA: Geology, v. 49, p. 1198-1203.*

Economy, K. 1996. Memo to Records (Subject: Drilling Into a Salado Contaminated Plume Within the Controlled Area, FEP Side Effort – S9). (July15, 1996). Albuquerque, NM: Sandia National Laboratories. ERMS 416367.

Edwards, J. 2011. Letter to Mr. Edward Ziemianski (Acting CBFO Manager) (Subject: Approval of DOE's PCR to emplace RH waste in shielded containers). (August 8, 2011). U.S. Environmental Protection Agency, Washington, DC.

Ewing, J.E., V.A. Kelley, T.L. Jones, T. Yan, A. Singh, D.W. Powers, R.M. Holt, and J.M. Sharp. 2012. Final Groundwater Availability Model Report for the Rustler Aquifer: report for Texas Water Development Board.*

Falta, R., M. Hu, E. M. Kwicklis, C. I. Steefel, S. C. Williams-Stroud, and J. A. Thies. 2021. Additional Panels Performance Assessment (APPA) Changed Conceptual Models Peer Review Report. Carlsbad, NM: U.S. Department of Energy, Carlsbad Field Office.*

Felicione, F.S., K.P. Carney, and C.C. Dwight. 2001. Results from the Gas Generation Experiments at Argonne National Laboratory-West. Sandia National Laboratories Technical Baseline Reports. Carlsbad, NM: Sandia National Laboratories. July 31, 2001. ERMS 518970.

Feng, L. and D. Kicker. 2025. Input Parameter Report for the 2026 Compliance Recertification Application Performance Assessment: Interim State Repository (CRA-2026 IS). Revision 0. Carlsbad, NM: Sandia National Laboratories*

Flemming, H.-C., J. Wingender, U. Szewzyk, P. Steinberg, S.A. Rice, and S. Kjelleberg. 2016. Biofilms: an emergent form of bacterial life. Nature Reviews Microbiology 14: 563-575.*

Francis, A.J. 1985. Low-Level Radioactive Wastes in Subsurface Soils, in Soil Reclamation Processes: Microbiological Analyses and Applications. R.L. Tate, III and D.A. Klein, eds. New York: Marcel Dekker, Inc. (pp. 279–331). ERMS 241227.

Francis, A.J., and J.B. Gillow. 1994. Effects of Microbial Gas Processes on Generation Under Expected Waste Isolation Pilot Plant Repository Conditions, Progress Report through 1992. Albuquerque, NM: Sandia National Laboratories. SAND93-7036. ERMS 210673.

Francis, A.J., J.B. Gillow, C.J. Dodge, M. Dunn, K. Mantione, B.A. Strietelmeier, M.E. Pansoy-Hjelvik, and H.W. Papenguth, H.W. 1998. Role of Bacteria as Biocolloids in the Transport of Actinides from a Deep Underground Radioactive Waste Repository. Radiochimica Acta 82: 347-354.*

Francis, A.J., and J.B. Gillow. 2000. Memorandum to Y. Wang (Subject: Progress Report: Microbial Gas Generation Program). (January 6, 2000). Upton, NY: Brookhaven National Laboratory. ERMS 509352.

Francis A.J., J.B. Gillow, and M.R. Giles. 1997. Microbial Gas Generation under Expected Waste Isolation Pilot Plant Repository Conditions. Albuquerque, NM: Sandia National Laboratories. SAND96-2582. ERMS 244125.

Froelich, C., H. DeShon, B. Stump, C. Hayward, M. Hornbach, and J.I. Walter. 2016. A historical review of induced earthquakes in Texas: Seismological Research Letters, v. 87, p. 1022-1038.*

Gaona, X., V. Montoya, E. Colàs, E., M. Grivé, and L. Duro. 2008. Review of the Complexation of Tetravalent Actinides by ISA and Gluconate under Alkaline to Hyperalkaline Conditions. Journal of Contaminant Hydrology, vol. 102:217–227.

Gauthier-Lafaye, F., F. Weber, and H. Ohmoto. 1989. Natural Fission Reactors of Oklo, Economic Geology, 84(8), 2286.*

Gillow, J.B., M. Dunn, A.J. Francis, D.A. Lucero, and H.W. Papenguth. 2000. The Potential of Subterranean Microbes in Facilitating Actinide Migration at the Grimsel Test Site and Waste Isolation Pilot Plant, Radiochemica Acta, vol. 88: 769–774.

Gillow, J.B., and A.J. Francis. 2001a. Re-Evaluation of Microbial Gas Generation under Expected Waste Isolation Pilot Plant Conditions: Data Summary Report, January 24, 2001. Carlsbad, NM: Sandia National Laboratories. Sandia National Laboratories Technical Baseline Reports, WBS 1.3.5.4, Repository Investigations Milestone RI010, January 31, 2001 (pp. 19–46). ERMS 516749.

Gillow, J.B., and A.J. Francis. 2001b. Re-Evaluation of Microbial Gas Generation under Expected Waste Isolation Pilot Plant Conditions: Data Summary and Progress Report (February 1 – July 13, 2001), July 16, 2001, Rev. 0. Carlsbad, NM: Sandia National Laboratories. Sandia National Laboratories Technical Baseline Reports, WBS 1.3.5.4, Repository Investigations Milestone R1020, July 31, 2001 (pp. 3-1 through 3-21). ERMS 518970.

Gillow, J.B., and A.J. Francis. 2002a. Re-Evaluation of Microbial Gas Generation under Expected Waste Isolation Pilot Plant Conditions: Data Summary and Progress Report (July 14, 2001 - January 31, 2002), January 22, 2002. Carlsbad, NM: Sandia National Laboratories. Sandia National Laboratories Technical Baseline Reports, WBS 1.3.5.3, Compliance Monitoring; WBS 1.3.5.4, Repository Investigations, Milestone RI110, January 31, 2002 (pp. 2.1-1 through 2.1-26). ERMS 520467.

Gillow, J.B., and A.J. Francis. 2002b. Re-Evaluation of Microbial Gas Generation under Expected Waste Isolation Pilot Plant Conditions: Data Summary and Progress Report (February 1 – July 15, 2002), July 18, 2002. Carlsbad, NM: Sandia National Laboratories. Sandia National Laboratories Technical Baseline Reports, WBS 1.3.5.3, Compliance Monitoring; WBS 1.3.5.4, Repository Investigations, Milestone RI130, July 31, 2002 (pp. 3.1-1 through 3.1-A10). ERMS523189.

Goodbar, A.K., D.W. Powers, J.R. Goodbar, and R.M. Holt. 2020. Karst and sinkholes at Nash Draw, Southeastern New Mexico (USA), Proceedings of the Sixteenth Multidisciplinary Conference on Sinkholes and the Engineering and Environmental Impacts of Karst (first ed.): NCKRI Symposium 8, National Cave and Karst Research Institute, Carlsbad, NM, p. 287-298.*

Goodbar, J., and A. Goodbar. 2014. A Method to Investigate Karst Groundwater Flow in Nash Draw, Eddy County, New Mexico, to Delineate Potential Impacts of Potash Industry Discharge and Runoff, *in* Kuniansky EL, Spangler LE, editors. US Geological Survey Karst Interest Group Proceedings, Carlsbad, New Mexico, April 29 – May 2, 2014. US Geological Survey Scientific Investigations Report 2014-5035, p. 98-107.*

Gougar, M.L.D., B.E. Scheetz, and D.M. Roy. 1996. Ettringite and C-S-H Portland Cement Phases for Waste Ion Immobilization: A Review. Waste Management, vol. 16, no. 4: 295–303.

Grieve, R.A.F. 1987. Terrestrial Impact Structures. Annual Review of Earth and Planetary Sciences, vol. 15: 245–70. ERMS 241228.

Griswold, G.B. and J.E. Griswold. 1999. Method of Potash Reserve Evaluation in New Mexico Bureau of Mines & Mineral Resources (pp. 33–67), Circular 207 (1999).

Hall, S.A., and R.J. Goble. 2012. Berino Paleosol, Late Pleistocene argillic soil development on the Mescalero sand sheet in New Mexico: The Journal of Geology, v. 120, p. 333-345, University of Chicago, Chicago, IL.*

Hall, S.A., and R.J. Goble. 2023a. Quaternary and Archeological Geology of the Mescalero Plain, Southeastern New Mexico: Bulletin 165, New Mexico Bureau of Geology and Mineral Resources, Socorro, NM.*

Hall, S.A., and R.J. Goble. 2023b. Late middle Pleistocene OSL age of the upper Gatuña Formation, southeastern New Mexico: New Mexico Geological Society Guidebook, 73rd Fall Field Conference, Third-Day Road Log.*

Halliday, I. 1964. The Variation in the Frequency of Meteorite Impact with Geographic Latitude. Meteoritics, vol. 2, no. 3: 271–278. ERMS 241229.

Hansen, C.W., L.H. Brush, M.B. Gross, F.D. Hansen, B.Y. Park, J.S. Stein, and T.W. Thompson. 2004. Effects of supercompacted waste and heterogeneous waste emplacement on repository performance, Revision 2. Carlsbad, NM: Sandia National Laboratories. ERMS 533551.

Hansen, C., S. King, J. Bethune, S. Brunell. 2023. Analysis Plan for the Performance Assessment for the Replacement Panels Planned Change Request. AP-204. Carlsbad, NM: Sandia National Laboratories. ERMS 579449.*

Hansen, C., S. Brunell, B. Day, S. King, J. Wilgus. AP-214, Analysis Plan for the 2026 WIPP Compliance Recertification Application Performance Assessment. Carlsbad, NM: Sandia National Laboratories.*

Hardin, E., K. Kuhlman, and F. Hansen. 2014. Technical Feasibility of Measuring Low-Stress, Low Strain-Rate Deformation Relevant to a Salt Repository. Sandia National Laboratories. Tech Report FCRD-UFD-2014-000614.*

Harris, A.H. 1987. Reconstruction of Mid-Wisconsin Environments in Southern New Mexico, National Geographic Research, vol. 3, no. 2: 142–51.

Harris, A.H. 1988. Late Pleistocene and Holocene Microtus (pitymys) (Rodentia: cricetidae) in New Mexico. Journal of Vertebrate Paleontology, vol. 8, no. 3: 307–13.

Harrison, J.J., H. Ceri, and R.J. Turner. 2007. Multimetal resistance and tolerance in microbial biofilms. Nature Reviews Microbiology 5: 928-938.*

Hart, D.B., R.M. Holt, and S.A. McKenna. 2008. Analysis Report for Task 5 of AP-114: Generation of Revised Base Transmissivity Fields. Carlsbad, NM: Sandia National laboratories. ERMS 549597.

Hartmann, W.K. 1965. Terrestrial and Lunar Flux of Large Meteorites in the Last Two Billion Years. ERMS 241230. Icarus, vol. 4, no. 2: 157−65.

Hartmann, W.K. 1979. Long-Term Meteorite Hazards to Buried Nuclear Waste Report 2, in Assessment of Effectiveness of Geologic Isolation Systems: A Summary of FY-1978 Consultant Input for Scenario Methodology Development. B.L. Scott, G.L. Benson, R.A. Craig, and M.A. Harwell, eds. Richland, WA: Pacific Northwest Laboratory. PNL-2851. ERMS 241232.

Haug, A., V.A. Kelley, A.M. LaVenue, and J.F. Pickens. 1987. Modeling of Ground-Water Flow in the Culebra Dolomite at the Waste Isolation Pilot Plant (WIPP) Site: Interim Report, Albuquerque, NM: Sandia National Laboratories. SAND86-7167. ERMS 228486.

Hawley, J.W. 1993. The Ogallala and Gatuña Formation in the Southeastern New Mexico and West Texas. New Mexico Geological Society, Forty-Fourth Annual Field Conference, Carlsbad, NM, October 6-9, 1993 (pp. 261–69). D.W. Love et al., eds. Socorro, NM: New Mexico Geological Society. ERMS 241431.

Hayes, P.T., and G.O. Bachman. 1979. Examination and reevaluation of evidence for the Barrera fault, Guadalupe Mountains, New Mexico: Open-file Report 79-1520, US Geological Survey, Denver, CO, 11 p.*

Helton, J.C., J.E. Bean, J.W. Berglund, F.J. Davis, K. Economy, J.W. Garner, J.D. Johnson, R.J., MacKinnon, J. Miller, D.G. O'Brien, J.L. Ramsey, J.D. Schreiber, A. Shinta, L.N. Smith, D.M. Stoelzel, C. Stockman, and P. Vaughn. 1998. Uncertainty and Sensitivity Analysis Results Obtained in the 1996 Performance Assessment for the Waste Isolation Pilot Plant. Albuquerque, NM: Sandia National Laboratories. SAND98-0365. ERMS 252619.

Herrick, C.G. 2012. JAS3D Calculations Performed in Support of the PCS-2012 PA Parameter Selections. Carlsbad, NM: Sandia National Laboratories. ERMS 557354.

Herzig, J.P., D.M. Leclerc, and P. Le Goff. 1970. Flow of Suspensions Through Porous Media: Application to Deep Filtration. Industrial and Engineering Chemistry 62: 8-35.*

Heyn, D.W. 1997. Letter from IMC Kalium to the U.S. EPA on Potash Solution Mining at WIPP Site. February 26, 1997. Washington, DC. ERMS 530221.

Hicks, T.W. 1996. Memorandum. (Thermal Convection and Effects of Thermal Gradients, Summary Memorandum of Record for GG-4 and S-10). (May 29, 1996). Albuquerque, NM: Sandia National Laboratories. SWCF-A 1.2.07.3: PA: QA: TSK: S10,GG4. ERMS 411687.

Hofmann-Wellenhof, B. and H. Moritz. 2006. Physical Geodesy. Second Edition. Equations 2-146 and 3-26).*

Holt, R.M., 1997, Conceptual model for transport processes in the Culebra Dolomite Member, Rustler Formation: SAND97-0194, Sandia National Laboratories, Albuquerque, NM.*

Holt, R.M., R.L. Beauheim, and D.W. Powers. 2005. Predicting fractured zones in the Culebra Dolomite, in Faybishenko, B, Witherspoon, P.A., and Gale, J., eds., Dynamics of Fluids and Transport in Fractured Rock: AGU Geophysical Monograph Series, v. 162, p. 103-116*.

Holt, R.M., and D. W. Powers. 1984. Geotechnical Activities in the Waste Handling Shaft, Waste Isolation Pilot Plant (WIPP) Project, Southeastern New Mexico: WTSD-TME 038. Carlsbad, NM: U.S. Department of Energy. ERMS 241347.

Holt, R.M., and D.W. Powers. 1986. Geotechnical Activities in the Exhaust Shaft, Waste Isolation Pilot Plant (WIPP) Project, Southeastern New Mexico: DOE-WIPP 86-008. Carlsbad, NM: U.S. Department of Energy. ERMS 241696.

Holt, R.M., and D.W. Powers. 1988. Facies Variability and Post-Depositional Alteration within the Rustler Formation in the Vicinity of the Waste Isolation Pilot Plant, Southeastern New Mexico. Carlsbad, NM: U.S. Department of Energy. DOE/WIPP 88-004. ERMS 242145.

Holt, R.M., and D.W. Powers. 1990. Geotechnical Activities in the Air Intake Shaft, Waste Isolation Pilot Plant. Carlsbad, NM: U.S. Department of Energy. WIPP-DOE 90-051.

Holt, R.M., and D.W. Powers. 2002. Impact of Salt Dissolution on the Transmissivity of the Culebra Dolomite Member of the Rustler Formation, Delaware Basin Southeastern New Mexico. Geological Society of America Abstracts with Programs, vol. 34, no. 6: 215.

Holt, R.M., and D.W. Powers. 2010. Evaluation of halite dissolution at a radioactive waste disposal site, Andrews County, TX: Geological Society of America Bulletin, v. 122, p. 1989-2004. DOI: 10.1130/B30052.1.*

Holt, R.M., and D.W. Powers. 2011. Synsedimentary dissolution pipes and the isolation of ancient bacteria and cellulose: Geological Society of America Bulletin, v. 123, p. 1513-1523. DOI:10.1130/B30197.1.*

Holt, R.M., and L. Yarbrough. 2002. Analysis Report: Task 2 of AP-088; Estimating Base Transmissivity Fields (July 8). Carlsbad, NM: Sandia National Laboratories. ERMS 523889.

Huber, H., M.J. Hohn, R. Rachel, T. Fuchs, V.C. Wimmer, and K.O. Stetter. 2002. A New Phylum of Archaea Represented by Nanosized Hyperthermophilic Endosymbiont. Nature 417: 63-67.*

Hudec, M.R., and Jackson, M.P.A., 2007, Terra infirma: Understanding salt tectonics: Earth-Science Reviews, v. 82, p. 1-28.*

Idaho National Engineering and Environmental Laboratory (INEEL), 1999. TRUPACT-II Matrix Depletion Program Final Report, Rev. 1. Prepared for the U.S. Department of Energy, Idaho Operations Office, Idaho Falls, Idaho. INEL-99-00987.

Imbrie, J., and J.Z. Imbrie. 1980. Modeling the Climatic Response to Orbital Variations. ERMS 241338. Science, vol. 207, no. 4434: 943–953.

Ingebritsen, S.E., and Manga, M., 2019, Earthquake hydrogeology: Water Resources Research, v. 55, p. 5212-5216.*

Jensen, R., S. Broome, C. Herrick, and B. Reedlunn. 2023. Improved Compaction Experiments and Modeling of Waste Isolation Pilot Plant Standard, Non-degraded, Waste Containers. Sandia National Laboratories. Tech Report SAND2023-04823.

Jewett, D.G., T.A. Hilbert, B.E. Logan, R.G Arnold, and R.C. Bales. 1995. Bacterial Transport in Laboratory Columns and Filters: Influence of Ionic Strength and pH on Collision Efficiency. Water Research 29: 1673-1680.*

Johnson, K.S. 1989. Development of the Wink Sink in West Texas, USA, Due to Salt Dissolution and Collapse. Environmental Geology and Water Science, vol. 14: 81–92.

Johnson, K.S., E.W. Collins, and S. Seni. 2003. Sinkholes and Land Subsidence due to Salt Dissolution near Wink, West Texas, and Other Sites in West Texas and New Mexico. K.T. Johnson and J.T. Neal, eds. Norman, OK: Oklahoma Geological Survey. Evaporite Karst and Engineering/Environmental Problems in the United States (pp. 183–96).

Johnson, K.W., 2005, Subsidence hazards due to evaporite dissolution in the United States: Environmental Geology, v. 48, p. 395-409.*

Jones, C.L., 1972, Permian basin potash deposits, southwestern United States, in Geology of Saline Deposits, UNEXCO, Earth Science Series, No. 7, p. 191-201.*

Jones, C.L., Cooley M.E., and Bachman, G.O., 1973, Salt deposits of Los Medaños area, Eddy and Lea Counties, New Mexico: Open-file Report 73-135 (also USGS-4339-7), US Geological Survey, Reston, VA.*

Jones, C.L. 1981. Geologic Data for Borehole ERDA-6, Eddy County, New Mexico. Denver, CO: U.S. Geological Society. ERMS 242321. Open-File Report 81-468.

Kaplan, U., J. Swanson, and C. K. Aslani. 2025. LANL ACRSP Parameter Recommendations for CRA-2026 Performance Assessment. Los Alamos National Laboratory; Carlsbad, NM. LCO-ACP-41, Revision 1.*

Kärnbränslesakerhet. 1978. Handling of Spent Nuclear Fuel and Final Storage of Vitrified High Level Reprocessing Waste. Stockholm: Kärnbränslesakerhet. ERMS 242406.

Kastenberg, W.E., P.F. Peterson, J. Ahn, J. Burch, G. Casher, P.L. Chambre, E. Greenspan, D.R. Olander, J.L. Vujic, B. Bessinger, N.G.W. Cook, F.M. Doyle, and L.B. Hilbert. 1996. Considerations of Autocatalytic Criticality of Fissile Materials in Geologic Repositories, Nuclear Technology 115(3), 298-310.*

Kato, C., T. Sato, M. Smorawinska, and K. Horikoshi. 1994. High Pressure Conditions Stimulate Expression of Chloramphenicol Acetyltransferase Regulated by the Iac Promoter in Escherichia coli. FEMS Microbiology Letters, vol. 122, nos. 1-2: 91–96. ERMS 241233.

Kelley, V.C., 1971, Geology of the Pecos Country, southeastern New Mexico: Memoir 24, New Mexico Bureau of Geology and Mineral Resources, Socorro, NM, 75 p. *

Kelley, V.C., 1972, Geometry and correlation along Permian Capitan escarpment, New Mexico and Texas: Bulletin, American Association of Petroleum Geologists, v. 56, p. 2192-2211.*

Kenward P.A., D. Fowle, R. Goldstein, M. Ueshima, L. Gonzalez, and J. Roberts. 2013. Ordered low-temperature dolomite mediated by carboxyl-group density of microbial cell walls. AAPG Bulletin 97: 2113-2125.*

Kicker, D. 2019. Radionuclide Inventory Screening Analysis for the 2019 Compliance Recertification Application Performance Assessment (CRA-2019 PA). Carlsbad, NM: Sandia National Laboratories. ERMS 571659.

Kicker, D. 2023. Radionuclide Inventory Screening Analysis for the Replacement Panels Planned Change Request Performance Assessment (RPPCR PA). Carlsbad, NM: Sandia National Laboratories. ERMS 578878.*

Kicker, D. 2025. Analysis Report for Radionuclide Inventory Screening in the 2026 Compliance Recertification Application Performance Assessment: Interim State Repository. Carlsbad, NM: Sandia National Laboratories.*

Kienzler, B., C. Borkel, V. Metz, and M. Schlieker. 2016. Long-Term Interactions of Full-Scale Cemented Waste Simulates with Salt Brines. Karlsruhe Institute of Technology, Karlsruhe, Germany. KIT Scientific Reports #7721.

Kim, H.N. and S. Walker. 2009. Escherichia coli transport in porous media: influence of cell strain, solution chemistry, and temperature. Colloids and Surfaces B: Biointerfaces 71: 160-167.*

King, P.B. 1948. Geology of the Southern Guadalupe Mountains, Texas. Washington, DC: U.S. Geological Survey. Professional Paper 215. ERMS 241749.

King, S. 2021. Recalculating of iron surface area for iron corrosion in the WIPP PA calculation. ERMS 576428. Carlsbad, NM: Sandia National Laboratories.*

King, S. 2025. Memo to Records. (Subject: Drilling Rate and Plugging Pattern Probabilities for the CRA-2026 PA Calculations). February 2025. Carlsbad, NM: Sandia National Laboratories.*

King, S., C. Hansen, P. Hora, 2023. Evaluation of radiolytic gas generation from adsorbed water and from CPR materials. Revision 1. Carlsbad, NM: Sandia National Laboratories. ERMS 579454.*

Kirkes, L., M. Farinacci, M-E. M. Akara, and O. Lofton. 2022. Analysis Report for AP-194: Analysis Report for Evaluation and Analysis of Current and Historical WIPP Culebra Groundwater Quality

Data, under Analysis Plan: AP-194, Rev. 0. Carlsbad, NM: Sandia National Laboratories. ERMS 578504.*

Kirkes, G.R. 2008. Features, Events and Processes Assessment for the Compliance Recertification Application—2009 (Revision 0). Carlsbad, NM: Sandia National Laboratories. ERMS 550489.

Kirkes, G.R. 2013. Features, Events and Processes Assessment for the Compliance Recertification Application—2014 (Revision 0). Carlsbad, NM: Sandia National Laboratories. ERMS 560488.

Kirkes, G.R. 2019a. Features, Events, and Processes Assessment for the 2019 Compliance Recertification Application Performance Assessment (CRA-2019 PA). Carlsbad, NM: Sandia National Laboratories. ERMS 571366.

Kirkes, L. 2019b. Lead Inventory Impact on Gas Generation. Carlsbad, NM. Sandia National Laboratories. ERMS 571255.

Kirkes, G.R. and J. McCormick. 2023. Analysis Report for the Reassessment of Features, Events, and Processes for the 2024 Compliance Recertification Application, Revision 0. December 2023. Carlsbad, NM: Sandia National Laboratories. ERMS 580866.*

Kirkes, G.R. 2024. Activity/Project Specific Procedure SP 9-4: Performing FEPs Baseline Impact Assessments for Planned or Unplanned Changes (Revision 6, March 28, 2024). Carlsbad, NM: Sandia National Laboratories. ERMS 581421.*

Kish, A., P.L. Griffin, K.L. Rogers, M.L. Fogel, R.J. Hemley, and A. Steele. 2012. High-pressure tolerance in *Halobacterium salinarum* NRC-1 and other non-piezophilic prokaryotes. Extremophiles 16: 355-361.*

Kuhlman, K.L. 2010. Analysis Report for the CRA-2009 PABC Culebra Flow and Transport Calculations. Carlsbad, NM: Sandia National Laboratories. ERMS 549013.

Kuhlman K.L., and T.F. Corbet. 2017. Memo to Records Center (Subject: WIPP Milestone Report: 2016 Culebra Groundwater Level Fluctuations). May 19, 2017. Carlsbad, NM: Sandia National Laboratories. ERMS 568172.

Lado, B.H. and A.E. Yousef. 2002. Alternative Food-Preservation Technologies: Efficacy and Mechanisms. Microbes and Infection 4:

Land, L. 2013. Evaporite Karst in the Permian Basin Region of West Texas and Southeastern New Mexico: The Human Impact. In: Proceedings of the 13th Sinkhole Conference, Carlsbad, New Mexico, 2013, Volume Sinkholes and the Engineering and Environmental Impacts of Karst.

Lambert, S.J. 1978. The Geochemistry of Delaware Basin Groundwaters. Geology and Mineral Deposits of Ochoan Rocks in Delaware Basin and Adjacent Areas. G.S. Austin, ed. Circular 159. Socorro, NM: New Mexico Bureau of Mines and Mineral Resources. ERMS 504429.

Lambert, S.J. 1983. Dissolution of Evaporites in and Around the Delaware Basin, Southeastern New Mexico and West Texas. Albuquerque, NM: Sandia National Laboratories. SAND82-0461. ERMS 227520.

Lambert, S.J. 1986. Stable-Isotope Studies of Groundwaters in Southeastern New Mexico, The Rustler Formation at the WIPP Site, EEG-34. Santa Fe, NM: New Mexico Environmental Evaluation Group. SAND85-1978C.

Lambert, S.J., and J.A. Carter. 1987. Uranium-Isotope Systematics in Groundwaters of the Rustler Formation, Northern Delaware Basin, Southeastern New Mexico. Principles and Methods. Albuquerque, NM: Sandia National Laboratories. SAND87-0388. ERMS 245158.

Lambert, S.J., and D.M. Harvey. 1987. Stable-Isotope Geochemistry of Groundwaters in the Delaware Basin of Southeastern New Mexico. Albuquerque, NM: Sandia National Laboratories. SAND87-0138. WPO 24150. ERMS 224150.

Lappin, A.R., R.L. Hunter, D.P. Garber, P.B. Davies, R.L. Beauheim, D.J. Borns, L.H. Brush, B.M. Butcher, T. Cauffman, M.S.Y. Chu, L.S. Gomez, R.V. Guzowski, H.J. Iuzzolino, V. Kelley, S.J. Lambert, M.G. Marietta, J.M. Mercer, E.J. Nowak, J. Pickens, R.P. Rechard, M. Reeves, K.L. Robinson, and M.D. Siegel (eds.). 1989. Systems Analysis, Long-Term Radionuclide Transport, and Dose Assessments, Waste Isolation Pilot Plant (WIPP), Southeastern New Mexico. Albuquerque, NM: Sandia National Laboratories. SAND89-0462. ERMS 210281.

Lasaga, A.C., J.M. Soler, J. Ganor, T.E. Burch, and K.L. Nagy, K.L. 1994. Chemical Weathering Rate Laws and Global Geochemical Cycles. ERMS 241234. Geochimica et Cosmochimica Acta, vol. 58, no. 10: 2361–2386.

Lee, W.T. 1925. Erosion by Solution and Fill. ERMS 252969. Contributions to Geography in the United States: U.S. Geological Survey Bulletin 760-C (pp. 107–21).

Leith, D. 1987. Drag on Nonspherical Objects, Aerosol Science and Technology, 6:2, 153-161*

Lenhardt, W.A. 1988. Damage Studies at a Deep Level African Gold Mine. C. Fairhurst, ed. Brookfield, VT: A.A. Balkema. Rockbursts & Seismicity in Mines, Proceeding of the Second International Symposium, Minneapolis, MN, June 8-10, 1988 (pp. 391–93).

Levandowski, W., R.B. Hermann, R. Briggs, O. Boyd, and R. Gold. 2018, An updated stress map of the continental Unites States reveals heterogeneous intraplate stress: Nature Geoscience, v. 11, p. 433-437.*

Litherland, M. 2023. History of monitoring induced seismicity in New Mexico, *in* Buchanan, R.C., Young, M.H., and Murray, K.E., eds., Recent Seismicity in the Southern Midcontinent, USA:

Scientific, Regulatory, and Industry Responses: Geological Society of America Special Paper 559.*

Litherland, M., and A. Record. 2023a. A report on the seismicity of the WIPP site for the period January 1 2023 through March 31 2023 for Nuclear Waste Partnership LLC, 12 p. + Excel records.*

Litherland, M., and A. Record. 2023b A report on the seismicity of the WIPP site for the period April 1 2023 through June 30 2023 for Nuclear Waste Partnership LLC, 12 p. + Excel records.*

Lorenz, J.C., 2006a. Assessment of the potential for karst in the Rustler Formation at the WIPP site: SAND2005-7303, Sandia National Laboratories, Albuquerque, NM, 102 p.

Lorenz, J.C., 2006b, Assessment of the geological evidence for karst in the Rustler Formation at the WIPP site, in Caves & Karst of Southeastern New Mexico, Land, L., and others, eds., NM Geological Society Fifty-seventh Annual Field Conference Guidebook, p. 243-251.

Lowenstein, T.K. 1987. Post Burial Alteration of the Permian Rustler Formation Evaporites, WIPP Site, New Mexico: Textural, Stratigraphic and Chemical Evidence. EEG-36, DOE/AL/10752-36. Santa Fe, NM: Environmental Evaluation Group. ERMS 241237.

Lucero, D.A., Y.K. Behl, G.O. Brown, K.G. Budge, M. Dunn, A.J. Francis, J.B. Gillow, and H.W. Papenguth. 1996. Laboratory Evaluation of Colloid Transport under Simulated Subsurface Conditions at the Waste Isolation Pilot Plant (WIPP): 2. Large-Scale-Intact-Core Column Flow Experiments. SAND96-2741J. Sandia National Laboratories; Albuquerque, NM.*

Lucchini, J. and J. Swanson. 2023. LANL ACRSP Parameter Recommendations for CRA-2024 Performance Assessment. Report LCO-ACP-34. Los Alamos National Laboratory; Carlsbad, NM. LA-UR-23-23839.*

Lüdeling, C., R. M. Günther, A. Hampel, J. Sun-Kurczinski, R. Wolters, U. Düsterloh, K. H. Lux, S. Yildirim, D. Zapf, S. Wacker, I. Epkenhans, J. Stahlmann, and B. Reedlunn. 2022. WEIMOS: Creep of Rock Salt at Low Deviatoric Stresses. The Mechanical Behaviour of Salt X. Editors: J.H.P. de Bresser and M.R. Drury and P. A. Fokker and M. Gazzani and S.J.T. Hangx and A.R. Niemeijer and C.J. Spiers. DOI: 10.1201/9781003295808.

Lund Snee, J. E., and M. Zoback. 2018. State of stress in Permian Basin, Texas and New Mexico: Implications for induced seismicity: The Leading Edge, v. 37, issue 2.*

Lund Snee, J-E., and M.D. Zoback. 2022. State of stress in areas of active unconventional oil and gas development in North America: American Association of Petroleum Geologists, v. 106, p. 355-385.*

Lundstern, J. E., and M. Zoback. 2016. State of stress in Texas: Implications for induced seismicity: Geophysical Research Letters, v. 43, p. 10,208–10,214, doi: 10.1002/2016GL070974.*

Madigan, M.T., K.S. Bender, D.H. Buckley, W.M. Sattley, and D.A. Stahl. (eds.). 2018. Brock Biology of Microorganisms. 15th Edition. Pearson Higher Education; New York.*

Mansure, A., and M. Reiter. 1977. An accurate equilibrium temperature log in AEC No. 8, a drill test in the vicinity of the proposed Carlsbad Disposal site: Open-file Report No. 80, New Mexico Bureau of Geology and Mineral Resources, Socorro, NM, 2 p.*

Mariner, P. 2019. A Summary of Humic Colloid Parameter Values to be Implemented in the CRA-2019 Deferred Performance Assessment. Albuquerque, NM: Sandia National Laboratories. ERMS 571250.

Mariner, P. E. 2025. CRA-2026 IS updates to the WIPP humic colloids models for An(III) and An(IV). Memo to Sandia National Laboratory WIPP Records Center, July 9, 2025. Sandia National Laboratories, Carlsbad, New Mexico.*

McCormick, J., and G.R Kirkes. 2025. Features, Events, and Processes Assessment for the Compliance Recertification Application—2026. Carlsbad, NM: Sandia National Laboratories.

Melzer, L.S. 2023. An Updated Assessment of the CO_2-Enhanced Oil Recovery Potential in the Vicinity of the Waste Isolation Pilot Plant (August). Midland, TX: Melzer Consulting.*

Melzer, S. L., and R.K. Hall. 2023. Report on Drilling, Production, Well Stimulation, Water Injection, and Seismic Activity in the Vicinity of the WIPP Site, Eddy County, New Mexico. Russell K. Hall and Associates, Incorporated. Midland, Texas.*

Menking, K.M., V. Polyak, R. Anderson, and Y. Asmeron. 2018. Climate History of the Southwestern United States based on Estancia Basin Hydrologic Variability from 69 to 10 ka: Quaternary Science Reviews, v. 200, p. 237-252.*

Mercer, J.W., R.L. Beauheim, R.P. Snyder, and G.M. Fairer. 1987. Basic Data Report for Drilling and Hydrologic Testing of Drillhole DOE-2 at the Waste Isolation Pilot Plant (WIPP) Site. Albuquerque, NM: Sandia National Laboratories. SAND86-0611. ERMS 227646.

Mercer, J.W., D.L. Cole, and R.M. Holt. 1998. Basic Data Report for Drillholes on the H-019 Hydropad (WIPP). Albuquerque, NM: Sandia National Laboratories. SAND98-0071. ERMS 252240.

Mijnendonckx, K., N. M. Bassil, S. Nixon, A. Boylan, and N. Leys. 2021. Organic Materials and their Microbial Fate in Radioactive Waste. Chapter 10 in The Microbiology of Nuclear Waste Disposal. J.R. Lloyd and A. Cherkouk Eds. Elsevier.*

Molecke, M.A. 1979. Gas Generation from Transuranic Waste Degradation. Albuquerque, NM: Sandia National Laboratories. SAND79-0911C. ERMS 228093.

Mondal, P.K. and B.E. Sleep. 2012. Colloid Transport in Dolomite Rock Fractures: Effects of Fracture Characteristics, Specific Discharge, and Ionic Strength. Environmental Science & Technology 46: 9987-9994.*

Morrill, C., D. Lowry, and A. Hoel. 2018. Thermodynamic and Dynamic Causes of Pluvial Conditions During the Last Glacial Maximum in Western North America: Geophysical Research Letters, v. 45, p. 335-345.*

Muehlberger, W.R., R.C. Belcher, and L.K. Goetz. 1978. Quaternary Faulting on Trans-Pecos, Texas. ERMS 241238. Geology, vol. 6, no. 6: 337–340.

Murray, R.L. 1957. *Nuclear Reactor Physics*, Prentice-Hall.*

National Academies/ National Research Council (NA/NRC). 2020. Review of the Department of Energy's Plans for Disposal of Surplus Plutonium in the Waste Isolation Pilot Plant. The National Academies Press.*

New Mexico Bureau of Mines and Mineral Resources (NMBMMR). 1995. Final Report Evaluation of Mineral Resources at the Waste Isolation Pilot Plant (WIPP) Site. March 31, 1995. 4 vols. Socorro, NM: New Mexico Bureau of Mines and Mineral Resources, Campus Station. ERMS 239149.

New Mexico Oil Conservation Division (OCD). 1994. Attachment to Discharge Plan BW-26 Approval Salado Brine Sales No. 3 Brine Facility Discharge Plan Requirements. Attachment to letter from W.J. LeMay, (Oil Conservation Division, Santa Fe, New Mexico) to W.H. Brininstool (Salado Brine Sales, Jal, New Mexico). January 12, 1994

Nicholson, A., Jr., and A. Clebsch, Jr. 1961. Geology and Ground-Water Conditions in Southern Lea County, New Mexico. Ground-Water Report 6. Socorro, NM: New Mexico Bureau of Mines and Mineral Resources. ERMS 241583.

Oelkers, E. H. 1996. Physical and Chemical Properties of Rocks and Fluids for Chemical Mass Transport Calculations. Reviews in Mineralogy, vol. 34: 131–191.

Otto, S. 2017. Salt Disposal Investigations Test Plan SDI-TP-002-Revision 1, Testing of a Prototype Canister Heater in the WIPP Underground. April 13, 2017. Carlsbad, NM: Los Alamos National Laboratory.

Park, B.Y. and F.D. Hansen. 2005. Determination of the Porosity Surfaces of the Disposal Room Containing Various Waste Inventories for WIPP PA. SAND2005-4236. Albuquerque, NM: Sandia National Laboratories.

Peake, T. 1996. Memorandum to Public Rulemaking Docket A-92-56 (Subject: WIPP–Examination of Mining and Hydraulic Conductivity). (January 31 1996). Washington, DC: U.S. Environmental Protection Agency. ERMS 241239.

Pedersen, K. 1999. Subterranean Microorganisms and Radioactive Waste Disposal in Sweden. Engineering Geology, vol. 52: 163–176.

Pedersen, K., and F. Karlsson. 1995. Investigations of Subterranean Microorganisms: Their Importance for Performance Assessment of Radioactive Waste Disposal. Stockholm, Sweden: Swedish Nuclear Fuel and Waste Management Co. SKB Technical Report 95-10.

Pepper, I.L., C.P. Gerba, and T.J. Gentry (eds.). 2014. Environmental Microbiology, 3rd Edition. Academic Press: London.*

Phillips, F.M., A.R. Campbell, C. Kruger, P.S. Johnson, R. Roberts, and E. Keyes. 1992. A Reconstruction of the Water Balance in Western United States Lake Basins in Response to Climate Change, New Mexico Water Resources Research Institute Report 269. Las Cruces, NM: New Mexico Water Resources Research Institute.

Pointeau, I., B. Piriou, M. Fedoroff, M.G. Barthes, N. Marmier, and F. Fromage. 2001. Sorption Mechanisms of Eu^{3+} on CSH Phases of Hydrated Cements. Journal of Colloid and Interface Science, vol. 236, no. 2: 252–259.

Popielak, R.S., R.L. Beauheim, S.R. Black, W.E. Coons, C.T. Ellingson, and R.L. Olsen. 1983. Brine Reservoirs in the Castile Formation, Waste Isolation Pilot Plant (WIPP) Project, Southeastern New Mexico. Carlsbad, NM: U.S. Department of Energy. TME-3153. ERMS 242085.

Powers, D.W. 1996. Tracing Early Breccia Pipe Studies, Waste Isolation Pilot Plant, Southeastern New Mexico: A Study of the Documentation Available and Decision-Making During the Early Years of WIPP. Albuquerque, NM: Sandia National Laboratories. SAND94-0991. ERMS 230968.

Powers, D.W., J.M. Sigda, and R.M. Holt. 1996. Probability of Intercepting a Pressurized Brine Reservoir under the WIPP. Carlsbad, NM: Sandia National Laboratories. ERMS 240199.

Powers, D.W. 2000. Evaporites, Casing Requirements, Water-Floods, and Out-of-Formation Waters: Potential for Sinkhole Developments: Technical Class – Sinkholes And Unusual Subsidence Over Solution-Mined Caverns And Salt And Potash Mines. San Antonio, TX: Solution Mining Research Institute.

Powers, D.W. 2003a. Analysis Report, Task 1 of AP-088: Construction of Geologic Contour Maps (January). Albuquerque, NM: Sandia National Laboratories. ERMS 522086.

Powers, D.W. 2003b. Jal Sinkhole in Southeastern New Mexico: Evaporite Dissolution, Drill Holes, and the Potential for Sinkhole Development in Johnson, K.S., and Neal, J.T., eds., Evaporite Karst and Engineering/Environmental Problems in the United States: Oklahoma Geological Survey Circular 109, p. 219-226.*

Powers, D.W., and R.M. Holt. 1990. Sedimentology of the Rustler Formation near the Waste Isolation Pilot Plant (WIPP) Site. Geological and Hydrological Studies of Evaporites in the

Northern Delaware Basin for the Waste Isolation Pilot Plant (WIPP), New Mexico (pp. 79–106). Geological Society of America Field Trip No. 14 Guidebook. Dallas, TX: Dallas Geological Society.

Powers, D.W., and R.M. Holt. 1995. Regional Processes Affecting Rustler Hydrogeology. Carlsbad, NM: Sandia National Laboratories. ERMS 244173.

Powers, D.W., and R.M. Holt. 1999. The Los Medaños Member of the Permian (Ochoan) Rustler Formation. New Mexico Geology, vol. 21, no. 4: 97–103. ERMS 532368.

Powers, D.W., and R.M. Holt. 2000. The Salt that Wasn't There: Mudflat Facies Equivalents to Halite of the Permian Rustler Formation, Southeastern New Mexico. Journal of Sedimentary Research, vol. 70, 29–39. ERMS 532369.

Powers, D.W., and R.M. Holt. 2021. Evaporite dissolution and the Waste Isolation Pilot Plant (WIPP) in the northern Delaware Basin, southeastern New .Mexico. in Johnson, K.S ., Land. L., and Decker. D.D., eds., Evaporite karst in the Greater Permian Evaporite Basin (GPEB) of Texas, New Mexico. Oklahoma. Kansas, and Colorado: Oklahoma Geological Survey, Circular113, p. 125-149.*

Powers, D.W., S.J. Lambert, S.E. Shaffer, I.R. Hill, and W.D. Weart, eds. 1978. Geological Characterization Report, Waste Isolation Pilot Plant (WIPP) Site, Southeastern New Mexico. Albuquerque, NM: Sandia National Laboratories. SAND78-1596. ERMS 205448 (vol. 1). ERMS 205448 (vol. 2).

Powers, D.W., R.M. Holt, R.L. Beauheim, and S.A. McKenna. 2003. Geological factors related to the transmissivity of the Culebra Dolomite Member, Permian Rustler Formation, Delaware Basin, Southeastern New Mexico, in Johnson, K.S., and Neal, J.T., eds., Evaporite Karst and Engineering/Environmental Problems in the United States: Oklahoma Geological Survey Circular 109, p. 211-218.*

Powers, D.W., R.M. Holt, R.L. Beauheim, and R.G. Richardson. 2006a. Advances in depositional models of the Permian Rustler Formation, southeastern New Mexico, in Caves & Karst of Southeastern New Mexico, L. Land and others, eds., NM Geological Society Fifty-seventh Annual Field Conference Guidebook, p. 267-276.*

Powers, D.W., R.L. Beauheim, R.M. Holt, and D.L. Hughes. 2006b. Evaporite karst features and processes at Nash Draw, Eddy County, New Mexico, in Caves & Karst of Southeastern New Mexico, Land, L., and others, eds., NM Geological Society Fifty-seventh Annual Field Conference Guidebook, p. 253-266.*

Powers, D.W., R.M. Holt, R. Salness, B. Seal, A. Hall, and J. Thurston. 2018, Geology of C-3977 (Pre-shaft corehole) for Waste Isolation Pilot Plant (WIPP): report to Nuclear Waste Partnership, Carlsbad, NM. DOI: 10.13140/RG.2.2.29086.84801.*

Powers, D.W., R. Salness, B. Seal, A. Hall, J. Thurston, and R.M. Holt. 2019a, Basic data report for C-3976-1 (Dewey Lake 1) for Waste Isolation Pilot Plant (WIPP): report to Nuclear Waste Partnership, Carlsbad, NM. DOI: 10.13140/RG.2.2.34532.19847.*

Powers, D.W., J. Thurston, R.M. Holt, R. Salness, B. Seal, and A. Hall, 2019b, Basic data report for C-3976-2 (shallow subsurface water 1) for Waste Isolation Pilot Plant (WIPP): report to Nuclear Waste Partnership, Carlsbad, NM. DOI: 10.13140/RG.2.2.19432.70406.*

Powers, D.W., B. Seal, A. Hall., J. Thurston, R.M. Holt, and R. Salness. 2019c, Basic data report for C-3976-3 (Dewey Lake 2) for Waste Isolation Pilot Plant (WIPP): report to Nuclear Waste Partnership, Carlsbad, NM. DOI: 10.13140/RG.2.2.29499.03361*

Powers, D.W., A. Hall, J. Thurston, R.M. Holt, R. Salness, and B. Seal. 2019d, Basic data report for C-3976-4 (shallow subsurface water 2) for Waste Isolation Pilot Plant (WIPP): report to Nuclear Waste Partnership, Carlsbad, NM.*

Powers, D.W., and R.M. Holt, 2021, Evaporite dissolution and the Waste Isolation Pilot Plant (WIPP) in the northern Delaware Basin, southeastern New Mexico, in Johnson, K.S., Land, L., and Decker, D.D., eds., Evaporite karst in the Greater Permian Evaporite Basin (GPEB) of Texas, New Mexico, Oklahoma, Kansas, and Colorado: Oklahoma Geological Survey, Circular 113, p. 125-149.*

Powers, D.W., R.H. Vreeland, and W.D. Rosenzweig, 2001, How old are bacteria from the Permian age?–Reply: Nature, v. 411, p. 155-156.*

Prichard, D.A. 2003. E-mail to Mary-Alena Martell (Subject: Potash Solution Mining at WIPP). 6 April 2003. Carlsbad, NM: IMC Global, Inc. ERMS 525161.

Qiu, X., Y. Yao, H. Wang, A. Shen, and J. Zhang. 2019. Halophilic archaea mediate the formation of proto-dolomite in solutions with various sulfate concentrations and salinities. Frontiers in Microbiology 10: 480.*

Railsback, L.B., G. Brook, B. Ellwood, F. Liang, H. Heng, and R. Edwards. 2015. A Record of Wet Glacial Stages and Dry Interglacial Stages Over the Last 560 kyr from a Standing Massive Stalagmite in Carlsbad Cavern, New Mexico. Paleogeography, Paleoclimatology, Paleoecology, v. 438, p. 256-266.*

Ramsey, J. L., R. Blaine, J. W. Garner, J. C. Helton, J. D. Johnson, L. N. Smith, and M. Wallace. 2000. "Radionuclide and Colloid Transport in the Culebra Dolomite and Associated Complementary Cumulative Distribution Functions in the 1996 Performance Assessment for the Waste Isolation Pilot Plant," Reliability Engineering and System Safety, 69(1-3), 397-420.*

Rappé, M.S., S.A. Connon, K.L. Vergin, and S.J. Giovannoni. 2002. Cultivation of the Ubiquitous SAR11 Marine Bacterioplankton Clade. Nature 418: 630-632.*

Rawson, D., C. Boardman, and N. Jaffe-Chazan. 1965. Project Gnome, the Environment Created by a Nuclear Explosion in Salt. Lawrence Radiation Laboratory, University of California, Livermore, CA. Springfield, VA: National Technical Information Service. PNE-107F. ERMS 241242.

Rechard, R.P., 2025a. Low-Probability Rationale for Excluding Post-Closure Criticality at the Waste Isolation Pilot Plant along with Risk Perspective, Memorandum to Steve Wagner, 8881; Ross Kirkes, 8881; October 2025, Albuquerque, NM: Sandia National Laboratories.*

Rechard, R.P., 2025b. Fissile Mass and Concentration Necessary for Post-Closure Criticality in Geologic Media Near Bedded Salt Repository, Memorandum to Steve Wagner, 8881; Ross Kirkes, 8881; October 2025, Albuquerque, NM: Sandia National Laboratories.*

Rechard, R.P., A.C. Peterson, J.D. Schreiber, H.J. Iuzzolino, M.S. Tierney, and J.S. Sandha. 1991. Preliminary Comparison with 40 CFR Part 191, Subpart B for the Waste Isolation Pilot Plant, December 1991, Volume 3: Reference Data. SAND91-0893/3, Albuquerque, NM: Sandia National Laboratories.

Rechard, R.P., L.C. Sanchez, H.R. Trellue, and C.T. Stockman. 2001. Unfavorable Conditions for Nuclear Criticality Following Disposal of Transuranic Waste at the Waste Isolation Pilot Plant. Nuclear Technology, 136(1), 99-129.*

Rechard, R.P., B. Reedlunn, J.E. Bean, Jr., B.A. Day, L.C. Sanchez 2025a. Improbability of Post-Closure Criticality in Array of Transuranic Waste Containers after Compaction by Salt Creep at Waste Isolation Pilot Plant, SAND2025-XXXX. Albuquerque, NM: Sandia National Laboratories.*

Rechard, R.P., and P.V. Brady, 2025. Hydrologic and Geochemical Constraints on Post-Closure Criticality in Geologic Media Near Waste Isolation Pilot Plant, Memorandum to Steve Wagner, 8881; Ross Kirkes, 8881; October 2025, Albuquerque, NM: Sandia National Laboratories.*

Rechard, R.P. M.S. Tierney, L.C. Sanchez, and M.-A. Martell. 1997. Bounding Estimates for Critical Events When Directly Disposing Highly Enriched Spent Nuclear Fuel in Unsaturated Tuff, Risk Analysis 17(1), 19-35.*

Rechard, R.P., B.A. Day, B. Reedlunn, and J.E. Bean, Jr. 2025b. Improbability of Post-Closure Criticality in Compacted Criticality Control Overpacks after Room Closure at Waste Isolation Pilot Plant, SAND2025-XXXX. Albuquerque, NM: Sandia National Laboratories.*

Reed, D.T., S. Okajima, L.H. Brush, and M.A. Molecke. 1993. Radiolytically-Induced Gas Production in Plutonium-Spiked WIPP Brine, Scientific Basis for Nuclear Waste Management XVI, Materials Research Society Symposium Proceedings, Boston, MA, November 30 – December 4, 1992. C.G.. terrante and R.T. Pabalan, eds. Materials Research Society, Pittsburgh, PA. Vol. 294, pp. 431–438. SAND92-7283C. ERMS 228637.

Reed, D.T., J.S. Swanson, J.-F. Lucchini, and M.K. Richmann. 2013. Intrinsic, Mineral, and Microbial Colloid Enhancement Parameters for the WIPP Actinide Source Term. Los Alamos National Laboratory; Carlsbad, NM. LCO-ACP-18, LA-UR-13-20858

Reed, D., J. Swanson, and F. Stanley. 2019. LANL/ACRSP Parameter Recommendations for the CRA-2019 Deferred Performance Assessment, Rev. 1. Los Alamos National Laboratory, Carlsbad, NM. ERMS 571296.

Reedlunn, B., and J. Bean. 2019. Simulations of Pipe Overpack Container Compaction at the Waste Isolation Pilot Plant. October 2019. Albuquerque, NM: Sandia National Laboratories. SAND2019-12111.

Reedlunn, B., J.E. Bean, Jr., J. Wilkes, and J. Bignell. 2023. Simulations of Criticality Control Overpack Container Compaction at the Waste Isolation Pilot Plant. Albuquerque, NM: Sandia National Laboratories. SAND2023-10477.*

Reedlunn, B., S. King, B. Day, C. Hamel, and J. Bean. 2025. An Assessment of the Error Due to Computing Waste Isolation Pilot Plant Porosity Using the Porosity Response Surface Approach. , Albuquerque, NM: Sandia National Laboratories SAND2025-12225.

Reiter, M., M.W. Barroll, and J. Minier. 1991. An Overview of Heat Flow in Southwestern United States and Northern Chihuahua, Mexico. D.B. Slemmons, E.R. Engdahl, M.D. Zoback, and D.D. Blackwell, eds. Boulder, CO: Geological Society of America. Neotectonics of North America (pp. 457–66). ERMS 241575.

Reyes, J. 2008. Letter to D.C. Moody (5 Enclosures). 11 February 2008. Washington, DC: U.S. Environmental Protection Agency, Office of Air and Radiation.

Richardson, S. M. and H.Y. McSween, Jr. 1989. Geochemistry: Pathways and Processes. Prentice Hall.

Roberts, R.M., R.L. Beauheim, and P. Domski. 1999, Hydraulic testing of Salado Formation evaporites at the Waste Isolation Pilot Plant site: final report: SAND98-2537, Sandia National Laboratories, Albuquerque, New Mexico.*

Robinson, J.Q., and D.W. Powers. 1987. A Clastic Deposit Within the Lower Castile Formation, Western Delaware Basin, New Mexico. D.W. Powers and W.C. James, eds. El Paso, TX: El Paso Geological Society Guidebook 18, El Paso Geological Society. Geology of the Western Delaware Basin, West Texas and Southeastern New Mexico (pp. 69–79). ERMS 241368.

Ropp, R.C. 2013. Encyclopedia of the Alkaline Earth Compounds, Elsevier, UK.*

Rosholt, J.N., and C.R. McKinney. 1980. Uranium Series Disequilibrium Investigations related to the WIPP Site, New Mexico, Part II, Uranium Trend Dating of Surficial Deposits and Gypsum Spring Deposits near WIPP Site, New Mexico. Denver, CO: U.S. Geological Survey. Open-File Report 80-879.

Roselle, G.T. 2013. Determination of Corrosion Rates from Iron/Lead Corrosion Experiments to be used for Gas Generation Calculations. Carlsbad, NM: Sandia National Laboratories. ERMS 559077.

Samari-Kermani, M., S. Jafari, M. Rahnama, and A. Raoof. 2021. Ionic Strength and Zeta Potential Effects on Colloid Transport and Retention Processes. Colloid and Interface Science Communications 42: 100389.*

Sanchez, L.C., and H.R. Trellue. 1996. Memorandum to T. Hicks (Galson Sciences Ltd.). Estimation of Maximum RH-TRU Thermal Heat Load for WIPP. (January 17, 1996). Albuquerque, NM: Sandia National Laboratories. ERMS 231165.

Sánchez-Roman M., J. McKenzie, A. de Luca Rebello. A. Wagener, C. Romanek, A. Sánchez-Navas, and C. Vasconcelos. 2011. Experimentally determined biomediated Sr partition coefficient for dolomite: significance and implication for natural dolomite. Geochimica et Cosmochimica Acta 75: 887-904.*

Sanford, A.R., L.H. Jakasha, and D.J. Cash. 1991. Seismicity of the Rio Grand Rift in New MexicoD.B. Slemmons, E.R. Engdahl, M.D. Zoback, and D.D. Blackwell, eds. Boulder, CO: Geological Society of America. Neotectonics of North America (pp. 229–44). ERMS 241571.

Santen, R.A. 1984. The Ostwald Step Rule. J. Phys. Chem., 88(24) 5768-5769.

Sandia National Laboratories (SNL). 2022. Software Problem Report for PRELHS Version 2.45 ERMS 577795. Carlsbad, NM: Sandia National Laboratories.

Santillan, J. 2023. “PBRINE Telecon, Issue 4 (Pu oxidation state), and Issue 19 (Boreholes)”, an email to Anderson Ward. February 24, 2023. ERMS 579254.*

Sarathi, R. 2019. Analysis Package for Actinide Mobilization and Salado Transport in the 2019 Compliance Recertification Application Performance Assessment (CRA-2019 PA). Carlsbad, NM: Sandia National Laboratories. ERMS 571371.

Savvaidis, A., B. Young, G-c.D. Huang, and A. Lomax. 2019. TexNet: A statewide seismological network in Texas: Seismological Research Letters, v. 90, p. 1702-1705.*

Savvaidis, A., A. Lomax, and C. Breton. 2020. Induced seismicity in the Delaware Basin, west Texas, is caused by hydraulic fracturing and wastewater disposal: Bulletin of the Seismological Society of America, v. 110, p. 2225o-2241.*

Schreiber, J. 1991. Updated Waste Storage Volumes. Carlsbad, NM: Sandia National Laboratories. ERMS 237713.

Schiel, K.A. 1994. A New Look at the Age, Depositional Environment and Paleogeographic Setting of the Dewey Lake Formation (Late Permian). West Texas Geological Society Bulletin, vol. 33, no. 9: 5–13. ERMS 220465.

Sehrawat, R.; Kaur, B.P.; Nema, P.K.; Tewari, S.; Kumar, L. 2021. Microbial inactivation by high pressure processing: principle, mechanism and factors responsible. Food Science and Biotechnology 30: 19-35.*

Serber, R. 1992. *The Los Alamos Primer: The First Lectures on How to Build an Atomic Bomb*, University of California Press, Berkeley (1992).*

Serne, R.J. 1992. Current Adsorption Models and Open Issues Pertaining to Performance Assessment. In Proceedings of the DOE/Yucca Mountain Site Characterization Project Radionuclide Adsorption Workshop at Los Alamos National Laboratory, September 11-12, 1990. Comp. J.A. Canepa. Los Alamos, NM: Los Alamos National Laboratory. 43–74. LA-12325-C. ERMS 241243.

Servant, J. 2001. The 100 kyr Cycle of Deglaciation During the Last 450 kyr: A New Interpretation of Oceanic and Ice Core Data. Global and Planetary Change, vol. 29: 121–133.

Sharma, K., N. Gillum, J.L. Boyd, and A. Schmid. 2012. The RosR transcription factor is required for gene expression dynamics in response to extreme oxidative stress in a hypersaline-adapted archaeon. BMC Genomics 13: 351.*

Siasou, E., D. Johnson, and N.J. Willey. 2017. An extended dose-response model for microbial responses to ionizing radiation. Frontiers in Environmental Science 5: article 6. *

Siegel, M.D., S.J. Lambert, and K.L. Robinson, eds. 1991. Hydrogeochemical Studies of the Rustler Formation and Related Rocks in the Waste Isolation Pilot Plant Area, Southeastern New Mexico. Albuquerque, NM: Sandia National Laboratories. SAND88-0196. ERMS 225624.

Silva, M.K. 1994. Implications of the Presence of Petroleum Resources on the Integrity of the WIPP. Albuquerque, NM: Environmental Evaluation Group. ERMS 241470. EEG-55.

Snelling, A.A. 1992. Alligator Rivers Analogue Project Final Report, Volume 2, Geologic Setting. Her Majesty's Inspectorate of Pollution of the Department of the Environment, London. Stockholm, Sweden: Swedish Nuclear Fuel and Waste Management Co. UK DOE Report DOE/HMIP/RR/92/072, SKI Report SKI TR, vol. 92:20-2. ERMS 241471.

Snider, A.C. 2001. The Hydration of Magnesium Oxide in the Waste Isolation Pilot Plant, December 2001. Boston, MA: MRS Fall 2001 Conference.

Snyder, R.P. 1985. Dissolution of Halite and Gypsum, and Hydration of Anhydrite to Gypsum, Rustler Formation, in the Vicinity of the Waste Isolation Pilot Plant, Southeastern New Mexico. Denver, CO: U.S. Geological Survey. Open-File Report 85-229.

Snyder, R.P., and L.M. Gard, Jr. 1982. Evaluation of Breccia Pipes in Southeastern New Mexico and Their Relation to the Waste Isolation Pilot Plant (WIPP) Site. Denver, CO: U.S. Geological Society. Open-File Report 82-968. ERMS 241244.

Stenhouse, M.J., N.A. Chapman, and T.J. Sumerling. 1993. SITE-94 Scenario Development FEP Audit List Preparation: Methodology and Presentation. Stockholm: Swedish Nuclear Power Inspectorate. SKI Technical Report 93:27. ERMS 241371.

Stoelzel, D.M., and D.G. O'Brien. 1996. The Effects of Salt Water Disposal and Waterflooding on WIPP. Summary Memorandum of Record for NS-7a. Albuquerque, NM: Sandia National Laboratories. ERMS 240837.

Stoelzel, D.M., and P.N. Swift. 1997. Supplementary Analyses of the Effect of Salt Water Disposal and Waterflooding on the WIPP. Albuquerque, NM: Sandia National Laboratories. ERMS 244158.

Stone, C.M. 1997. Final disposal room structural response calculations. SAND97-0795. Albuquerque, NM: Sandia National Laboratories.*

Stratton, W.R., and D.R. Smith. 1989. A Review of Criticality Accidents. DOE/NCT-04. US Department of Energy, Office of Environment, Safety, and Health, (1989).

Stroes-Gascoyne, S., and J.M. West. 1994. Microbial Issues Pertaining to the Canadian Concept for the Disposal of Nuclear Fuel Waste. Atomic Energy of Canada Ltd. Manitoba, Canada: Whiteshell Labs, Pinawa. AECL Report No. AECL-10808, COG-93-54. ERMS 241639.

Sturchio, N.C. 2016. Results of Radiokrypton Analyses of Monitoring Wells AEC-7R, H-12R, and SNL-16 Near the Waste Isolation Pilot Plant, New Mexico. Carlsbad, NM: Sandia National Laboratories. ERMS 566236.*

Sturchio, N.C., K. Kuhlman, R. Yokochi, P. Probst, W. Jiang, Z. Lu, P. Mueller, and G. Yang. 2014. Krypton-81 in Groundwater of the Culebra Dolomite near the Waste Isolation Pilot Plant, New Mexico: Journal of Contaminant Hydrology, v. 160, p. 12-20.*

Swanson, J.S., F.E. Stanley, and D.T. Reed. 2019. Review of the Microbial Colloid Contribution to the WIPP Actinide Source Term. LCO-ACP-23, Rev. 0. Carlsbad, NM: Los Alamos National Laboratory. LA-UR-19-22310.

Swanson, J.S., and K.A. Simmons. 2013. Update on Microbial Characterization of WIPP Groundwaters. Carlsbad, NM: Los Alamos National Laboratory. Report LCO-ACP-20, LA-UR 13-20623.

Swanson, J., D. T. Reed, M.K. Richmann, and D. Cleveland. 2015. Investigation into the post-excavation sources of methane from INL TRU waste drums. Report LA-UR-15-26657. Carlsbad, NM: Los Alamos National Laboratory.

Swanson, J.S., and D.T. Reed. 2018. Update on Microbiology Research for the Waste Isolation Pilot Plant. LAUR 18-31313. Los Alamos, NM: Los Alamos National Laboratory.

Swanson, J. 2025a. Microbial Influence on Radionuclide Transport through the Culebra. Report LCO-ACP-37, Rev. 0. LAUR-25-30024. Carlsbad, NM: Los Alamos National Laboratory.*

Swanson, J. 2025b. Biologically Influenced Transport of the +3 Actinide Oxidation State From the WIPP Environment, Using Neodymium as an Analog. Report LCO-ACP-32, Rev. 1. Carlsbad, NM: Los Alamos National Laboratory. LA-UR-25-30181.*

Swift, P.N., W.D. Weart, S. G. Bertram-Howrey, R.V. Guzowski, K.F. Brinster, and S.B. Pasztor. 1991. Long-Term Climate Variability at the Waste Isolation Pilot Plant, Background Information Presented to the Expert Panel on Inadvertent Human Intrusion into the Waste Isolation Pilot Plant. R.V. Guzowski and M.M. Gruebel, eds. Albuquerque, NM: Sandia National Laboratories. SAND91-0928.

Swift, P.N. 1992. Long-Term Climate Variability at the Waste Isolation Pilot Plant, Southeastern New Mexico, USA. Albuquerque, NM: Sandia National Laboratories. SAND91-7055. ERMS 227093.

Tamada, K. and H. Fujikawa. 1957. The Steady Two-Dimensional Flow of Viscous Fluid at Low Reynolds Numbers Passing Through an Infinite Row of Equal Parallel Circular Cylinders. The Quarterly Journal of Mechanics and Applied Mathematics, vol. 10, Issue 4: 425-432.*

Tasi, A., X. Gaona, D. Fellhauer, M. Böttle, J. Rothe, K. Dardenne, R. Polly, M. Grivé, E. Colàs, J. Bruno, K. Källström, M. Altmaier, and H. Geckeis. 2018. Thermodynamic Description of the Plutonium – α-D-Isosaccharinic Acid System I: Solubility, Complexation and Redox Behavior. Applied Geochemistry, vol. 98: 247–264.*

Tedesco, E.F. 1992. Ceres. McGraw-Hill Encyclopedia of Science & Technology. 1992 ed. Vol. 3. p. 443.

Telander, M.R., and R.E. Westerman. 1993. Hydrogen Generation by Metal Corrosion in Simulated Waste Isolation Pilot Plant Environments: Progress Report for the Period November 1989 through 1992. Albuquerque, NM: Sandia National Laboratories. SAND92-7347. ERMS 223456.

Telford, W.M., L.P. Geldart, R. E. Sheriff, and D.A. Keys. 1976. Applied Geophysics. Cambridge, MA: Cambridge UP.

Thompson, G.A., and M.L. Zoback. 1979. Regional Geophysics of the Colorado Plateau. ERMS 241603. Tectonophysics, vol. 61, nos. 1-3: 149–81.

Thorne, B.J., and D.K. Rudeen. 1981. Regional Effects of TRU Repository Heat. Albuquerque: Sandia National Laboratories. SAND80-7161. WPO 10281. ERMS 210281.

Thorne, M.C. 1992. Dry Run 3 - A Trial Assessment of Underground Disposal of Radioactive Wastes Based on Probabilistic Risk Analysis - Volume 8: Uncertainty and Bias Audit. London: Her Majesty's Inspectorate of Pollution (HMIP) of the Department of the Environment. DOE/HMIP/RR/92.040. ERMS 241245.

Tounsi, H., J. Rutqvist, M. Hu, R. Wolters, and S. Lerche. 2023. Long-term sinking of nuclear waste canisters in salt formations by low- stress creep at high temperature. Acta Geotechnica. Vol. 18. Pg. 3469-3484. DOI: 10.1007/s11440-023-01900-w.

U.S. Congress. 1992. Waste Isolation Pilot Plant Land Withdrawal Act. ERMS 239105. Public Law 102-579, October 1992. 102nd Congress, Washington, DC.

U.S. Department of Energy (DOE). 1980. Final Environmental Impact Statement, Waste Isolation Pilot Plant (October). 2 vols. Washington, DC: U.S. Department of Energy. DOE/EIS-0026. ERMS 238835 and ERMS 238838.

U.S. DOE. 1996a. Title 40 CFR Part 191 Compliance Certification Application for the Waste Isolation Pilot Plant (October). Carlsbad, NM: Carlsbad Field Office. 21 vols. DOE/CAO-1996-2184.

U.S. DOE. 1996b. Transuranic Waste Baseline Inventory Report (Revision 3). U.S. Department of Energy, Carlsbad, NM. DOE/CAO-95-1121. ERMS 243330.

U.S. DOE. 2000. MgO Mini-Sack Elimination Proposal (July 21). Carlsbad, NM: Carlsbad Area Office. ERMS 519362.

U.S. DOE. 2004. Title 40 CFR Part 191 Compliance Recertification Application for the Waste Isolation Pilot Plant (March). Carlsbad, NM: Carlsbad Field Office. 10 vols. DOE/WIPP 2004-3231.

U.S. DOE. 2009. Title 40 CFR Part 191 Subpart B and C: WIPP Compliance Recertification Application. Carlsbad NM: U.S. Department of Energy, Carlsbad Area Office. DOE/WIPP-2009-3424.

U.S. DOE. 2014. Title 40 CFR Part 191 Subparts B and C Compliance Recertification Application for the Waste Isolation Pilot Plant. Carlsbad, NM: Carlsbad Field Office. DOE/WIPP 2014-3503.

U.S. DOE. 2015a. RH-TRAMPAC, Revision 3, Carlsbad, NM: U.S. Department of Energy, Carlsbad Field Office.

U.S. DOE. 2015b. RH-TRU 72-B Safety Analysis Report, Revision 7. Carlsbad, NM: U.S. Department of Energy, Carlsbad Field Office.

U.S. DOE. 2018a. Delaware Basin Monitoring Annual Report, Revision 1. September 2018. Carlsbad, NM: Carlsbad Field Office. DOE/WIPP-18-2308.*

U.S. DOE. 2018b. 40 CFR Part 194.4(b)(4) Annual Change Report 2017/2018. Carlsbad, NM: Carlsbad Field Office.

U.S. DOE. 2019a. Title 40 CFR Part 191 Subparts B and C Compliance Recertification Application for the Waste Isolation Pilot Plant. Carlsbad, NM: Carlsbad Field Office. DOE/WIPP-10-3609.

U.S. DOE. 2019b. Delaware Basin Monitoring Annual Report: DOE/WIPP-19-2308, US Department of Energy, Carlsbad, NM.*

U.S. DOE. 2020a. Waste Isolation Pilot Plant Delaware Basin Monitoring Annual Report: DOE/WIPP-20-2308, US Department of Energy, Carlsbad, NM.*

U.S. DOE. 2020b. Letter from R. Knerr to L. Veal (Subject: Planned Change Notice for Alternative Panel Closure Locations for Panels 1 and 2). ERMS 574284.

U.S. DOE. 2020c. Response 2 to U.S. Environmental Protection Agency's 2019 Compliance Recertification Application Completeness Comments Letter dated March 23, 2020 from Tom Peake to Mike Brown. Letter from Gregory Sosson (DOE) to Lee Veal (EPA). CBFO:OEP:MRB:MC:20-0248:UFC 5486.00. Carlsbad, New Mexico. July 9, 2020. (Second Response Package). EPA-HQ-OAR-2019-0534-0013 *

U.S. DOE. 2020d. Response 7 to U.S. Environmental Protection Agency's 2019 Compliance Recertification Application Completeness Comments Letters dated May 6, 2020, June 12, 2020, July 17, 2020 and September 11, 2020 from Tom Peake to Mike Brown. U.S. Department of Energy, Carlsbad Field Office, Carlsbad, New Mexico. Letter to L.B. Veal, U.S. Environmental Protection Agency Radiation Protection Division, Washington, D.C. December 1, 2020. EPA-HQ-OAR-2019-0534-0018.

U.S. DOE. 2021a. Department of Energy Response 10 to U.S. Environmental Protection Agency's Completeness Comments, Letter dated September 11, 2020, and November 13, 2020, from Tom Peake to Mike Brown. U.S. Department of Energy, Carlsbad Field Office, Carlsbad, New Mexico. March 30, 2021.*

U.S. DOE. 2021b. Department of Energy Response 12 to U.S. Environmental Protection Agency's 2019 Compliance Recertification Application Completeness Comments Letter dated September 11, 2020, from Tom Peake to Mike Brown. U.S. Department of Energy, Carlsbad Field Office, Carlsbad, New Mexico. May 27, 2021.*

U.S. DOE. 2021c. Department of Energy Response 9 to EPA Completeness Comments. March 4, 2021.*

U.S DOE. 2021d. Delaware Basin Monitoring Annual Report. September 2021. Carlsbad, NM: U.S. Department of Energy, Carlsbad Field Office. DOE/WIPP-21-2308.*

U.S. DOE. 2022a. Delaware Basin Monitoring Annual Report, Revision 0. December 2022. Carlsbad, NM: U.S. Department of Energy, Carlsbad Field Office. DOE/WIPP-22-2308.*

U.S. DOE. 2022b. Waste Isolation Pilot Plant Annual Site Environmental Report for 2021. Carlsbad, NM: Carlsbad Field Office. DOE/WIPP-22-3591.*

U.S. DOE. 2022c.Transuranic Waste Acceptance Criteria for the Waste Isolation Pilot Plant. DOE/WIPP-02-3122, Revision 11. Carlsbad, NM: US Department of Energy, Carlsbad Field Office.*

U.S. DOE. 2022d. CH-TRAMPAC, Revision 6. U.S. Department of Energy, Carlsbad Field Office.*

U.S. DOE. 2023. Planned Change Notice. Subject: Addition of Four Shielded Containers. Letter dated April 25, 2023, from Mark Bollinger to Lee Ann B. Veal. U.S. Department of Energy, Carlsbad Field Office, Carlsbad, NM. CBFO:ERCD:MG:JV:23-0090 *

U.S. DOE. 2024a. Planned Change Request for the Use of Replacement Panels 11 and 12. Letter dated March 12, 2024, from Mark Bollinger to Lee Anne B. Veal. U.S. Department of Energy, Carlsbad Field Office, Carlsbad, NM. CBFO:ERCD:MG:SV:24-0168*

U.S DOE. 2024b. Delaware Basin Monitoring Annual Report, Revision 0. January 2024. Carlsbad, NM: U.S. Department of Energy, Carlsbad Field Office. DOE/WIPP-23-2308.*

U.S DOE. 2025a. Delaware Basin Monitoring Annual Report, Revision 0. February 2025. Carlsbad, NM: U.S. Department of Energy, Carlsbad Field Office. DOE/WIPP-24-2308.*

U.S. DOE. 2025b. Waste Isolation Pilot Plant Annual Site Environmental Report, Revision 0. September 2025. Carlsbad, NM: U.S. Department of Energy, Carlsbad Field Office. DOE/WIPP-25-3591.*

U.S. Environmental Protection Agency (EPA). 1993. 40 CFR Part 191: Environmental Radiation Protection Standards for the Management and Disposal of Spent Nuclear Fuel, High-Level and Transuranic Radioactive Wastes; Final Rule. Federal Register, vol. 58 (December 20, 1993): 66398–416.

U.S. EPA. 1996a. 40 CFR Part 194: Criteria for the Certification and Recertification of the Waste Isolation Pilot Plant's Compliance With the 40 CFR Part 191 Disposal Regulations; Final Rule. Federal Register, vol. 61 (February 9, 1996): 5224–45.

U.S. EPA. 1996b. Compliance Application Guidance for 40 CFR Part 194 (March 29). Washington, DC: Office of Radiation and Indoor Air. EPA 402-R-95-014. ERMS 239159.

U.S. EPA. 1996c. Criteria for the Certification and Re-Certification of the Waste Isolation Pilot Plant's Compliance with the 40 CFR Part 191 Disposal Regulations, Background Information Document for 40 CFR Part 194. Washington, DC: Office of Radiation and Indoor Air. 402-R-96-002.

U.S. EPA. 1998a. 40 CFR Part 194: Criteria for the Certification and Recertification of the Waste Isolation Pilot Plant's Compliance with the Disposal Regulations; Certification Decision; Final Rule. Federal Register, vol. 63 (May 18, 1998): 27353–406.

U.S. EPA. 1998b. Technical Support Document for Section 193.32: Scope of Performance Assessments (May). Washington, DC: Office of Radiation and Indoor Air.

U.S. EPA. 1998c. CARD No. 33: Consideration of Drilling Events in Performance Assessments. Compliance Application Review Documents for the Criteria for the Certification and Recertification of the Waste Isolation Pilot Plant's Compliance with the 40 CFR 191 Disposal Regulations: Final Certification Decision (May) (pp. 33-1 through 33-31). Washington, DC: Office of Radiation and Indoor Air.

U.S. EPA. 1998d. Response to Comments: Criteria for the Certification and Recertification of the Waste Isolation Pilot Plant's Compliance with the 40 CFR Part 191 Disposal Regulations (May). Washington, DC: Office of Radiation and Indoor Air.

U.S. EPA. 2001. Letter from Frank Marcinowski, EPA to Dr. Ines Triay. (Subject: Approval for the elimination of magnesium oxide mini-sacks from the Waste Isolation Pilot Plant). DOE. Washington, DC: Office of Radiation and Indoor Air. ERMS 519362.

U.S. EPA. 2006. Criteria for the Certification and Recertification of the Waste Isolation Pilot Plant's Compliance with the 40 CFR Part 191 Disposal Regulations: Recertification Decision. Washington, DC: Office of Radiation and Indoor Air. EPA-HQ-OAR-2004-0025.

U.S. EPA. 2010. 40 CFR Part 194 Criteria for the Certification and Recertification of the Waste Isolation Pilot Plant's Compliance with the Disposal Regulations: Rectification Decision; Final Notice. Federal Register, vol. 75 (November 18, 2010): 70584 – 595.

U.S. EPA. 2014. 40 CFR Part 194 Criteria for the Certification and Recertification of the Waste Isolation Pilot Plant's Compliance with the Disposal Regulations; Panel Closure Redesign. Federal Register, vol. 79 (October 8, 2014): 60750 – 756.

U.S. EPA. 2015. Letter from J. Edwards to D. Bryson. Fourth Set of Completeness Comments Related to the 2014 WIPP Compliance Recertification Application, Response 4-C-2. July 30, 2015. EPA Docket EPA-HQ-OAR-2014-0609-0024.

U.S. EPA. 2017a. Criteria for the Certification and Recertification of Waste Isolation Pilot Plant's Compliance with Disposal Regulations; Recertification Decision. Washington, D.C.: Office of Radiation and Indoor Air. Federal Register, vol. 82 (July 19, 2017). 2017-15182. EPA-HQ-OAR-2014-0609.

U.S. EPA. 2017b. Probability of Encountering Castile Brine Beneath the WIPP Waste Panels Using the TDEM Block Method. June, 2017. Office of Radiation and Indoor Air, Docket EPA-HQ-OAR-2014-0609-0047.

U.S. EPA. 2017c. Technical Support Document (TSD) for Sections 194.23, 194.32, and 194.33 Review of Changes to WIPP Performance Assessment Features, Events, and Processes in the 2014 CRA. July 2017. Washington, DC: Office of Radiation and Indoor Air. EPA Docket FDMS Docket ID No. EPA-HQ-OAR-2014-0609.

U.S. EPA. 2017d. Technical Support Document for Section 194.24, Evaluation of the Compliance Recertification Actinide Source Term, Gas Generation, Backfill Efficacy, Water Balance and Culebra Dolomite Distribution Coefficient Values. June, 2017. Office of Radiation and Indoor Air, Docket EPA-HQ-OAR-2014-0609-0054.

U.S. EPA. 2017e. Technical Support Document for Section 194.23, EPA Review of Proposed Modification to the Waste Shear Strength Parameter TAUFAIL. July, 2017. Office of Radiation and Indoor Air, Docket EPA-HQ-OAR-2014-0609-0052.

U.S. EPA. 2020a. U.S. Environmental Protection Agency's 2019 Compliance Recertification Application Completeness Comments #1. Letter from Tom Peake (EPA) to Mike Brown (DOE). Washington, D.C. March 23, 2020. EPA-HQ-OAR-2019-0534-0005.*

U.S. EPA. 2020b. Fifth set of EPA Completeness Comments and Questions for CRA 2019. September 11, 2020.*

U.S. EPA. 2020c. Sixth set of EPA Completeness Comments and Questions for CRA 2019. November 3, 2020.*

U.S. EPA. 2020d. Third set of EPA Completeness Comments and Questions for CRA 2019. June 12, 2020*

U.S. EPA. 2021. Letter from L. Veal to R. Knerr (Subject: Approval of PCR to place run-of-mine (ROM) salt in alternate locations for Panels 1 and 2 at the Waste Isolation Pilot Plant. Office of Radiation and Indoor Air. ERMS 575058.

U.S. EPA. 2022a. Technical Support Document (TSD) for Section 194.33 Review of Borehole Drilling Rate and Plugging Pattern Frequency Calculations in the CRA-2019 Performance Assessment. April 2022. Washington, DC: Office of Radiation and Indoor Air. EPA Docket FDMS Docket ID No. EPA-HQ-OAR-2019-0534.*

U.S. EPA. 2022b. Review of the planned change notice for a fifth shaft at the WIPP repository. Technical Support Document for Section 194.23 and 194.34. Washington, D.C. EPA-HQ-OAR-2019-0534.*

U.S. EPA. 2022c. Evaluation of the Compliance Recertification Application (CRA-2019) Actinide Source Term, Gas Generation, Backfill Efficacy, Water Balance, and Culebra Dolomite Distribution Coefficient Values. Technical Support Document for Section 194.24. Washington, DC. EPA-HQ-OAR-2019-0534. *

U.S. EPA. 2022d. Technical Support Document (TSD) for Section 194.23, 194.32, and 194.54 Review of Changes to WIPP Performance Assessment Features Events, and Processes in the CRA-2019. April 2022. Washington, DC: Office of Radiation and Indoor Air. EPA Docket FDMS Docket ID No. EPA-HQ-OAR-2019-0534.*

U.S. EPA. 2022e. Criteria for the Certification and Recertification of Waste Isolation Pilot Plant's Compliance with Disposal Regulations; Recertification Decision. Federal Register, vol. 87 (May 3, 2022). EPA–HQ–OAR–2019–0534. Washington, D.C.: Office of Radiation and Indoor Air.*

U.S. Nuclear Regulatory Commission (NRC). 2016. Model RH-TRU 72-B Package Certificate of Compliance Number 9212, Revision 10. March 2016. Washington, DC: U.S. Nuclear Regulatory Commission.

U.S. NRC. 2019. Certificate of Compliance for Radioactive Material Package RH-TRU 72-B, Revision 11, Docket 71-9212. Washington DC: US Nuclear Regulatory Commission.*

Van Hullenbusch, E.D., M.H. Zandvoort, and P.N.L. Lens. 2003. Metal immobilization by biofilms: mechanisms and analytical tools. Re/Views in Environmental Science & Bio/Technology 2: 9-33.*

Van Santen, R.A. 1984. The Ostwald Step Rule. J. Phys. Chem., vol. 88: 5768-5769.

Van Soest, G. 2012. Performance Assessment Inventory Report-2012. (Revision 0, November). Los Alamos National Laboratory, Carlsbad, NM. INV-PA-12, LA-UR-12-26643, INV-1211-05-01-01.

Van Soest, G.D. 2018. Performance Assessment Inventory Report – 2018. INV-PA-18, Revision 0. Los Alamos National Laboratory, Carlsbad, NM. LA-UR-18-31882, INV-1812-09-01-01.

Van Soest, G. D. 2025. Interim State Performance Assessment Inventory Report – 2024. INV-IPA-24, Revision 0. Carlsbad, NM: Los Alamos National Laboratory.*

Veal, L. 2019. Letter to T. Shrader, Manager, Carlsbad Field Office, U.S. Department of Energy. (Subject: Approval of Planned Change Notice for Run-of-Mine Panel Closure System Installation and Abandonment of Waste Emplacement in Panel 9 at the Waste Isolation Pilot Plant). (March 21, 2019). Washington, D.C. U.S. Environmental Protection Agency.

Vignes, C., J. Bean, B. Reedlunn. 2023. Improved Modeling of Waste Isolation Pilot Plant Disposal Room Porosity. SAND2023-04826. Albuquerque, NM: Sandia National Laboratories.*

Vine, J.D. 1963. Surface Geology of the Nash Draw Quadrangle, Eddy County, New Mexico. Bulletin 1141-B. Washington, DC: U.S. Geological Survey. ERMS 239558.

Waber, N. 1991. Mineralogy, Petrology and Geochemistry of the Poços de Caldas Analogue Study Sites, Minas Gerais, Brazil, I:. Osamu Utsumi Uranium Mine. Baden, Switzerland: National Genossen Schaft für die Lagerung Radioaktiver Abfalle (NAORA). Nagra Report NTB-90-20.

Wagner, J.D.M., J. Cole, J. Beck, P. Patchett, G. Henderson, and H. Barnett. 2010. Moisture Variability in the Southwestern United States Linked to Abrupt Glacial Climate Change. Nature Geoscience, v. 3, p. 110-113.*

Wagner, S., R. Kirkes, and M.A. Martell. 2003. Features, Events and Processes: Reassessment for Recertification Report. Carlsbad, NM: Sandia National Laboratories. ERMS 530184.

Wall, N. A. 2005. Preliminary Results for the Evaluation of Potential New MgO. Carlsbad, NM: Sandia National Laboratories. ERMS 538514.*

Wallace, M. 1996a. Leakage from Abandoned Boreholes. Summary Memorandum of Record for NS-7b. Albuquerque, NM: Sandia National Laboratories. SWCF-A 1.1.6.3:PA:QA:TSK:NS-7b. ERMS 240819.

Wallace, M. 1996b. Pumping from the Culebra Outside the Controlled Area. Summary Memorandum of Record for NS-5. Albuquerque, NM: Sandia National Laboratories. SWCF-A 1.1.6.3:PA:QA:TSK:NS-5. ERMS 240831.

Wallace, M. 1996c. Records Package for Screening Effort NS11: Subsidence Associated with Mining Inside or Outside the Controlled Area (November 21). Carlsbad, NM: Sandia National Laboratories. ERMS 412918.

Wallace, M., R. Beauheim, C. Stockman, M. Alena Martell, K. Brinster, R. Wilmot, and T. Corbert. 1995. Summary Memorandum of Record for NS-1. (Subject: Dewey Lake Data Collection and Compilation). Albuquerque: Sandia National Laboratories. SWCF-A 1.1.6.3:PA:QA:TSK:NS-1. ERMS 222508.

Wallner, M. 1981. Critical Examination of Conditions for Ductile Fracture in Rock Salt. Proceedings of the Workshop on Near-Field Phenomena in Geologic Repositories for Radioactive Waste, Seattle, WA, August 31–September 3, 1981 (pp. 243–53). Paris: Organisation for Economic Co-operation and Development. ERMS 241372.

Wang, Y. 1996a. Memorandum to Internal Distribution (Subject: Evaluation of the Thermal Effect of Exothermal Chemical Reactions for WIPP Performance Assessment: A revised version) (August 19, 1996). Albuquerque, NM: Sandia National Laboratories. ERMS 240633.*

Wang, Y. 1996b. Memorandum to Internal Distribution (Subject: Evaluation of the Thermal Effect of MgO Hydration for the Long-Term WIPP Performance Assessment). (May 9, 1996). Albuquerque, NM: Sandia National Laboratories. ERMS 237743.

Wang, Y. 1998. Memorandum to Malcolm D. Siegel (Subject: On the Matrix Pore Plugging Issue). (August 8, 1998). Albuquerque, NM: Sandia National Laboratories. ERMS 421858.

Wang, Y., and L.H. Brush. 1996a. Memorandum to M.S. Tierney (Subject: Estimates of Gas-Generation Parameters for the Long-Term WIPP Performance Assessment). (January 26, 1996). Albuquerque, NM: Sandia National Laboratories. ERMS 231943.

Wang, Y., and L.H. Brush. 1996b. Memorandum to M.S. Tierney (Subject: Modify the Stoichiometric Factor y in the BRAGFLO to Include the Effect of MgO Added to WIPP Repository as a Backfill). (February 23, 1996). Albuquerque, NM: Sandia National Laboratories. ERMS 232286.

Warrick, R., and J. Oerlemans. 1990. Sea Level Rise, in Climate Change: The IPCC Scientific Assessment. J.T. Houghton, G.J. Jenkins, and J.J. Ephraums, eds. Sweden: Intergovernmental Panel on Climate Change. (pp. 257–81).

Westinghouse Electric Corporation. 1994. Backfill Engineering Analysis Report, Waste Isolation Pilot Plant. Carlsbad, NM. Westinghouse Electric Corporation. WPO 37909. ERMS 237909.

Weinberg, R.F., 1993. The upward transport of inclusions in Newtonian and power-law salt diapirs. Tectonophysics. Vol. 228. Pg. 141-150.

Wierczinski, B., S. Helfer, M. Ochs, and G. Skarnemark. 1998. Solubility Measurements and Sorption Studies of Thorium in Cement Pore Water. Journal of Alloys and Compounds, vol. 271: 272−276.

Wilgus, J., and J. Bethune. 2025. Analysis Report for Culebra Flow and Transport in the 2026 Compliance Recertification Application Performance Assessment, Revision 0. November 2025. Carlsbad, NM: Sandia National Laboratories.*

Wilmot, R.D., and D.A. Galson. 1996. Memorandum of Record for NS17 and NS18, SWCF-A 1.1.6.3:PA:QA:TSK; NS-17, NS-18 (Subject: Human-Initiated Brine Density Changes). Albuquerque, NM: Sandia National Laboratories. ERMS 238748.

Wilson, C., D. Porter, J. Gibbons, E. Oswald, G. Sjoblom, and F. Caporuscio. 1996. Conceptual Models Supplementary Peer Review Report (December). Carlsbad, NM: Carlsbad Area Office. ERMS 243153.

WIPP Performance Assessment Department. 1991. Preliminary Comparison with 40 CFR Part 191, Subpart B for the Waste Isolation Pilot Plant, December 1991, Volume 1: Methodology and Results. Albuquerque, NM: Sandia National Laboratories, WIPP Performance Assessment Department. SAND91-0893/1. ERMS 226404.

WIPP PA Department 1992. Preliminary Performance Assessment for the Waste Isolation Pilot Plant, December 1992—Volume 3: Model Parameters. Albuquerque, NM: Sandia National Laboratories. SAND92-0700/3.

WIPP Performance Assessment Department. 1993. Preliminary Performance Assessment for the Waste Isolation Pilot Plant, December 1992, Volume 4: Uncertainty and Sensitivity Analyses for 40 CFR 191, Subpart B. Albuquerque, NM: Sandia National Laboratories. SAND92-0700/4.UC-721. ERMS 223599.

WIPP Performance Assessment. 2025. Design Document and User's Manual for BRAGFLO, Version 8.00. Carlsbad, NM: Sandia National Laboratories. EIMS-0004430695.

WIPP Performance Assessment. 2022a. Design Document and User's Manual for NUTS, Version 2.08. Albuquerque, NM: Sandia National Laboratories. ERMS 573824.

WIPP Performance Assessment. 2022b. Design Document and User's Manual for SECOTP2D, Version 1.44. Carlsbad, NM: Sandia National Laboratories. ERMS 573879.

Witherspoon, P.A., J.S.Y. Wang, K. Iwai, and J.E. Gale. 1980. Validity of Cubic Law for Fluid Flow in a Deformable Rock Fracture. Water Resources Research, vol. 16: 1016−24. ERMS 238853.

Wolery, T.J. 1992. EQ3NR—A Computer Program for Geochemical Aqueous Speciation Solubility Calculations: Theoretical Manual, User's Guide, and Related Documentation (Version 7.0). Berkeley, CA: Lawrence Livermore National Laboratory. UCRL-MA-110662 PT III.

Woo, J.U., and W.L. Ellsworth. 2023. Reactivation of Precambrian faults by deep wastewater injection in Midland Basin, Texas, and performance evaluation of seismic response areas: Bulletin of Seismological Society of America, v. 20, p. 1-14.*

Wood, B.J., R.E. Snow, D.J. Cosler, and S. Haji-Djafari. 1982. Delaware Mountain Group (DMG) Hydrology – Salt Removal Potential, Waste Isolation Pilot Plant (WIPP) Project, Southeastern New Mexico. Albuquerque NM: U.S. Department of Energy. TME 3166. ERMS 241602.

Xu, S., and L. Feriancikova. 2014. Transport of Manure-Derived Escherichia coli Within Naturally-Fractured Dolomite. Groundwater Research Report, Project ID WR12R003. University of Wisconsin Water Resources Institute.*

Yelton, W.G., Y.K. Behl, J.W. Kelly, M. Dunn, J.B. Gillow, A.J. Francis, and H.W. Papenguth. 1996. Laboratory Evaluation of Colloidal Actinide Transport at the Waste Isolation Pilot Plant (WIPP): 1. Crushed-Dolomite Column Flow Experiments. SAND96-2894C. Sandia National Laboratories; Albuquerque, NM.*

Zhai, G., Shirzaei, M., and Manga., M. 2021. Widespread deep seismicity in the Delaware Basin, Texas, is mainly driven by shallow wastewater injection: Proceedings of the National Academy of Sciences, v. 118, no. 20, 7 p.*

Zeitler, T.R. 2015. Memo to Records. (Subject: Evaluation of Brine Flow Through Panel Closures using CRA-2014 BRAGFLO Results). June 2015. Carlsbad, NM: Sandia National Laboratories. ERMS 564062.

Zeitler, T.R., and C. Hansen. 2015. Cumulative Distribution for STEEL:CORRMCO2. Carlsbad, NM: Sandia National Laboratories. ERMS 565005.

Zeitler, T.R., and B. Day. 2016. CRA14_SEN4 Sensitivity Study, Revision 1. Carlsbad, NM: Sandia National Laboratories. ERMS 567505.

Zeitler, T.R., and B. Day. 2017. Analysis Plan for the Assessment of Abandoned Panel Closures in South End of Repository and Lack of Waste Emplacement in Panel 9, Revision 0. July 13, 2017. Carlsbad, NM: Sandia National Laboratories. AP-177. ERMS 568138.

Zeitler, T.R., B.A. Day, J. Bethune, R. Sarathi, and J. Long. 2017. Assessment of Abandoned Panel Closures in South End of Repository and Lack of Waste Emplacement in Panel 9, Revision 0." August 31, 2017. Carlsbad, NM: Sandia National Laboratories. ERMS 568459.*

Zeitler, T.R. 2018a. Bounding Calculation of the Cumulative Distribution for STEEL:HUMCORR. Sandia National Laboratories. Carlsbad, NM. ERMS 569807.

Zeitler, T.R. 2018b. Cumulative Distribution for STEEL:CORRMCO2 for the CRA-2019 PA. Carlsbad, NM: Sandia National Laboratories. ERMS 570869.*

Zeitler, T. R. 2019a. Analysis Plan for the 2019 WIPP Compliance Recertification Application Performance Assessment. Carlsbad, NM: Sandia National Laboratories. AP-181. ERMS 571150. *

Zeitler, T.R. 2019b. Calculation of Shaft and Experimental Area Dimensions for Use in the CRA-2019 PA. Sandia National Laboratories. Carlsbad, NM. ERMS 571045.*

Zeitler, T.R., J. Bethune, S. Brunell, B. Day, D. Kicker, J. Long, and R. Sarathi. 2019. Summary Report for the 2019 Compliance Recertification Application Performance Assessment (CRA-2019 PA). 2019. Carlsbad, NM: Sandia National Laboratories. ERMS 571376.

Zengotita F.E., H.P. Emerson, F.E. Stanley, T.M. Dittrich, M.K. Richmann, D. Reed, J. Swanson. 2019. Potential for biocolloid transport of cesium at high ionic strength. Chemosphere, Volume 235, Pages 1059-1065.*

Zerwekh, A. 1979. Gas Generation from Radiolytic Attack of TRU-Contaminated Hydrogenous Waste. Los Alamos National Laboratory, Los Alamos, NM. LA-7674-MS.

Zerwekh, A., J. Warren, and S. Kosiewicz, 1993. The Effect of Vibration on Alpha Radiolysis of Transuranic (TRU) Waste, Proceedings of Symposium on Waste Management, Tucson, AZ.

Zoback, M.D., and M.L. Zoback. 1991. Tectonic Stress Field of North America and Relative Plate Motions. D.B. Slemmons, E.R. Engdahl, M.D. Zoback, and D.D. Blackwell, eds. Boulder, CO: Geological Society of America. Neotectonics of North America (pp. 339–66). ERMS 241601.

Zoback, M.L., and Zoback, M.D. 1980. State of Stress in the Conterminous United States. Journal of Geophysical Research, vol. 85, no. B11: 6113–56. ERMS 241600.

Zoback, M.L., M.D. Zoback, J. Adams, S. Bell, M. Suter, G. Suarez, C. Estabrook, and M. Magee. 1991. Stress Map of North America. Continent Scale Map CSM-5, Scale 1:5,000,000. Boulder, CO: Geological Society of America.